AD-A033 774 BOEING AEROSPACE CO SEATTLE WASH F/G 21/5
INTEGRATED PROPULSION CONTROL SYSTEM (IPCS). VOLUME II. TECHNIC--ETC(U)
AUG 76 L O BILLIG F33615-73-C-2035
UNCLASSIFIED AFAPL-TR-76-61-VOL-2 NL

1 OF 3
AD
A033774

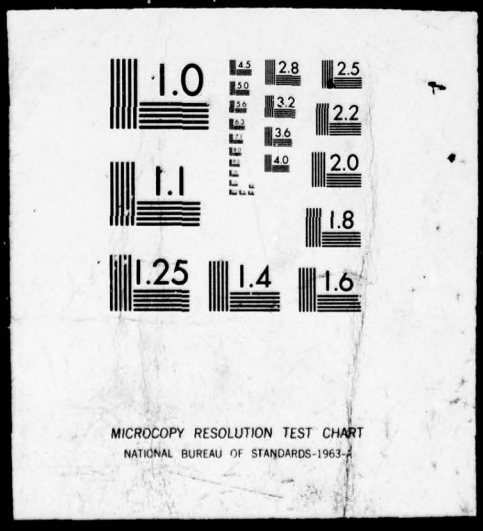

AFAPL-TR-76-61
VOLUME II

INTEGRATED PROPULSION CONTROL SYSTEM (IPCS)
FINAL REPORT
VOLUME II
TECHNICAL DESCRIPTION

BOEING AEROSPACE COMPANY
P.O. BOX 3999
SEATTLE, WA. 98124

AUGUST 1976

TECHNICAL REPORT AFAPL-TR-76-61 VOLUME II
FINAL REPORT FOR PERIOD 1 MARCH 1973 - 30 AUGUST 1976

Approved for public release; distribution unlimited

AIR FORCE AERO-PROPULSION LABORATORY
AIR FORCE WRIGHT AERONAUTICAL LABORATORIES
AIR FORCE SYSTEMS COMMAND
WRIGHT-PATTERSON AIR FORCE BASE, OHIO 45433

NOTICE

When Government drawings, specification, or other data are used for any purpose other than in connection with a definitely related Government procurement operation, the United States Government thereby incurs no responsibility nor any obligation whatsoever; and the fact that the government may have formulated, furnished or in any way supplied the said drawings, specifications, or other data, is not to be regarded by implication or otherwise as in any manner licensing the holder or any other person or corporation, or conveying any rights or permission to manufacture, use, or sell any patented invention that may in any way be related thereto.

This final report was submitted by Boeing Aerospace Company, under contract F33615-73-C-2035. The effort was sponsored by the Air Force Aero Propulsion Laboratory, Air Force Systems Command, Wright-Patterson AFB, Ohio under Project Number 3066, Task Number 03 and Work Unit Number 42 with Joseph J. Batka, AFAPL/TBC as Project Engineer. Mr. G. W. N. Lampard of Boeing Aerospace Company was technically responsible for the work.

This report has been reviewed by the Information Office, (ASD/OIP) and is releasable to the National Technical Information Service (NTIS). At NTIS, it will be available to the general public, including foreign nations.

This technical report has been reviewed and is approved for publication.

Joseph J. Batka

JOSEPH J. BATKA
Project Engineer

FOR THE COMMANDER

Charles E. Bentz

CHARLES E. BENTZ
Technical Area Manager - Controls

Copies of this report should not be returned unless return is required by security considerations, contractual obligations, or notice on a specific document.

UNCLASSIFIED

SECURITY CLASSIFICATION OF THIS PAGE (When Data Entered)

REPORT DOCUMENTATION PAGE

READ INSTRUCTIONS BEFORE COMPLETING FORM

1. REPORT NUMBER: AFAPL-TR-76-61-Volume II

2. GOVT ACCESSION NO. (9) Final

3. RECIPIENT'S CATALOG NUMBER

4. TITLE (and Subtitle): (16) (IPCS). Integrated Propulsion Control System Final Report, Volume II, TECHNICAL DESCRIPTION

5. TYPE OF REPORT & PERIOD COVERED: Technical Report (Final) 1 March 1973-30 August 1976

6. PERFORMING ORG. REPORT NUMBER

7. AUTHOR(s): (10) Leon O. Billig

8. CONTRACT OR GRANT NUMBER(s): (15) F33615-73-C-2035

9. PERFORMING ORGANIZATION NAME AND ADDRESS: Boeing Aerospace Company, P. O. Box 3999, Seattle, WA 98124

10. PROGRAM ELEMENT, PROJECT, TASK AREA & WORK UNIT NUMBERS: P.E. 62203F, PROJ 3066, Task 306603, W.U. 30660342

11. CONTROLLING OFFICE NAME AND ADDRESS: Air Force Aero-Propulsion Laboratory (AFAPL/TBC), Air Force System Command, Wright Patterson AFB OH 45433

12. REPORT DATE: August 1976

13. NUMBER OF PAGES: 197

14. MONITORING AGENCY NAME & ADDRESS (if different from Controlling Office): (16) 3066 (17) 03

15. SECURITY CLASS. (of this report): UNCLASSIFIED (12) 200 p.

15a. DECLASSIFICATION/DOWNGRADING SCHEDULE

16. DISTRIBUTION STATEMENT (of this Report)

Approved for Public Release; Distribution Unlimited.

17. DISTRIBUTION STATEMENT (of the abstract entered in Block 20, if different from Report): (18) AFAPL (19) TR-76-61-Vol-2

18. SUPPLEMENTARY NOTES

19. KEY WORDS (Continue on reverse side if necessary and identify by block number)

Gas turbine testing, digital controls, propulsion controls, F-111, TF30, flight testing, integrated control

20. ABSTRACT

The Integrated Propulsion Control System (IPCS) program was conducted to pursue and demonstrate the advantages of integrated propulsion controls. The program encompassed the design, build, flight qualification, and flight testing of control modes, software, and hardware. The flight test vehicle was an F-111E. The left inlet and TF30-P-9 engine were modified to operate under control of an HDC-601 computer. Two sets of hardware were built or modified and two sets of software were developed; one implemented the bill-of-materials control laws and one implemented control laws developed under contract. A step-by-step sequence of tests of increasing complexity demonstrated suitability for flight. Fifteen flights were conducted to evaluate the IPCS. This document describes the design, fabrication, and ground testing of the IPCS.

DD FORM 1 JAN 73 1473 EDITION OF 1 NOV 65 IS OBSOLETE

UNCLASSIFIED

SECURITY CLASSIFICATION OF THIS PAGE (When Data Entered)

059610

CONTENTS

ILLUSTRATIONS

TABLES

IPCS NOMENCLATURE

A/B	Afterburner
ABC1-ABC8	Afterburner Control Scheduled Functions in BOMDIG
Aj	Nozzle Area
A/D	Analog-to-Digital
ATP	Acceptance Test Procedure
BITE	Built In Test Equipment
BLFT	Baseline Flight Test
BOM	Bill-of-Materials
BOMDIG	Bill-of-Material Digital Control
CADC	Central Air Data Computer
CCU	Computer Control Unit
CDR	Critical Design Review
CFE	Contractor Furnished Equipment
CLBT	Closed-Loop Bench Test
CMU	Computer Monitor Unit
CPC	Computer Program Component
CPCEI	Computer Program Contract End Item
CPU	Central Processor Unit
D/A	Digital-to-Analog
dB	Decibel
DCS	Digital Computer System
DCU	Digital Computer Unit
DEM	Diffuser Exit Mach Number
DFRC	Dryden Flight Research Center
DIB	Discrete Input Buffers
DIO	Direct Input/Output Channel
DMA	Direct Memory Access Channel
DOB	Discrete Output Buffers
DPCU	Digital Propulsion Control Unit
DS	Design Specifications
ECS	Environmental Control System
EIB	Engine Interface Box
ENC	Exhaust Nozzle Control
ENC1-ENC8	Exhaust Nozzle Scheduled Control Functions in BOMDIG
EPR	Engine Pressure Ratio
EX	Excitation
FAT	Flight Assurance Test
FBCANG	Feedback Cam Angle
FMEA	Failure Mode & Effect Analysis
FMECA	Failure Mode, Effect, and Criticality Analysis
GFE	Government Furnished Equipment
GSE	Ground Support Equipment
HPC	High Pressure Compressor
HSPT	High Speed Paper Tape Punch & Reader
HMC	Hydromechanical Control
Hz	Hertz (= cycles per second)
I.C.	Initial Condition
ICD	Interface Control Document
IFU	Interface unit
I/O	Input/Output
KD	Distortion Index
LLMUX	Low Level Multiplexer
LM	Local Mach Number
LPC	Low Pressure Compressor
LRD	Lamp and Relay Drivers
LVDT	Linear Variable Differential Transformer

MFC	Main Fuel Control
MFC1-MFC7	Scheduled Functions in the BOM fuel Control, Represented by Tables or Polynominal Curve Fits in BOMDIG
MN	Airplane Mach Number
MSB	Most Significant Bit
MTBF	Mean Time Between Failures
MUX	Multiplex or Multiplexer
NSP	Non Standard Part
N1	Low Pressure Rotor Speed, PRM
N2	High Pressure Rotor Speed, RPM
OCV	Oscillator Controlled Voltage Circuits Demodulators
P	Pressure, See Illustration page 33 for Station Designations
Pb	Burner static pressure
PC	Programmable Clock
P/C	Printed Circuit
PCM	Pulse Code Modulation
PDR	Preliminary Design Review
PIL	Priority Interrupt Lines
PLA	Power Lever Angle
PLM	Local-Mach Total Pressure Signal
P/N	Part Number
POT	Potentiometer
PPH	Pounds Per Hour
PPS	Pounds Per Second
PRBC	Pressure Ratio Bleed Control (12th Stage Bleed)
PRI	Power Recovery Interrupt
PSLM	Local-Mach Static Pressure Signal
PSU	Power Supply Unit
RAM	Random Access Memory
RFD	Recycling Frequency-to-Digital Converters
RMS	Root Mean Square
ROM	Read Only Memory
RNI	Reynolds Number Index
RSS	Root Sum Square
RTC	Real Time Clock
RTD	Recycling Time-to-Digital Converters
SFCO	Software Field Change Order
S&H	Sample and Hold
SIA	Simulation Interface Adapter
SLS	Sea Level Static
SMD	Stepping Motor Drivers
SMITE	P&WA Technique for Iterative Solutions in Digital Simulation Program
S/N	Serial No.
SOAPP	P&WA Modular Program Assembly Procedure
SOD	Solenoid Drivers
STE	Special Test Equipment
T	Temperature
T/C	Thermocouple
TIGT	Turbine Inlet Gas Temperature
TSU	Test Set Unit
TTY	Teletype
VCO	Voltage Controlled Oscillator
Vex	Sensor Excitation Voltage
Vo	Sensor Output Voltage
Wa	Airflow Rate, lb/hour
WAR2	Corrected Air Flow Rate at Station 2
Wf	Fuel Flow Rate, Gas Generator, lb./hr.
WFG	Commanded Fuel Flow Rate, Gas Generator
WFZi	Commanded Afterburner Fuel Flow, ith Zone, i=1,..., 5
XAJP	Resolver Angle on Nozzle Position Feedback
XAJV	Nozzle Control Pilot Valve Position
XCON	Cone Actuator Position
XOO	Afterburner Control Power Piston Position
XSPK (XORLS)	Spike Position (normalized spike position)

A suffix "S" indicates a sensed variable.

SUMMARY

The operational capability of aircraft can be expanded by use of integrated propulsion controls. Steady-state engine performance (thrust, SFC) can be improved by operating closer to the engine limits. External disturbances can be tolerated by shifting the engine operating point for the duration of the disturbance. Faster, smoother transients can be accomplished by retreating from the operating limits (sacrificing fuel economy or peak thrust momentarily) during accels and decels. Engine life and time between overhauls can be extended by more consistent avoidance of momentary over-temperature and over-stress conditions and by minimizing temperature cycling. Crew work load may be reduced through a greater degree of automation. Ground trimming of the engines can be reduced or eliminated. While these improvements are applicable to both military and civilian aircraft, implementation has been impeded by the inherent limitations of hydromechanical controls and by the fact that the newer, more complex propulsion systems are more difficult to control.

The Air Force sponsored the Integrated Propulsion Control System (IPCS) program under Contract No. F33615-73-C-2035 to pursue and demonstrate the advantages of integrated propulsion controls. The program encompassed the design, build, flight qualification and flight testing of propulsion control modes, software, and hardware. The flight test vehicle was an F-111E airplane owned by the government. The left-hand inlet and TF30-P-9 engine were modified to operate under control of an HDC-601 digital computer mounted in the aircraft weapons bay. Key tests were conducted and specialized technical guidance was provided by NASA; the Dryden Flight Research Center and the Lewis Research Center. Major contractors were Boeing Aerospace Company, Honeywell, Inc., G&AP Division, and Pratt and Whitney Division of United Technology.

The contract date was 1 March 1973. An analysis and design phase of about fifteen months followed; the final design review was conducted late in May 1974. Baseline tests were conducted to document the characteristics of the test engines and aircraft.

Two complete sets of hardware were fabricated or modified for the IPCS program. The first set of hardware and software was delivered by Honeywell on 28 October 1974. System level tests at the P&WA fuel system test bench facility began immediately. The electronic hardware was mated with the modified Bendix fuel controls and a modified F-111 inlet actuation module and operated, closed loop, using simulations of the engine and inlet aerodynamics to close the loop. A two-month test series followed during which various hardware and software deficiencies were identified and corrected.

The modified fuel controls were then installed on the two TF30-P-9 engines that were dedicated to the IPCS program, engines P-676627 and P-676629. Testing commenced in the sea-level test cell on 21 January 1975 and continued through 27 March 1975. A total of 97 hours and 57 minutes running time were accumulated on the two engines during the sea level tests.

One engine (P-676629) and set of controller hardware were subjected to extensive tests in the NASA/LeRC altitude facility. The comprehensive nature of the tests resulted in the accumulation of 243 hours of run time and 70 stalls on the engine. The engine was sent to the Air Force overhaul facility after the altitude test and subsequently returned to inventory.

The other engine (P-676627) and associated electronic equipment was shipped to NASA/DFRC where it was installed in the F-111E test aircraft by a NASA crew. After a comprehensive ground checkout, a flight test series was conducted to evaluate the IPCS in a flight environment.

A full set of steady-state and transient engine and aircraft events were conducted over a spectrum of test conditions. Seventy-seven operating hours were accumulated on the engine during thirty five ground runs and fifteen flights.

The IPCS program successfully demonstrated operational advantages on the test airframe/engine installation, it demonstrated in a flight environment advanced technical features that had previously been studied only theoretically or in a laboratory environment, and it demonstrated a management methodology that can be applied to reduce cost and risk in the development of an integrated propulsion control system for a high performance aircraft of the future.

1.0 INTRODUCTION AND SUMMARY

Controls for early turbojet engines were direct and simple. Engine geometry was fixed and operating margins were generous, with engine fuel flow as the only independent variable. Satisfactory control was achieved through a simple speed governor. Acceleration and deceleration fuel flow limiting could be done with open-loop schedules. These requirements were readily satisfied by positioning a fuel valve through a system of cams and linkages that come to be known as the hydromechanical fuel control. Since the engine requirements were minimal, a suitable fuel control could be compact, lightweight, and highly reliable.

Twin-spool engines, turbofan engines, variable compressor geometry, and afterburners engendered a corresponding increase in the complexity of the control required for satisfactory operation. The progression to turbofan engines with fully modulated afterburners and exhaust nozzles placed severe demands upon hydromechanical control technology. The added complication of operation behind a supersonic inlet pushed the current technology of hydromechanical controls to an apparent limit, with costs increasing and little hope of maintaining a reputation for reliability. By contrast, both the cost and reliability of digital electronic controls have been improving rapidly and this improvement appears to be destined to continue. Furthermore, integration into a modern flight system demands communication, and direct communication with a hydromechanical unit is inherently difficult.

The Air Force* recognized the problems associated with propulsion controls and sponsored the Integrated Propulsion Control System (IPCS) program under Contract No. F33615-73-C-2035 to address those problems.

The Integrated Propulsion Control System (IPCS) program encompassed the design, build, flight qualification, and flight testing of propulsion control modes, software, and hardware. The flight test vehicle was an F-111E airplane owned by the government. The L-H inlet and TF30-P-9 engine were modified to operate under control of an HDC-601 digital computer mounted in the aircraft weapons bay. The flight-test aircraft is shown in Figure 1.0-1. Technical support was being provided by NASA; the Flight Research Center (FRC)** and the Lewis Research Center (LeRC). Major contractors were Boeing Aerospace Company, Honeywell, Inc., G&AP Division, and Pratt and Whitney Division of United Technology (P&WA™). A diagram showing organizational responsibilities is given in Figure 1.0-2. The IPCS program and schedule is diagrammed in Figure 1.0-3.

This, the second volume of the IPCS final report, contains a technical description of the IPCS program; goals and philosophy, analytical design of control modes, the design, development and testing of hardware and software, and ground testing of the IPCS on an engine under sea-level and simulated altitude conditions. The flight evaluation of the IPCS is described in Volume III. IPCS methodology that may be relevant to future programs is described in Volume IV along with specific recommendations based on IPCS experience.

1.1 IPCS PROGRAM GOALS

The goals of the Air Force in funding the IPCS program were two fold:

1. Improve aircraft systems performance through technological advances.
2. Reduce the cost and risk of future development programs through an expanded technical data base and demonstrated management methodology.

Specific goals established for the IPCS pursued the goals of the Air Force Exploratory Development Programs. The first of these was to develop, demonstrate, amd evaluate in a flight environment, certain advanced technical features that have to date been explored only under very restricted conditions. These are listed in Table 1.0-1.

The second major goal was the development of an intercompany management approach applicable to the design and development of integrated systems. The IPCS management methodology addresses three areas of potential concern; assignment of responsibilities, communication and coordination between geographically remote organizations, and

*Air Force Aero Propulsion Laboratory
Air Force Systems Command
United States Air Force
Wright-Patterson AFB, Ohio

**NASA/FRC has subsequently been designated the Hugh L. Dryden Flight Research Center (NASA/DFRC)

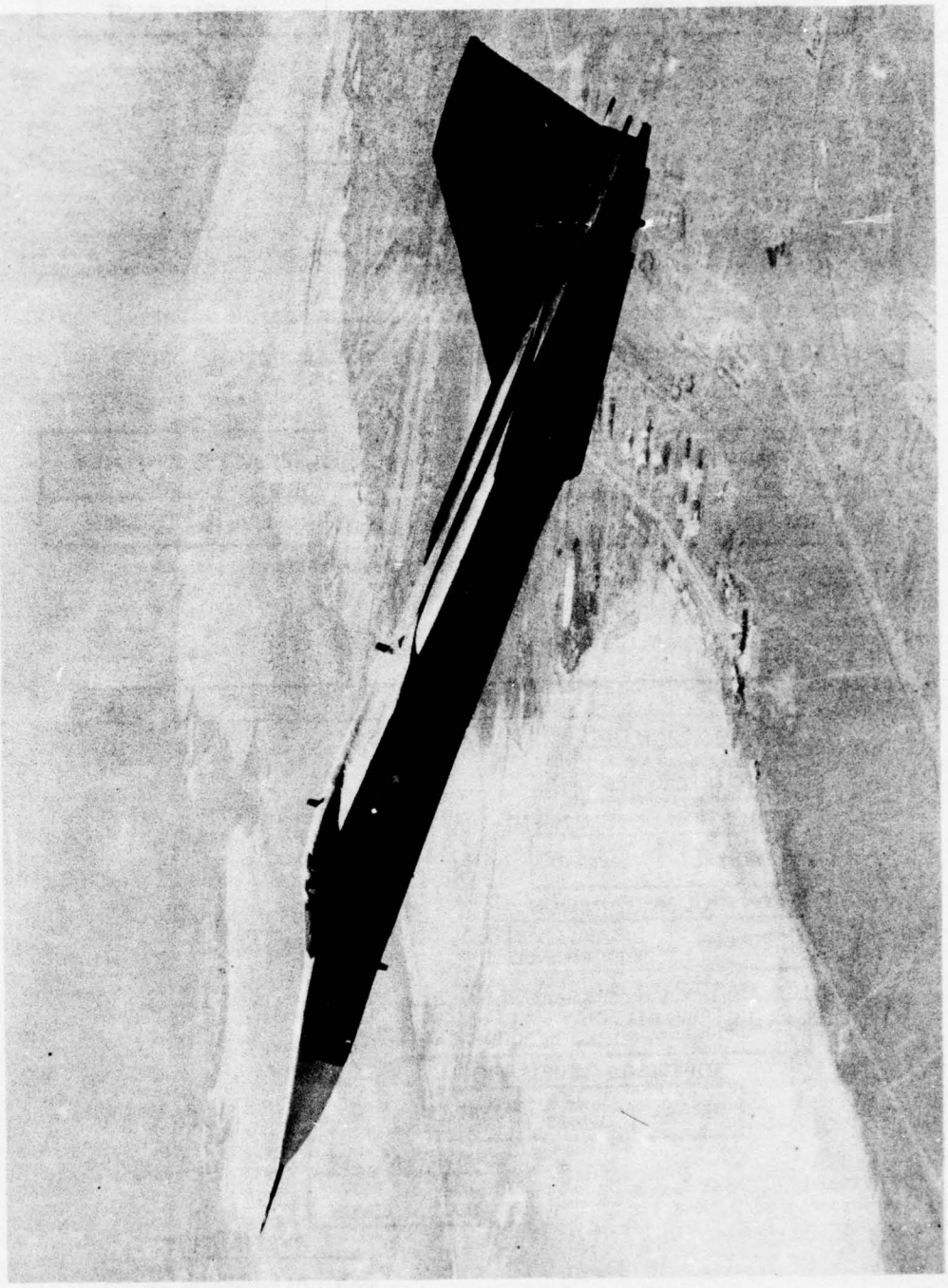

Figure 1.0-1 IPCS Flight Test Aircraft

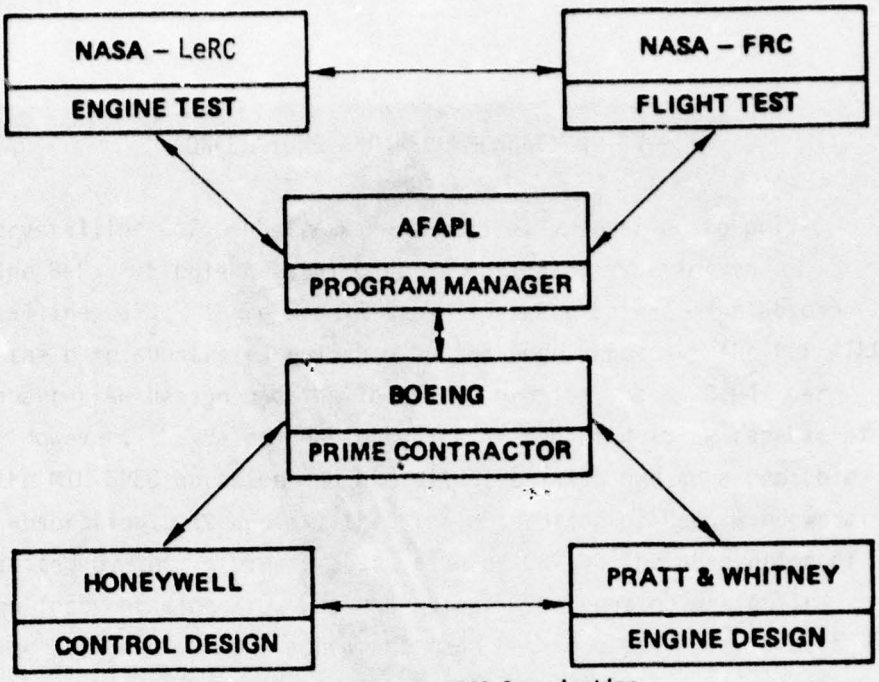

Figure 1.0-2 IPCS Organization

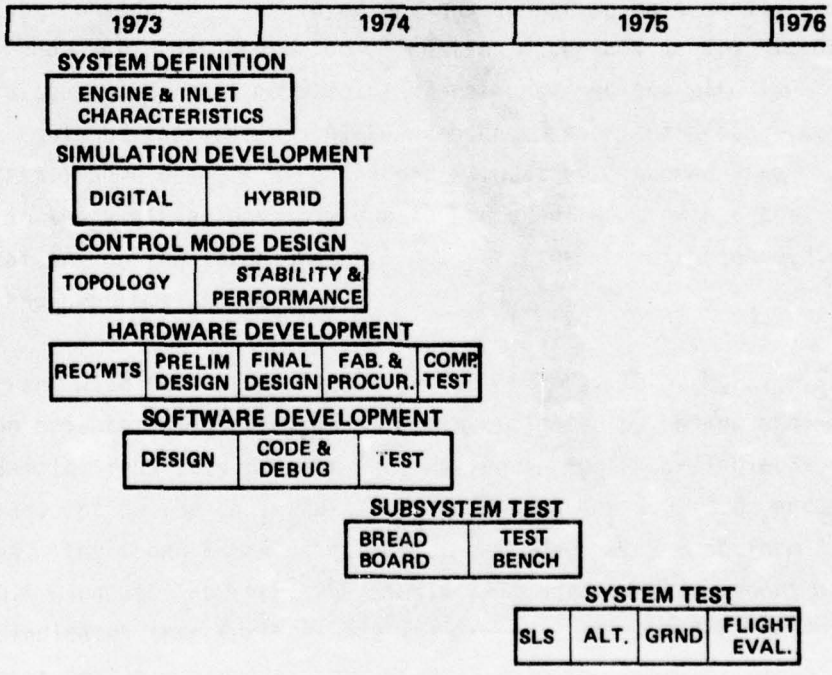

Figure 1.0-3 Integrated Propulsion Control System Program

1.1 IPCS PROGRAM GOALS (Continued)

minimization of technical risk and cost through a timely test sequence. The salient features of the IPCS management approach are listed in Table 1.0-2.

Achievement of these program goals has identified potential development problem areas. It has generated a body of technical data upon which to base further development work and has provided a basis for estimating the time and cost of development of an operational IPCS.

Table 1.0-1

IPCS Advanced Technical Features

Integration of engine and inlet controls.

Full authority digital propulsion control with hydromechanical backup. This permitted control law changes without hardware modification.

Closed loop control on turbine-inlet gas temperature (TIGT)

Use of compressor discharge Mach number for surge protection during engine transients.

Automatic detection and suppression of inlet buzz so that engine airflow can be reduced during airplane deceleration.

Continuous monitoring of distortion to extend the operating envelope with the compressor surge bleeds closed.

Fuel manifold prefill logic to smooth afterburner transients.

Table 1.0-2

SALIENT FEATURES OF IPCS INTERCOMPANY MANAGEMENT APPROACH

Horizontal assignment of responsibility - each organization exercised its own area of expertise over the entire range of the program.

Direct communication at the working level was stressed.

Regular (monthly) coordination meetings were attended by representatives of the prime and major subcontractors.

Periodic working sessions were conducted with attendance by technical personnel of each of the three firms.

Progressive step-by-step hardware and software test sequence.

Final decisions were made by the prime contractor at government direction.

1.2 SYSTEM DESCRIPTION

The IPCS consisted of flight hardware, control modes, and ground support hardware. A brief description of each of these items, intended to help the reader to understand subsequent material, is given below. Additional information is given in the sections of this report that treat the design, fabrication, and testing of the individual component and subsystems.

Two complete sets of hardware were fabricated or modified for the IPCS program.

1.2.1 IPCS Flight Hardware

A diagram of the IPCS is shown in Figure 1.2-1. The TF30-P-9 engine was modified by P&WA to the extent required to interface with the Digital Propulsion Control Unit (DPCU). Pressure transducers temperature sensors and tachometers defined the engine state to the DPCU, which evaluated this information and generated commands that were transmitted to the modified fuel and nozzle controls. An electrical torque motor servo first stage was installed on the main fuel control. A selector solenoid was added so that the fuel metering valve could be driven either by the electrical first stage or by the hydromechanical bill-of-materials fuel controller, which was retained. Metering valves for each of the five afterburner zones were driven by stepper motors acting through hydraulic boosters. The exhaust nozzle actuator pilot valve was also driven by a hydraulically boosted stepper motor. Position feedback sensors were provided for all fuel metering valves the exhaust nozzle pilot valve, and for the nozzle itself. Solenoids were added to operate the shut-off valves for the five afterburner zones and the nozzle. These solenoids, as well as the main fuel control sector solenoid, were selected so that interruption of electrical excitation would drive the engine to a safe operating condition; afterburner off, nozzle closed and gas generator under hydromechanical control. The 7th stage compressor bleeds were made to be operable under either DPCU or bill-of-materials control. The DPCU could open the 12th stage bleeds but could not override the bill-of-materials (PRBC) control to close them.

No changes were made to the engine cycle or to the gas path except as required for the installation of sensors. Only the actuation system was modified in the fuel and exhaust nozzle controls; all the service-proven fuel plumbing was retained.

The inlet actuation system was also modified as necessary to interface with the DPCU. The bill-of-materials hydromechanical inlet control was removed and replaced by a servo module that responds to computer commands. This module also had a solenoid-operated selector valve that caused the inlet surfaces to move to the low-speed configuration when excitation was interrupted. Pressure transducers were provided to sense inlet control signals and position feedback sensors were provided to close the position loops. The inlet aerodynamic configuration was not modified in any way.

The DPCU consisted of four major components; the digital computer unit (DCU) and interface unit (IFU), a power supply unit (PSU) and a computer monitor unit (CMU). The DCU was a Honeywell HDC-601 digital computer with a repertory of 84 instructions. It has a core memory with 16,384 words divided into 32 sectors of 512 (1000_8) words each. Word length was 16 bits and memory cycle time was 1.2 microseconds.

The IFU was designed and built especially for the IPCS program. The input and output capability of the unit is given in Table 1.2-1. The IFU incorporated three custom input channels based on the Supersonic transport buzz detector circuit (reference 1), one each to detect inlet buzz, inlet air turbulence associated with distortion, and afterburner rumble.

The CMU was mounted in the cockpit and was the interface between the flight crew and the DPCU. All control switches and displays were mounted on the CMU panel, which is diagrammed in Figure 1.2-2.

It was originally intended that the power supply be incorporated in the IFU. This plan was modified when it was determined that the flight-qualified stepper motors available for the fuel system modification required 32 vdc rather than the 28 vdc ship's power. The requirements for 32 vdc for the stepper motors imposed the requirement for a separate PSU.

The layout of the IPCS on the aircraft is shown in Figure 1.2-3. The figure also shows a shock position probe and an instrumentation package. The shock probe was flown for evaluation only during preliminary (baseline) tests; the results of these tests are discussed in paragraph 2.1.3 below. The instrumentation package supplied by NASA/FRC, is discussed in paragraph 5.2.2.2.

The IPCS was installed in the aircraft by NASA personnel. Wire bundles and tubing runs were fabricated by NASA to Boeing drawings. Engineering support was provided on-site by the contractor team during the installation.

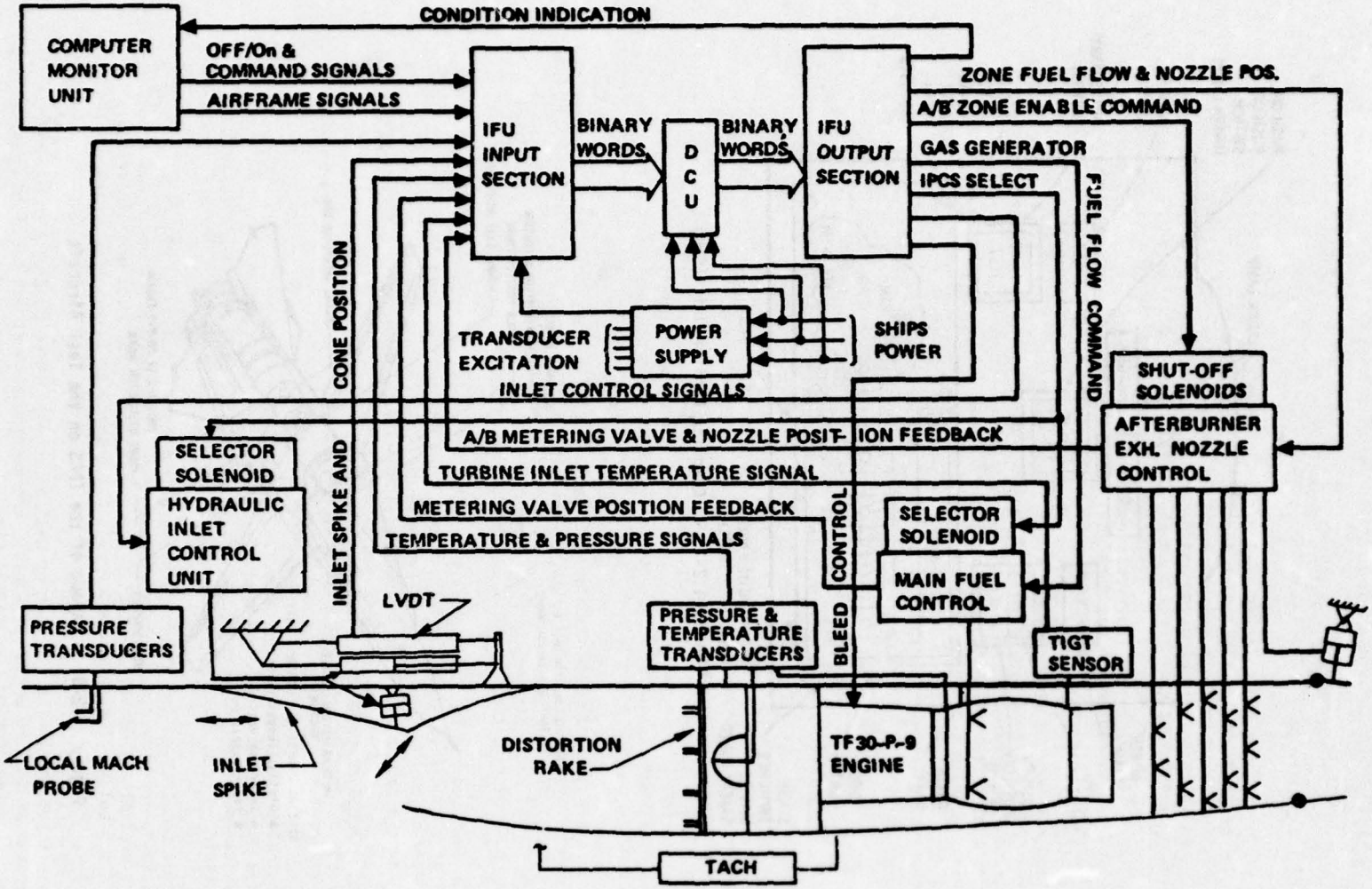

Figure 1.2-1 Integrated System Diagram

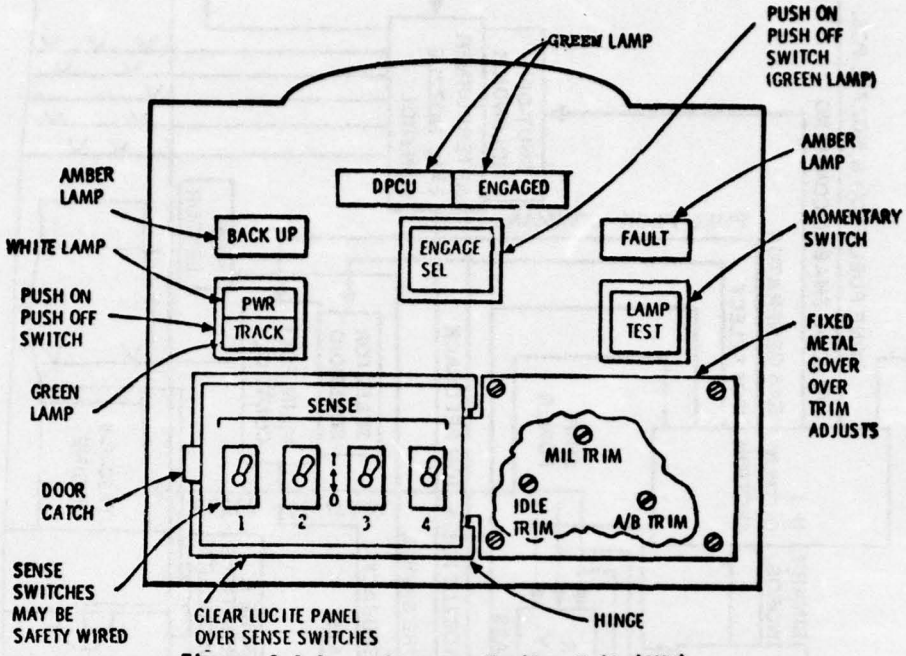

Figure 1.2-2 Computer Monitor Unit (CMU)

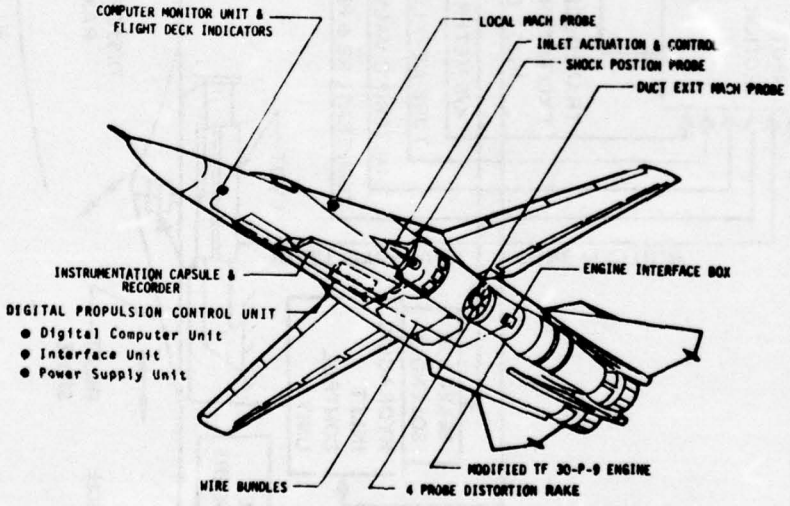

Figure 1.2-3 Layout of the IPCS on the Test Aircraft

Table 1.2-1

Input/Output Capability of the Interface Unit

INPUT:	
Low-level analog (30 mv)	32 channels
High-level analog (5.12 volt)	32 channels
16-bit discrete word	1
Resolver signal processing	8 channels*
Frequency output pressure transducer	8 channels*
Tachometer	2 channel*
TIGT sensor	1 channel*
LVDT (converted to analog)	5 channels
OUTPUT:	
Analog (±10.24 volts dc)	16 channels
Torque motor drivers (amplify D/A output)	3 channels
Stepper motor drives (from DIO)	6 channels
16-bit discrete words	3 channels
PCM interface	59 words

*Direct conversion from frequency signal to digital word.

1.2.2 Control Modes

The IPCS engine could be operated in any one of three control modes; hydromechanical, under computer control using a digital representation of the bill-of-materials controller (BOMDIG), or under computer control using software (IPCS) that implemented the advanced technical features listed in Table 1.0-1.

The hydromechanical mode employed the bill-of-materials unit that was retained for the gas generator only. This control mode was used both for a back-up in case of computer failure and as a baseline to evaluate the performance of the digital system.

The BOMDIG program incorporated the same schedules, setpoints, and logic that the hydromechanical controller was designed to implement. No attempt was made to simulate the dynamics of the hardware components or the hysteresis, deadbands, stiction or other idiosyncracies of mechanical devices.

The IPCS software program implemented the control laws that are discussed in Section 2.3 of this document. A continuing effort was made during software development to achieve maximum commonality between the two programs. Commonality was pursued in the area of DCU self test, transducer signal conditioning, actuator command processing, etc.

1.2.3 Ground Support Hardware

Ground support equipment (GSE) was provided to service and test the flight hardware and to communicate with the DCU. The GSE consisted of a Test Set Unit (TSU) and an ASR-35 teletypewriter (TTY), associated software, and interconnections. The TSU was a rack-mounted system consisting of a computer control unit (CCU), a high speed paper tape reader a paper tape punch, a duplicate of the CMU that was mounted in the cockpit, a DVM, displays, and specialized simulation and test circuitry.

The TSU could be used to check out the IFU and DCU when these components were disconnected from the engine installation. Steady-state and sinusoidal perturbations of sensor outputs for selected engine operating conditions could be presented to the IFU input. The IFU outputs could be monitored at test jacks on the TSU front panel.

The TSU also incorporated a recorder monitor panel that simulated the NASA PCM data system. This feature made it possible to display on-line and in realtime, any one of fifty-nine preselected words directly from the computer memory. Any variable that was assigned a permanent location in memory could be selected for display. This capability was extremely useful during ground-test operations.

1.3 TEST PROGRAM

A sequence of hardware tests was conducted to evaluate the IPCS. This series progressed from baseline evaluation of the bill-of-materials system in a low risk, step-by-step manner through flight evaluation of the IPCS. The test flow is diagrammed in Figure 1.3-1. This test program provided high confidence of success at each phase due to the gradually increasing complexity of the tests.

Hardware components were subjected to flight assurance tests under the appropriate government specifications. The software was loaded into the control computer at Honeywell and checked out using a real-time engine simulation to close the loop. The Digital Propulsion Control Unit (DPCU) met the modified engine fuel controls for the first time at a closed-loop bench test at the P&WA facility. Again a real-time engine simulation was used to close the loop.

A series of three ground tests with the engine run under DPCU control followed; a sea-level static test at P&WA, an altitude test at NASA/LeRC, and a ground test, with the engine installed in the aircraft at NASA/FRC. These tests provided further flight assurance and verified hardware and software compatibility. They provided the means for refining the control modes and software and bringing them to maturity.

The system-level test points are shown on Figure 1.3-2, which also shows the operating envelope of the TF30-P-9 engines as modified for the IPCS program. The philosophy was to operate along lines of constant Reynolds index and to limit the maximum engine operating pressure, thereby reducing structural loads on engine components and restricting the range of operation of the pressure sensors.

1.3.1 Baseline Tests

Baseline engine and flight tests were designed to document the performance of the F-111E/ TF30-P-9 system prior to the IPCS modifications. During the baseline engine test the two engines to be modified for IPCS were tested over a range of flight conditions to establish steady-state and transient performance and distortion tolerance. Data from the test have been analyzed and used to update the dynamic simulation. The baseline flight test provided similar data for the airplane and inlet.

The Distortion Computer shown in Figure 1.3-3 with its test set was a useful asset to the baseline tests. *The computer is installed in the instrumentation* package in the airplane and computes KD2 in-flight. The distortion level is thus known to the pilots via a cockpit guage and to the engineers via telemetered data, permitting exploration of the operating limits of the propulsion system.

The baseline test program is discussed in Section 5.0 of this document.

1.3.2 Subsystem Tests

Individual component performance and physical integrity were demonstrated, where necessary, through component and subsystem test. Individual components were subject to environmental tests, temperature cycling and vibration in particular, as required by the NASA specification 21-2. The DPCU hardware and software were thoroughly checked out prior to shipment from the Honeywell facility as indicated earlier.

The control software was loaded into the HDC-601 flight computer and tested in real time with the loop closed by the hybrid simulation. The flight conditions explored were sea level static and three Mach numbers at 45,000 feet: 0.9, 1.6, and 2.1. A full complement of power transients was executed. Typical flight disturbances were presented to the system. The effect of transducer failure was evaluated by disconnecting the signal lines to simulate failure. This extensive in-house test program drastically reduced the number of "bugs" encountered during subsequent system-level testing and thereby effected significant savings in both cost and calendar time.

1.3.3 Closed-Loop Bench Test

A comprehensive closed-loop bench test followed the component tests, References 2 and 3. The TF30 fuel control, modified to incorporate electrical interfaces, was installed in the P&WA fuel bench test facility. The flight DPCU was connected to the fuel control through electrical cables of length chosen to simulate the aircraft installation. The inlet

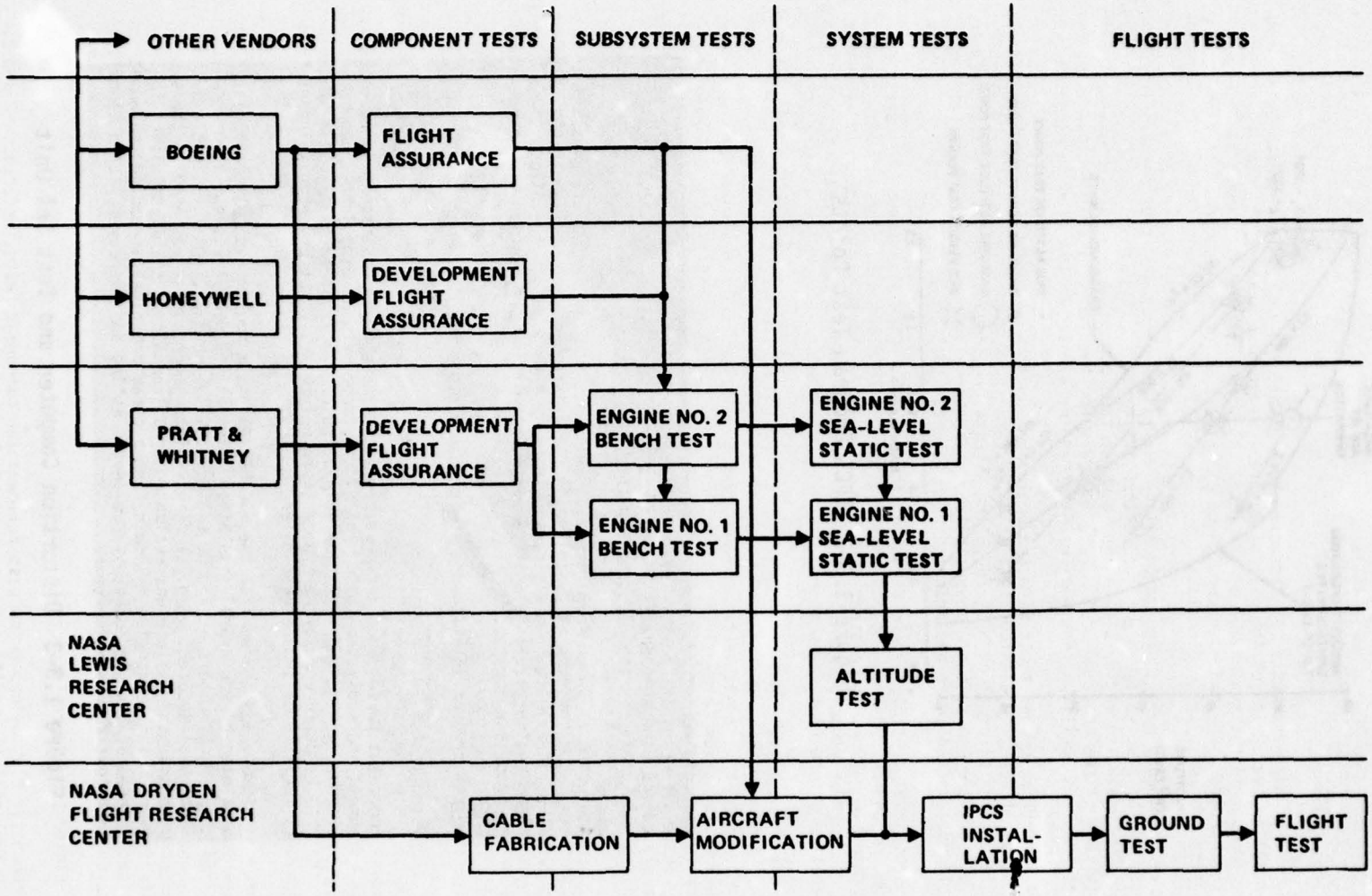

Figure 1.3-1 Test Flow

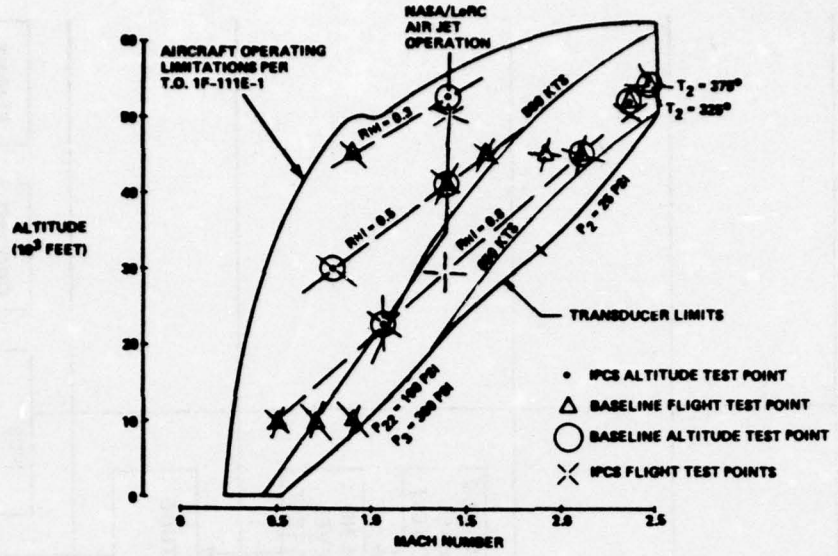

Figure 1.3-2 IPCS Program Test Points

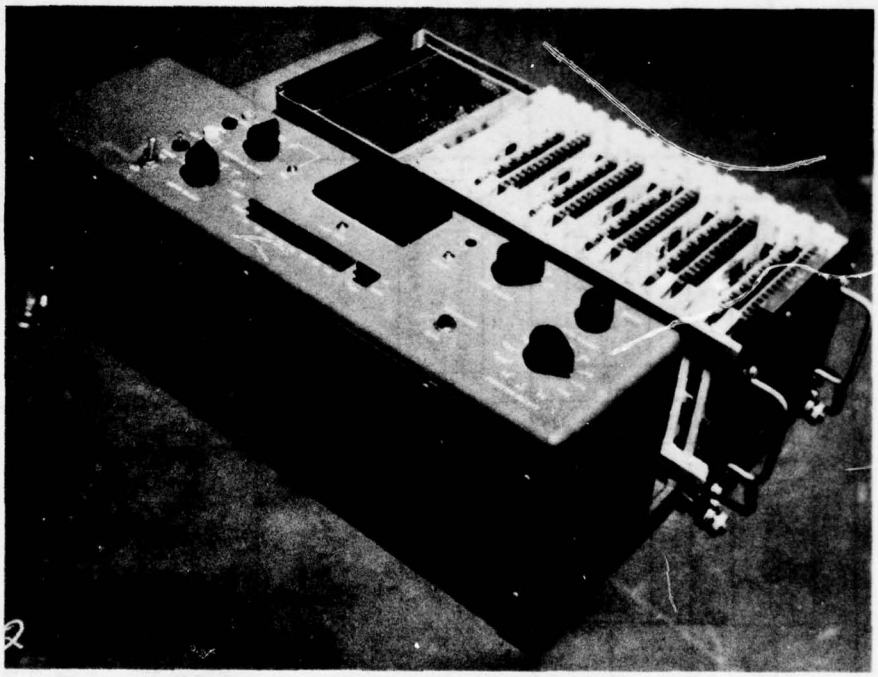

Figure 1.3-3 Distortion Computer and Test Set Unit

1.3.3 Closed-Loop Bench Test (Continued)

actuators, with their position feedback transducers, were installed in a jig, supplied with hydraulic power, and connected to the DPCU. Analog simulations of the engine and the inlet aerodynamics were provided to close the loops and generate the signals that would be sensed by transducers in the aircraft. In some cases, simulation interface adapters were provided to simulate the transducer output format. This test provided a functional check out of the modified fuel control unit and established compatibility between the DPCU, with its software and the engine and inlet control hardware. The closed-loop bench test is discussed in Section 6.0 of this document.

1.3.4 Sea-Level Static Test

The sea level static (SLS) test was conducted at the P&WA facility in East Hartford, Connecticut. (References 4 & 5.) The modified fuel controls were installed on the TF30-P-9 engines that also had been modified for the IPCS program. The principal objectives of the test were to verify the structural integrity of the engine and fuel system modifications and to evaluate and refine the IPCS control modes and software with actual engine hardware. A total of 98 hours running time was accumulated on the two engines during the test. Most of this time was spent under DPCU control.

Evaluation of system operation indicated that performance of the IPCS components in the sea level engine environment was consistent with design objectives. The DPCU software and the control modes implemented in the software for both BOMDIG and IPCS exhibited several anomalies relative to design operational requirements. These anomalies were corrected through Software Field Change Orders (SFCO) during the engine testing and then retested to demonstrate acceptable engine operation.

Satisfactory completion of 98 hours of steady state and transient testing, and satisfactory periodic inspections of engine hardware and IPCS probes provided assurance of the structural integrity of the engine modifications, and they were judged acceptable for further testing at NASA/LeRC and NASA/FRC. The concluding acceptance test run on both engines per T.O. documented acceptable engine performance on both engines with no deviations.

1.3.5 Altitude Facility Test

The investigations begun at the SLS test were continued and greatly expanded at the altitude test conducted at NASA/LeRC. The objective of the test was to demonstrate that the IPCS hardware, control modes, and software were flight worthy and that the system was ready to proceed to the flight test phase of the program. A comprehensive set of steady-state and transient events was performed. These included accels, decels, bodies, DPCU engage and disengage events, and operation of the facility "puff-jets" to simulate inlet distortion and buzz. Two hundred forty three operating hours and seventy nine stalls were accumulated on the engine during the altitude test program.

The altitude test is discussed in detail in Section 8.0 of this document and in references 6 & 7.

1.3.6 Flight Evaluation of the IPCS

The final checkout of the IPCS system was the flight evaluation test series conducted at NASA/DFRC. The DPCU and a TF30-P-9 engine modified for the IPCS program were installed in a F-111E aircraft. The objectives of the tests were to demonstrate hardware capability and to evaluate operation of IPCS control modes and hardware in an actual F-111E aircraft flight environment. The flight tests also provided the first opportunity for evaluation of the inlet buzz detector and closed-loop control on sensed inlet distortion in a realistic environment.

A full set of steady-state and transient engine events (accels, decels, bodies, DPCU engage and disengage events, etc) were conducted at all test conditions shown in Figure 1.3-2. Operation of the IPCS system was also demonstrated for steady-state and transient aircraft events (accels, decels, angle-of-attack pull ups, etc.). Seventy-seven operating hours were accumulated on the engine during thirty five ground runs and fifteen flights.

The flight evaluation of the IPCS is discussed in detail in Volume III "Flight Test Report.

2.0 ANALYTICAL TASKS

The analysis performed under the IPCS contract supported the hardware and software design tasks as diagrammed in Figure 2.0-1. Preliminary exploration of the new control modes to be implemented was performed prior to contract; these new control modes are listed in Table 2.0-1. The data required for detail control mode design were identified during these preliminary studies or very early in the contract period.

Work began immediately after contract on three key tasks shown in Figure 1.0-3. System Definition Documentation (Task I-A), Preliminary Control Mode Design (Task I-C), and Preliminary Hardware Selection & Design (Task I-D). The development and refinement of dynamic simulations (Task I-B) was initiated approximately 30 days after contract.

The analytical tasks, Tasks I-A, I-B, and I-C are described in this section. The hardware design effort is described in Section 3.0.

2.1 SYSTEM DEFINITION

The development of propulsion system baseline data was required to supply the empirical portions of the dynamic simulations needed for control analysis and to provide comparative performance data for the subsequent IPCS controls evaluation testing. The data were obtained from two major sources; existing F-111E/TF30-P-9 performance data and the baseline testing of the IPCS aircraft and engines conducted by the Government in support of the IPCS program.

2.1.1 Compilation of Existing Data

A thorough search of published data was conducted to compile information relevant to the F-111E/TF30-P-9 configuration. In addition, previously unpublished data from sources internal to P&WA and General Dynamics were obtained under subcontract and screened for relevant information. While the information thus obtained was very useful in developing the dynamic simulations required for controls analysis, it was determined that adequate data did not exist in several areas. Most notable of these were inlet distortion and shock position measurement, and the performance and distortion tolerance of the TF30-P-9 engines to be used in the IPCS program. Therefore, it was decided that a series of baseline tests would be conducted on the unmodified airplane and engines to obtain the needed data. The test conditions for the flight and the engine altitude tests were chosen to match those planned for the IPCS evaluation tests to provide direct correlation of data. See Figure 1.3-2.

2.1.2 Baseline Engine Test

The baseline engine tests were conducted at NASA/LeRC from September 1973 to February 1974. A total of 115.5 hours of testing was conducted on engine S/N 676629 with an additional 49.7 hours of testing on engine S/N 676627.

The data compiled from these tests substantially increased the engine data base available to the IPCS program. Test results have defined steady state and transient operating characteristics for both the primary and backup engines at seven flight conditions, four compressor bleed settings, and three exhaust nozzle configurations. In addition, tests with the NASA distortion generator established the distortion tolerance levels of both engines.

Test results such as those shown in Figure 2.1-1 were used to refine the TF30-P-9 dynamic simulation and thus improve the accuracy of the IPCS control mode and scheduling studies.

2.1.3 Baseline Flight Test

The baseline flight testing on the unmodified F-111E was initiated on 9 October 1974, and completed on 17 January 1975. A total of ten flight tests were conducted by NASA/FRC with the primary goals being to obtain adequate high response inlet data, examine the adequacy of the shock position sensor, and to establish a data base for subsequent IPCS testing. All test objectives were achieved. Although it was decided not to incorporate the shock position sensor as an IPCS control signal, the test data verified that the shock probe operated as expected. The tests showed that it is feasible to measure a shock position parameter using a single transducer. This could have possible future application to in-flight optimization of installed propulsion performance through closed loop control of shock position and, thus, spillage drag.

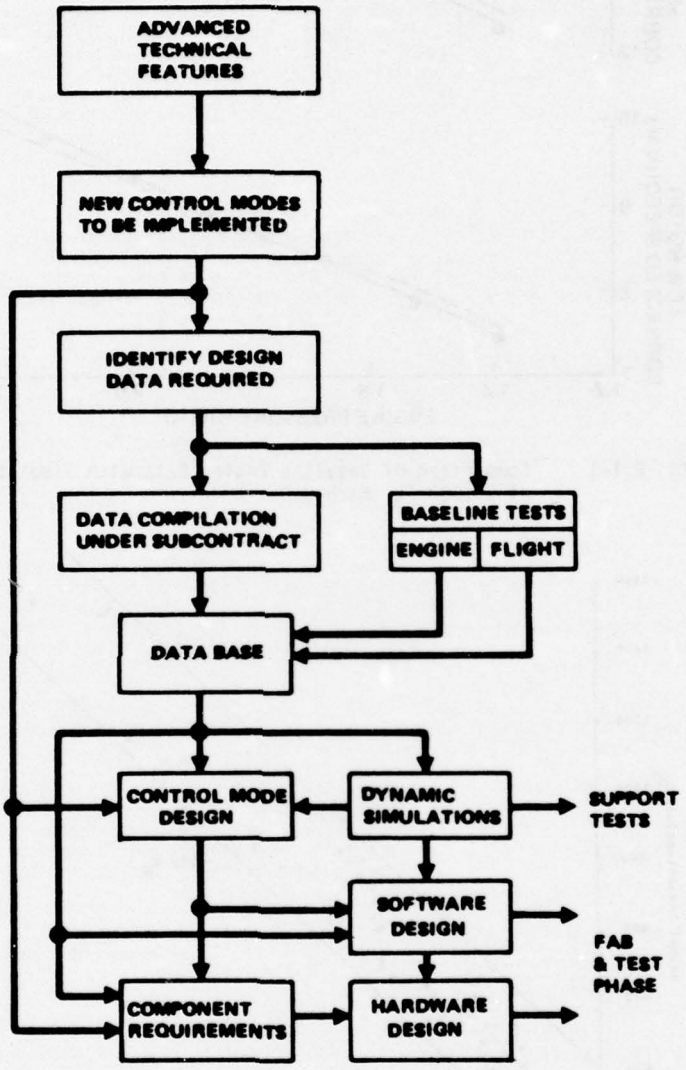

Figure 2.0-1 Analytical Design Approach

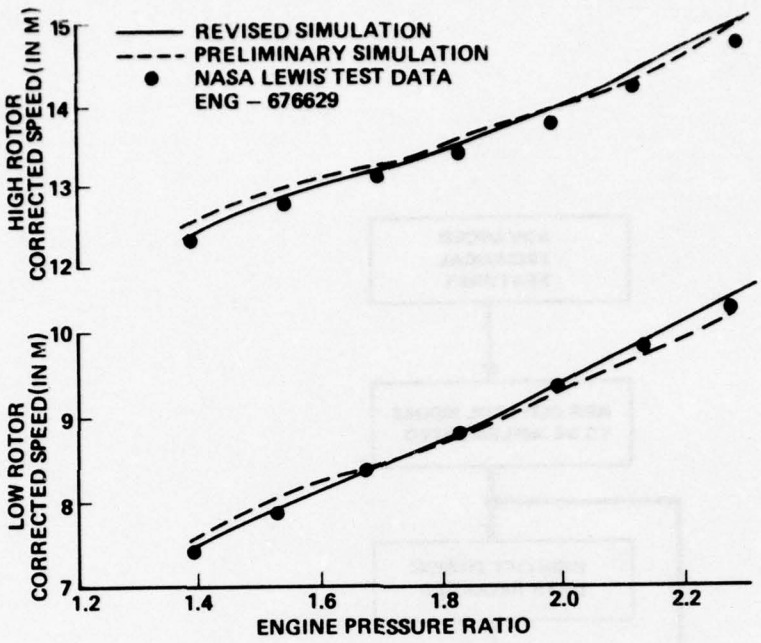

Figure 2.1-1 Comparison of Baseline Engine Data with Simulation at 30,000 Ft, Mach 0.8

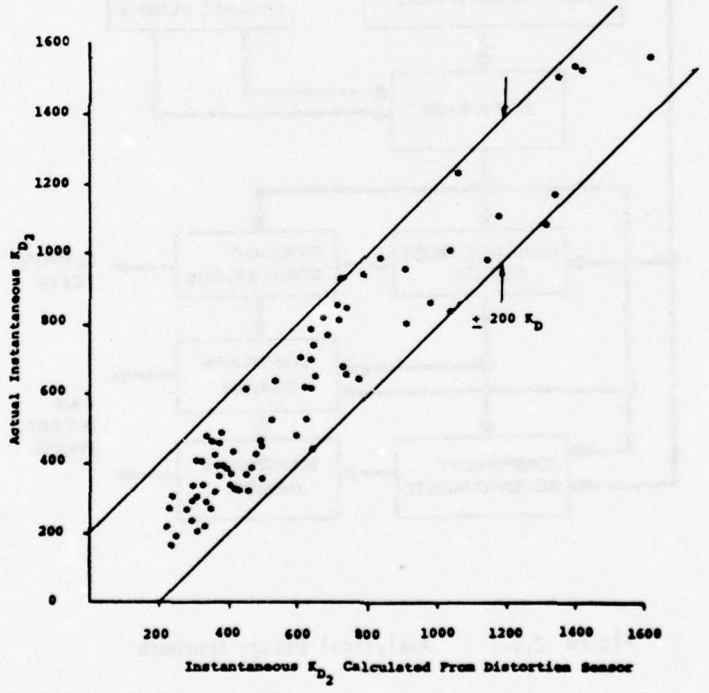

Figure 2.1-2 Correlation of Distortion Sensor Output with Instantaneous Distortion

2.1.3 Baseline Flight Test (Continued)

Adequate high response inlet data were obtained to permit evaluation of an instantaneous distortion sensing scheme using five (5) pressure probes located at the compressor face. Results showed that this method of distortion measurement is sufficient for use of the signal as an IPCS control signal, (See Figure 2.1-2). The distortion signal was used to control engine bleeds and thus engine surge margin.

The baseline flight tests generated a large F-111E airframe data base that was used to update and supplement that previously available. The data were used to refine the dynamic simulations and to provide a baseline against which to access the performance of subsequent IPCS testing. In addition, the experience obtained from conducting the baseline tests was valuable in planning and conducting the IPCS flight evaluation tests.

A complete discussion of the baseline flight testing is covered in Section 5.2.

2.2 DYNAMIC SIMULATIONS

Dynamic simulations of the F-111 propulsion systems formed the foundation for the IPCS control system development and software validation. Two types of simulation were generated. The first is an entirely digital simulation developed for use on a large digital computer such as a CDC 6600. P&WA provided that portion of the program that represents engine operation; Boeing provided the simulation of the inlet and airframe effects. The second is a comprehensive hybrid simulation, based on the digital simulation, that was developed by Honeywell.

The simulations incorporated much of the system definition data discussed in para 2.1 above and hence formed a compact and convenient repository for masses of information. Linear state models extracted from the digital simulation were used to study control system stability and response. The digital simulation was the principal test bed for evaluating new control modes. The hybrid simulation was used to evaluate the response of the system to selected failures and to check out both the digital propulsion control unit (DPCU) and its software prior to shipment.

2.2.1 Digital Simulation

The digital simulation employs the SOAPP system developed by P&WA. With this modular system, most of the simulation is created from routines drawn from the SOAPP library. This library is a major reason for the development of SOAPP. It forms a repository for up-to-date versions of those utility routines that determine the speed and accuracy of the simulation.

The SOAPP program generates both steady-state and transient engine performance data. This feature is made possible by the application of a technique called SMITE, originally conceived by the Air Force Aero Propulsion Laboratory. It uses the solution to a set of linearized adjunct equations to obtain an iterative solution to the complex non-linear equations in the simulation. Steady-state solutions are obtained merely by setting all the temporal derivatives to zero. The simulation was adjusted periodically, as data became available, to improve its fidelity. Figure 2.1-2 illustrated the simulation adjustment. Data generated by the digital program are compared to corresponding baseline engine test data obtained at NASA/LeRC. Adjustment improved the fidelity of the simulation significantly.

The inlet simulation developed by Boeing for the IPCS program is a lumped mass, one-dimensional flow representation of the F-111 inlet. A block diagram of the inlet simulation is shown in Figure 2.2-1. Given time-dependent free-stream conditions (Mach number, ambient temperature, pressure, and airplane angle of attack) and engine corrected weight flow, the inlet simulation program will calculate the engine face total pressure (P2), inlet control signals, surface positions, and a distortion index (KD). The inlet control signals are the pressure ratios for the local Mach number (PRLM) and duct exit Mach number (PRDEM). The surface positions are the cone angle (θ2) and the spike translation ratio (X/R).

No attempt was made to simulate abnormal operating conditions (e.g., buzz, stall, afterburner rumble). This did not present any handicap during the control design process. These conditions are not encountered in practice if the control is operating properly and steady-state operation in such a situation is neither desirable nor necessary. It is desirable, however, to delineate the normal system operating boundaries and provide a gross representation of certain system variables if control action is required for recovery. The inlet buzz detector falls into this category. Figure 2.2-2 shows how the buzz signal was generated in the simulation.

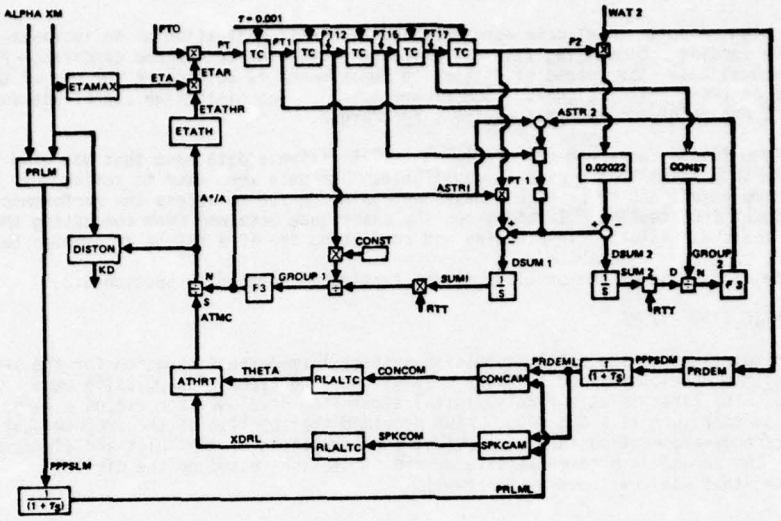

Figure 2.2-1 Boeing Inlet Simulation

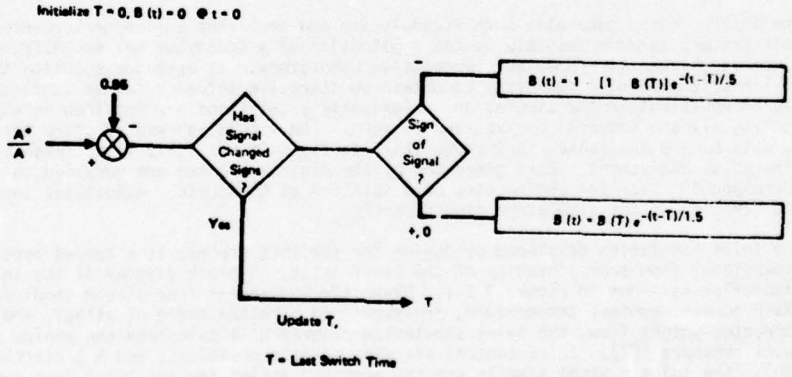

Figure 2.2-2 Buzz Signal Simulation

2.2.2 Hybrid Simulation

The hybrid simulation of the propulsion system prepared by Honeywell used two 781 EAI analog computers, two 231R EAI analog computers, a PACER 16K digital computer, and a SIGMA 5 40K digital computer. The PACER was used solely for generating bivariate functions, for on-line analysis, and for problem setup. The Σ5 computer was used to generate the control functions and to drive a scope display. The system was designed to run ten times slower than real time when under control of the Σ5.

The principal functions of the hybrid simulation are listed in Table 2.2-1.

The results of typical sample rate studies are shown in Figure 2.2-3. These studies confirmed that the sampling period of 30 milliseconds that had been tentatively selected would provide satisfactory performance and that there was no incentive to accept the cost and risk associated with a shorter sampling period.

Checkout of the DPCU hardware and software was done by replacing the Σ5 by the HDC 601 flight computer with its interface unit (IFU). A custom built simulation interface adapter (SIA) conditioned signals from the analog computers to simulate the outputs from the flight transducers. In this service, the simulation ran in real time. All time-dependent functions were performed in the 781 EAI computers to facilitate time scale switching.

2.3 CONTROL MODES

Aircraft mission capability hinges upon the characteristics of the propulsion system in two areas:

1. Steady-state performance; which may be defined as the ability to deliver the most thrust per pound of fuel, airflow, engine weight, etc.
2. Transient performance or system responsiveness to required thrust changes; this may be expanded to include propulsion system stability and tolerance to changes in the operating environment.

One way to increase steady-state performance is to sacrifice operational stability so that pressure ratios and stage loadings can be increased further. This, of course, infringes on the second area because safe, reliable operation during engine transients requires that the current stability margins be maintained.

The goal in the selection and design of the IPCS control modes was to maximize steady-state and transient performance without compromising engine/inlet stability. To achieve this goal, an extensive control mode design task was performed to integrate the control of the inlet, gas generator, and afterburner.

This work was divided into two general categories or sub tasks: control mode identification and loop design. Control mode identification consisted of selecting the signals required to implement each technical feature, the logic and timing relationships, and developing the block diagrams that define the information flow from the sensors to the actuators. Loop design consisted of selecting gains, compensation, and switching logic.

These two subtasks were carried out concurrently and, to a great extent, by the same personnel The lines of demarkation between these tasks, the software design and checkout, and system-level tests were indistinct and, in many cases, indistinguishable.

An overview of the control mode design effort is given in the paragraphs below.

2.3.1 Control Mode Identification

The first step in the design and development of the IPCS controller was the selection of critical engine parameters and control modes. Several advanced technical features, listed in Table 1.0-1 were tested for the first time. The propulsion system variables over which the DPCU had control were:

a) Gas generator fuel flow
b) Compressor bleeds - 7th and 12th stage
c) Afterburner fuel flow
d) Exhaust nozzle area

TABLE 2.2-1 HYBRID COMPUTER SYSTEM STUDIES

SAMPLE RATE STUDIES
CONTROL BLOCK DIAGRAM CONFIRMATION
CONTROL INSENSITIVITY TO MODEL
COMPONENT FAILURES
NOISE SENSITIVITY
DIGITAL FILTER DESIGN
STABILITY STUDIES
SOFTWARE CHECKOUT
DPCU HARDWARE CHECKOUT

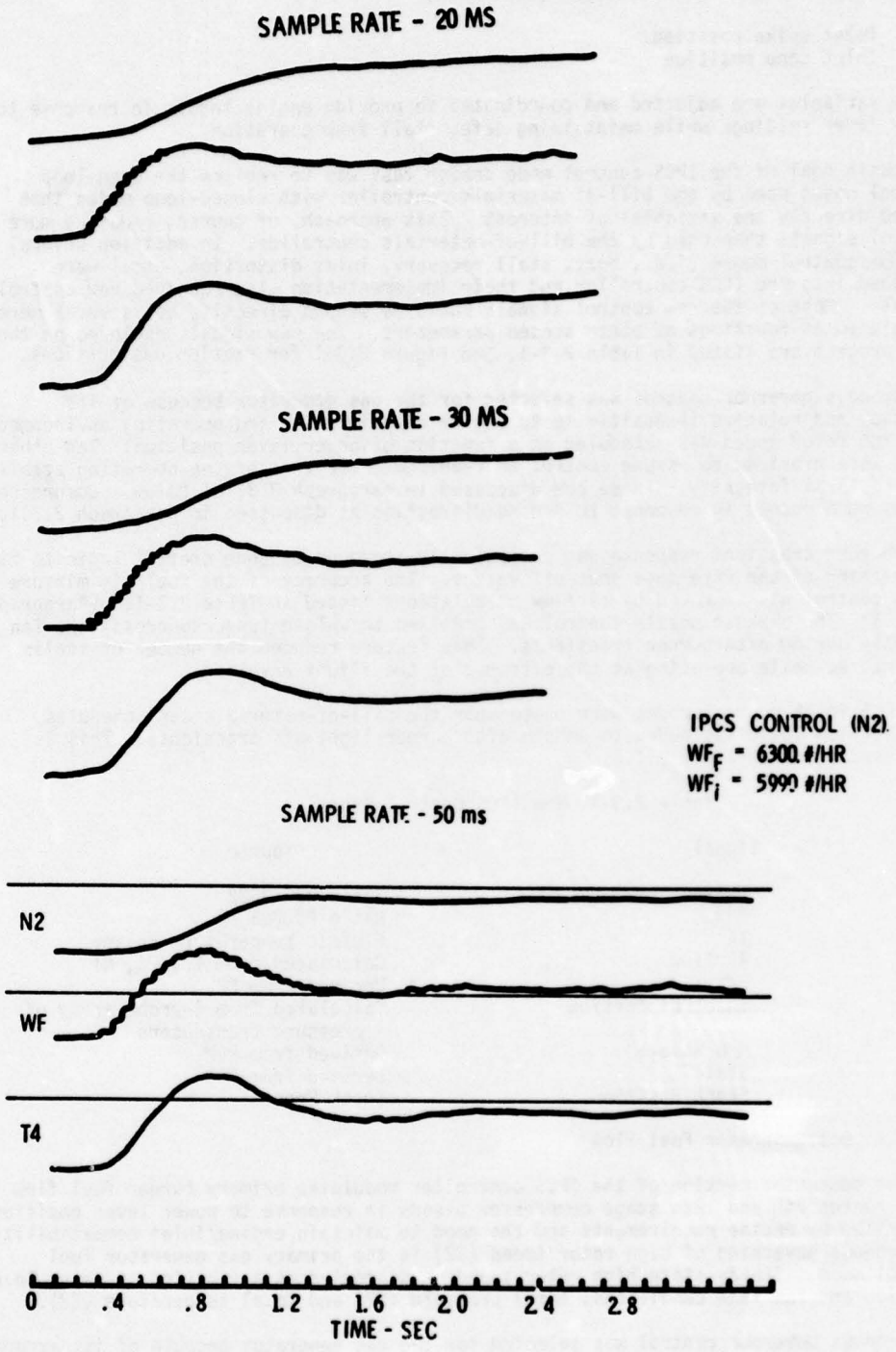

Figure 2.2-3 Sample Rate Studies

2.3.1 Control Mode Identification (Continued)

e) Inlet spike position
f) Inlet cone position

These variables are adjusted and coordinated to provide engine thrust in response to power lever settings while maintaining safe, stall free operation.

The basic goal of the IPCS control mode design task was to replace the open-loop control modes used by the bill-of-materials controller with closed-loop modes that sensed directly the variables of interest. This approach, of course, required more control signals than used by the bill-of-materials controller. In addition several advanced control modes (i.e., buzz, stall recovery, inlet distortion, etc.) were designed into the IPCS controller and their implementation also required new control signals. Most of the new control signals could be sensed directly, but several were calculated as functions of other sensed parameters. The new signals explored on the IPCS program are listed in Table 2.3-1. See Figure 2.3-1 for station designations.

Isochronous governor control was selected for the gas generator because of its accuracy and relative insensitivity to engine deterioration and operating environment; the high rotor speed was scheduled as a function of power lever position. Ten other loops were provided to assume control as required to protect engine operating stability or structural integrity. These are discussed in paragraph 2.3.1.1 below. Compressor bleeds were opened in response to sensed distortion as discussed in paragraph 2.3.1.2

Afterburner transient response was dramatically improved by zone prefill logic to time the opening of the five zone shut-off valves. The accuracy of the fuel/air mixture ratio control was improved by airflow calculations listed in Table 2.3-1. (Paragraph 2.3.1.3) The exhaust nozzle control was modified to unload (undersuppress) the fan slightly during afterburner transients. This feature reduced the number of stalls encountered while operating at the extremes of the flight envelope.

The IPCS inlet control modes were based upon the bill-of-materials cam schedules. Anticipation logic was added to smooth afterburner light-off transients. This is discussed in paragraph 2.3.1.5.

Table 2.3-1 New IPCS Control Signals

Signal	Source
MN22	Ratio P22/PS22
MN3	Ratio P3/PS3
T4	Fluidic temperature sensor
Airflow	Calculated from T2, P2, N1
Buzz	Derived from P2
Inlet Distortion	Calculated from 4-probe array of pressure transducers
A/B Rumble	Derived from P6M
Stall	Derived from PS3
Shock Position	Shock Probe

2.3.1.1 Gas Generator Fuel Flow

The gas generator portion of the IPCS controller modulates primary burner fuel flow and actuates 7th and 12th stage compressor bleeds in response to power lever position, as limited by engine requirements and the need to maintain engine/inlet compatibility. Isochronous governing of high rotor speed (N2) is the primary gas generator fuel control mode. Steady-state high rotor speed is scheduled as a function of power lever position and fan face conditions; total pressure (P2) and total temperature (T2).

Isochronous governor control was selected for the gas generator because of its accuracy and relative insensitivity to engine deterioration and operating environment. Isochronous control holds thrust more nearly constant during bleed and shaft power extraction than does droop control and it also provides better thrust response during part power excursions.

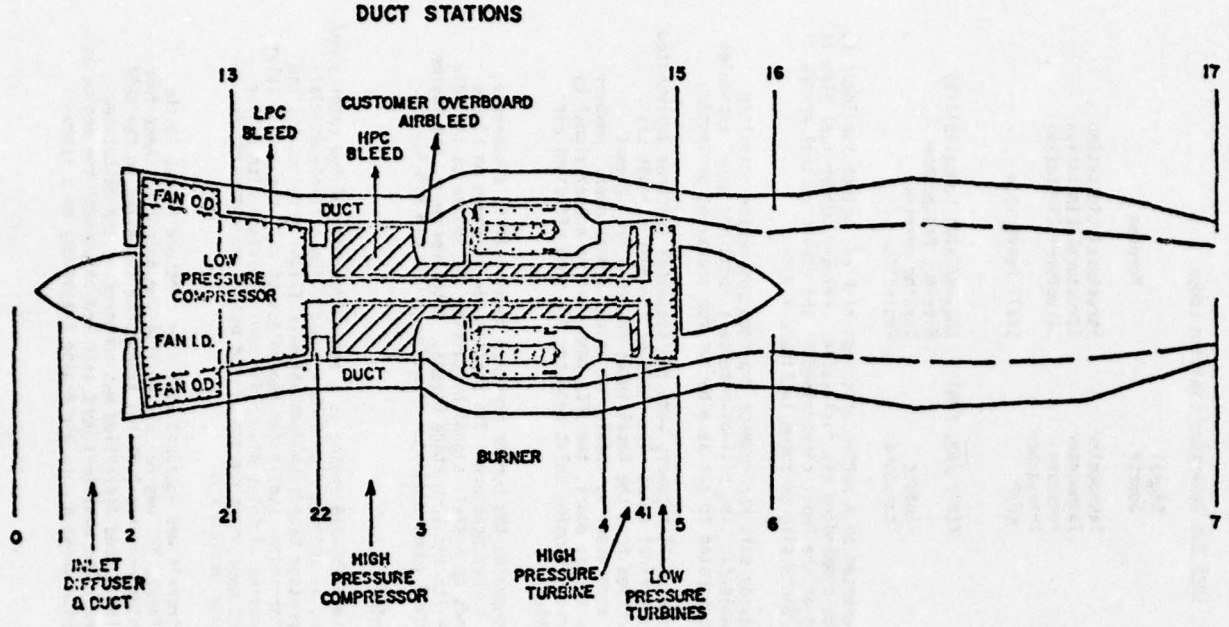

Figure 2.3-1 Station Identification

2.3.1.1 Gas Generator Fuel Flow (Continued)

Ten limiting loops are provided to override the N2 loop when required to protect engine integrity or operating stability. The IPCS design approach was to provide direct measurement of critical parameters to maintain the limits. Those parameters which are not directly measureable with existing technology have been synthesized to permit direct comparison with the limiting value. The limiting variables are listed in Table 2.3-2.

Table 2.3-2 IPCS Gas Generator Limiting Loops

Limited Variable	Signal Source	Purpose
Low Rotor Speed	Tachometer	Structural Limitation
High Rotor Speed	Tachometer	Structural Limitation
Burner Pressure	Pressure Transducer	Structural Limitation
Compressor Exit Mach No.	$\Delta P/P$	Stall Prevention
Airflow	$f(N1/\sqrt{\theta 2}, EPR)$	Engine/Inlet Compatibility
Fuel/Air Ratio		Blow-out Protection
Turbine Inlet Temperature	Fluidic Transducer	Turbine Overtemp Protection

The limiting loops were implemented by a series of select high and select low logic to determine which loop should be commanding the fuel valve. Primary burner fuel flow is determined by the integration of the least constrained of the eleven control errors indicated on the generalized block diagram shown in Figure 2.3-2.

Closed-loop control of compressor exit Mach number provided compressor stability protection during engine transients. The bill-of-materials accel and decel schedules based on Wf/Pb were also incorporated to act as a backup for transient protection.

Inlet buzz and automatic engine stall recovery were two technical features implemented in an engine controller for the first time. Operation of the buzz circuit was continuous with the signal derived from the total inlet pressure (P2) signal. Normally inlet buzz would be suppressed by opening an inlet bypass door. However, since the F-111 does not have bypass doors, the IPCS responded to a buzz signal by accelerating the engine and repositioning inlet geometry for more efficient air spillage as rapidly as possible.

Engine stall was sensed by comparing the burner pressure decay rate to a schedule, FSTLL, that is a function of burner pressure. The stall logic is shown on Figure 2.3-3. The controller responds to a stall signal by setting the engine to the idle power setting and opening the 7th and 12th stage bleeds. After recovery, the engine was accelerated to its pre-stall power setting. (See Vol. III, para 6.5.4).

2.3.1.2 Compressor Bleed Control

The distortion tolerance of the TF30-P-9 engine is a strong function of low rotor speed and compressor bleed position, as indicated by Figure 2.3-4. The bill-of-materials controller scheduled the compressor bleeds to open wherever flight test results had shown increased probability for engine stalls and regardless of what the actual inlet distortion was. By direct sensing of inlet distortion and comparison with engine distortion tolerance, the IPCS would open the compressor bleeds only when needed and thus increase propulsion system efficiency.

In operation the IPCS test aircraft was equipped with four pressure probes in the inlet duct. The distortion index, KD, was calculated from the output of these four probes plus the output of a high response (Kulite) transducer installed in the NASA test instrumentation rake. The sensed distortion was compared to the calculated distortion tolerance and bleed valve positions were selected to protect the engine as indicated on Figure 2.3-5, which shows a possible engine trajectory on a speed-distortion tolerance map.

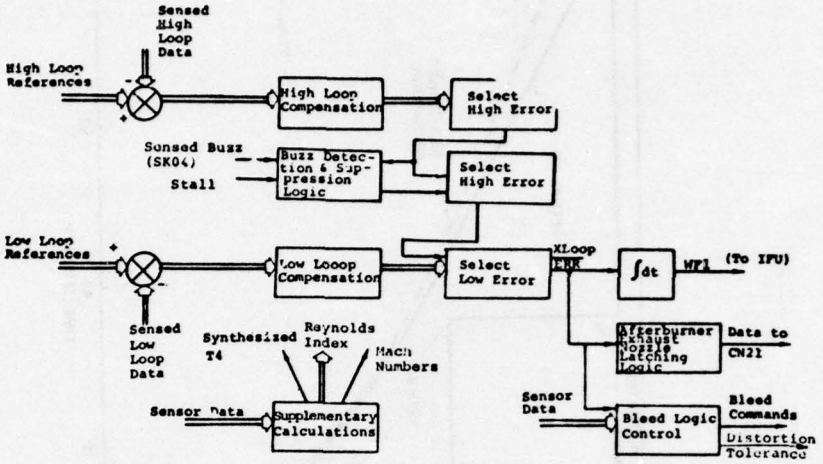

Figure 2.3-2 IPCS Gas Generator Control Block Diagram

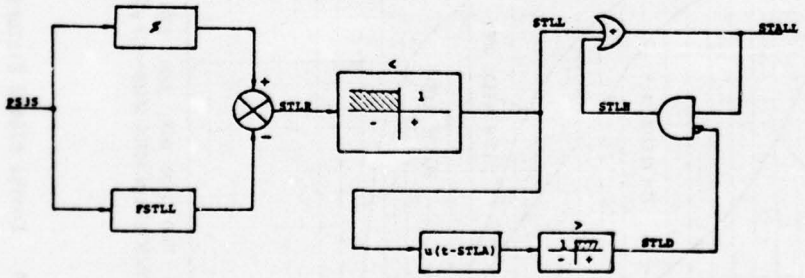

Figure 2.3-3 Stall Logic

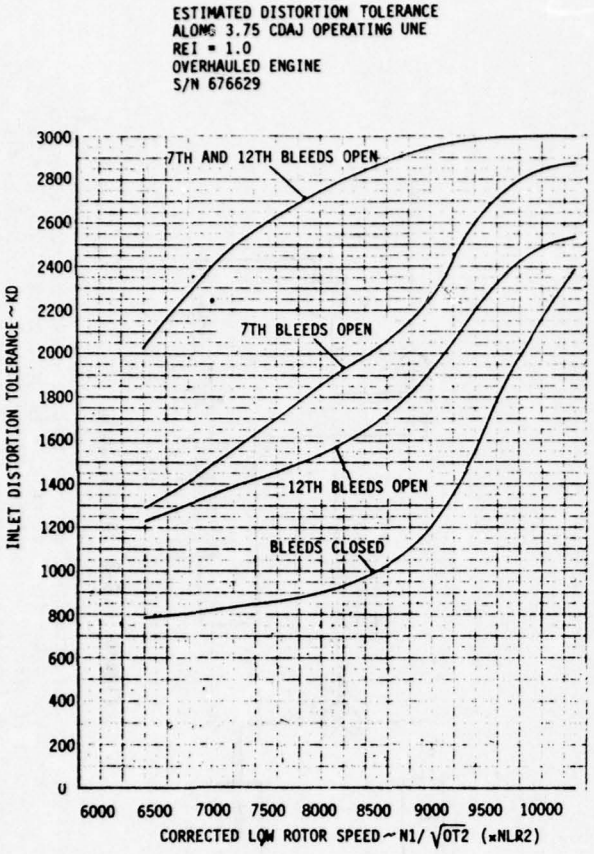

Figure 2.3-4 Engine 676629 Distortion Tolerance

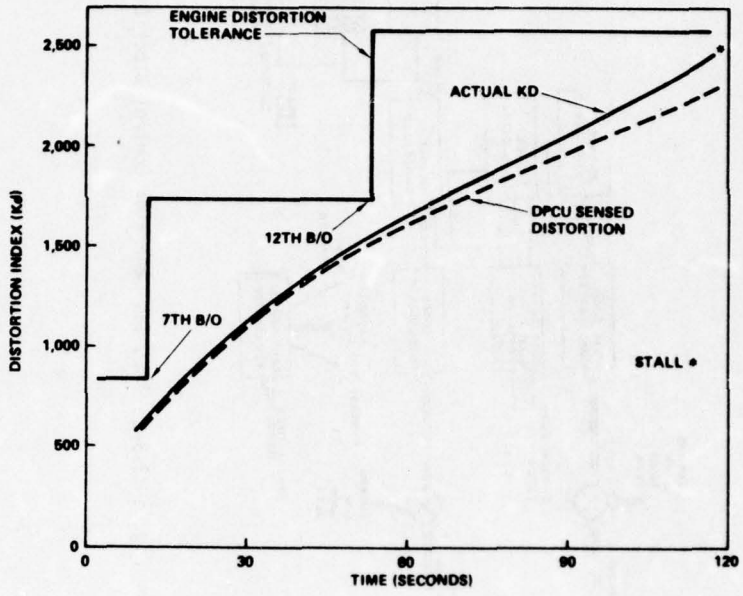

Figure 2.3-5 Compressor Bleed Operation

2.3.1.2 Compressor Bleed Control (Continued)

The correlation between the simplified four-probe parameter and KD computer from the forty-probe rake data was shown in Figure 2.1-2.

The compressor bleeds were also opened during engine deceleration to provide greater stall margin and during part-power operation on the ground to reduce thrust, and hence, brake wear during taxi operations.

2.3.1.3 Afterburner Fuel Control

The IPCS modulated afterburner fuel flow in response to thrust commands as limited by engine requirements and the need to maintain engine inlet compatibility. The design approach was to use direct (or synthesized) measurements to schedule fuel flow and maintain fan suppression limits. The afterburner control block diagram is shown in Figure 2.3-6.

The IPCS scheduled engine-stream and duct-stream afterburner fuel-air ratios as functions of a rate limited PLA. This signal was also used to schedule a base (reference) exhaust nozzle area. Engine stream airflow was calculated as a function of high compressor discharge pressure and temperature (P3, PS3, and T3). Duct stream airflow was obtained from the difference between total calculated airflow and engine stream airflow. Use of airflow calculations improved the accuracy of the fuel/air mixture ratio control.

A significant improvement in response time was obtained by optimizing the timing of the five afterburner zone valves to permit prefilling of the manifolds. Calculation of the zone fill time was performed as a function of a rate limited power lever angle, PLAP. Zone fill time, using flow rates and manifold volumes, determined the value of PLAP at which the zone fill valve was opened. The prefill logic is shown in Figure 2.3-7. Transient performance improvements are discussed under test results in Sections 7.0 and 8.0 of this volume and in Volume III.

2.3.1.4 Exhaust Nozzle Area Control

The rate limited PLA that schedules afterburner fuel air ratio is also used to schedule a nominal exhaust nozzle area. This schedule was set to minimize airflow trim requirements. The schedule was also designed to force the area open faster when fuel is added, and close slower when the fuel is decreased. This provided a fan operating point during A/B transients that was farther away from the stall line, resulting in a slight temporary under-suppression and reducing the number of stalls encountered while operating at the extremes of the flight envelope.

The IPCS fan suppression control for the TF30-P-9 engine used the fan match line as a reference schedule for trimming about the base area setting. An airflow reference was balanced against the airflow correlation measurement to trim area until the fan match was satisfied. If the fan match could not be satisfied due to area being at the maximum limit, trim authority was transferred to the afterburner fuel module. The main fuel module was also biased with a trim signal received from the inlet module to improve the off design engine/inlet airflow match.

2.3.1.5 Inlet Control

A sketch of the F-111 inlet installation is shown in Figure 2.3-8. The controllable aerodynamic surface is the spike, which translates fore and aft. The spike surface consists of two cones; the second cone may be expanded or contracted over the range of 8.5° to 26° included angle.

In the bill-of-materials (BOM) inlet control, both the spike and cone positions are scheduled as functions of local Mach number and duct exit Mach number. The BOM inlet control schedules were retained for the IPCS. They were supplemented by an anticipation function that momentarily resets the surfaces for smoothing the afterburner light-off or shut-down transients. A buzz detector, based on that developed for the supersonic transport was provided. It repositioned the surface for more efficient supersonic air spillage when buzz was sensed as well as sending a signal to the gas generator control as discussed above. Engine/inlet compatibility was enhanced by an airflow loop that shifted both engine and inlet operating points slightly to control the inlet throat Mach number.

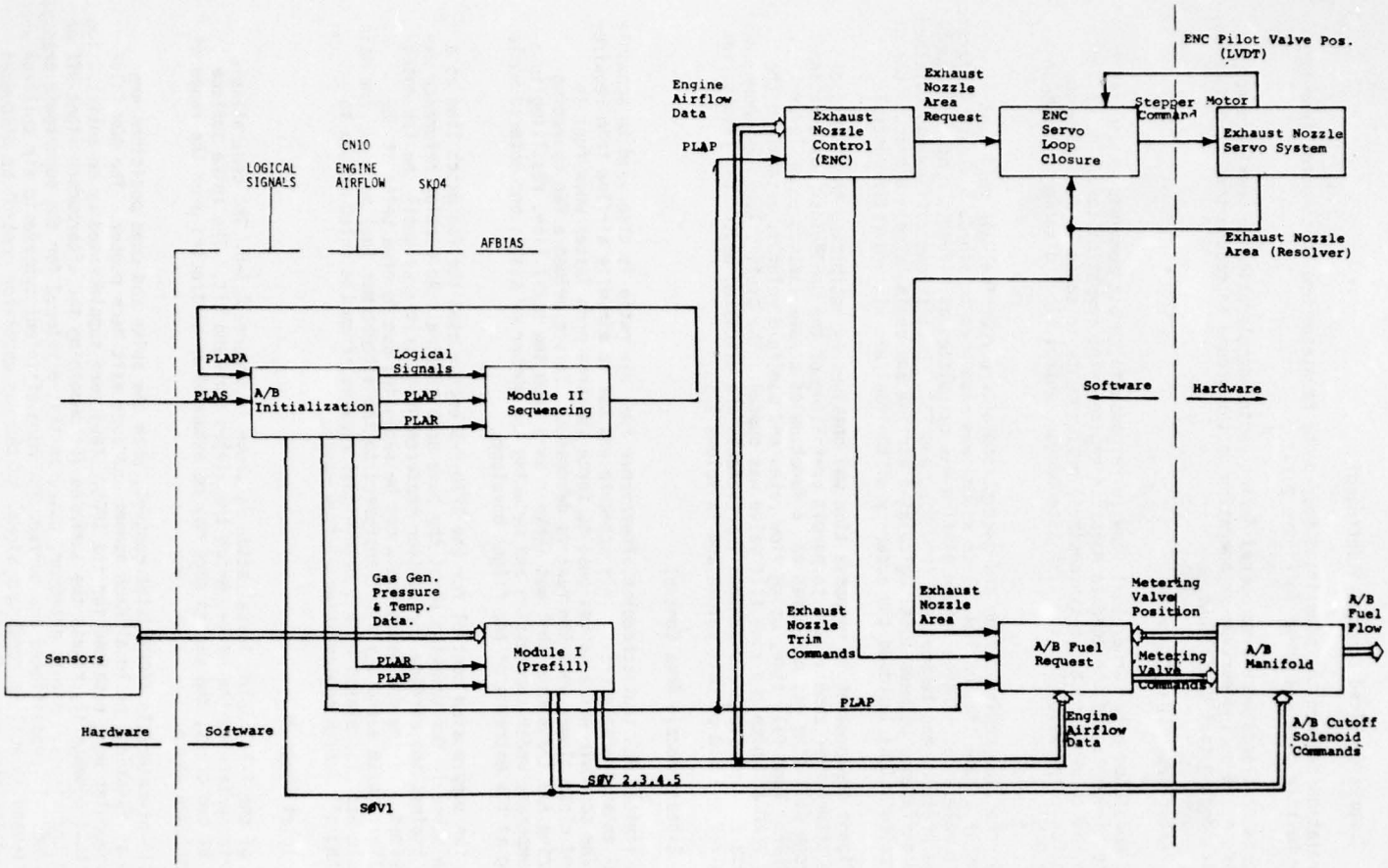

Figure 2.3-6 IPCS Afterburner Control Block Diagram

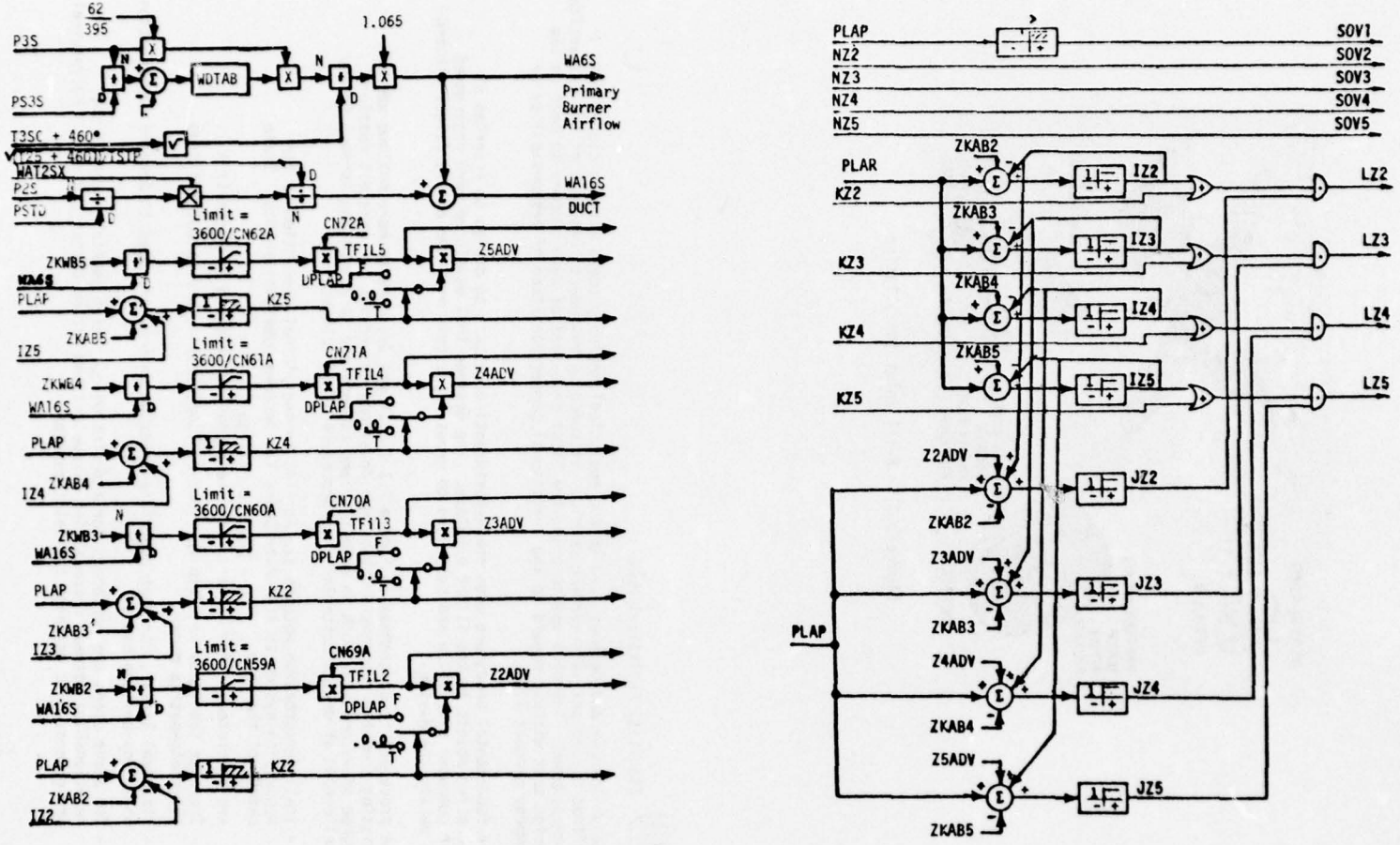

Figure 2.3-7 Afterburner Prefill Logic

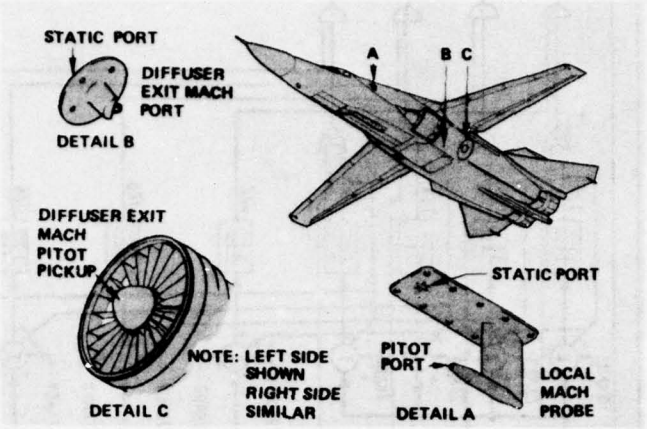

Figure 2.3-8 F-111 Inlet Installation

2.3.2 Stability Analytical Models

The philosophy and methods used in the analytical design process were developed and refined during analysis working sessions attended by engineers from each of the tripartite company teams. The goal was to bring the total resources of each company to bear on the design task without regard to the traditional compartmentation of responsibility by company product line.

The fundamental procedure uses small-perturbation methods to design to a series of operating points in the flight envelope. The designs thus developed were programmed for computer simulation and subjected to gross transients over the entire flight placard to verify the design.

The procedure is diagrammed in Figure 2.3-9. It was designed to make maximum use of existing computer programs and has been developed to provide the greatest feasible degree of automation, both to save time and expense and to assure consistency in the application of design criteria. The procedure is as follows:

- Small-perturbation methods are applied to the digital simulation of the propulsion system to linearize about the desired operation points. State models of the form $\dot{\underline{x}} = A\underline{X} + B\underline{U}$; $\underline{Y} = C\underline{X} + D\underline{U}$ are generated. (The linearization technique is sketched in Appendix A.)
- Transfer functions required for loop-by-loop analysis are calculated from the state-matrix model.
- Classical linear, constant coefficient design methods are used to develop compensation on a loop-by-loop basis.
- The above steps are performed for a series of operating points to obtain the relationships between compensation parameters and engine burner pressure. Polynominals are generated to describe the relationships.

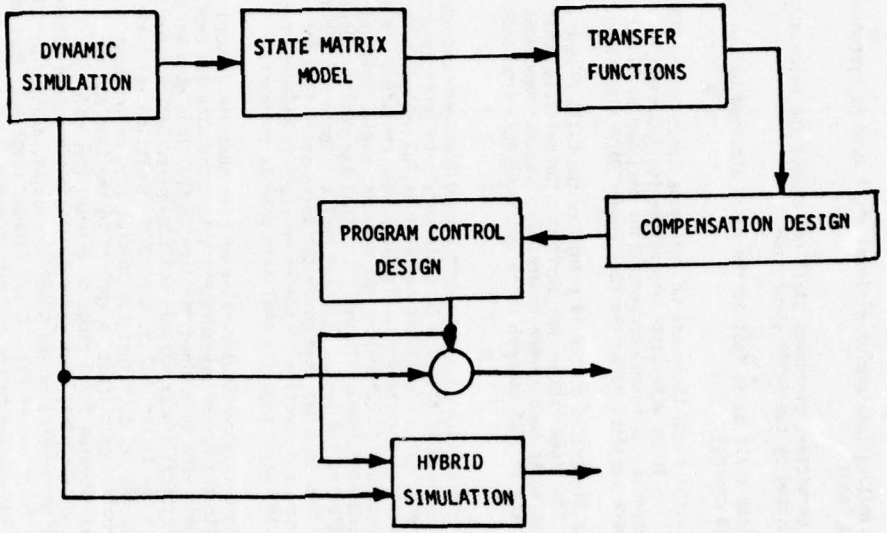

Figure 2.3-9 Analytical Design Procedure

2.3.2 Stability Analytical Models (Continued)

- The compensation polynominals are programmed into the nonlinear SOAPP simulation and subjected to standard disturbances over the flight envelope.

- Adjustment is made and the process is repeated if necessary.

In lieu of classical design specs, the following criteria were established as goals to be used in controller compensation design:

- Gain margin of all loops shall be at least 6 dB

- Loops designed as limiting (maximum or minimum) shall have no overshoot when subjected to a step input.

- Where overshoot is permitted, overshoot shall not exceed the value attained under BOM control as predicted by the SOAPP simulation.

- Rise time of each loop shall be as fast as the value attained by the SOAPP simulation under BOM control.

For some of the IPCS control loops there are no analogous loops in the BOM controller. Time domain specs for these loops were based on engineering judgement of what is required to attain good servo response. All loop compensations designed by linear single input/ single output methods were verified using the non-linear SOAPP simulation.

The SOAPP simulation was linearized at the 19 points in the F-111 flight envelope shown in Figure 2.3-10. The linearization was performed for multiple power settings so that a total of 38 linear state models were generated. Transfer functions required for the analysis of each of the 11 IPCS control loops were generated from each of the 38 linear state models.

Models of all dynamic elements significant to each closed loop were cascaded with the plant transfer functions developed from the 38 state models to generate open-loop transfer functions for each loop. Root locus and Bode design methods were then used to design dynamic compensation for the particular loop when required. In all cases analyzed, simple lead compensation cancelling the dominant engine pole was sufficient to compensate the gas generator loops. It was found that the dominant engine pole could be readily identified as the second negative real axis pole for the N1, N2, PB, and WAR2 control loops; this pole has been given the designation "XPOLE". A plot showing the value of XPOLE as a function of burner pressure is shown in Figure 2.3-11. In the T4 control loop, the third negative real axis pole is dominant.

For each control loop there is a particular value of gain that yields good loop response and can be identified with the burner pressure PS3 associated with the design point. Optimum values of loop gain were determined for each control loop at a series of burner pressures, using both classical linear methods and step perturbation "shot gun" runs with the SOAPP simulation. In the latter method, the SOAPP simulation is initialized at the selected flight condition and set such that the control loop of interest maintains control. A small perturbation step input is applied to the loop and the system response recorded; this process is repeated for a range of assumed loop gain values. Figure 2.3-12 shows the results of a typical shot gun run. The optimum gain values for a series of pressures were implemented in the SOAPP simulation, along with schedules of dynamic compensation, as functions of PS3. After further check-out, they were formally documented and implemented in the control software.

Loop design methods may be summarized as being classical, quasi-linear, and continuous. This does not imply that these are the best design methods but they rather were selected upon consideration of the program schedule, funding level, and available resources, especially computer programs. Some exploratory work was done with modern control theory. While promising,the state-of-the art of these techniques, as applied to propulsion control, were judged to involve long lead times and thus high risk. This conflicted with the IPCS schedule (the control mode topology was essentially frozen about a year after contract) and the conservative, success-oriented philosophy adapted for this program.

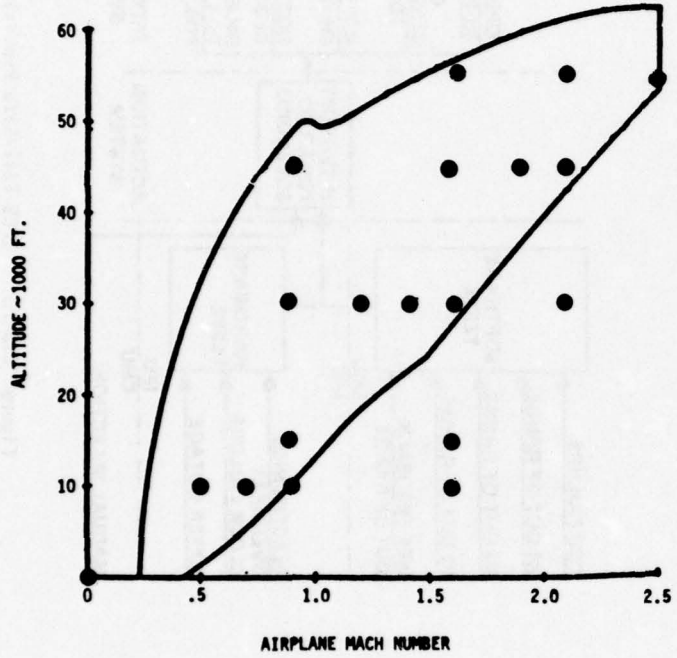

Figure 2.3-10 IPCS Control Design Points

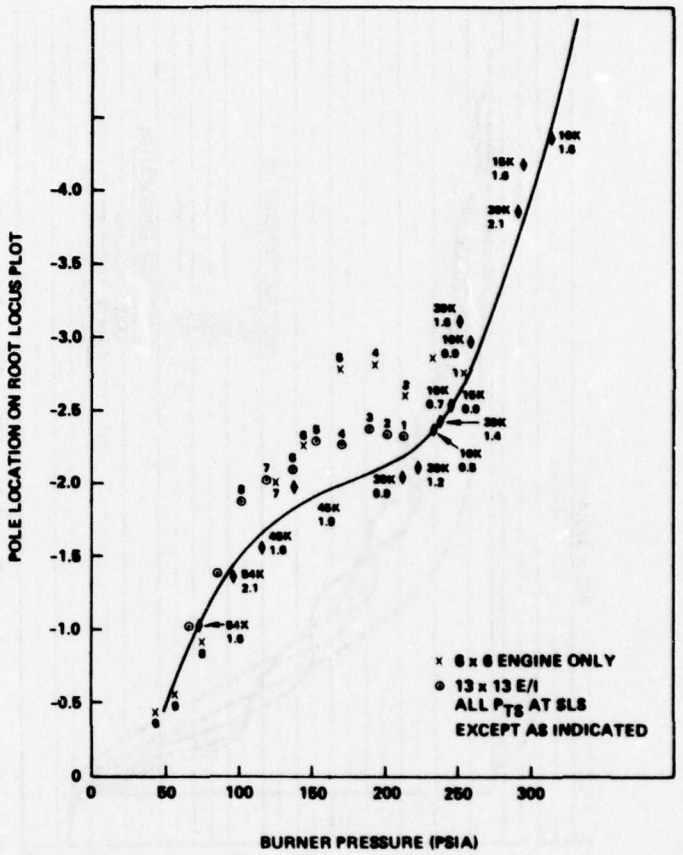

Figure 2.3-11 Dominant Pole Locations as Functions of PS3

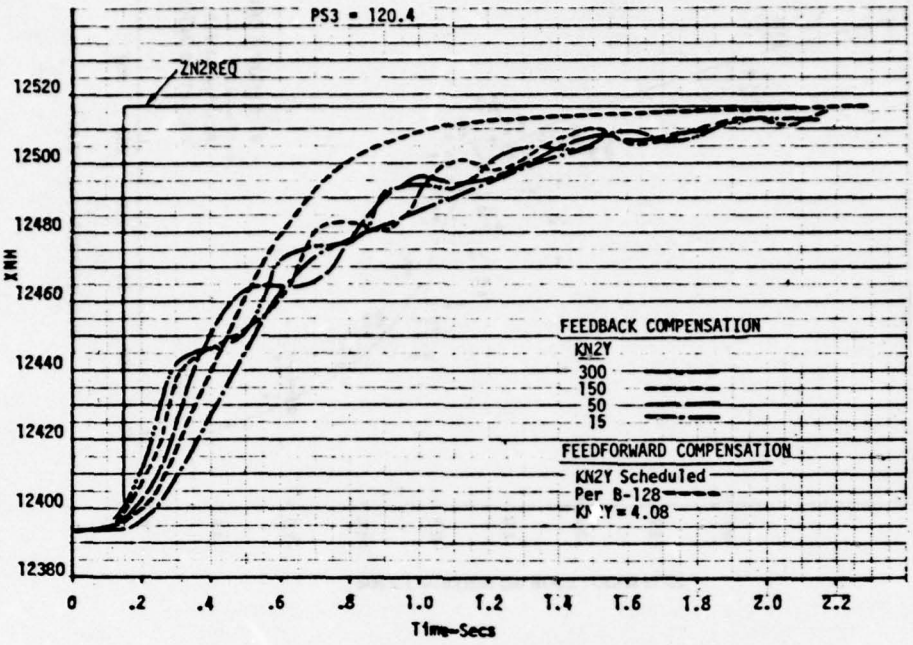

Figure 2.3-12 Closed Loop Step Response for Several Values of Gain

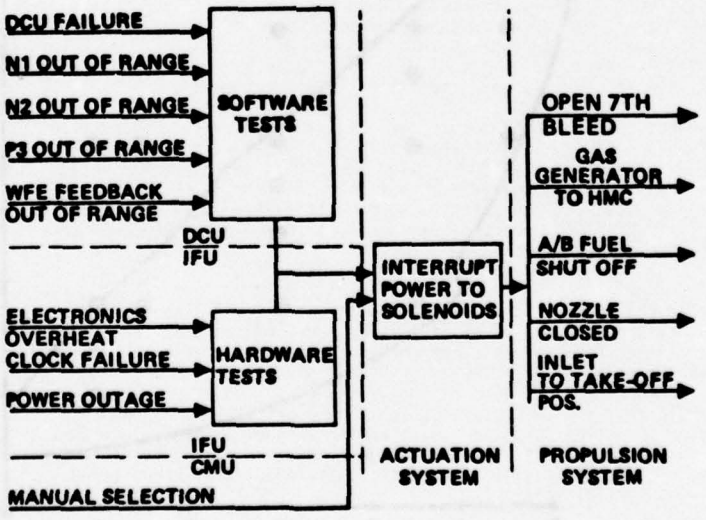

Figure 2.3-13 IPCS Fail-Safe Provisions

2.3.2 Stability Analytical Models (Continued)

The SOAPP simulation of the TF30-P-9 indicated that the engine may be represented adequately by a linear model provided that operating limits are avoided and that burner pressure, PS3, is held constant. Control reaction to encountering operating limits is typically binary (e.g., switch control loops) and the transition is not amenable to analysis. On the other hand, PS3 will change only a small amount during a controller sampling period. The scheduling of gains and time constants, as functions of PS3 accounted for non-linearities consequent to changes in PS3. The decision to use linear analysis for loop stability design was based in part upon these factors. Other factors that influenced the decision were the availability of computer programs and the backgrounds of personnel assigned to the IPCS program.

Continuous-design methods (as opposed to discrete methods) were used initially because they were immediately available. Some exploratory work was done with Z-transforms as a back-up in case the target 30-millisecond sampling period could not be achieved with the software. This work was dropped as confidence was gained that a 30-millisecond interval was both achievable and satisfactory.

The validity of the IPCS analytical design approach has been verified by subsequent engine testing. The regulation portion of the IPCS control mode has been remarkably trouble free. On occasions where adjustment was required, the problems were traceable to discrepancies between the digital simulation and the actual engine, or, more commonly, lack of precise definition of control signals. The fact that work could proceed on schedule in absence of firm data on control signal characteristics is due entirely to the flexibility afforded by the digital computer system.

2.3.3 Failure Detection, Fail-Safe, and Redundancy Provisions

Failure safety and back-up provisions were provided in both the hardware and IPCS software to protect the aircraft and engine, to demonstrate automatic failure detection and signal synthesis, and to minimize test aborts due to certain hardware failures. The hierarchy of hardware redundancy and back-up features was as follows:

a. The aircraft was equipped with two engines, either of which had enough power to return the aircraft to base subsequent to failure. Furthermore, the right-hand engine remained in the bill-of-materials (unmodified) configuration.

b. The hydromechanical gas generator control was retained on the test engine so that the engine could operate at power settings up to Military without depending on the DPCU.

c. Transfer between the DPCU and the back-up hydromechanical control was effected by solenoid valves selected such that interruption of electrical power caused reversion to the back-up hydromechanical mode. Hydromechanical control could be selected by the flight crew or it was selected automatically consequent to several classes of failure. DPCU control, on the other hand, could be selected only by the crew; it was never selected automatically.

d. Upon reversion to hydromechanical control, the inlet surfaces translated to the take-off position at a rate compatible with aircraft deceleration at minimum power settings. Thus if reversion occurred at high flight speeds, aircraft speed would be reduced below the inlet buzz threshold before the inlet reaches the low speed configuration. The 7th stage bleed also opened for three seconds to limit N1 speed excursions encountered if reversion occurred when the afterburner was in operation.

e. Electrical power to the DPCU was interrupted automatically by the IFU if an over-temperature were sensed or if a timer were not reset by the DCU at regular intervals. This latter feature protected the system against both clock failures and a large class of software failures.

f. Signals from transducers determined to be critical to flight safety were examined each major sampling period to determine whether the signal was within the normal operating range. If an out-of-range condition were detected, the signal was synthesized, if feasible, or control was immediately transferred to the hydromechanical unit.

2.3.3 Failure Detection, Fail-Safe, and Redundancy Provisions (Continued)

The fail-safe provisions implemented on the IPCS flight-test airplane are summarized by Figure 2.3-13. The signal monitoring is described by Table 2.3-3.

Table 2.3-3 Sensor Validity Tests & System Response

SIGNAL	UNITS	LOWER LIMIT	UPPER LIMIT	NOTES/FAILURE RESPONSE (1)
N1S	RPM	1050	10,400	N1 not computed if N2 .95 x N2 Min Lower limit not checked in PLA 8°, SQUAT on If failure revert to track and display Fault light
N2S	RPM	2400	15,100	Lower limit not checked if PLA 8°, SQUAT on If failure revert to track and display Fault light
WFGS	PPH	100	16,380	If stall flag set do not check lower limit If failure revert to track and display Fault light
P3S	PSIA	20	298.	If N2 10,000 RPM P3S lower limit = 4 PSIA
PS3S	PSIA	4	298.	
PD3S	PSID	.29	24.	If N2 4000 RPM PD3 lower limit = 0. If Any station 3 pressure fails sythesize from remaining two and display backup
PS22	PSIA	4.	98.	Display backup (BOMDIG Only). Compute PS22S = P22S - PD22S
P2KDAS	PSIA	2.8	26.25	Display BACKUP status Compute P2 by setting P2S = PDEMS
P2KDBS	PSIA	2.8	26.25	
P2KDCS	PSIA	2.8	26.25	
P2KDDS	PSIA	2.8	26.25	
PLMS	PSIA	1.5	26.25	Synthesize PRLMS and display BACKUP status. BOMDIG only
PSLMS	PSIA	1.5	26.25	(1) For Any Two Sensor Failures Revert To Track and Display Fault Light
PDEMS	PSIA	2.85	26.25	Display BACKUP status
PSDEMS	PSIA	2.85	26.25	

3.0 HARDWARE DESIGN, FABRICATION AND TESTING

The hardware-oriented tasks performed on the IPCS program consisted of the design and development of electronic computer equipment, the installation of that equipment on the flight-test aircraft, and the modification of the engine and inlet to permit those subsystems to communicate with the computer. A hardware block diagram is shown in Figure 3.0-1.

A brief introduction to the IPCS hardware was given in Section 1.2. The work loading to the delivery of flight qualified hardware is described in this section.

3.1 ENGINE MODIFICATIONS

A number of engine modifications were necessary to convert a TF30-P-9 engine to the IPCS configuration. Some case modifications were required to incorporate new gas path probes. The requirements for some of these probes were determined by the preliminary control mode studies. Part of the hardware configuration was determined by interface definitions such as the electrical connector interface bracket and the pressure line interface bracket. These helped to define the electrical harness configuration and the flexible pressure line configuration. The transducer box was designed to house the pressure transducers, the thermistors and the thermocouple compensating probes. Some of the rigid steel tubing had to be redesigned to avoid interferences with new IPCS hardware or to provide new pressure signals to the IPCS control system.

3.1.1 Probes and Sensors

3.1.1.1 Gas Path Probes

The overall engine layout SL95884, showing final pressure and temperature probe configuration was completed at the time of Preliminary Design Review. The final probe selection was as follows:

Station	Type	Quantity
P2	Airframe Inlet	4
T2	Bill of Materials - TF30 Thermocouple Harness	2
P22, T22	Combination Probe Developed for CSAP Program	1
P3	TF30 Experimental	4
T3	Bill of Materials - TF30 Thermocouple Harness	2
T4	P&WA/FRDC Design from J58 Program	1
P6M	Bill of Materials - TF30 EPR System	6

The final selection of the pressure ports used to measure the gas path static pressure was also presented at PDR. The selection was as follows:

Station	Type	Quantity
PS22	BOM - Bleed Control Port	1
PS3	New Design	4

The following is a description of the probes which involved a new design effort for the IPCS program. Engine signal designations are explained in Table 3.1-1.

P22, T22 Combination Probe

This probe is the same type as was used in the Compressor Stability Assessment Program. The probe is shown in Figure 3.1-1 and 3.1-2. The selection of this probe allows the measurement of both pressure and temperature at the exit of the low compressor with the least amount of stress on the engine high rotor. To use this type probe in the IPCS program the connection end of the probe was reworked to measure the average pressure and temperature of the five radial pickup points on the kiel head of the probe. The location of this probe has been established at the existing borescope hole in the engine, and no engine case modifications were necessary.

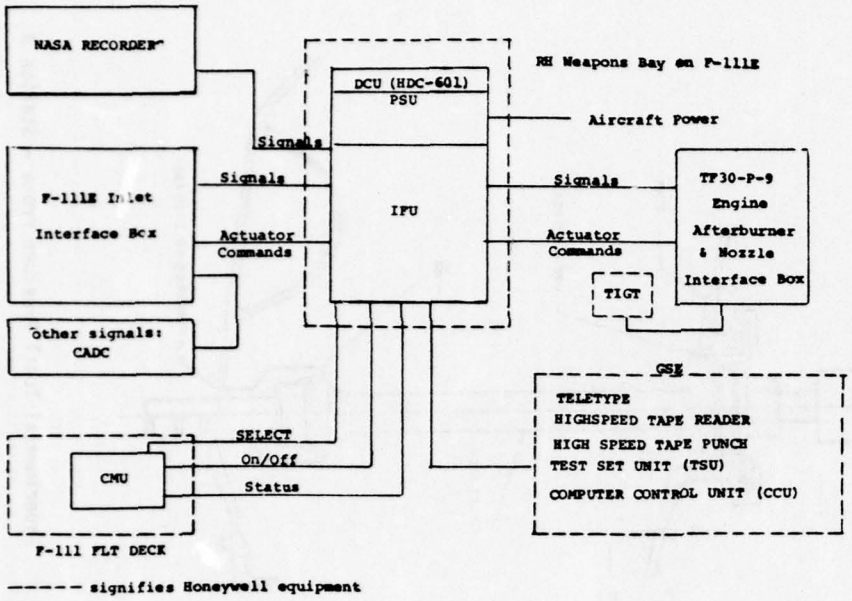

Figure 3.0-1 IPCS Hardware Block Diagram

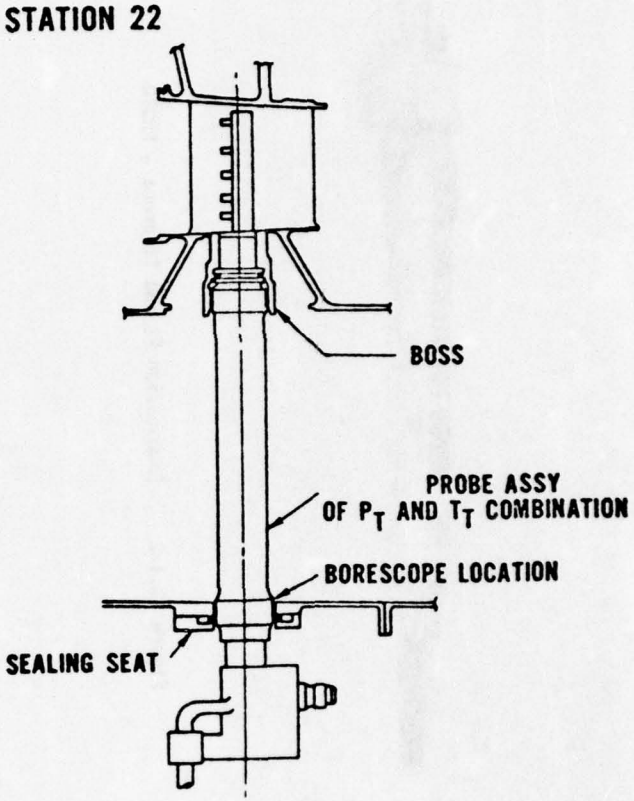

Figure 3.1-1 Combination Pt and Tt probe

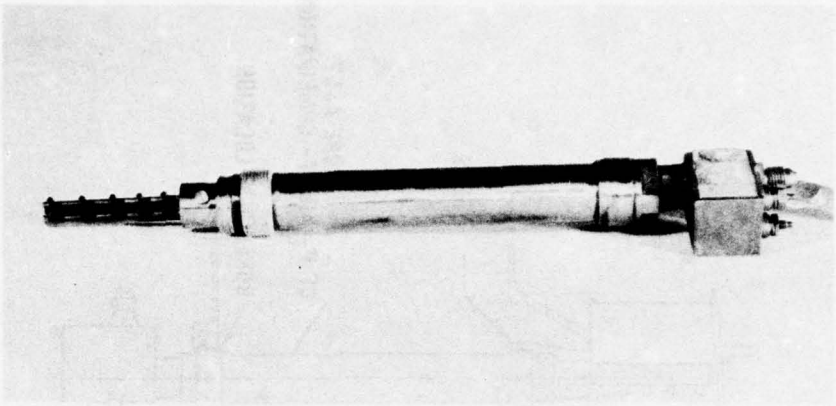

Figure 3.1-2 Combination Pt and Tt probe - PHOTO

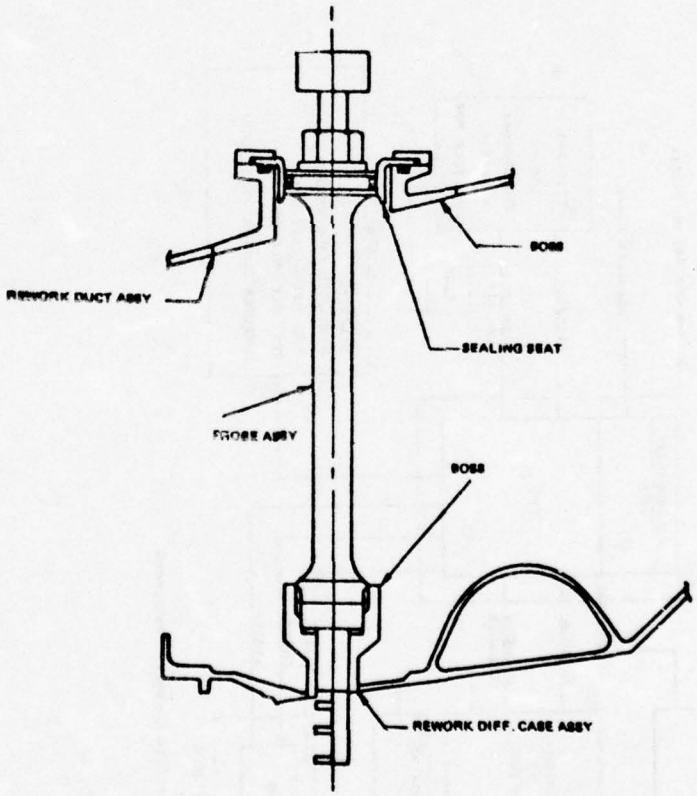

Figure 3.1-3 Experimental Total Pressure Probe - Station 3

3.1.1.1 Gas Path Probes (Continued)

P3 TF30 Experimental Probe

An existing TF30 experimental probe design as shown in Figure 3.1-3 and 3.1-4 was selected to sense the total pressure at Station 3. It was used in conjunction with the wall static pressure in the same plane to determine the high compressor Mach number instead of developing a new Mach number probe design. This selection assured the reliability of the IPCS system without imposing a performance penalty.

The new wall static pickups at the high compressor exit consisted of 3 static pressure taps welded to the diffuser case and one tap bolted to a boss that is welded to the case. These modifications are shown in Figure 3.1-5.

Table 3.1-1

Engine Control Signals

Sensed Parameters

Low Rotor Speed, N1
High Rotor Speed, N2
LPC Exit Total Pressure, P22
LPC Exit Static Pressure, PS22
LPC Exit Differential Pressure, (P-PS) 22
HPC Exit Total Pressure, P3
HPC Exit Static Pressure, PS3
HPC Exit Differential Pressure, (P-PS) 3
LP Turbine Exit Total Pressure, P5
Compressor Face Total Temperature, T2
LPC Exit Total Temperature, T22
HPC Exit Total Temperature, T3
Turbine Inlet Gas Temperature, T4

It was determined using data from a NASA test of an F100 Compressor that a minimum of four (4) Pt probes with three (3) radial location each were required for consistent measurement. The location of these probes in the engine is as nearly equally spaced circumferentially as possible due to internal and external interferences.

Turbine Inlet Gas Temperature Probe

The final design of the turbine inlet temperature probe installed in the TF30-P-9 IPCS engine is shown in Figure 3.1-6. A study based on turbine inlet temperature profiles revealed that the probe could be located in any burner can except the bottom two. The probe was located 22 degrees below the left hand horizontal center line when viewed from the rear, which allows the probe to be removed for inspection with the engine installed in the aircraft.

3.1.1.2 Transducer Box Installation

The transducer box installation, shown in Figure 3.1-7 consists of the silicone oil filled transducer box which houses the pressure transducer, the thermistors, and the cold reference junction probes. The transducer box was designed with the pressure transducers installed in individual rubber vibration isolators and with thermistors and cold reference junction probes in the silicone oil to provide temperature compensation for the transducers and a reference junction for the thermocouple system. The original system design called for fuel cooling the transducer box but manufacturing problems with the first unit led to an unsuccessful vibration test and the decision was made to fill the box with silicone oil to avoid delaying the program for additional flight assurance testing. The box is also insulated with a 1/2" molded blanket of Johns-Manville MIN-K insulation to help minimize the temperature changes around the transducers due to environmental temperature variations.

The thermistor probes use the same thermistor as used to measure compressor inlet temperature in the TF30-P-100 engine and the probe design is the same as the oil temperature immersion thermocouple probe used in the F100 engine.

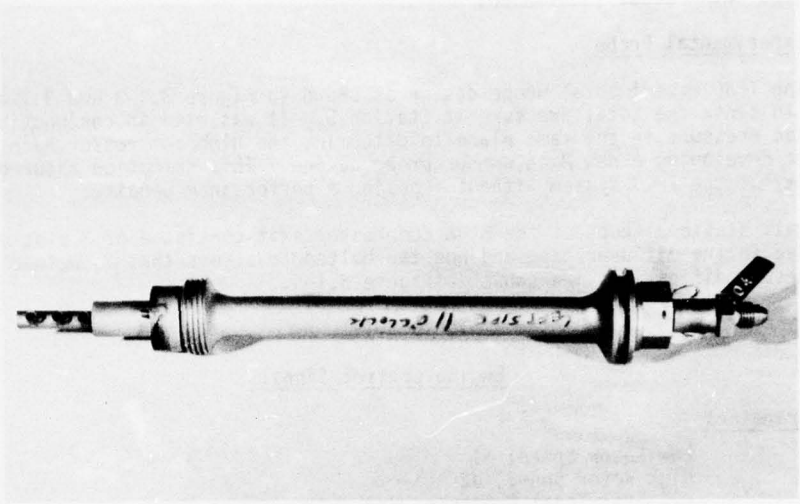

Figure 3.1-4 Probe - Station 3 - PHOTO

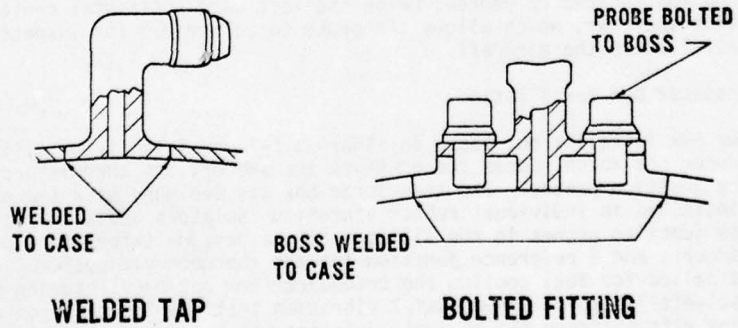

Figure 3.1-5 High Compressor Exit Ps3 Wall Static Configuration

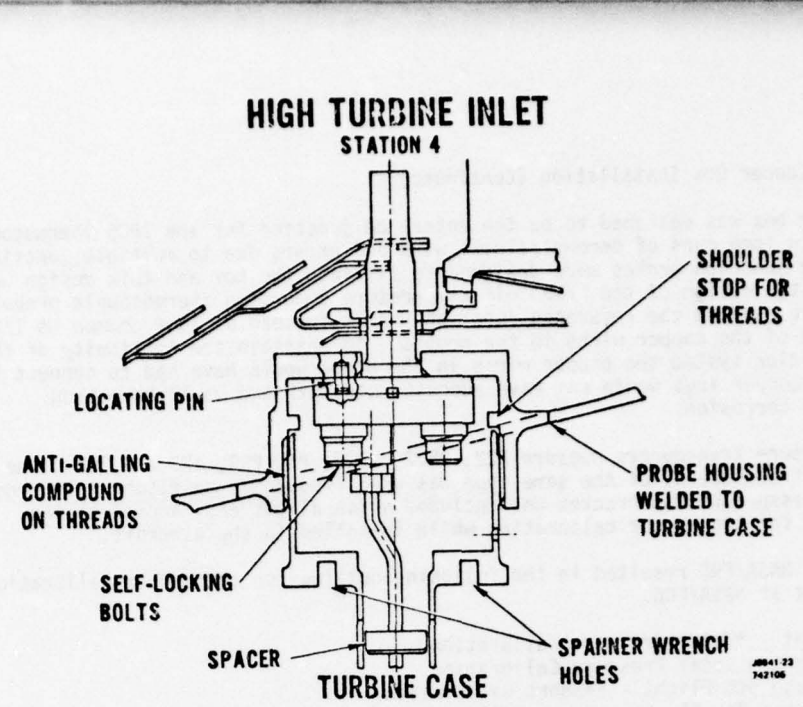

Figure 3.1-6 Turbine Inlet Temperature Probe

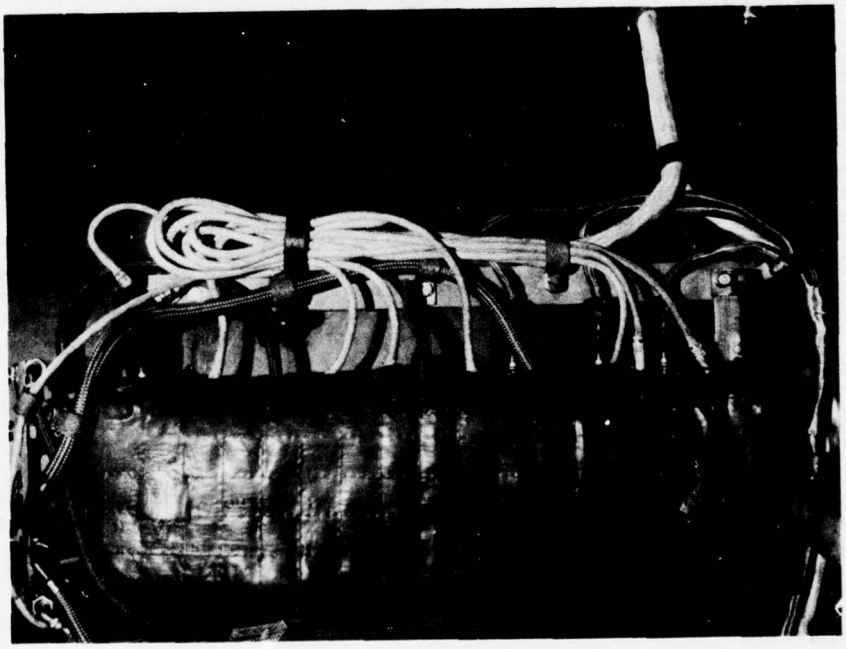

Figure 3.1-7 Transducer Box Installation

3.1.1.2 Transducer Box Installation (Continued)

The transducer box was designed to be the reference junction for the IPCS thermocouple system to avoid long runs of chromel/alumel wire and errors due to multiple junctions. Cold reference junction probes were designed to fit into the box and this design was also based on the design of the F100, oil temperature immersion thermocouple probe. Connectors were used on the reference junction probes instead of lugs common to T/C probes because of the copper wires in the probes. To maintain the continuity of the reference junction system the copper wires in the probe would have had to connect to copper lugs. Copper lugs would not have adequate strength and would have been susceptible to corrosion.

The seven pressure transducers measure P22, PS22, ΔP22, P3, PS3, ΔP3 and P6M. They are MB/Alinco transducers, of the same type was used frequently on flight test programs at P&WA. A pressure pickup bracket was included which allows easy access to the pressure lines for transducer calibration while installed in the aircraft.

Discussions at NASA/FRC resulted in the following outline for transducer calibration for flight test at NASA/FRC.

Pre 1st Flight - *Total Pressure Calibration
Post 1st Flight - Total Pressure Calibration
Pre 2nd through 9th Flight - **Short Calibration
Post 2nd through 9th Flight - Short Calibration
Pre 10th Flight - Total Pressure Calibration
Post 10th Flight - Total Pressure Calibration
Pre 11th through 25th - Short Calibration
Post 11th through 25th Flight - Short Calibration
Post Last Flight - Total Pressure Calibration

The outline was contingent on the day to day flight test experience. If any suspected problem arose which involved the transducers or associated hardware, a complete pressure calibration was required.

3.1.2 Fuel System Modifications

Modifications to the fuel system were made only to the extent required to meet the objectives of the IPCS program. These modifications were based on three ground rules:

1. Provide the accuracy, flexibility, and response required for IPCS control modes.
2. Minimize component and plumbing changes to avoid fuel system hardware development problems.
3. Retain the hydromechanical gas generator control capability as a backup to the IPCS.

These guidelines were met by providing an electromechanical device at each key metering and actuating location in the fuel system. Component housings, structural mounts, and plumbing were retained intact, as were several secondary fuel-handling and pump-sequencing functions. External modifications were confined essentially to the addition of electrical connectors on the engine and afterburner fuel control housings, and installation of several solenoid valves. Fuel pumps, filters, actuators, and heat exchangers were retained as fully qualified, service-proven components, and were not affected by IPCS operation.

The control system vendor, Bendix Energy Control Division, had extensive experience with the installation of electromechancial interface devices and the IPCS modifications posed no new problems. Design features and components incorporated in the F100-PW-100 control system, which have several similar interfaces, were incorporated wherever practical. The previous use of the control electrical components is shown in Table 3.1-2.

**Short Calibration
(1) Ambient pressure check for absolute pressure transducers
(2) Zero pressure check for differential pressure transducers

*Total Pressure Calibration
(1) 4 to 6 point calibration
(2) Use leak-tek on pressure fitting to check for air leaks while engine is running

Table 3.1-2 IPCS Electrical Component Substantiation

COMPONENT	CONTROL APPLICATION	ENGINE
RESOLVERS	FJ-A3	F100
SOLENOIDS	AA-J2	TF30
STEPPER MOTORS	FJ-A2	F100
TORQUEMOTORS	CJ-T1	SIMILAR TO GE-J101*
LVDT	CJ-T1	GE-J101

*ELECTRICAL PARTS COMMON, HYDRAULIC INTERFACE CHANGED FOR PACKAGING CONSIDERATIONS

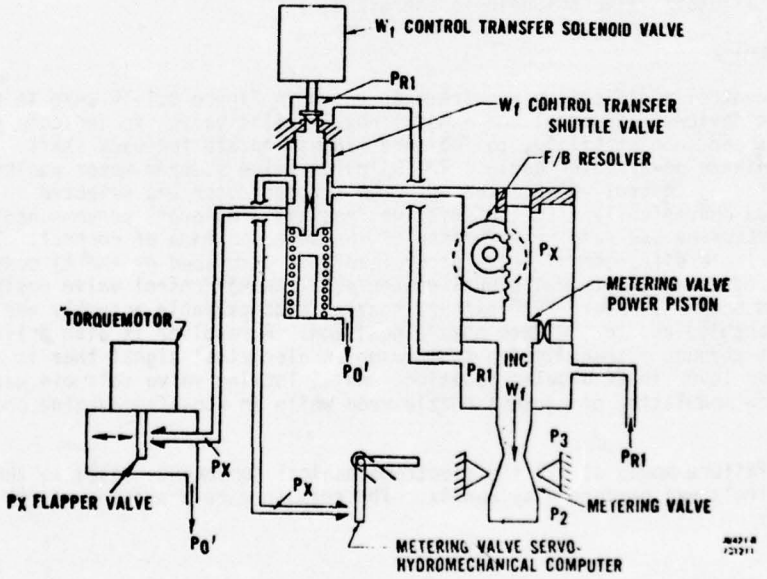

Figure 3.1-8 Main Fuel Control

3.1.2.1 Main Fuel Control

The main fuel control modification requirements were to add an electro-hydraulic device to indicate metering valve position, and to add an electrically actuated switching device to permit selection between electrical or hydromechanical control of metering valve. These requirements were met with a torque motor driven flapper valve servo to control metering valve position, a rack and pinion driven resolver to indicate metering valve position, and a fuel control transfer solenoid for control mode selection, as shown in Figure 3.1-8. The torque motor was selected because it provided a simple interface compatible with the existing servomechanism, and met the accuracy and response requirements of the selected mode of control. The transfer solenoid was designed to transfer metering valve control to the hydromechanical mode in the event of a solenoid failure or loss of electrical power. A separate module was added to the main fuel control at the location of the Bill of Material A/B reset piston and A/B blowout signal valve to incorporate the torque motor, resolver, and transfer solenoid. Separate electrical connectors were provided for each device.

3.1.2.2. Afterburner and Exhaust Nozzle Control

Afterburner Control

The afterburner control modification requirements, shown in Figure 3.1-9 were to add electrohydraulic devices to position the five zone metering valve positions and to add electrohydraulic devices to control five cutoff valves. A stepper motor acting through a transmission positions each metering valve. The stepper motor was selected because it was compatible with the existing hydromechanical "position follower" servomechanism, and could meet the accuracy and rate requirements of the selected mode of control. In addition, the implementation was similar to the approach used in the F100 control which provided confidence in the design. A resolver driven by the stepper motor through a transmission indicates the metering valve position. The cutoff valves are opened or closed by a solenoid valve acting through a hydraulically powered three-way shuttle valve. Another feature incorporated in the afterburner control is the A/B pump turn-on and A/B igniter signal shuttle valve. This valve supplies servo pressure to the A/B pump turn-on switch and supplies a pressure arming signal to the A/B igniter valve when the Zone 1 cutoff valve solenoid is energized.

Exhaust Nozzle Control

The exhaust nozzle control modification requirements shown in Figure 3.1-10 were to add electrical interface devices to control the exhaust nozzle pilot valve, to indicate pilot valve position for inner loop stability, to indicate exhaust nozzle feedback shaft position, and to indicate power lever angle. The Aj pilot valve stepper motor positions the servo valve of the Aj control valve actuator. The stepper motor was selected because it interfaced conveniently with the existing "position follower" servomechanism, and could meet the accuracy and rate requirements of the selected mode of control. The core of a linear variable differential transformer (LVDT) is displaced by the Aj control valve actuator to provide an electrical signal proportional to Aj control valve position. A resolver is driven by the standard TF30 exhaust nozzle feedback cable assembly and shaft, through a transmission, to indicate nozzle position. A resolver is also driven by power lever shaft through a transmission to provide an electrical signal that is a function of the power lever shaft angular position. An Aj locking valve solenoid was incorporated to allow modulation of exhaust nozzle area while in non-afterburning operation if required.

An analysis of the failure modes of all the electromechanical components added to the main and afterburner controls was performed by Bendix. The results were presented at the Final Design Review.

3.1.3 Engine Wiring Harness and Plumbing

3.1.3.1 Electrical Harnesses

A sketch of the IPCS engine harness configuration is shown in Figure 3.1-11. Besides the N1 tach harness and the T/C harness, there are four separate harnesses to facilitate separation of the low level signals from the high level signals. There are two harnesses for the A/B control, the resolver harness which contains low level signals and the stepper motor and solenoid harness which contains high level signals. A third harness includes

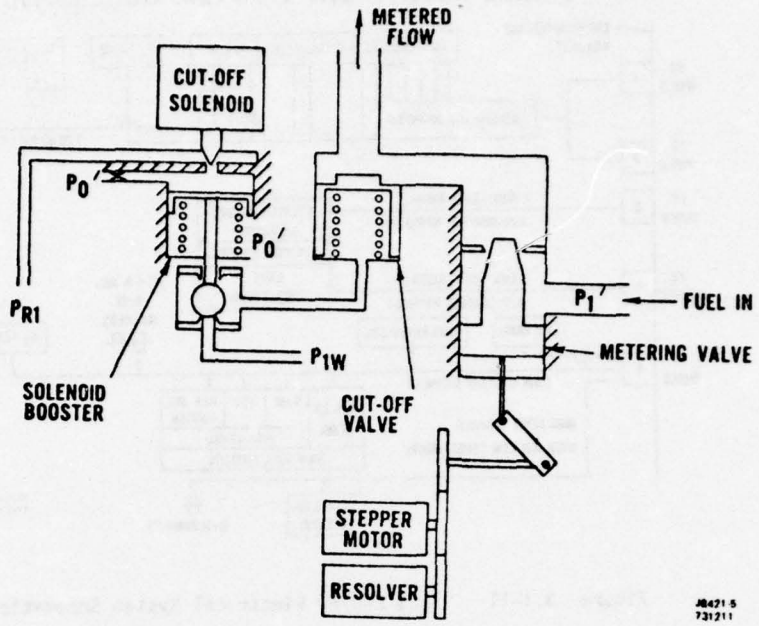

Figure 3.1-9 Afterburner Control

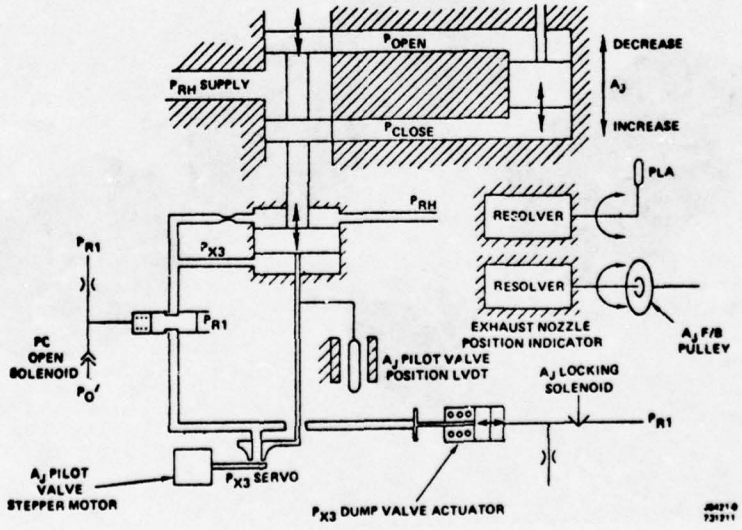

Figure 3.1-10 Exhaust Nozzle Control

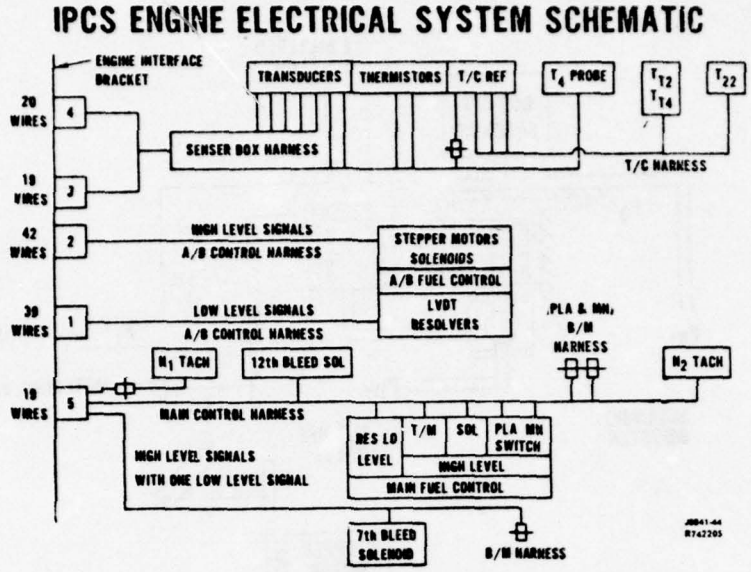

Figure 3.1-11 IPCS Engine Electrical System Schematic

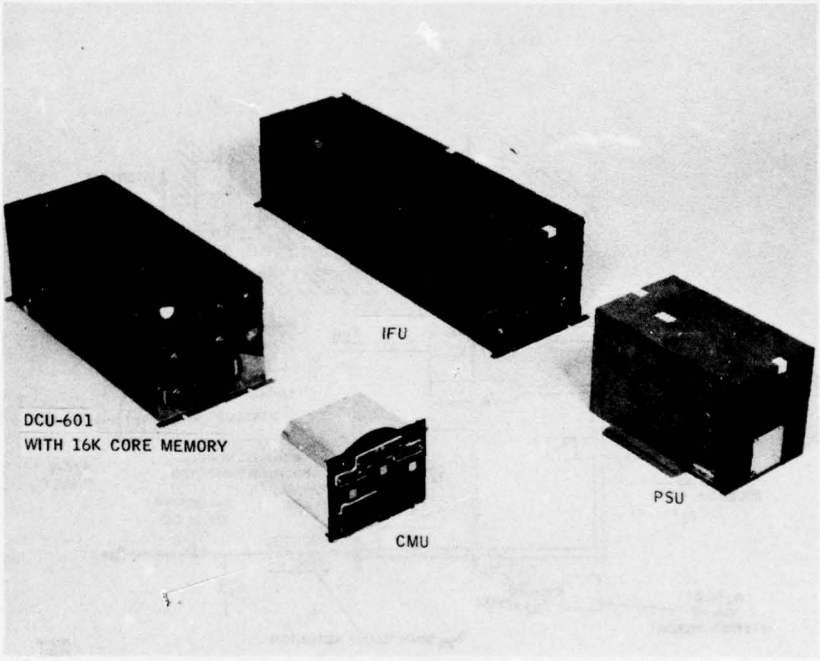

Figure 3.2-1 Digital Propulsion Control Unit

3.1.3.1 Electrical Harnesses (Continued)

the transducers, thermistors, T4 probe, and the copper wires from the T/C cold reference junction - all low level signals. The fourth harness includes the main fuel control torque motor, resolver and solenoid, and two tachometers, the twelfth bleed solenoid, and the seventh stage bleed modified wiring. The only low level signal in the fourth harness is the MFC resolver which is terminated at a distance from the high level signals in the interface connector and shielded from them.

Aside from segregating the high and low level signals in the harnesses, the harnesses were also constructed in such a way as to maintain signal integrity to and from the DPCU. The harnesses were mainly constructed of individual twisted, shielded pairs to prevent cross talk between the different signals. In addition, the entire wire bundle in each harness was covered with an outer shield to prevent RF interference. In addition, the Bendix harnesses had an outer fiberglass braid to minimize the risk of chafing and handling damage. The harnesses used MIL Spec connectors that are used on many other aircraft engine applications. As part of the acceptance test of the harnesses at the vendor, they were checked for continuity and insulation resistance. The harnesses were clipped in place on the engine as required to minimize flexing.

3.1.3.2 Plumbing Modifications

The plumbing modifications to the engine consisted of both flex lines and steel hard pipes. The flex lines were used for the air pressures going to the transducer box while hard pipes were used for fuel pressure lines and internal air pressure lines. Fourteen steel hard pipes required for the engine modifications, of which ten were new and four were modifications to existing pipes.

The flex lines originally selected for the high compressor discharge and turbine discharge pressures contained convoluted steel cores, while teflon core lines were selected for low compressor discharge. This selection was made to minimize the deteriorating effect of high temperature gas leakage if a leak should develop. Vibration test of the transducer box assembly indicated the steel core lines would not withstand the engine vibration environment and a change was instituted to make all the flex lines of teflon core material. Since the sense lines do not normally flow, the impact of the change was not considered major. The lines were all pressure tested as part of the acceptance procedure and were clipped in place on the engine according to P&WA standard practice.

The steel lines were designed and built to the same standards as all the BOM steel lines on the TF30 engine. In most cases the new lines were routed and clipped in a similar manner to the BOM tubes they replaced. Any all-new tubes were clipped according to P&WA standard practice.

3.2 ELECTRONIC HARDWARE

The Honeywell Digital Propulsion Control Unit (DPCU) provides hardware and the software programs required for implementation of the Integrated Propulsion Control System (IPCS). The DPCU is designed to control an entire aircraft propulsion module--inlet, engine, afterburner, and nozzle, and inclusion of the DPCU with the input/output hardware and the aircraft propulsion module constitutes an IPCS. Figure 3.2-1 shows the flight hardware components of the DPCU: a Digital Computer Unit (DCU), an Interface Unit (IFU), a Power Supply Unit (PSU), and a Computer Monitor Unit (CMU). The DCU, IFU, and PSU are installed in an aircraft installation box that is mounted in the weapon's bay of an F-111E for flight testing. Figure 3.2-2 shows these units. The aircraft installation is shown in Figure 4.1-10 of Volume III.
In addition to the flight hardware, the DPCU also provides two flight software programs: Bill-of-Material-Digital (BOMDIG) and IPCS. The BOMDIG software program represents a digital version of the present hydromechanical TF30-P-9 (F-111E) Propulsion Control System. The IPCS software program provides for advance control modes.

The modularized design of the DPCU makes it a general-purpose controller that may be used for data acquisition and control of various systems. It is possible to reconfigure the interface unit (IFU) by changing the number and type of plug-in cards. The IFU is structured with computer interface logic, a real time clock, and direct-memory address (DMA) control such that a number of the cards can be considered computer-peripherals for both input and output signal conditioning.

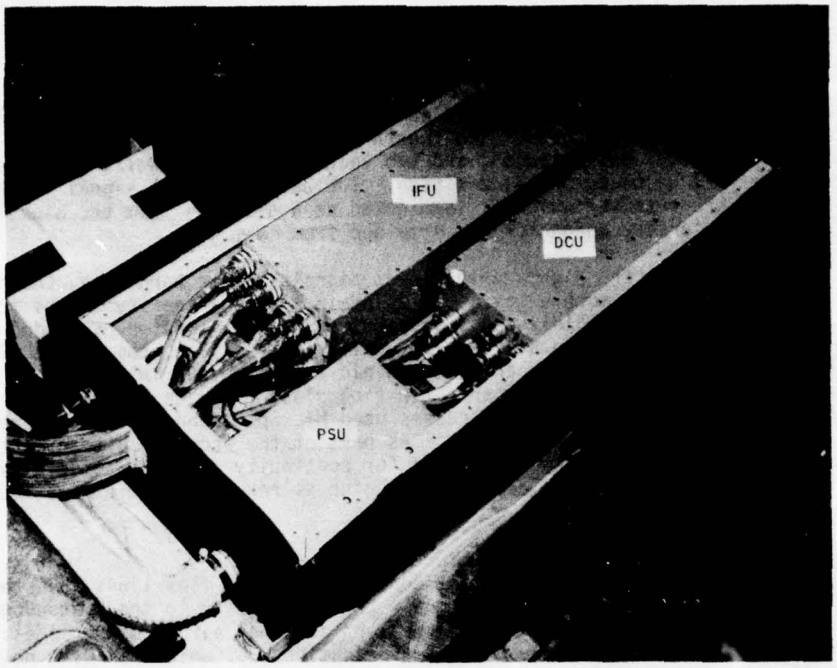

Figure 3.2-2 Aircraft Installation Box

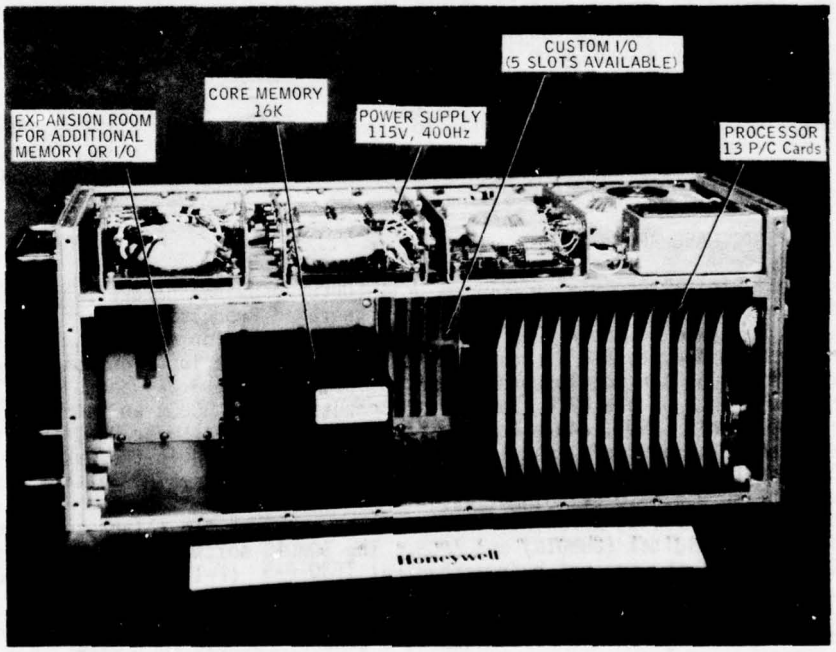

Figure 3.2-3 The HDC-601 Computer

Support test hardware and software were also supplied with this system. A test set unit (TSU) provides the support hardware for field use. The TSU, when supplemented with an oscilloscope, low-frequency function generator, and a precision digital voltmeter (DVM), provides complete capability for performance of the system acceptance test procedures (ATP). A short-form, quick, semi-automatic ATP can be run to provide system functional checkout. The test software includes a long-form ATP, short-form ATP, and "MEDIC" test programs.

Test equipment other than the TSU is available at Honeywell in Minneapolis. This equipment includes three printed circuit card testers and a simulation interface adapter (SIA). The card testers are factory-bench fixtures used for calibration and testing of the IFU printed circuit cards. The SIA is a specially designed rack that provides the circuitry to interface the hybrid computer simulation of the TF30-P-9 engine and the F-111 inlet to the DPCU.

Honeywell also supplied cables for engine testing at Pratt and Whitney Aircraft and NASA-Lewis Research Center. The design of these cables provided the basis for specification of aircraft wiring.

The following subsections provide a technical description of the DPCU hardware; the DPCU software is described in Section 4.0, and testing of the DPCU is discussed in Section 3.4.

3.2.1 Digital Control Unit (HDC-601)

The Honeywell (Florida) HDC-601 Computer was selected for this program. It has a 16K core memory supplied by Electronic Memories. A picture of the computer with the cover removed is shown in Figure 3.2-3. The computer consists of a central processor unit (CPU), memory, power supply, crystal clock, and associated wiring, mounting, and cooling facilities. The CPU is constructed of TTL flat-pack circuitry mounted on 13 P/C cards. The CPU contains timing and control, interface addressing (I/O and interrupt channels), direct-memory access (DMA), and arithmetic processing functions. Timing circuits provide signals that establish orderly processing of data in the correct sequence. Control circuits interpret commands and ensure that the required circuits are activated to accomplish a given processing operation. Interface circuits provide the capability to transfer computer compatible data to and from the external devices. Addressing circuits permit random access of memory and the means by which address can be altered. Arithmetic circuits provide parallel processing of arithmetic functions in two's complement form.

The functional elements of the CPU are:

- A Register
- B Register
- Program Counter
- Memory Address (Y) Register
- External Priority Interrupt
- External Interrupt Register
- Discrete Decode Function
- Instruction Decode
- Timing
- Direct Input/Output Channel (DIO)
- Direct Memory Access Channel (DMA)
- Adder
- F Register (4 Bits of OP Code)
- M Register
- Shift Counter
- Index Register
- Interrupt Mask Register
- Interrupt Control

The CPU is not packaged along functional lines; e.g., the A register is a part of CPU P/C cards A1, A3, A5, and A7

3.2.1 Digital Control Unit (HDC-601) Continued

Word size is 16 bits, but double-precision arithmetic is possible. Eighty-four instructions are available . The timing control is derived from a 2.5 MHz crystal-controlled clock.

The DCU power supply is a switching regulator operating at 10 kHz from a Royer oscillator. The 5-Vdc output is used for feedback control of the regulator to ensure regulated control of the 5-Vdc power. The other output voltages then track the 5-Vdc power as a function of the switching regulator power transformer turns ratios. Protection and monitor circuits are provided to protect against over voltage, over current, and to provide normal power up/down control.

The 16K core memory supplied by Electronic Memories (16384) is a cubic model SEMS-9. Word size is 16 bits, and there is no hardware parity bit. Construction is of the coincident current configuration with the inhibit current and sense lines as a common line for each bit. The read/write cycle time for the memory is 1.2 microseconds.

3.2.2 Interface Unit (IFU)

The Interface Unit (IFU) interfaces the DCU to the engine, inlet, CMU, recorder, and the TSU. It conditions analog signals to digital signals for input to the DCU and controls digital signals from the DCU to analog outputs. It also provides total system hardware mode control in the STATUS and ENGAGE control logic. Built-in-test (BITE) features are incorporated into the IFU circuitry to provide automatic hardware function monitoring.

The IFU can be described in terms of four basic blocks: 1) input electronics, 2) output electronics, 3) computer interface electronics, and 4) power supply electronics. Figure 3.2-4 is a block diagram of the IFU.

Input Electronics - The input electronics provides capacity for 64 analog-to-digital (A/D) input channels. Two A/D converters are used to convert simultaneously. The 32-input high-level A/D digitizes analog signals within a ±5 Vdc range; the 16-input (16 spares available) low-level A/D digitizes analog signals within a ±30 mVdc range. The least significant bit is approximately 15 microvolts for the low-level A/D. The conversion accuracy from IFU input to digital word is ±0.1 percent, and the average conversion time is 105 microseconds (two simultaneous conversions at 210 microseconds each). Input filters roll off the analog inputs to 13 ± 3 Hz. All inputs are differential, with common voltage capability of +5 Vdc and common mode rejection ratios of 10,000 for low-level A/D conversion and 500 for high-level A/D conversion. Both A/D converters use automatic null correction circuitry to ensure operation to ±0.1 percent over the full temperature range.

The input electronics also provide conversion of 11 frequency inputs:

Two rotor speed tachometers (N_1/N_2) to ±0.5% of full scale
One special temperature sensor (TIGT-T4) to ±1% of full scale
Eight special pressure transducers (inlet pressures) to ±0.06% of full scale

Resolver-to-digital converters are provided for eight positional inputs. These converters provide digital representations of actual positions to within ±0.5 degree.

Other input features provided are:

Buzz - 10 ±1 Hz breakpoint frequency detector
Turbulence - 50 ±5 Hz breakpoint frequency detector
Rumble - 40 ± 4 Hz breakpoint frequency detector
Five full-demod converters for LVDT inputs (spike, cone, internal 1-KHZ excitation, AJPVS, internal 3.9-KHz excitation). With an accuracy of ±3.5% of input signal, much better than 2.5% accuracy is obtained by software techniques.
Sixteen buffered input discrete lines (six spares)
Hardware closed loop main fuel control circuit

Output Electronics -- The output electronics provides 16 D/A outputs of +10.24 Vdc with an accuracy of ±1 percent of full scale. Eleven of these outputs provide analog data output for test purposes. The other five outputs are:

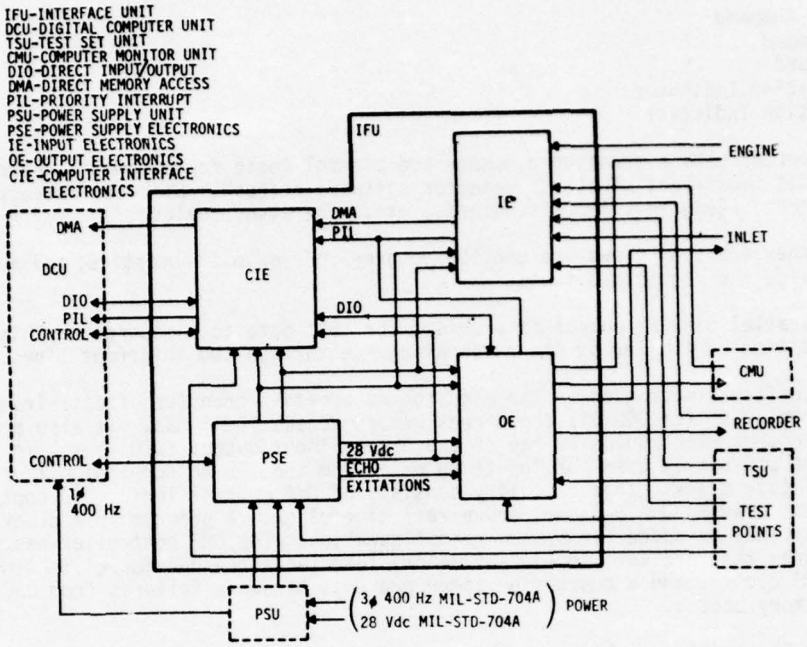

Figure 3.2-4. Interface Unit (IFU) Block Diagram

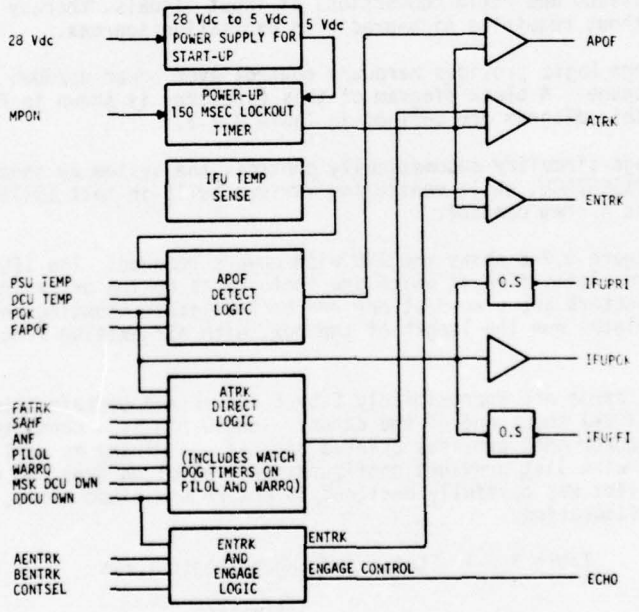

Figure 3.2-5. Status and Engage Logic Block Diagram

3.2.2 Interface Unit (IFU) Continued)

Main Fuel Command
Spike Command
Cone Command
Spike Position Indicator
Cone Position Indicator

The D/A converter uses a scratchpad memory and control logic for automatic refresh of outputs. This feature eliminates a need for software refresh. Discrete outputs for driving solenoids (engage solenoids, bleeds, etc.) are also provided.

The afterburner A/B fuel flows are controlled grey-code output converters, and associated drivers provide the required outputs.

A 16-bit, parallel digital output is provided for test data to a recorder. This interface is time-controlled by the external device through two interrupt lines.

Computer Interface Electronics -- The electronics provides transfer of data from the input electronics to the DCU via the direct memory access (DMA) bus. It also provides data to the output electronics by way of the direct input/output (DIO) bus. In addition, the DIO bus is used for inputting data from the IFU DMA control circuitry and the IFU real time clock. This circuitry consists of DMA control logic, DIO control logic, DMA bus driver, DMA decoder, and a real time clock. A programmable clock and a DIO repeater may be added for system reconfiguration. The DMA controller has some design features that prevent "lockup" of memory interface; the DMA access is limited to alternate DMA cycles, and a conversion timer prevents hardware failures from causing lockup of memory access.

Power Supply Electronics -- Power supply electronics in the IFU provide precision excitation sources and system power up/down, engage/disengage control. Excitation generators of +5 Vdc, -5 Vdc, 5 mA/D constant current sources, 1 kHz a-c, and 3.9 kHz a-c are provided. Analog-to-digital conversions of these excitations provide capability for software corrections and ratio conversions of input signals, thereby enhancing system accuracy without requiring high-precision excitation sources.

The status and engage logic provides hardware control over power up/down and control system engage/disengage. A block diagram of this circuitry is shown in Figure 3.2-5. The terms used in this diagram are defined in Table 3.2-1.

The status and engage circuitry automatically controls the system by sequencing power ON/OFF and ENGAGE/DISENGAGE, while monitoring various built-in-test (BITE) circuits to provide fail safe system control.

IFU Packaging -- Figure 3.2-6 shows the IFU with covers removed. The IFU contains 46 printed circuit card slots, five of which are included as option or expansion features. The connectors are placed at one end to facilitate mounting and for cable access. Two cold plates run the length of the box, with air exiting from connector end.

The printed circuit cards are approximately 6 by 6 inches and contain primarily TTL circuitry. Figure 3.2-7 shows one of the cards. The 90 pin card connectors plug into a mother board connector that provides printed circuit bus wiring as well as wire-wrap wiring. A detailed wire list provides configuration control on type and routing of wiring. This wire list was carefully designed to ensure a minimum noise, cross talk, and ground-loop configuration.

Table 3.2-1 Status and Engage Logic Terms

Term	Definition
MPON	Main Power On (from CMU)
POK	Power OK (from PSU)
FAPOF	Force Automatic Power Off (from Software)
FATRK	Force Automatic Track (from Software)
SAHF	Sample and Hold (Circuit) Failure
ANF	Auto-Null (Circuit) Failure

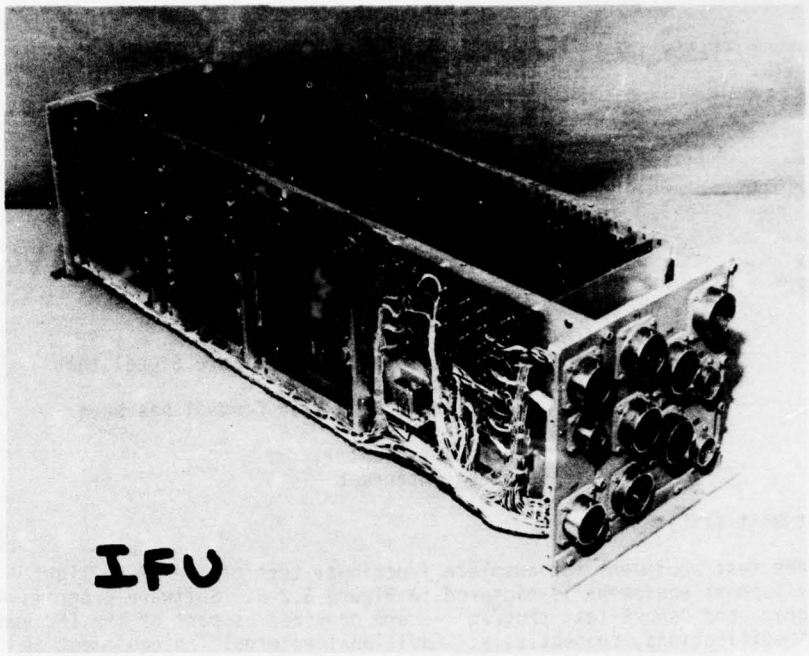

Figure 3.2-6 Interface Unit (IFU)

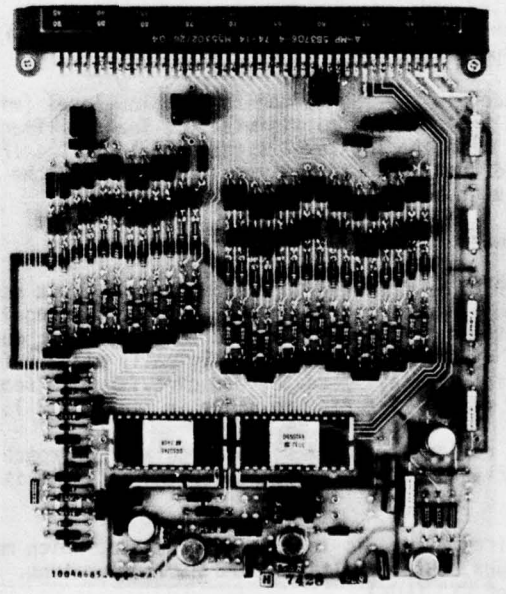

Figure 3.2-7 IFU Printed Circuit Card

Table 3.2-1 Status and Engage Logic Terms (Continued

Term	Definition
PIL01	Priority Interrupt 1 (Real Time Clock)
WRRQ	Write Request (DMA)
MSK DCU DWN	Mask DCU Down (from Software)
D DCU DWN	Disable DCU Down (Test Point)
AENTRK	"A" Enable Track (from Software)
BENTRK	"B" Enable Track (from Software)
CONTSEL	Control Select (from CMU)
APOF	Auotmatic Power Off
ATRK	Automatic Track
ENTRK	Enabled Track (Hardware and Software Signal that Enables Control Engagement)
ECHO	Return "Echo" indicating that Control has been Engaged
PFI	Power Failure Interrupt
PRI	Power Recovery Interrupt

3.2.3 Test Set Unit (TSU)

The DPCU includes test equipment for complete functional test of the DPCU flight hardware. This support equipment is pictured in Figure 3.2-8. Software programs -- "long-test program" and "short-test program" -- are provided as part of the IFU and system design specifications, respectively. Additional external lab equipment is required to run the long-test program as this is the full acceptance test procedure for verification of system compliance to detailed specification requirements. The short program, however, provides a quick functional test of the system. The long-form program requires 6 to 8 hours of testing (including setup time) to complete, whereas the short-form program can be set up and run in 20 minutes. The DCU peripheral equipment is included in the TSU, and is shown in Figure 3.2-9. The peripheral equipments include:

CCU - Computer Control Unit
TTY (ASR-35) - Teletypewriter
HSTR (EEC09300) - High-Speed Paper Tape Reader
HSP (Tally P1200) - High-Speed Paper Tape Punch

A breakout box is also included in the TSU to monitor the low-level (millivolt) signals into the IFU, and amplifiers are provided to minimize the loading effect caused by inserting this box in series with the low-level signals cable to the IFU. These buffer amplifiers are powered from a Ni-Cad battery located inside the breakout box. Figure 3.2-10 shows the breakout box.

3.2.4 Other Electronic Hardware

3.2.4.1 Power Supply Unit (PSU) -- The need for a power supply unit became evident after the inception of the program. Then it was found that +33 Vdc was required for the various Bendix actuators. This requirement more than doubled the DPCU power supply output requirement, and volume on the side of the IFU, which was originally planned for the +5, ±15 Vdc supplies, was then required for special 33-Vdc driver circuitry. A separate box was then designed to supply DPCU power. The PSU was shown in Figure 3.2-1.

To expedite the power supply design, a simple series regulator approach was selected. This approach provides a quick, reliable, low-noise design, although it is not the most efficient design.

A sensing circuits printed circuit card is included in the PSU, which monitors all the power supply input voltages, output voltages, and PSU temperature. The output of this card is the signal "Power OK" (POK).

3.2.4.2 Computer Monitor Unit (CMU) -- The computer monitor unit was also shown in Figure 3.2-1. This unit is mounted in the cockpit and provides switches and indicators for the pilot. The pilot may switch power on/off, engage/disengage control, or modify software (combinations of four sense switches). Indicator lights are provided for engage, backup, fault, track, and power. In addition, a switch is provided for lamp test. The

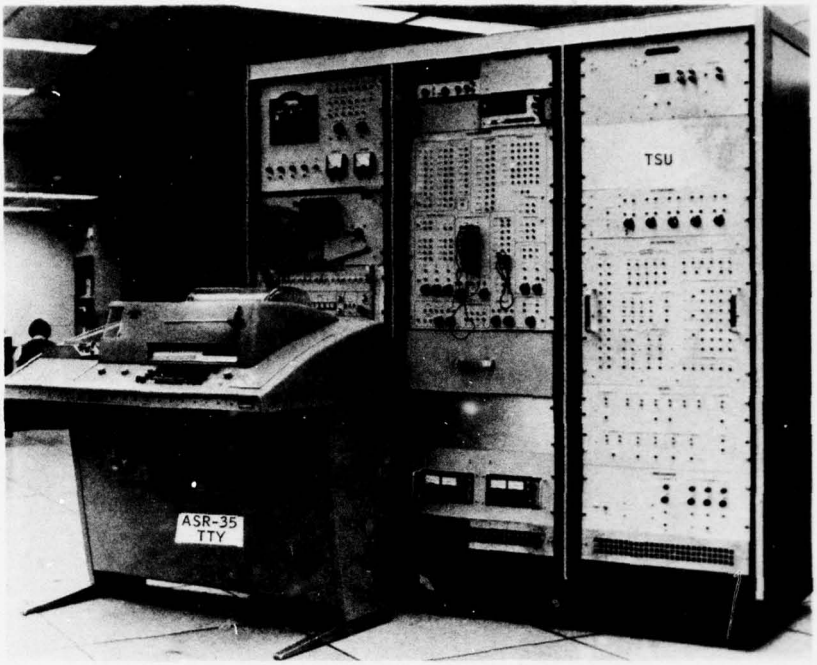

Figure 3.2-8 Test Set Unit (TSU)

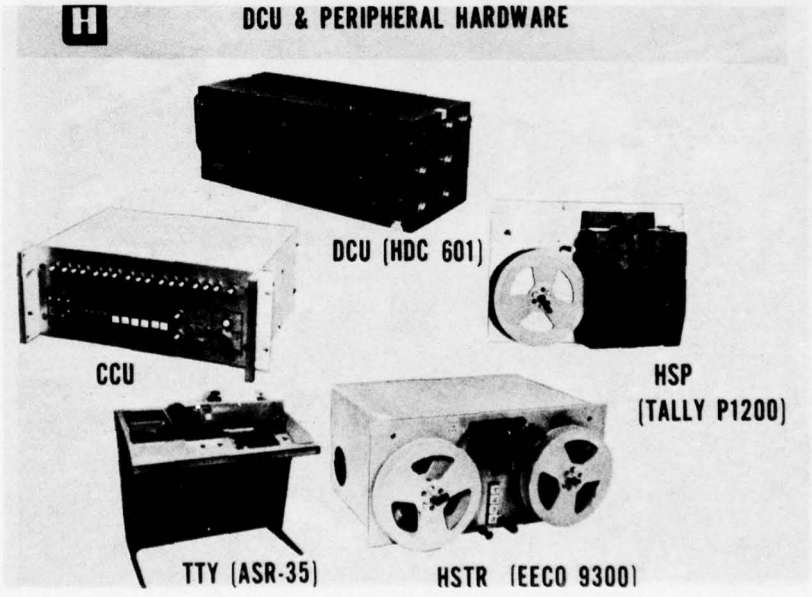

Figure 3.2-9 Digital Computer Unit With Peripheral Test Equipment

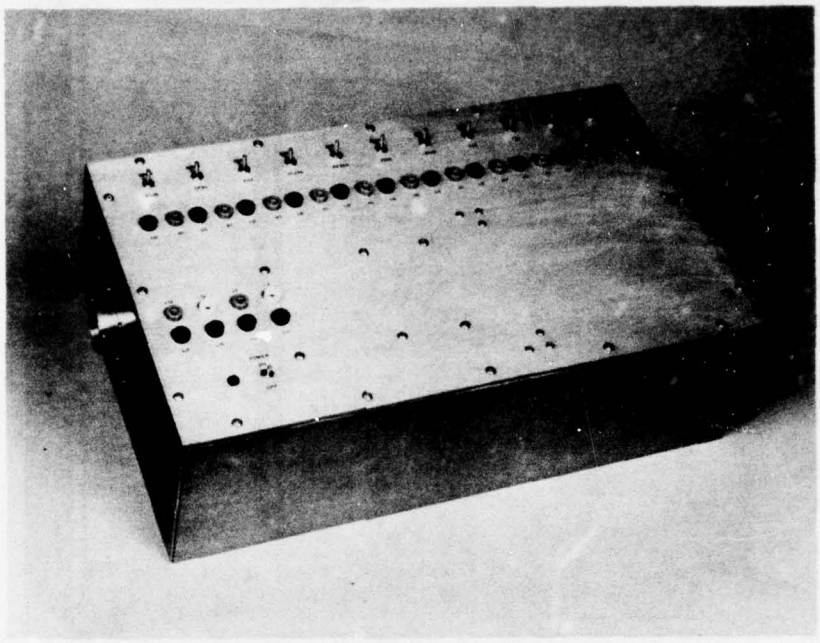

Figure 3.2-10 Breakout Box (Part of TSU)

Figure 3.2-11 SIA and System Breadboard

3.2.4.2 Computer Monitor Unit (CMU) (Continued)

CMU logic circuitry is constructed of 28 Vdc electromechanical circuitry, relays, switches, and indicator lamps. Engine trim potentiometers are also provided which may be screwdriver adjusted from the cockpit for idle, military, and A/B engine trimming. These parts have +5 volt excitation voltage across them. Their outputs are digitized by the A/ D converter, and if the CMU sense switches are set to some particular condition, these digital values will be stored by software in the DCU memory, thus permanently storing the trim values.

3.2.4.3 Simulation Interface Adapter -- The simulation interface adapter (SIA) was designed for use in the Honeywell Hybrid Computer Laboratory. This equipment provides the necessary circuitry to connect the DPCU to the Honeywell hybrid computers simulation of the TF-30-P-9 engine. Fox example, level-shift circuits take 100-Vdc signals and convert them to millivolt signals as inputs to the IFU. Voltage-to-frequency converters and sine wave function generators provide other simulated inputs to the IFU. Figure 3.2-11 shows the SIA in use early in the program in conjunction with the bread-board IFU and the DCU. The SIA is the relay rack console on the left side of the photograph.

The top two sections of the SIA are the DVM and frequency meter, which are used for calibration and monitor of inputs and outputs. The next section down is a test panel for the IFU input/outputs, which provides monitor jacks and circuit opening switches. The next panel simulated the CMU, manual inlet control and throttle inputs. The blank panel (with the handles) contains the printed circuit cards for converter circuits, buffers, function generators, and dividers. The panel below the handles contains the test and monitor facility for the simulation interface. Monitor test jacks and switches are also provided. The bottom panel contains the power supplies for the SIA circuitry.

The installation illustrated in Figure 3.2-11 is in the IPCS lab at Honeywell. This lab was directly below the Hybrid Computer Engine Simulator Laboratory. A 100-foot long cable runs from the SIA up through the ceiling to the Simulation Lab. This installation provided a functional DPCU system for I/O testing, simulating real-time checkout, and software development early in the program.

3.2.4.4 Cables -- Poor cable design can cause noisy signals, ground loop problems, cross-talk problems, random intermittent failure, inductive load transient problems, unbalanced Thevenin driving impedance effects, and RF noise problems. It was for these reasons that Honeywell designed the cabling for the bench sea-level-static and altitude test installations. The engine cables were provided by Pratt and Whitney Aircraft and Bendix. The control cables connected with the engine cables at a five-connector interface on a forward rib of the engine. The cable design used for the test installations was used for the baseline specification for the aircraft cabling. Double-shielded balanced lines were used for low-level differential sources, distributed ground returns were maximized where ground loops existed (signal-ground return), heavy multiline ground returns were used, and RF shield terminations were box-connected to a close proximity central point. The single-point system ground exists on the inboard cold plate connector end of the IFU.

All system ground and signal lines were analyzed with reference to this single-point system ground. In some cases it was necessary to isolate certain lines: TIGT (T4) sensor required isolation transformers, inlet pressure transducers required an isolated floated ground return for the special power supply for these devices, the DCU/IFU interface required a cable driver buffer design, inductive load lines required clamps at the proper location, and shields were required to prevent cross talk from high-power switched lines.

3.3 AIRFRAME AND INLET HARDWARE

3.3.1 DPCU Box and Mounts

The DCU, the IFU, and the PSU were installed in a box assembly that was mounted in the right-hand side of the F-111 weapons bay. The box was designed to be supported from the existing weapons attachment fittings without modification to the existing structure or installed aircraft equipment. The box provided environmental protection to the electronic equipment and was designed and tested to withstand the vibration environment described by curve B of Figure 3.4-1, which was extracted from NASA FRC Process Specification 21-2 (Reference 8). A fairlead for the DPCU wiring was provided in the box. The box assembly is shown in Figure 3.3-1; Figure 3.3-2 shows the box installation.

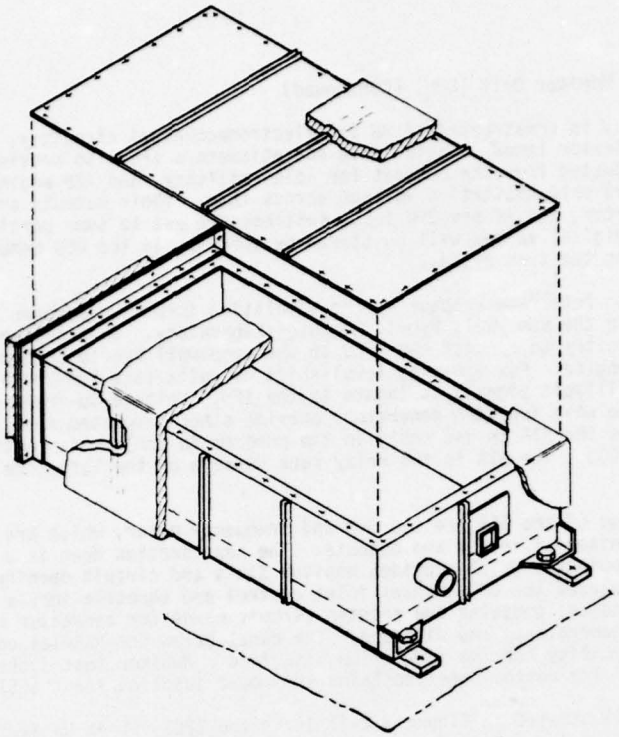

Figure 3.3-1 DPCU Box Assembly

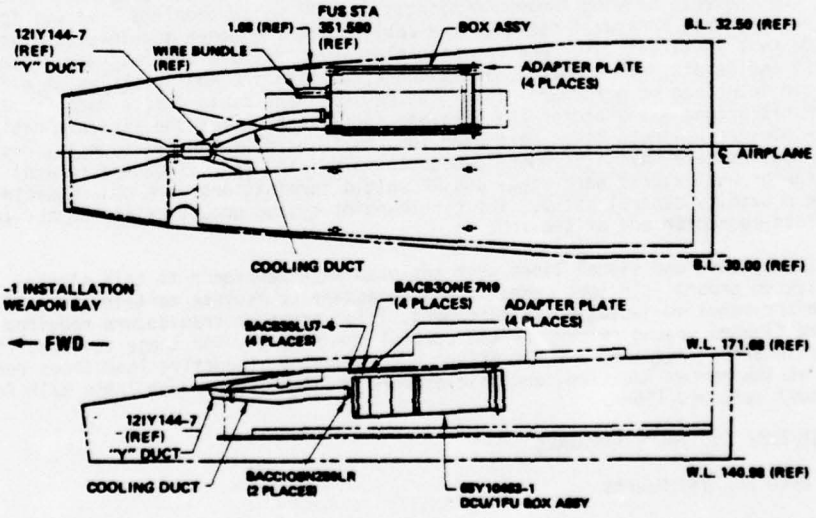

Figure 3.3-2 DPCU Box Installation in Weapons Bay

3.3.1 DPCU Box and Mounts (Continued)

The DPCU System components were installed in the box assembly with the Power Supply Unit connected directly to the cooling system air. (see Figure 3.2-2). This air was then exhausted thru a venturi into the box assembly. The venturi regulated the air flow into the box assembly to 3.0 - 3.4 lb/min. The ΔP across the box varied from .07 psid at sea level to .64 psid at 55,000 ft. The cooling air flowed thru the IFU and DCU and was exhausted into the weapons bay thru the aft end of the Box Assembly.

The DPCU box assembly was suspended from four shockmounts which were attached to the weapons attach fittings. The box assembly was covered with a foam rubber insulation to reduce heat transfer from the weapons bay. The permanent system wiring was installed thru a fairlead in the forward end of the box. Connectors were installed in the box end plate to permit test equipment hookup without opening the box.

The only testing required on the box was to vibrate it to show that the box would not amplify the input loads to a level unacceptable to the DPCU components mounted inside. It became apparent from the start of vibration testing that the box assembly was amplifying the input load by 4-5 times with loads to +19G's indicated. After some experimentation with rubber pads, commercially available shockmounts were selected and installed on the box assembly. The tests were repeated; the maximum load observed was 5.4G's. This occurred at 14 Hz. From 27 Hz to 500 Hz the loads were damped by the shockmounts to a level significantly below the levels of reference 8.

It was decided that the loads were satisfactory and the second DPCU system was then vibration tested within the box assembly.

A drawing change was made to show the changes required for installation of the shock mounts.

3.3.2 Shock Position Probe

The shock position probe is a tapered tubular probe that extends 16.0 inches forward of the air induction inlet. It was mounted on the outboard side of the left hand air induction system cowl lip, 45° below the horizontal spike centerline. No protrusions were permitted to extend into the inside surface of the air induction lip and the probe assembly was required to be removable.

The probe consists of a probe body, a pressure transducer, and a housing assembly as shown in Figure 3.3-3. The probe body was a tapered tube with .062 inch diameter holes spaced .50 inches apart along its length, starting 2.0 inches from the probe tip. The holes were in line on the side next to the inlet. The holes were all vented into a common plenum running the length of the probe. The pressure in the plenum was measured by a MB Electronics 25 PSIA pressure transducer threaded into the probe body plenum. The probe body was installed in the housing assembly that was attached to the inlet cowl. The inlet structure had to be modified to provide adequate strength for the shock probe assembly. The shock probe installation is shown in Figure 3.3-4.

The shock probe assembly and pressure transducer had to be operable from -65°F to +275°F, from sea level to 60,000 ft and had to withstand vibration as defined by curve "D" of reference 8.

The shock probe was used during baseline tests only and its use is discussed in Section 5.2.

The original design of the shock probe housing assembly had the housing welded to the mounting plate. During initial FAT testing the weld joint had started to fail when the test was completed. A modification to the weld was made as to joint preparation, size and length of the weld. This caused unacceptable material distortion and weld cracks when attempts were made to minimize distortion.

It was then decided to machine the base plate in one piece. This was done and the FAT testing was repeated successfully. The probe was tested to curve "D" of reference 8. The transducer was not installed in the probe during tests as it had passed flight assurance tests prior to purchase. The transducer weight and C.G. was simulated during shock probe tests.

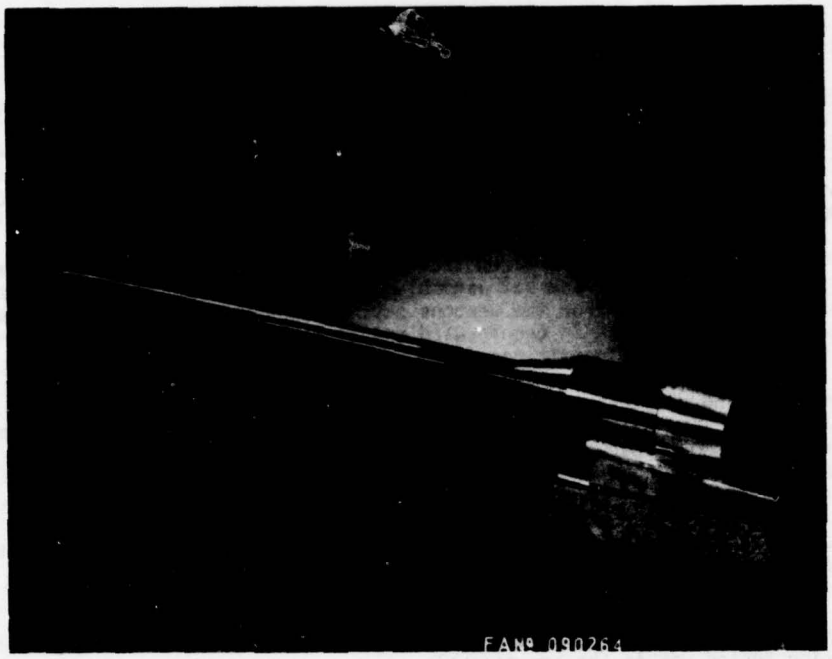

Figure 3.3-3 Shock Probe Assembly

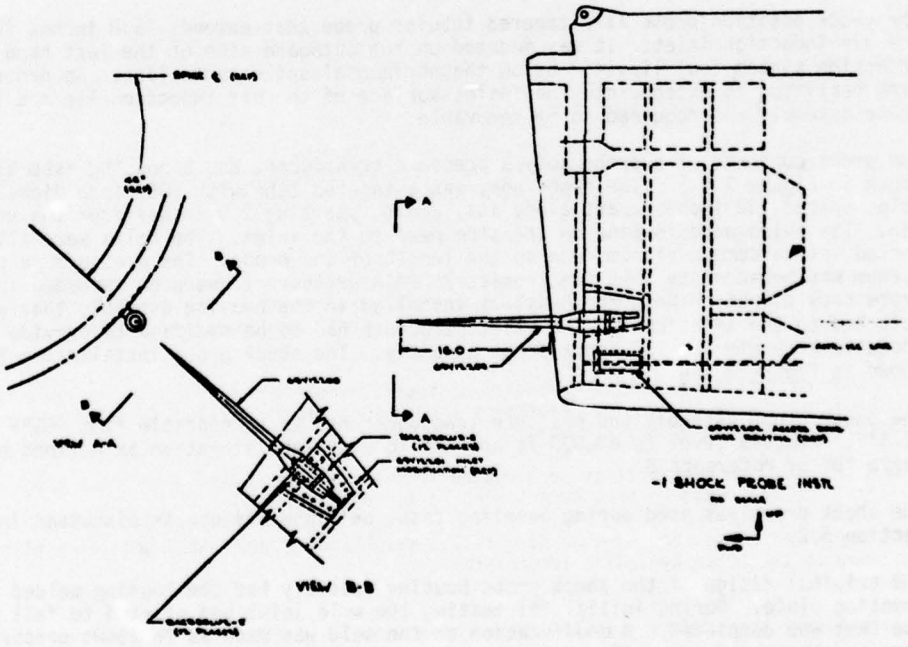

Figure 3.3-4 Shock Probe Installation

3.3.3 Transducers and Mounts

The transducer installations included the local Mach pitot and static probe diffuser exit Mach pitot and static and the distortion probe sensor installations.

3.3.3.1 Local Mach Sensor Installation

The bill-of-materials local Mach pitot probe and static port are made in one unit that is located forward of the air induction inlet on the lower surface of the wing glove.

Two (2) pressures, a pitot and a static, are picked up and transmitted to pressure transducers mounted in the well above the local Mach mounting base. The existing tubing was disconnected at the probe. The PLM and PSLM pressure transducers were connected directly to the probe with short lengths of tubing. The transducers were insulated from the skin surface for thermal protection. Wiring was routed from the transducers thru the existing sensor pneumatic lines to the aircraft weapons bay.

The transducers used were Paroscientific Inc. Model 230-A, 0-30 psia.

The local Mach pitot and static installations are shown in Figure 3.3-5.

3.3.3.2 Diffuser Exit Mach Sensor Installation

The diffuser exit Mach pitot pressure is picked up at the nose cone on the front of the engine. The diffuser exit Mach static pressure is picked up by a static port located within the air induction inlet duct. These pressures are transmitted to their respective pressure transducers mounted in the main landing gear wheel well and in the area behind the left hand inlet control unit. The existing probe, port and pneumatic lines were used.

The diffuser exit Mach static transducer installation was mounted on a plate that is attached to the upper surface of the wheel well top panel. The pneumatic line to the transducer connected to the existing diffuser exit Mach static line in this area. A shock isolator was installed to protect the transducer from impact loads that could damage the unit.

The diffuser exit Mach pitot transducer was also mounted in the wheel well, on a plate at the aft left hand side. The pneumatic line for the transducer was connected to the existing diffuser exit Mach pitot line at the engine firewall.

3.3.3.3 Distortion Probe Sensor Installation

Four steady-state total pressure probes located immediately forward of the engine compressor face were used for direct distortion measurement as discussed in para 2.3.1.2. The pressures picked up were transmitted to pressure transducers mounted in the main landing gear wheel well.

The four distortion probes were mounted on four of the eight existing rakes which were mounted forward of the engine compressor face. (See Figure 5.2-10). Design and installation of the probes was done by NASA-FRC.

Four 1/8" O.D. pneumatic lines were routed from the pressure rakes, thru the engine firewall to the pressure transducers mounted in the wheel well.

The pressure transducers were mounted in the main landing gear wheel well on a plate clamped to the brake hydraulic accumulators.

All pressure transducers installed were Paroscientific Model 230-A 0-30 psia units.

3.3.3.4 Position Transducers for Inlet Surfaces

The position signals that were required for closing the inlet surface position loops were generated by linear variable differential transformers (LVDTs) that were mechanically coupled to the spike and cone actuators. The LVDTs were built by Kavlico Electronics. The units were standard designs modified as required to match the strokes of the actuators.

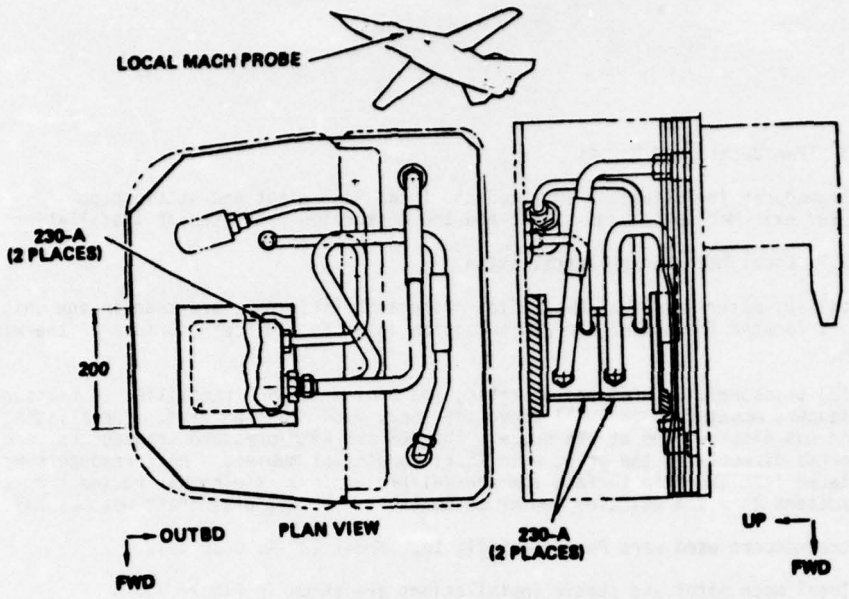

Figure 3.3-5 Local Mach Probe Transducer Installation

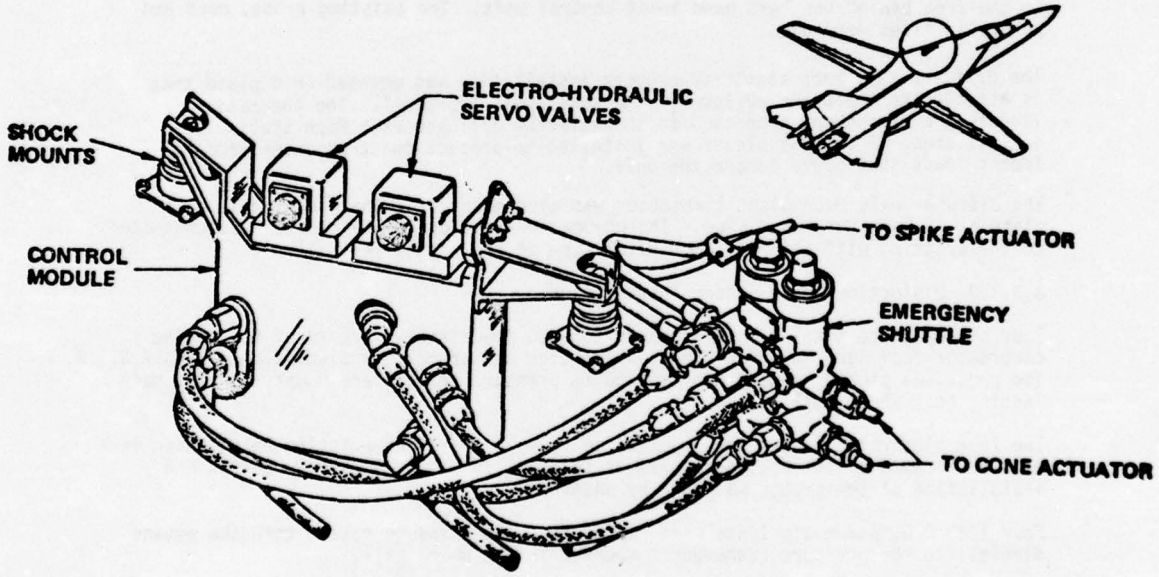

Figure 3.3-6 Inlet Control Module Installation

3.3.4 Hydraulic Inlet Control Module

The left-hand Hamilton-Standard hydromechanical inlet control was removed from the aircraft and replaced by a custom-built electrohydraulic unit that interfaced with the IFU. The installation is shown in Figure 3.3-6. The unit was designed around electrohydraulic servovalves that drive the actuators in the conventional fashion. It also incorporated a solenoid operated shuttle valve assembly to drive the inlet surfaces to the take-off position (spike forward, cone contracted) if electrical power is interrupted. Flow control orifices were installed in the shuttle-valve plumbing to increase the time for full stroke travel to 150 +30 seconds. This was to allow sufficient time for the aircraft to slow below the inlet buzz threshold speed in event of an inadvertent reversion at high speed.

The module was designed to be completely interchangeable with the mounting of the normal aircraft unit. The ports were located to allow the use of the existing hydraulic hoses. The gas-driven emergency inlet actuation system that is provided to drive the inlet surfaces to the take-off position in event of hydraulic power failure were retained, unaffected by the IPCS installation.

The subcontract to design and develop the Inlet Control Module was performed by E-Systems, Inc. Montik Division. The module was designed to the requirements of Specification Control Drawing D251-10023.

3.3.5 Manual Inlet Control

The test airplane was equipped with a Hamilton-Standard "AIC-11-3" manual inlet control unit for the baseline flight test. NASA-FRC personnel installed the unit in the airplane. Spike and cone position indication was provided by indicators mounted on the manual control panel.

Modification to the system was required prior to IPCS flight tests. These modifications included replacement of the 16 VDC spike position indicator with a similar 6 VDC unit, and rewiring of the unit from the control panel to the DPCU.

The IFU provided the excitation for the manual inlet control AUTO/MAN switch and the command potentiometers. Two (2) outputs were provided by the IFU which drove the spike and cone position indicators. Hence the manual inlet control operable only when the DPCU power was on. (The DPCU could be either engaged or disengaged.) This limitation did not impose any penalty on any of the test operations.

3.4 DEVELOPMENT AND FLIGHT ASSURANCE TESTING

3.4.1 DPCU

Development Testing--Development testing of the DPCU followed the classical design and development test sequence. Breadboards were constructed of special IFU circuits, tested, modified as required, and retested to ensure proper function and the ability of the design to meet specification requirements. Also, the actual transducers and actuators with which the IFU had to interface were obtained, and tests were performed to ensure compatibility.

The next phase of development testing consisted of constructing breadboards of the additional IFU circuitry required to complete the construction of a functional system breadboard. Figure 3.2-11 is a picture of the system breadboard. Real-time DPCU-breadboard to simulation tests were run to verify the system design.

The next phase of development testing consisted of tests of IFU production-version printed circuit cards. Three card test boxes were constructed to facilitate these tests. The printed circuit cards were tested to design specifications as outlined in the Design Specifications DS24715-01, Part II, Section 6. Temperature tests were performed on selected cards, which had critical temperature-sensitive requirements. The tested printed circuit cards were then assembled into the IFU chassis a few at a time, and IFU build-up was tested with interface to the DCU, PSU, CMU, and TSU. The DCU, PSU, CMU, and TSU had undergone their related design specification acceptance test procedures (ATP) tests prior to these tests. These IFU build-up tests are specified in DS24715-01, Part II. They constitute the long-form ATP for the DPCU. Upon completion of the build-up testing ATP for the first IFU, this first DPCU system was used in the Hybrid-Simulation Laboratory for continued real-time testing of the system and for software development.

3.4.1 DPCU (Continued)

During this time the second DPCU system was tested in like manner to prepare it for flight assurance testing (FAT). Both DCU's had undergone FAT at Honeywell-Florida prior to shipment to Minneapolis, and therefore did not require FAT as a subassembly. The DCU did undergo additional FAT, however, as part of the total DPCU.

Flight Assurance Testing - Flight assurance testing (FAT) of the DPCU system consisted of tests of the flight hardware as subassemblies and of the system with the DCU, IFU, and PSU mounted in the DPCU aircraft mounting box as shown in Figure 3.2-2. The tests were performed to ensure compliance to the design specifications (DS) for the specific devices and for the system. Test plans and ATPs were written based on these specifications to provide procedures for orderly, recordable test sequences. The requirements for these tests were therefore indirectly derived from reference 8.

Initial tests were performed on the DCU at Honeywell-Florida where temperature and vibration testing were also performed. Similar tests were performed later in Minneapolis on the IFU, PSU, and CMU. The TSU was tested functionally at room temperature only.

The IFU was initially tested to ATP by the long-form test program at room temperature and the results were recorded as previbration. Then, during vibration testing, the semi-automatic short-form test program was run. At the conclusion of vibration testing, the IFU was long-form tested, and these results were recorded as post-vibration. The same long-short-long form test approach was used for the temperature tests.

The temperature tests were performed with the IFU, DCU, and PSU mounted in the DPCU flight box. The box was placed in a pressurized altitude chamber, which was set to the worst case altitude of 8000 feet, and the minimum cooling air flow was provided. A temperature stabilization period was allowed, then power was applied, and the short-form test was performed. Testing with continuous worst-case 80°F input air at 3.35 lb/min) resulted in some failures which were subsequently overcome, but the purpose of the test was to ensure operation at nominal long time with the specified cooling air at 45 +5°F at 3.5 lb/min.

Momentary malfunctions of the altitude chamber caused over-temperature conditions to occur, but the automatic temperature-sensing, power-off circuitry of the DPCU provided protection.

Both DPCU systems were then shipped to Pratt and Whitney Aircraft in East Hartford, Connecticut for bench and sea level static (SLS) testing. At the conclusion of SLS testing, one of the DPCU systems was returned to Minneapolis where EMI tests were performed. The same basic test sequence was followed: pre-EMI long-form test, short-form tests during EMI environments, and finally post-EMI long-form tests. Figure 3.4-1 shows the equipment setup while running the short-form test program during vibration tests.

The software associated with the long-form and short-form ATP programs is described in Section 4.0

3.4.2 Transducer Box

The transducer box was originally designed to provide a fuel-cooled housing for the pressure transducers and mounting provisions for the thermistors and cold reference junction probes.

The analysis performed as part of the design effort is documented in "Pratt & Whitney Aircraft Design Data Summary, PWA Hardware," Integrated Propulsion Control System Components, revised March 15, 1974, reference 9.

The flight assurance testing of the transducer box consisted primarily of three stages; acceptance tests, vibration test, and engine ground test.

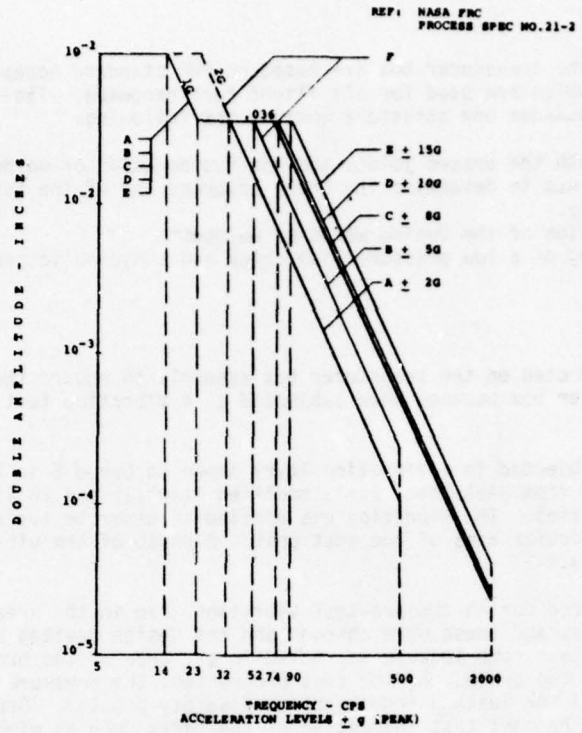

Figure 3.4-1 Vibration Test Envelope

Figure 3.4-2 Vibration Test Rig

3.4.2.1 Acceptance Tests

The acceptance tests of the transducer box are based on PWA standard acceptance inspection requirements which are used for all flight test hardware. The inspection requirements for the transducer box structure include the following:

Visual inspection of both the brazed joints and the fusion welds or weldments.
X-ray of the brazed joints to determine the braze coverage and of the fusion welds to determine integrity.
Fluoropenetrant Inspection of the fusion welds or weldments.
Pressure test consisting of a low pressure leak check and a hydraulic proof pressure test.

3.4.2.2 Vibration Test

A vibration test was conducted on the transducer box assembly to ensure the structural integrity of the transducer box package when subjected to a vibration test specified in reference 8.

The transducer box was subjected to a vibration level shown on Curve E in Figure 3.4-2, which is extracted from NASA Spec. 21-2, modified slightly due to limits of the vibration test facilities. The vibration was applied in separate tests to each of three mutually perpendicular axes of the test unit. A photo of the vibration test setup is shown in Figure 3.4-3.

Problem areas were uncovered during the pre-test vibration scan in the area of the brackets, clips and clamps, and these were changed and the design revised before the actual test. During the test some leakage was noted in the area of the braze joints which indicated cracks in the braze. As the test progressed, the pressure in the box was reduced to prevent the leakage from becoming a safety problem. Other minor deviations were noted in the post test inspection of the parts such as minor fatigue cracks in the mount pins and leakage from the steel convoluted flex lines.

Clips and Clamps

Some resonances were noted in the pretest vibration scan in the clips, clamps, and brackets. Minor revisions were made before the test and this configuration successfully completed the test. The design of the clips, clamps and brackets was changed in accordance with the test results.

Fuel Vessel Integrity

The vibration and post test inspection showed that all welds on the box were sound and no serious resonances were observed. The box as tested had encountered manufacturing difficulties which resulted in insufficient braze coverage. It was accepted that way because time did not permit rebrazing without impacting the overall test schedule. Comparison of the observed leakage locations with X-rays of the braze joints showed that the leaks were in areas of insufficient braze coverage, which resulted in braze cracking.

It was judged that the transducer box structure with sufficient braze coverage would have satisfactorily passed the vibration test. Since both program schedule and hardware availability precluded any additional vibration testing, it was decided to replace the pressurized fuel in the box with silicone oil as the heat transfer medium. The transducer boxes subsequently used for altitude and flight test were accepted with satisfactory braze joints.

Mounting Hardware

The mounting hardware passed the test with no noticeable problems. Post test fluoro-penetrant inspection revealed minor fatigue cracks in the mount pins, P/N 750356. Some galling was noted in the .370-.371 diameter of the pin which was most likely caused by the pin rotating in its mount. The pins were redesigned to press fit configuration to avoid a recurrance of the cracks and galling. A periodic inspection of the box mounts was recommended.

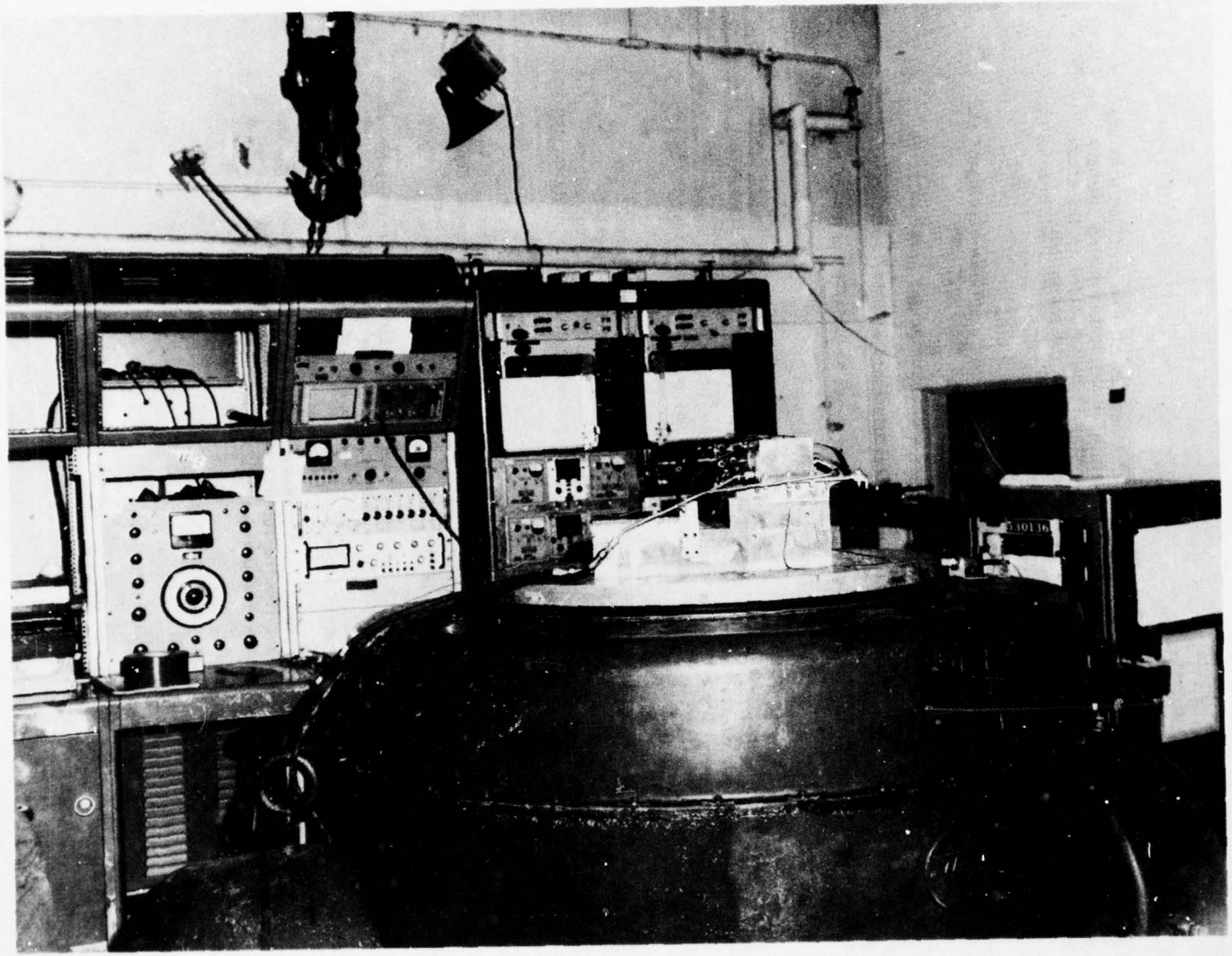

Figure 3.4-3 Vibration Test Setup

3.4.2.2 Vibration Test (Continued)

Tubes

Post test pressure test of the fuel lines and the flex lines revealed no problems with the fuel lines or the teflon flex lines. The steel convoluted lines leaked during pressure test from area under the collars where the convoluted steel tube is welded to the elbow. Teflon tubes were used to replace the steel convoluted tubes in the engine build.

3.4.2.3 Engine Ground Test

In addition to the acceptance tests and the vibration test, flight assurance testing of the transducer box was also conducted by the following engine ground testing.

- Approximately 100 hours on both P-676627 and P-676629 engine during sea level tests at PWA.
- Approximately 243 hours on P-676629 engine during altitude tests at NASA/Lewis Research Center.
- Approximately 15 hours on P-676627 engine during ground tests at NASA/FRC prior to the first flight.

3.4.3 Gas Path Probes

The gas path probes were structurally the same as the probe design from which they were derived, except for pressure and temperature connection changes external to the engine. Since extensive test experience already existed with the original designs, no separate flight assurance testing other than engine ground running was considered necessary. Table 3.4-1 summarizes this test experience.

The combination probe which measures total pressure (P22) and total temperature at the exit of the low compressor was identical to the probe designed for the "Compressor Stability Assessment Program (CSAP)," except for a slight modification. The connector end of the probe (external to the engine) was modified to average the 5 radial pressure and temperature measurements for IPCS.

The probe which senses total pressure (P3) at the exit of the high compressor in four locations was designed for and tested in experimental TF30 engines. It was also used in a specially instrumented TF30-P-3 engine tested at the Arnold Engineering Development Center as shown in Table 3.4-1. The connector end of the probe (external to the engine) was modified for the IPCS application to average the three radial pressure measurements.

The fluidic turbine inlet temperature probe was developed under an Air Force contract No. at PWA/FRDC for use in a J-58 engine and a design was developed for use in a TF30 engine. The probe ran approximately 50 hours of rig testing in a J58 rig and 50 hours in a TF30 rig in addition to the engine running shown in Table 3.4-1.

The T2, T3, and P6M probes which are used for IPCS measurements are Bill of Material in the TF30-P-9 engine, and therefore, did not require further flight assurance testing.

Table 3.4-2

Probe Substantiation

P22 Probe

Probe	Previous Use	Time	Remarks
Combination Probe	Dual Spool Rig	119 hrs.	No Probe Failures
P/N T686202	IPCS Baseline Engine Test S/N P-676629	34.5 hrs.	64 Induced Stalls No Probe Failures
	IPCS Sea Level Engine Test S/N P-676629	70 hrs.	10 Stalls No Probe Failures
P/N 724784	IPCS Sea Level Engine Test S/N P-676627	30 hrs.	No Probe Failures
	IPCS Altitude Engine Test S/N P-676629	243 hrs.	79 Stalls No Probe Failures
	IPCS Ground Test S/N P-676627	15 hrs.	2 Stalls No Probe Failures

P3 Probe

Experimental Probe	Experimental Engine Testing		No Probe Failures
P/N 483597	Special Instrumented Engine, S/N P-658886 Government Contract N00019-68-C-0414	10.86 hrs. at PWA 336 hrs. at AEDC	450 Induced Stalls at AEDC No Probe Failures
P/N 724786	IPCS Sea Level Engine Test S/N P-676629 and P-676627	100 hrs.	10 Stalls No Probe Failures
	IPCS Altitude Engine Test P-676629	243 hrs.	79 Stalls No Probe Failures
	IPCS Ground Test P-676627	15 hrs.	No Probe Failures

T4 Probe

FRDC Design Probe	J-58 Engine Test at PWA/FRDC	250 hrs.	No Probe Failures
	J-58 Altitude Test at NASA/LeRC	12 hrs.	No Probe Failures
P/N 764018	IPCS Sea Level Engine Test P-676629	70 hrs.	10 Stalls No Probe Failures
	IPCS Altitude Engine Test P-676629	243 hrs.	79 Stalls 2 Probe Failures*

*The two (2) probe failures were after 15 and 17 hours of running time respectively due to axial stress cracks imposed by the puller used to remove the probes from the engine for inspection. A modification to preclude this type of failure was made to three additional probes supplied to the IPCS program.

4.0 SOFTWARE

4.1 DESIGN

Two software items were developed to operate noncurrently within the same DPCU to provide two distinct propulsion control modes. The first of these is the Bill of Materials Digital or BOMDIG control computer program contract end item(CPCEI), and the second is the IPCS control CPCEI. Requirements and information peculiar to their design, development, performance, test and qualification were established and presented in design specification documents DS24716-01 and DS24717-01, respectively.

The implementation of the design was organized by dividing the programs into computer program components (CPC). Four basic CPCs were identified:

- Executive CPC
- Sensor Processing CPC
- Control CPC
- Output Processing CPC

In addition, a computer program data base was required.

The functions assigned to each component are described in Table 4.1-1.

Table 4.1-1 Functions of the Computer Program Components

Component	Function
Executive CPC	Concerned with interrupt processing, process scheduling and data input, mode identification/ selection, main fuel (WFGS) validity test, and DCU self test.
Sensor Processing CPC	Provides data conversion and compensation, sensor validity test, signal synthesis, and IFU voltage tests.
Control CPC	Performs control processing and back-up computations.
Output Processing CPC	Formats commands and generates command outputs.
Computer Program Data Base	Provides data storage for access by the other CPCs. Data is provided for CPCEI interface, CPC interface, and adaptation data.

The establishment of these components provides an orderly design methodology such that the software system can be developed in relatively small disassociated components that can be interfaced into a final system. This component design also has proven effective in simplifying the implementation of software changes.

The next phase of the design required development of flow diagrams for the various components and subcomponents of the program. These flow diagrams were preceded by identification of inputs, process requirements, and outputs for each sub-component of the CPCs. Analysis and coding in DAP-16*language of these flow diagrams then provided data relating to the number of memory words and the time required to process the various components. Tabulation of these results established the number of memory words required and the processing times for each program.

The processing times were then used to establish major frame times required for each program. BOMDIG was established at 20 milliseconds, and IPCS was established at 30 milliseconds. The minor cycle time is 5 milliseconds and is automatically established by the IFU real time clock (RTC) interrupt PIL01. Therefore, the executive CPC merely counts the RTC interrupts to establish the desired major cycle times.

*Honeywell symbolic assembly language for the HDC 601

4.1 DESIGN (Continued)

Allocation of memory to each component was then established, with some spare locations allotted to each component for expansion and modification.

Additional memory was allocated to a new CPC, a field maintenance program called MEDIC. The MEDIC program, described in Section 4.3.3, has proven invaluable as a resident tool for software development and troubleshooting.

The required performance of the computer programs was verified by the tests described in Table 4.1-2.

Table 4.1-2 Computer Program Tests

Test	Description
Category A	Open-loop tests of those requirements that were verifiable independent of the IFU, PSU, and CMU.
Category B	Open-loop tests of those requirements that could not be verified without interface to the IFU, PSU, and CMU.
Category C	Closed-loop testing using the total DPCU in a flight configuration interfaced with the hybrid simulation of the propulsion module.

At the conclusion of these tests, the computer program (BOMDIG) Part Number NH1007 AA01 was delivered. It consisted of a punched program tape and a source program listing. Likewise, the computer program IPCS, Part Number NH1008AA01, was delivered. The masters for these programs were retained on magnetic tape at Honeywell.

These magnetic tape programs are run on a Honeywell 516 computer system in Minneapolis. This computer lab facility provided invaluable support functions. It has the capability for converting the master (source file) programs from magnetic tape to disc file for easy random-access editing of the program.

The edited program on the disc file can then be replaced on magnetic tape for continued program source file storage. Then if a program listing is desired, this facility can access the magnetic-tape source file and provide a line printer printout of the program. Binary-executable punched paper tapes of the program were also provided for field use.

The computer lab facility expedited the development of the IPCS and BOMDIG software because of its debug capability and the hardware available. Because the IPCS and BOMDIG programs are written in DAP-16 language, a DAP-16M2 assembler was loaded into the 516 computer memory to operate the facility. The DEBUG program was used to handle and verify the data flow; i.e., a punched-tape program was generated and then verified against memory by using DEBUG. The magnetic tape handling equipment, disc files, high-speed paper-tape reader, high-speed paper-tape punch, and line printer facilitated development. It was possible through the use of extensive comments in the listing to provide an understandable definition of a large complex program, and random access was easy to obtain for program modifications.

4.2 SOFTWARE TESTING AND VERIFICATION

4.2.1 Open-Loop Testing

Open-loop testing of software included those Category A and Category B open-loop tests that were performed without the use of the hybrid simulation or the actual engine. These tests were performed in Minneapolis and some of the initial testing was done with the Honeywell 516 computer lab facility.

4.2.1 Open-Loop Testing (Continued)

The next test phase was accomplished by loading the binary-executable BOMDIG or IPCS punched-tape program into the HDC-601 DCU. The DCU, in conjunction with the MEDIC utility program, made the second phase of open-loop verification tests possible. This testing used the peripheral equipment associated with the HDC-601 (DCU) Computer: a teletype (TTY), a computer control unit (CCU), and a high-speed paper tape reader (Figure 3.2-9). The paper tape punch was not required. When punched-tape programs were required, the TTY paper-tape punch was used.

The availability of the DPCU system breadboard (shown in Figure 3.2-11) greatly expedited the next series of open-loop tests. The previous open-loop tests were relatively simple, but checking input and output processing comprises the greater part of the open-loop testing. For this test configuration the SIA was used to provide input signals, output loads, fault conditions, cockpit switching functions, cockpit indicator functions, and cockpit throttle input. By use of the MEDIC utility program and the TTY, it was possible to manually manipulate subcomponents of the program and to read out results. It was also possible to develop utility test routine loops through easy memory read/write access.

The final pre-delivery testing consisted of connection to the hybrid simulation, and performance of open-loop tests under static simulation conditions. In addition to software changes, recalibrations were required to the SIA and simulation during these tests. Completion of these open-loop tests prepared the system for the hybrid simulation to perform closed-loop testing. At this stage of the program, the first DPCU ship hardware was available. It consisted of the IFU, PSU, CMU, TSU, and DCU. After a recheck of the open-loop tests, the closed-loop testing started.

4.2.2 Hybrid Simulation

The Honeywell hybrid simulation of the TF30-P-9 engine and inlet was developed to provide for closed-loop testing in real time of the BOMDIG and IPCS programs. Also, this type of testing was developed because it is safer than running the actual engine. Software verification was accomplished by this powerful design tool, which has the following capabilities:

- Closed-loop testing
- Real-time testing
- Experimentation with different control concepts
- Real-time modeling with input sensors and output actuators
- Testing with actual controller hardware and software

The simulation was implemented by use of two 781 EAI analog computers, two 231R EAI analog computers, a PACER 16K digital computer, and a SIGMA-3 40K digital computer.

The PACER was used solely for generating bivariate functions, on-line analysis, and problem setup. The Sigma-5 computer was used to generate the control functions and to drive a scope display. The simulation was designed to run ten times slower than real time when under Sigma-5 control. Real-time operation with the HDC-601 Computer was accomplished by providing SIA interconnects. The use of the analog computers is given in Table 4.2-1.

Table 4.2-1 Functions of the Analog Computers

Computer	Function
781-1	FAN OD, FAN ID, LPC, Inlet
781-2	HPT, LPT, Engine Burner, Main Burner
231R-1	HPC, Tail Pipe
231R-2	Exhaust Nozzle, Duct Burner

The systems provided hard-copy recorder outputs of the dynamic closed-loop response of various control parameters.

Tests performed using the hybrid simulation were more extensive than software verification. The tests included:

4.2.2 Hybrid Simulation (Continued

Software Real-Time Verification
Sample Rate Studies
Control Block Diagram Confirmation
Control Algorithm Extensions
Component Failure Tests
Noise Sensitivity Tests
Digital Filter Design Tests
Stability Studies
I/O Time Skew Effect Studies

Formal documentation of control response was provided for both BOMDIG and IPCS. Tests were run at sea level and at 45,000 feet. The 45,000-foot runs were performed at 0.9, 1.6, and 2.1 Mach. Step response tests were run idle to max, max to idle, mil to 95°, max to 95°, max to mil to max, mil to idle to mil, 18° to 35°, 35° to 50°, and 50° to 69°. Additional IPCS tests were performed to check T4 sensor failure, WF sensor failure and delta P3 noise effects. Formal documentation plots were provided as a function of time for variables such as WFE, WFA/B, Aj, N1, N2, PLA, XLOOP, and others. In addition, plots of MN3 versus N2/ $\sqrt{\theta 22}$, Wf/Pb versus N2, and others were supplied.

4.3 GROUND SUPPORT SOFTWARE

4.3.1 Long-Form ATP

The initial test programs used for the DPCU system followed a long-test procedure. The chronological order of this procedure for system buildup is as follows:

1. TSU-ATP per Part II, DS24718-01
2. DCU-ATP per DS24713-01 (Reference Acceptance Test Procedure for the Integrated Propulsion Control System Digital Computer Unit and Support Equipment - ED 21540, from Honeywell-Florida).
3. PSU-ATP per section 4 of DS24933-01.
4. CMU-ATP per Part II, DS24714-01.
5. IFU-ATP per Part II, DS24715-01.

When the DPCU passed the initial build-up tests, performance of the IFU-ATP and running of the BOMDIG or IPCS programs was sufficient to verify DPCU acceptance. However, in-depth troubleshooting may require use of the subordinate ATP's for the DCU, PSU, CMU, or TSU. A malfunction of the CMU, PSU, or DCU will become evident during this IFU-ATP test procedure. The IFU-ATP included manual tests and software-controlled semi-automatic tests. The description and software coding for these tests are documented in the IFU Design Specification, Part II, DS24715-01. The program was written in conjunction with the MEDIC utility program.

The program consists of 23 stand-alone subprograms and uses the CCU sense switches along with the TTY for control. One of the subprograms is the Executive, two others are utility subroutines, and the remaining 20 programs test specific IFU functions. Hard-copy data out is provided via the TTY while performing these tests.

A punched tape is used to load the program into the DCU memory, and the MEDIC software program is also loaded into the computer memory. The TSU input signal generators are adjusted as required prior to each test, then the test is executed from the TTY by using MEDIC control "G". The results are then printed out on the TTY once or continuously as a function of CCU sense switch settings. If no sense switch (SS) is set, the program continuously cycles through the program. If SS1 is set, the sub-program stops or passes only once through that subprogram. If SS2 is set, the sub-program advances to the next subprogram in sequence and halts, or if SS3 is set, the program stops at the beginning address of the MEDIC program (16000). Other sense switch combinations are used for some of the other subprograms. Test data forms are available from Honeywell to assist in data recording, analysis, and specification requirements confirmation when required.

4.3.2 Short-Form ATP

The short-form ATP provides an automatic, fast functional test of the DPCU. The software for this procedure is described and is code listed in Design Specification DS24712-01, Part II, DPCU system. This test program inputs data from the IFU, checks it against limits, outputs data, and if all the input data passes the limits, prints "PROGRAM OK" on the TTY. Other semiautomatic and manual tests are performed to verify DPCU operation. The short-form ATP is also used in conjunction with the MEDIC program. Sense switch operations are: SS1-auto track test, SS2-auto power off test, and SS3-return to MEDIC. The program starts at location 5000 and can be entered while in MEDIC by typing line feed, 5000, followed by control "G".

Tests are run automatically and results are checked to preset limits. If the test passes the limits, it automatically performs the next test in sequence. At the conclusion of a successful complete test, the TTY prints "PROGRAM OK" and then re-initializes. If no SS is set, the program runs continuously.

If a test does not pass the limits, the program prints the following on the TTY as raw octal data: address, low limit value, high limit value, and actual value. Then the program automatically returns to 5000 and re-initializes.

Locations 5000 to 5027 initialize the DPCU. This establishes the DPCU initial conditions by properly setting up all the IFU outputs; e.g., AENTRK1, BENTRK1, FAULT, BACKUP are set to ones for DISO1; RTC-ADD setup; S/H OUTPUTS set; TTY initialize; and PROGRAM OK counter initialized. The main program starts at 5030, and through each pass routinely clears converters, starts F/D converters, counts RTC interrupts, and outputs DISO2. The DISO2 and recorder output is set all "1" then all "0" on alternate four passes through the program. It is during this re-initialization that the condition of the CCU sense switches are tested.

TSU inputs are set up to specified values for inputs to the IFU; monitor of these inputs is required to ensure that they do not drift. It is also necessary to monitor the IFU outputs on the TSU to ascertain proper DPCU function.

The main program can be used to test failure detection. By switching the CMU sense switches or manual inlet control switch, it is possible to force the program to sense an out-of-limit input from the TSU, thus causing a predictable failure printout on the TTY. It is also possible to vary other inputs such as P3S to produce a similar reaction.

The design specification DS24712-01, Part II, provides a description of the short-form ATP address assignments, software coding, and software limits table.

4.3.3 Medic

The MEDIC utility software program is used in conjunction with the long-form ATP, short-form ATP, BOMDIG and IPCS software programs. It is an on-line, octal-symbolic debugging package originally developed for the Honeywell DDP-516 Computer. MEDIC is completely self-contained, with its own bootstrap, loader, and punch routines. The TTY is its prime communication link.

Twelve utility routines are provided: Register, Examine, and Modify (A,B, index, and keys), Examine and Modify, Calculate Effective Address, Jump Option, Breakpoint, Dump Routine, Search Routines, Fill/Clear Routine, Transfer Routine, Program Loading, Program Saving, and Tape Verify. Unfortunately not all of these routines will function on the HDC-601 DCU, but a sufficient number of the routines do work to facilitate debug and modify capability. In this program for example, the Dump (to TTY or Punch), Search, Fill/Clear, Program Loading (from TTY or Reader), Tape Verify, Examine and Modify routines have been helpful in software development.

A description of MEDIC and its operating procedures has been provided in the field support data packages supplied with each DPCU.

4.4 SOFTWARE CONFIGURATION CONTROL

4.4.1 Honeywell In-Plant

Software configuration control in-plant at Honeywell follows Honeywell's conventional Engineering Change Order (ECO) procedures. The Honeywell Detail Specifications DS 24716-01 and DS 24717-01, together with the BOMDIG and IPCS programs, are therefore subject to the discipline of engineering change control. No change can be incorporated without the approval of the Honeywell IPCS Program Manager. Furthermore, all change orders processed subsequent to the commencement of bench tests were coordinated with Boeing to ensure accuracy and compatibility with the field-tested modifications.

Each computer program was revised via update of the source assembly language file (magnetic tape). Following the assembly process, the new source computer program listing was inspected in those areas which underwent modification.

Subsequent to the generation of the self-loading punched object tape, a comprehensive comparison was made of the original and revised self-loading object tapes. During that comparison, a listing was generated identifying each and every difference by DCU memory address. That listing was thoroughly inspected to ensure that each change was incorporated correctly and that no extraneous changes were introduced. Revision also included the necessary modifications to the specifications.

The self-loading object tapes, i.e., the computer programs themselves, cannot be modified in the field. Instead, the contents of the DCU memory are modified subsequent to software load by patch tapes. Such modifications are controlled through the mechanism of the Software Field Change Order (SFCO) as described in Paragraph 4.4.2.

4.4.2 Software Configuration Control in the Field

The Computer Program Contract End Item (CPCEI) configuration cannot be modified in the field. Instead, software field changes were accomplished by altering the contents of the DCU memory. Periodic CPCEI updates were accomplished through the formal Honeywell change control procedure upon Boeing request. These updates resulted in a new configuration identified by revision of the CPCEI identification number.

A formal Software Field Maintenance Procedure, approved by the government for the IPCS program was applied during the ground and flight tests. This procedure requires the use of a Software Maintenance Log (SML), a Software Maintenance Listing (SMLI) and a Software Field Change Order (SFCO).

The Senior Contractor Test Engineer on-site was responsible for software changes. He ensured that all proposed software changes were documented on SFCO's (Figure 4.4-1). The Senior Contractor Test Engineer approved all changes to be implemented and was responsible for maintaining an engineering log that documents the implementation of each SFCO and the reasons for the change.

During the flight test program, documentation describing changes made to the flight software was submitted to the NASA/FRC IPCS Program Manager or his designated representative prior to the first preflight briefing to be conducted subsequent to the change. The Senior Contractor Test Engineer discussed software configuration at preflight briefings, including the function of the CMU sense switches, and submitted a configuration report, listing the computer program (IPCS or BOMDIG), the patch tapes, and the SFCOs loaded into the computer, for incorporation in each IPCS flight report.

SOFTWARE FIELD CHANGE ORDER

Title of Program _____ (1) Change # _____ (4) [1]
Program Number _____ (2) Log Ref _____ (5)
Prog. Rev. Letter _____ (3) Date _____ (6)
Change Req. by _____

Reason for Change:

Method of Verification: [3]

Change:

Core Location	INSTR (ARG) or Loc Cont Octal	Address (Mnemonic)	Comments

Approved Rejected

Reviewed by _____
Approved by _____
[2] Paper Tape Pchd _____
Inc by _____
Verified by _____
DATE

[1] Change # composition is: (1), (3), Seq # Seq. # = 1 for 1st SFCO against a Rev. Letter
[2] All SFCOs longer than 10 words to be *punched on* paper tape. Label paper tape with change #.
[3] If method is complex, reference test procedure

Figure 4.4-1 Software Field Change Order

5.0 BASELINE TEST PROGRAM

5.1 BASELINE ENGINE TEST

5.1.1 Purpose and Scope

The baseline engine test was conducted at the NASA/LeRC altitude facility between September, 1973 and February, 1974. Its primary purpose was to catalog standard engine operating characteristics with the hydromechanical control over a broad range of flight conditions and power settings for use as reference data for dynamic simulation verification and comparative data for later integrated propulsion control system tests. Since it was the first test conducted in the IPCS program, it also served to establish procedures for test planning, coordination, and operations, and to check out data recording and processing systems.

When baseline engine testing was completed in February 1974, a substantial amount of data had been obtained during the 113 hours and 74 stalls accumulated on P-676629 and 50 hours and 70 stalls accumulated on P-676627. Both engines were shipped to P&WA following the test for incorporation of the IPCS sensors and fuel control modifications.

5.1.2 Test Operations

Pre-test coordination meetings were held in May, 1973 to aquaint the contractors with the NASA/LeRC altitude facility and to discuss test plans, instrumentation and data processing requirements and test procedures with NASA. Documents were issued for the baseline engine test plan (Reference 10) and the data reduction requirements (Reference 11) following these meetings.

Testing began in late September, 1973 with P-676629 installed in PSL #1. The engine was trimmed with a remote trimmer at a near sea level static condition (approx. 5000 ft/.05 Mn) in order to maintain sufficient cooling airflow through the cell. The following seven flight conditions were simulated in the altitude test chamber during the fall, 1973 testing of P-676629.

Altitude - ft.	Mach No.	T2 - °F	Reynolds Index
22000	1.06	85	0.8
41000	1.4	85	0.5
52000	1.4	85	0.3
30000	0.8	+6	0.5
45000	2.1	275	0.8
48500	2.25	325	0.8
51500	2.39	375	0.8

Steady state gas generator data were recorded for 4 compressor bleed configurations: closed; 7th open and 12th closed; 7th closed and 12th open; and 7th open and 12th open. Three exhaust nozzle positions were also tested for non-A/B operation: nominal (3.75 ft^2); full open (7.05 ft^2); and with a plug (6.0 ft^2). Gas generator transients and afterburner transients were conducted at each test condition except at the high supersonic Mach numbers where the gas generator operating range is small.

In early December, 1973 an excessive spread in low turbine discharge temperature was observed after approximately 80 hours of operation. Data analysis indicated the spread was coincident with a noticeable increase in secondary manifold nozzle pressure drop. P-676629 was removed from the test cell and shipped to the Oklahoma City Air Logistic Center where a hot section inspection verified that main engine burner nozzles exhibited streaky, low flow characteristics and showed evidence of coking in the secondary nozzle passages. Nozzle clusters were replaced and the engine was returned to NASA/LeRC for further testing.

The nozzle coking was attributed to sub-idle operation at the high Mach number test conditions. Normally, idle power setting is established with a Mach number bias on idle governing speed. The bias is implemented through a Mach lever on the fuel control which is positioned by a signal from the aircraft computer. The Mach lever was not used during NASA/LeRC because the function of the aircraft computer was not duplicated. Thus, when idle power lever angles were selected at high Mach numbers,

5.1.2 Test Operations (Continued)

rotor speeds and fuel flows were below nominal idle settings, and the low fuel flow rates at high compressor inlet temperatures were conducive to fuel coking. This problem was resolved for later testing by positioning the power lever manually to maintain idle speeds pre-determined for each test condition.

The removal of P-676629 was followed by installation of P-676627 and upstream airjets which were used to produce inlet distortion through a momentum exchange with the engine inlet airflow. Testing of P-676627 commenced on December 11, 1973 and ended on January 18, 1974 and was limited to inlet temperatures of 85°F and below. A total of 70 stalls (9 at 22000 ft/1.06 Mn, 0.8 RI2; 48 at 41000 ft/1.4 Mn, 0.5 RI2; and 13 at 52000 ft/1.4 Mn, 0.3 RI2) were induced with the distortion generated by the airjets over a period of 50 hours.

After P-676627 was removed, P-676629 was re-installed and testing resumed on January 28, 1975 with the airjets. Distortion tolerance of P-676629 was determined from a total of 74 stalls (67 at 41000 ft/1.4 Mn, 0.5 RI2; 3 at 52000 ft/1.4 Mn; 0.3 RI2; and 4 at 30000 ft/0.8 Mn, 0.5 RI2). Total P-676629 baseline test time was 113 hours.

5.1.3 Data Operations

Steady state and low frequency response (to approximately 50 Hz) data were recorded digitally and converted to engineering units by NASA/LeRC. Transient data were recorded and digitized at the rate of 20 samples/second. On-line steady state digital data were sent to Boeing and P&WA after completion of each test. Magnetic tapes with digital steady state and transient data were sent to Boeing for further processing and then to P&WA for machine plotting.

5.1.4 Results

The baseline engine tests conducted at NASA/LeRC substantially increased the engine data base for the IPCS program. They defined steady state and transient operating characteristics for both engines at seven flight conditions, four compressor bleed settings, and three exhaust nozzle areas. Distortion tests conducted with the NASA/LeRC airjet system defined the distortion tolerance levels of both engines. The large data matrix generated during baseline engine tests is shown in Table 5.1-1. These results were used to refine the TF30-P-9 dynamic simulation and thus improve the accuracy of IPCS control mode studies. They also served as reference data for later engine testing with the IPCS control.

Several conclusions were made after completion of the baseline engine tests. A comparative analysis of the baseline test engines showed engine P-676627 generally demonstrated better performance than engine P-676629. This was evidenced by approximately 1 percent better overall turbine efficiency, 0.5 percent better overall compressor efficiency, 1.5 percent lower low compressor operating line, and 300-400 Kd higher distortion tolerance for the backup engine. These performance differences were attributed to the 250 hours of prior operation accumulated on P-676629 before overhaul in November, 1972, versus no prior use of engine P-676627.

The P-676627 engine distortion tests generally substantiated the TF30-P-9 distortion tolerance predictions. One exception was the predicted effect of seventh stage compressor bleed on distortion tolerance. The engine demonstrated more distortion tolerance with 7th stage bleed than predicted. This same relative trend was observed in the P-676629 engine distortion tolerance test results. The under estimate of the 7th stage bleed effect on distortion tolerance was due to basing the TF30-P-9 distortion tolerance on test data for the TF30-P-412 which has a smaller 7th stage bleed port area. The TF30-P-9 distortion tolerance predictions were revised to account for the larger improvement in distortion tolerance with 7th stage bleed.

The distortion tolerance predictions were also revised to reflect the lower tolerances demonstrated by the P-676629. As described above, this 300-400 Kd difference between the two engines was attributed to the prior use of engine P-676629. The 1.5 percent higher engine P-676629 low compressor operating line accounted for approximately one third of the lower tolerance, and the remainder was attributed to a reduced low compressor surge line. The difference in distortion tolerances was reflected in the

5.1.4 Results (Continued)

IPCS control schedules for each engine (Figures 5.1-1 and 5.1-2). The distortion tolerances measured during the baseline tests were also used as a reference to gauge the effect of the IPCS engine modifications on engine performance during the IPCS altitude testing in the spring of 1975.

TABLE 5.1-1

BASELINE ENGINE TEST CONDITIONS

Test Condition	Reynolds Index	Inlet	Nozzle
Engine P-676629			
1. 22000 Ft./1.06 Mn	0.80	Clean	Closed, Plug, Open
2. 41000 Ft./1.4 Mn	0.50	Clean	Closed, Plug, Open
		Distorted	Closed, Plug, Open
3. 52000 Ft./1.4 Mn	0.30	Clean	Closed, Plug, Open
4. 30000 Ft./0.8 Mn	0.50	Clean	Closed, Plug, Open
5. 45000 Ft./2.1 Mn	0.80	Clean	Closed, Plug, Open
6. 48500 Ft./2.25 Mn	0.80	Clean	Closed, Plug
7. 51500 Ft./2.39 Mn	0.80	Clean	Closed, Plug
Engine P-676627			
1. 22000 Ft./1.06 Mn	0.80	Clean	Closed
		Distorted	Closed
2. 41000 Ft./1.4 Mn	0.50	Clean	Closed, Plug, Open
		Distorted	Closed, Plug, Open
3. 52000 Ft./1.4 Mn	0.30	Clean	Closed
		Distorted	Closed
4. 30000 Ft./0.8 Mn	0.50	Clean	Closed

An initial review of engine P-676629 on-line data received from NASA/LeRC revealed the measured total fan corrected airflow, WAR2, was 4 to 5 percent larger at high power settings than demonstrated in previous TF30-P-9 tests. A check of the engine nozzle flow parameter, FP6M, during choked operation showed a spread of 6 percent in the baseline data. Since this parameter can be expected to vary only 1 percent for nozzle choked operation, the total fan corrected airflows measured during the baseline testing were considered to be excessive. This flow measurement discrepancy was also reflected in the primary stream corrected airflow, W2R2, since it was calculated from total fan corrected airflow. IPCS control schedules were not affected, however, since they were based on a total fan corrected airflow calibration curve that was developed from numerous TF30-P-9 ground and flight tests.

Dynamic simulation predictions for engine operational characteristics were compared to the baseline test results in order to determine simulation accuracy. As shown in figs 5.1-3 thru 5.1-6 initial predictions for high rotor corrected speed and corrected fuel flow were higher than the baseline steady state data at the 22000 ft/1.06 Mn and 30000 ft/0.8 Mn conditions. Subsequent refinements were made to the engine component characteristics, and simulation predictions showed better agreement with the baseline test data as shown in these same figures.

A comparison of the gas generator transient response measured from baseline data and predicted by the simulation is shown in Figures 5.1-7 and 5.1-8. The predicted low and high rotor speed response for the same fuel flow input agrees well with the baseline data, indicating simulation heat transfer and inertia characteristics are acceptable. Good agreement between predicted and measured data during an afterburner retard is indicated in Figure 5.1-9 for the 30000 ft/0.8 Mn condition. This indicates the simulation A/B control characteristics reasonably approximate actual A/B control operation.

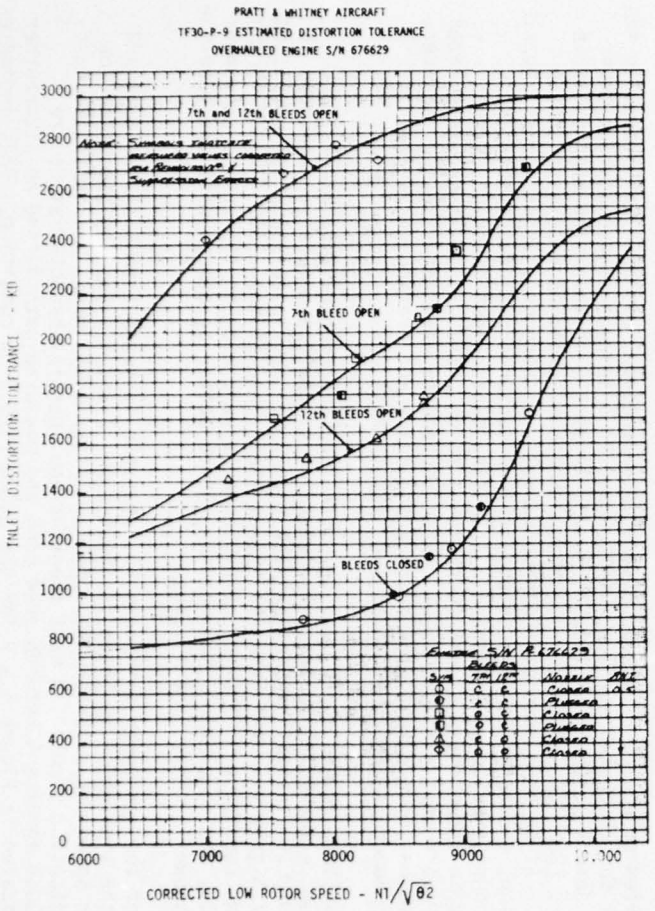

Figure 5.1-1 Base Distortion Tolerance - Engine S/N 676629

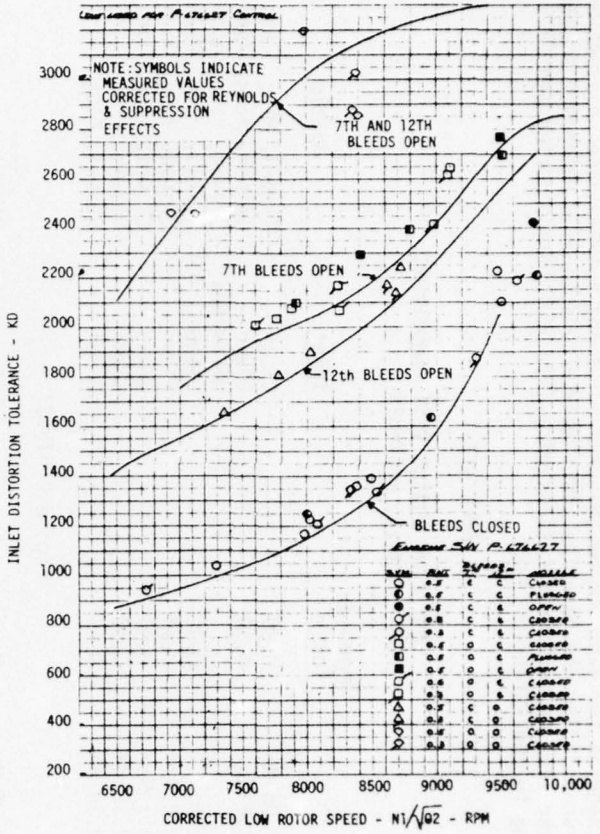

Figure 5.1-2 Base Distortion Tolerance - Engine S/N 676627

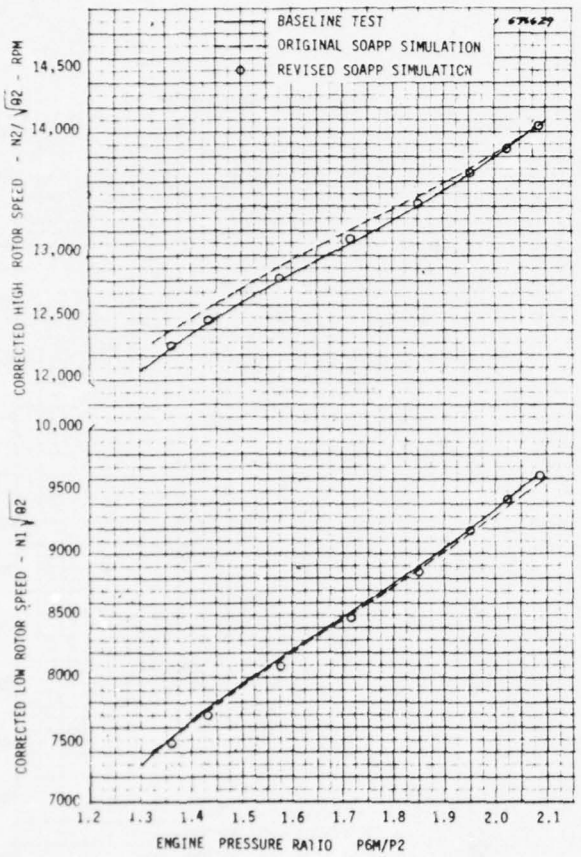

Figure 5.1-3 Engine Performance - 22K/1.06 Mn S/ N 676629

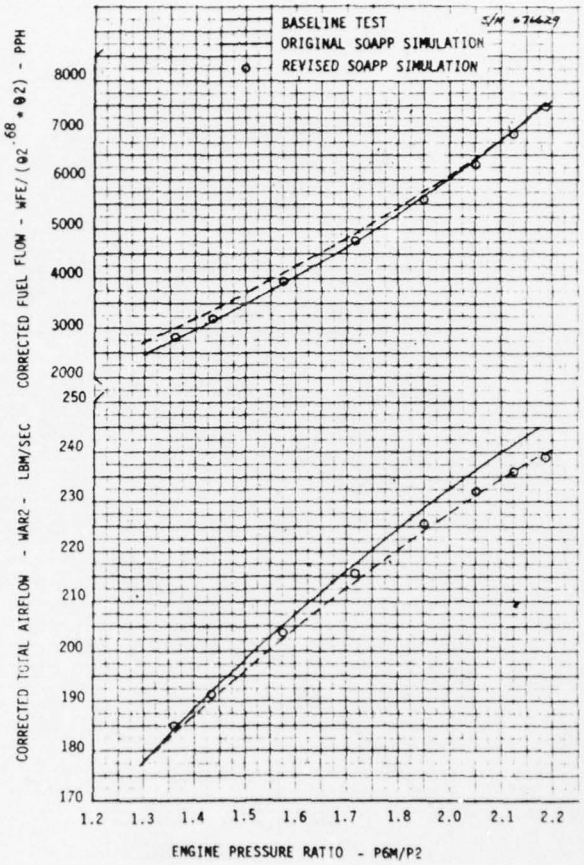

Figure 5.1-4 Engine Performance - 22K/1.06 Mn S/N 676629

AD-A033 774 BOEING AEROSPACE CO SEATTLE WASH F/G 21/5
INTEGRATED PROPULSION CONTROL SYSTEM (IPCS). VOLUME II. TECHNIC--ETC(U)
AUG 76 L O BILLIG F33615-73-C-2035
UNCLASSIFIED AFAPL-TR-76-61-VOL-2 NL

2 OF 3
AD
A033774

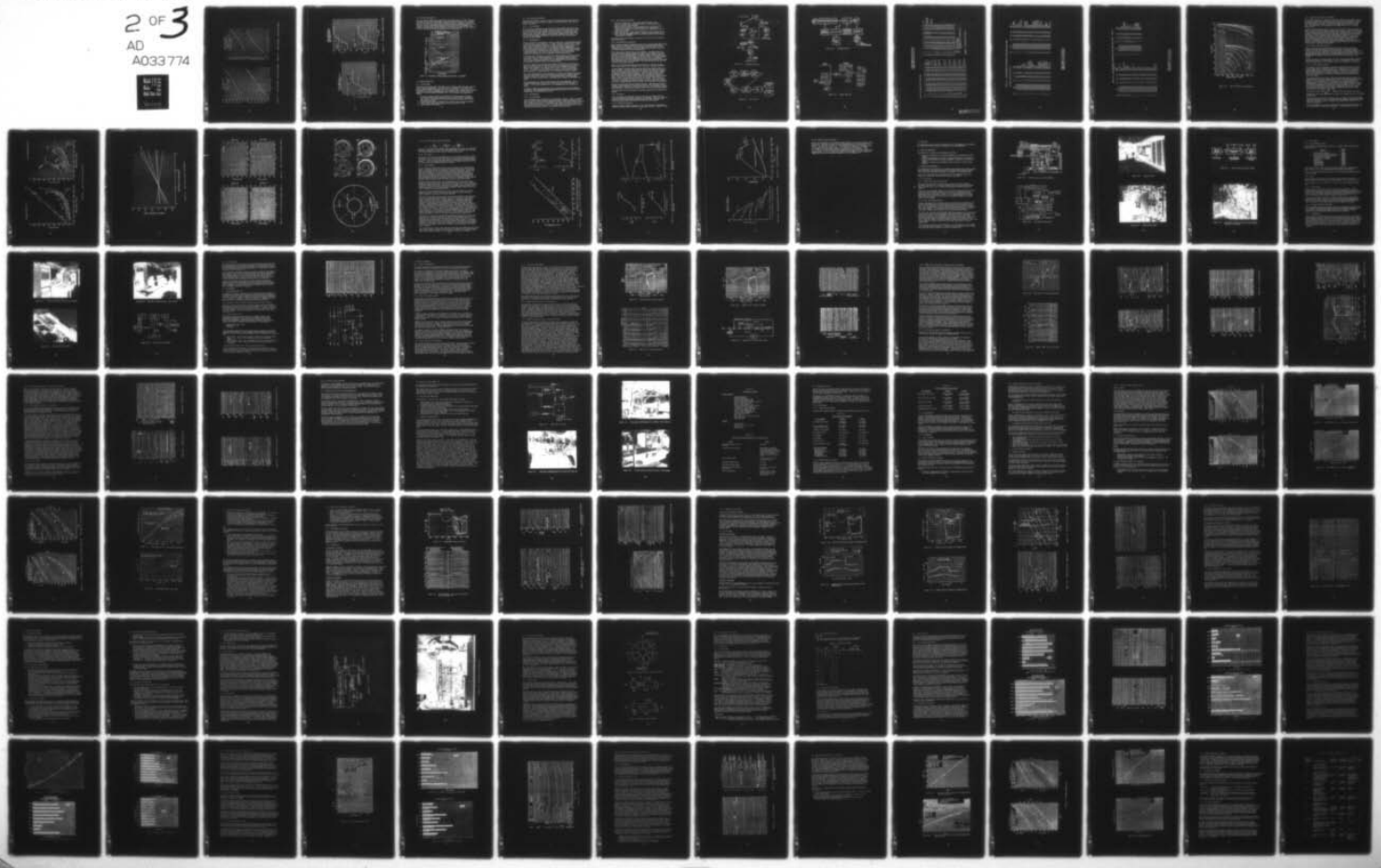

SIFIED

2 OF 3

AD

A033774

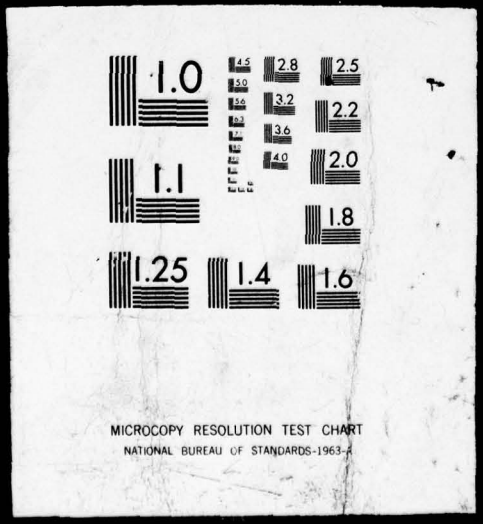

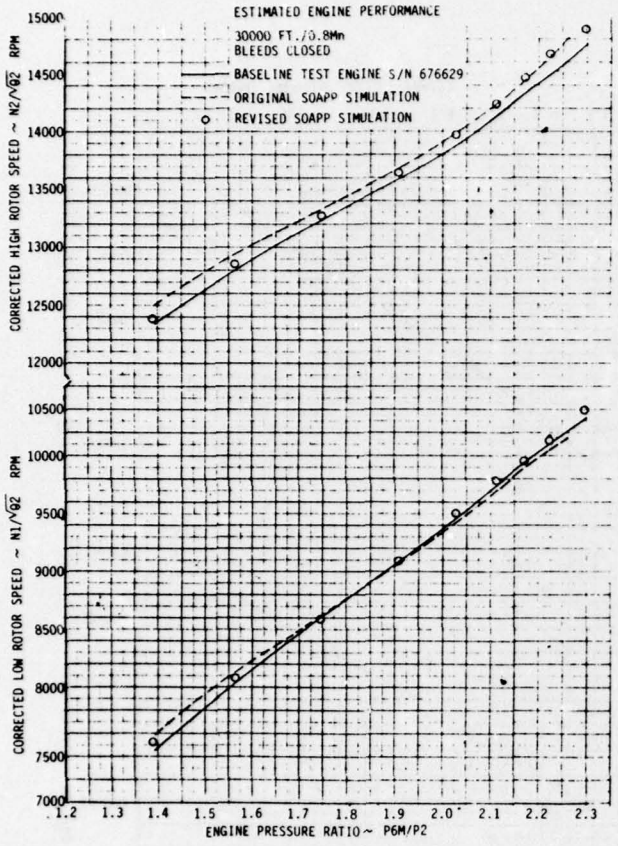

Figure 5.1-5 Engine Performance - 30K/0.8 Mn S/N 676629

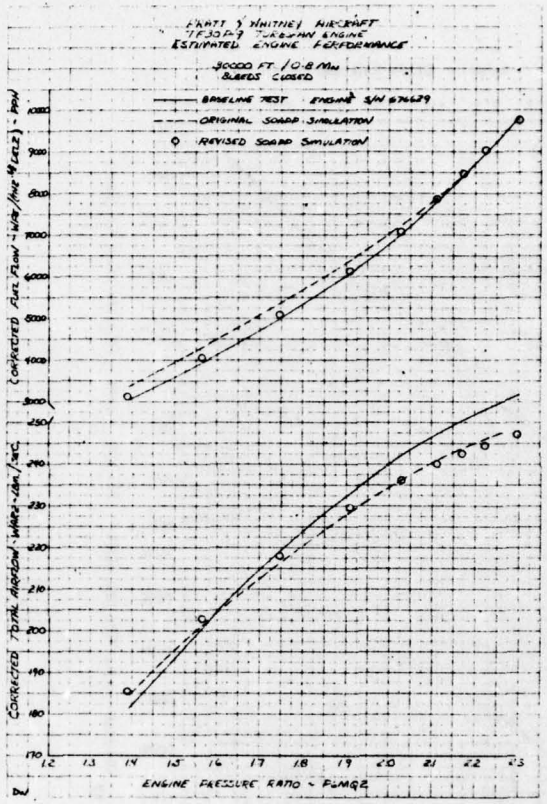

Figure 5.1-6 Engine Performance - 30K/0.8 Mn S/N 676629

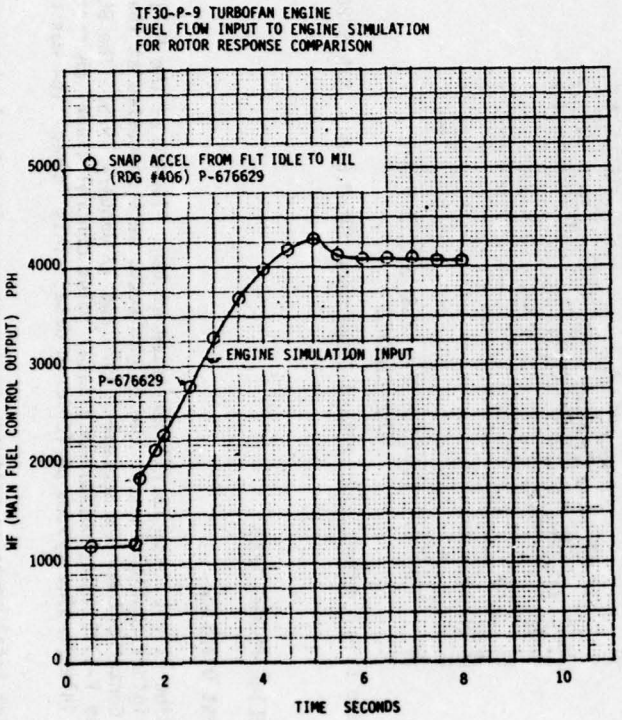

Figure 5.1-7 Fuel Flow to Engine Simulation

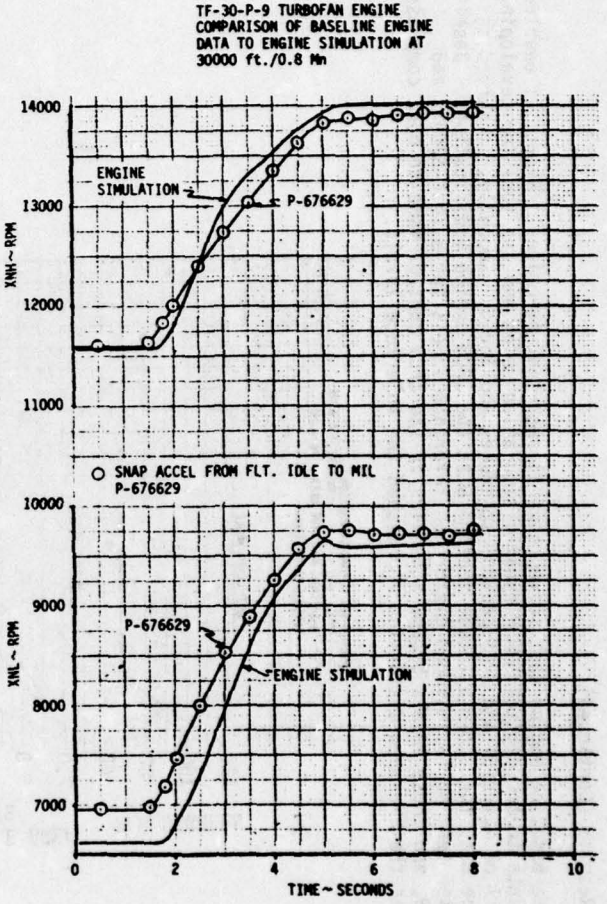

Figure 5.1-8 Rotor Response Comparison S/N 676629

5.1.4 Results (Continued)

Thus, the baseline engine test served several important functions. First, it enabled refinements to the digital SOAPP dynamic simulation which was the tool for developing both bill of material and IPCS control schedules and logic. Secondly, it served as reference data for later altitude testing with the IPCS engine modifications. Baseline distortion testing established distortion tolerance levels for both P-676627 and P-676629, and these levels became schedules in the IPCS control mode to open compressor bleeds as the measured distortion approached the tolerance levels.

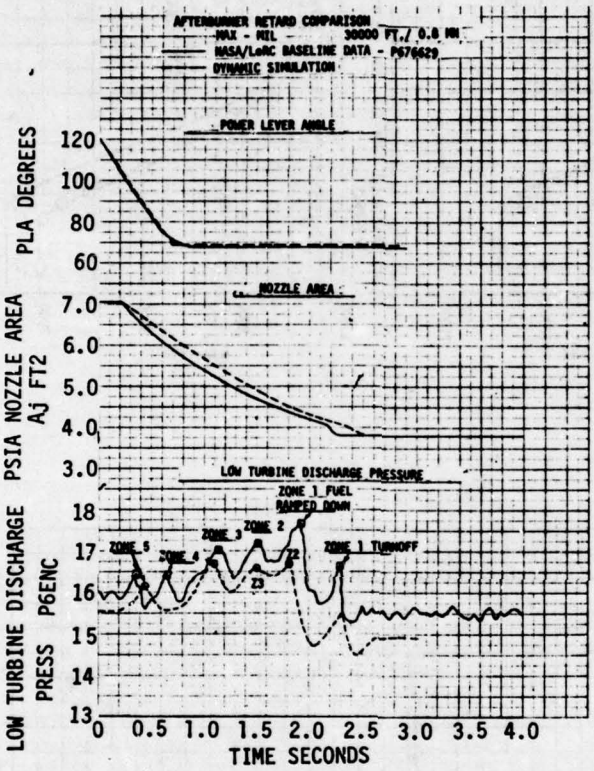

Figure 5.1-9 Afterburner Retard Comparison 30K/0.8 Mn - S/N 676629

5.2 BASELINE FLIGHT TEST

5.2.1 Test Overview

The baseline flight tests (BLFT) consisted of ten flights of the F-111E test aircraft in its original configuration. The flight tests were conducted at the NASA Flight Research Center between 24 September 1974 and 17 January 1975. The BLFT objectives were to provide F-111E inlet performance data, inlet control signal characteristics, and combined inlet/engine system performance data. This information was categorized as follows:

1. Inlet total pressure recovery and compressor face total pressure distortion as a function of mass flow and angle of attack for both the bill of materials inlet control cam schedule and off-design relationships between spike position and second cone angle.
2. Inlet and engine stability boundaries with respect to buzz, surge and flameout.
3. Inlet control signals, both standard and new with respect to IPCS.
4. System response to transients.

5.2.1 Test Overview (Continued)

Instrumentation hardware dedicated to the IPCS program which were installed during the BLFT consisted of the distortion computer, the shock position probe, and the manual inlet control.

5.2.1.1 F-111E Airplane

An F-111E aircraft (SN70115) was dedicated to the IPCS program to be used in both the baseline and IPCS flight testing. The test aircraft had Triple Plow II inlets, AIC11-3-6 inlet control cam schedule and TF30-P-9 engines. The left hand inlet/engine was the unit tested. Manual cockpit control of spike position and second cone angle was provided in addition to the standard automatic inlet control. The aircraft was also equipped with manual cockpit control of the left hand engine 7th and 16th stage bleeds.

5.2.1.2 Instrumentation

The test airplane was instrumented to obtain in-flight data. The parameters measured related directly to three categories: 1) general aircraft parameters, which include the aircraft configuration; the aircraft flight conditions, such as altitude, Mach number, angles of attack and sideslip; and aircraft stresses, temperatures, accelerations, and fuel quantities; 2) air-induction system instrumentation, which includes parameters pertaining to the inlet geometry and local flow conditions; and 3) propulsion system instrumentation, which consists of measured parameters related to engine performance, such as fuel flow rate, nozzle areas, engine speeds, temperatures, and pressure levels throughout the engine and fan duct.

A removable, inlet lip mounted, shock position sensing probe was provided by Boeing for the left hand inlet (see paragraph 3.3.2.) This tapered tubular probe was hollow with a series of holes spaced along its length vented into the plenum. A single pressure transducer mounted within the probe measured the plenum pressure. The probe was installed for most of the flight testing.

A 40 probe compressor face rake provided by NASA was installed on the left hand engine. An analog distortion computer was provided by Boeing which calculated the P&WA distortion parameter, KD, from the output of the 40 compressor face rake dynamic total pressures. The computer was installed in the FRC instrumentation capsule. In addition to being recorded, the output from the distortion computer was transmitted to a cockpit guage for online indication of distortion levels.

The flight instrumentation system incorporated a CT-77B Flexible Airborne Pulse Code Modulation (PCM) system which is a hard-wired programmable unit capable of multiplexing 80 channels at a frame rate of 200 frames per second, converting these channels to a 10 bit digital word at a sampling rate per channel of 200 samples per second.

Two subcommutators were used in conjunction with the prime commutator. The subcommutator channels were systematically substituted for the prime commutator channels. The resulting sampling rate for the subcommutators was 20 samples per second.

The eight-arm NASA 40 probe compressor face rake contained Kulite high frequency transducers. These measurements were recorded separately using an analog recording system capable of recording data to 500 Hz.

5.2.2 Test Operations

5.2.2.1 Test Procedures

Ten altitude/Mach number combinations were selected for the BLFT. Figure 1.3-2 shows these test points as they related to the other testing. These conditions provided good coverage of the inlet variable geometry requirements and an RI variation consistent with the baseline engine tests. Test events were selected to provide variation in engine operations and inlet distortion. A standard series of test events was normally conducted at each flight condition. Briefly these test events were:

5.2.2.1 Test Procedures (Continued)

1. Snap throttle transients - snap throttle movements between various PLA values, normally military maximum and idle. Each PLA was held long enough to stabilize engine operation.
2. Angle of attack transients - originally designed as an increase of angle of attack to the limit at a rate of approximately 1°/sec. After several flights this was changed to a more rapid maneuver to a specified "g" limit to protect the wing seals.
3. Yaw to sideslip limit - a nose left yaw transient at a rate of about 1/2° sec.
4. Manual spike and cone movements (MINKD) - variation in the spike position and second cone angle independently until a noticeable increase in KD was observed on the cockpit KD indicator.

Test events 1 and 4 were conducted at high angles of attack as well as at the normal cruise configuration.

5.2.2.2 Data Recording and Processing

Data recording was handled by NASA/FRC and processing was divided between NASA/ FRC and Boeing. Figure 5.2-1 shows the NASA/FRC data flow. An onboard tape was created containing 10 tracks of FM data, 1 track of PCM data, and 1 track with time of day. In addition data were telemetered to the Flight Research Center control room for on-line stripout and writing of a backup telemetry tape.

A data request based on the stripout data was submitted. The onboard tape was run through the FRC SEL 86 computer program which formats the data recorded on the PCM track and a series of formatted digitized tapes were created containing a sequential time history of the flight data desired. Calibration and zero shift information were then input to the FRC CDC CYBER computer for each data channel. The "CYBER compatible" PCM tape was then run through the CYBER BPCM program and a set of decommutated calibrated tapes created. These decommutated data tapes containing data in engineering units, along with a duplicate of the onboard tape containing FM data, were then sent to Boeing for additional processing.

Figure 5.2-2 illustrates the Boeing tape handling logistics. Basically the same digital programs were used for reduction of the high and low frequency response data.

The high frequency FM data were demultiplexed and digitized by the Boeing Test Data Processing Center. Figure 5.2-3 shows the data flow for the processing of the analog tapes. The FM signals, mostly signals from the compressor face rake, were digitized to compute instantaneous pressure distortion. In order to edit the data to permit processing only of the significant portions of data, oscillograph stripouts of the analog output from the distortion computer were used to identify the significant events. The typical data sample then consisted of a 200-millisecond interval centered about the event. The pressure signals were low-pass filtered (-3dB at 160 Hz) to retain only the frequency range of significance to the engine. Data were digitized at a rate of 1,000 samples per second per channel. The output digital data tape was converted to a format compatible with the CDC 6600 for the remainder of the processing.

Raw data from the analog tapes were digitized at Boeing. These data were processed through an input package and a calibration routine before being processed by the data reduction program. Figure 5.2-4 illustrates the data flow. All the digital processing was performed on the CDC 6600, which produced printed, microfilmed and plotted results.

The microfilmed results were transmitted to government agencies; AFAPL, NASA/LeRC and NASA/FRC.

5.2.3 Test Results

Out of an original plan consisting of 88 test events, 64 were completed and the other 24 eliminated as being either impractical or unnecessary. Table 5.2-1 summarizes the events flown during the baseline flight testing while Table 5.2-2 details the flight conditions for which high response distortion data were processed.

5.2.3.1 Recovery and Distortion

The engine throttle transients conducted at each flight condition were analyzed for effects of corrected airflow variations on recovery and distortion. Figure 5.2-5 shows

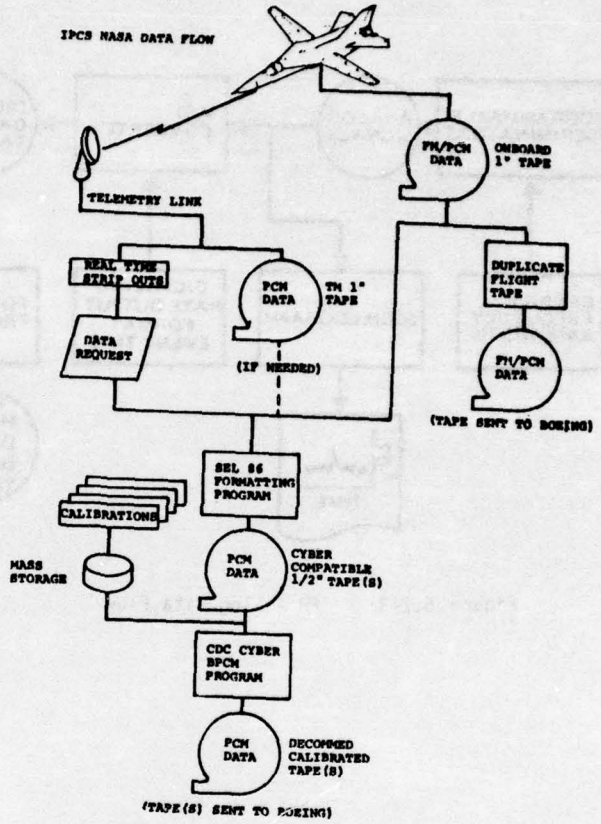

Figure 5.2-1 IPCS/NASA-FRC Data Flow

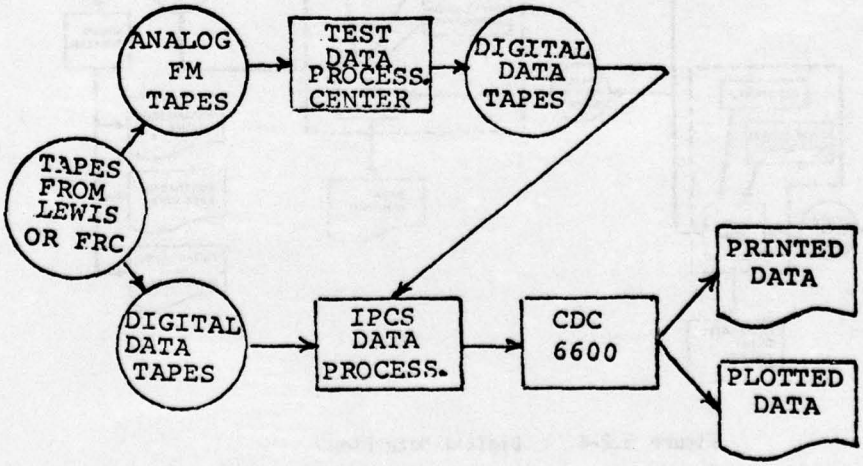

Figure 5.2-2 Tape Logistics

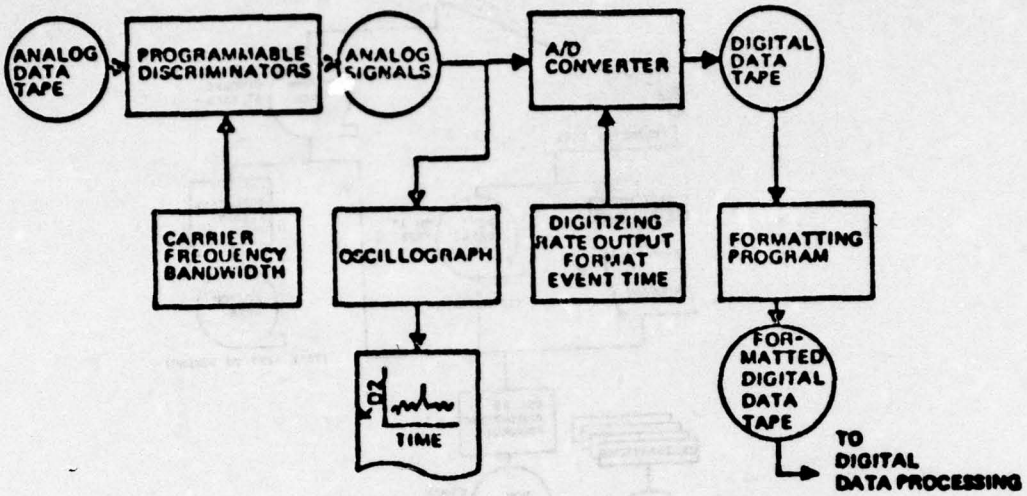

Figure 5.2-3 FM Analog Data Flow

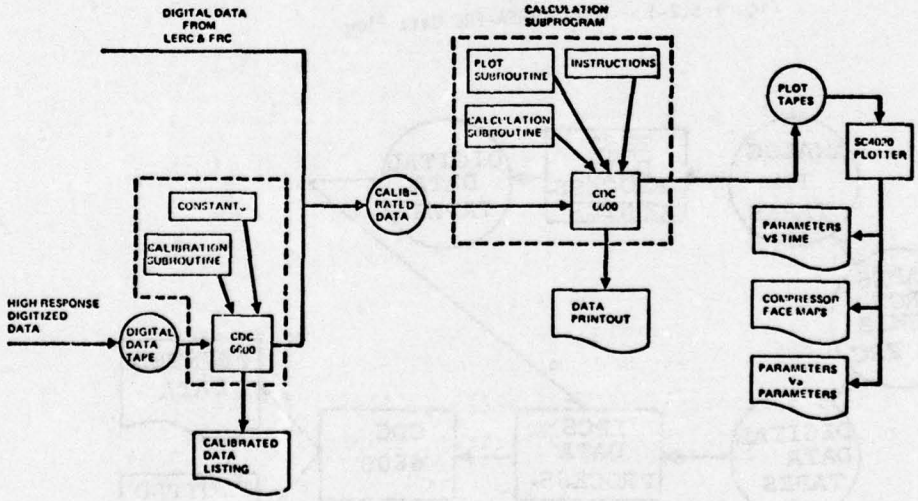

Figure 5.2-4 Digital Data Flow

Table 5.2-1 Baseline Flight Test Events

EVT	FLT	MACH	ALT	ALPHA	BETA	BLD ?	THROTTLE	SPIKE	CONE	REMARKS
1	9	2,47	50K	CRUISE	0	OPEN	MAXMIMAX	AUTO	AUTO	HOLD MIL TILL
2	9	2,47	50K	MUTLIM	0	OPEN	MAX	AUTO	AUTO	A/B OFF
3	*	2,47	50K	LIM	0	OPEN	MAXMIMAX	AUTO	AUTO	HOLD MIL TILL
4	*	2,47	50K	CRUISE	0	CLOSE	MAXMIMAX	AUTO	AUTO	A/B OFF
5	*	2,47	50K	MUTLIM	0	CLOSE	MAX	AUTO	AUTO	HOLD MIL TILL
6	1,2,8	2,30	50K	CRUISE	0	OPEN	MAXMIMAX	AUTO	AUTO	A/B OFF
7	8	2,30	50K	MUTLIM	0	OPEN	MAX	AUTO	AUTO	
8	*	2,30	50K	LIM	0	OPEN	MAXMIMAX	AUTO	AUTO	HOLD MIL TILL
9	1	2,30	50K	CRUISE	0	CLOSE	MAXMIMAX	AUTO	AUTO	A/B OFF
10	*	2,30	50K	MUTLIM	0	CLOSE	MAX	AUTO	AUTO	
11	1,6A	2,10	45K	CRUISE	0	OPEN	MIMAIDMI	AUTO	AUTO	HOLD MAX TILL
12	7	2,10	45K	MUTLIM	0	OPEN	MIL	AUTO	AUTO	ALL ZONES ON,
13	7	2,10	45K	LIM	0	OPEN	MIMAIDMI	AUTO	AUTO	IDLE TILL A/B
14	*	2,10	45K	CRUISE	0	CLOSE	MIMAIDMI	AUTO	AUTO	OFF
15	*	2,10	45K	MUTLIM	0	CLOSE	MIL	AUTO	AUTO	
16	*	2,10	45K	LIM	0	CLOSE	MIMAIDMI	AUTO	AUTO	HOLD MAX TILL
17	1,5	1,90	45K	CRUISE	0	OPEN	MIMAIDMI	AUTO	AUTO	ALL ZONES ON,
18	5	1,90	45K	MUTLIM	0	OPEN	MIL	AUTO	AUTO	IDLE TILL A/B
19	5	1,90	45K	LIM	0	OPEN	MIMAIDMI	AUTO	AUTO	OFF
20	5	1,90	45K	CRUISE	0	CLOSE	MIMAIDMI	AUTO	AUTO	
21	5	1,90	45K	MUTLIM	0	CLOSE	MIL	AUTO	AUTO	
22	5	1,90	45K	LIM	0	CLOSE	MIMAIDMI	AUTO	AUTO	
23	1,8	1,60	45K	CRUISE	0	OPEN	MIMAIDMI	AUTO	AUTO	HOLD MAX TILL
24	8B	1,60	45K	MUTLIM	0	OPEN	MIL	AUTO	AUTO	ALL ZONES ON,
25	8B	1,60	45K	LIM	0	OPEN	MIMAIDMI	AUTO	AUTO	IDLE TILL A/B
26	8	1,60	45K	CRUISE	0	CLOSE	MIMAIDMI	AUTO	AUTO	OFF
27	8	1,60	45K	MUTLIM	0	CLOSE	MIL	AUTO	AUTO	
28	8	1,60	45K	LIM	0	CLOSE	MIMAIDMI	AUTO	AUTO	
29	3,4	1,40	41K	CRUISE	0	OPEN	MIMAIDMI	AUTO	AUTO	HOLD MAX TILL
30	3,6A	1,40	41K	MUTLIM	0	OPEN	MIL	AUTO	AUTO	ALL ZONES ON,
31	3,6A,7	1,40	41K	LIM	0	OPEN	MIMAIDMI	AUTO	AUTO	IDLE TILL A/B
32	8	1,40	41K	CRUISE	0	CLOSE	MIMAIDMI	AUTO	AUTO	OFF
33	6A	1,40	41K	MUTLIM	0	CLOSE	MIL	AUTO	AUTO	
34	6A	1,40	41K	LIM	0	CLOSE	MIMAIDMI	AUTO	AUTO	
35	3,6A	.90	45K	CRUISE	0	OPEN	MIMAIDMI	AUTO	AUTO	HOLD MAX TILL
36	3,7	.90	45K	MUTLIM	0	OPEN	MIL	AUTO	AUTO	ALL ZONES ON,
37	3,8	.90	45K	LIM	0	OPEN	MIMAIDMI	AUTO	AUTO	IDLE TILL A/B
38	3,6	.90	45K	CRUISE	0	CLOSE	MIMAIDMI	AUTO	AUTO	OFF
39	3,7	.90	45K	MUTLIM	0	CLOSE	MIL	AUTO	AUTO	
40	3,8	.90	45K	LIM	0	CLOSE	MIMAIDMI	AUTO	AUTO	
41	1,2,6B	.90	10K	CRUISE	0	OPEN	MIMAIDMI	AUTO	AUTO	HOLD MAX TILL
42	1,2	.90	10K	MUTLIM	0	OPEN	MIL	AUTO	AUTO	ALL ZONES ON,
43	1	.90	10K	LIM	0	OPEN	MIMAIDMI	AUTO	AUTO	IDLE TILL A/B
44	1,3,6B	.90	10K	CRUISE	0	CLOSE	MIMAIDMI	AUTO	AUTO	OFF
45	3	.90	10K	MUTLIM	0	CLOSE	MIL	AUTO	AUTO	
46	3	.90	10K	LIM	0	CLOSE	MIMAIDMI	AUTO	AUTO	
47	6A	.70	10K	CRUISE	0	OPEN	MIMAIDMI	AUTO	AUTO	HOLD MAX TILL
48	*	.70	10K	MUTLIM	0	OPEN	MIL	AUTO	AUTO	ALL ZONES ON,
49	*	.70	10K	LIM	0	OPEN	MIMAIDMI	AUTO	AUTO	IDLE TILL A/B
50	6A	.70	10K	CRUISE	0	CLOSE	MIMAIDMI	AUTO	AUTO	OFF
51	*	.70	10K	MUTLIM	0	CLOSE	MIL	AUTO	AUTO	
52	*	.70	10K	LIM	0	CLOSE	MIMAIDMI	AUTO	AUTO	
53	1,6A	.50	10K	CRUISE	0	OPEN	MIMAIDMI	AUTO	AUTO	HOLD MAX TILL
54	1	.50	10K	MUTLIM	0	OPEN	MIL	AUTO	AUTO	ALL ZONES ON,
55	1	.50	10K	LIM	0	OPEN	MIMAIDMI	AUTO	AUTO	IDLE TILL A/B
56	1,6A	.50	10K	CRUISE	0	CLOSE	MIMAIDMI	AUTO	AUTO	OFF
57	*	.50	10K	MUTLIM	0	CLOSE	MIL	AUTO	AUTO	
58	*	.50	10K	LIM	0	CLOSE	MIMAIDMI	AUTO	AUTO	
59	*	2,47	50K	MUTLIM	0	AUTO	MAX	AUTO	AUTO	SHOCK PROBE
60	*	2,30	50K	MUTLIM	0	AUTO	MAX	AUTO	AUTO	INSTALLED
61	*	2,10	45K	MUTLIM	0	AUTO	MIL	AUTO	AUTO	
62	*	1,90	45K	MUTLIM	0	AUTO	MIL	AUTO	AUTO	
63	*	1,60	45K	MUTLIM	0	AUTO	MIL	AUTO	AUTO	
64	2,8	2,30	50K	CRUISE	0	AUTO	MAX	AUTO	MINRD	
65	8	2,30	50K	LIMIT	0	AUTO	MAX	AUTO	MINRD	
66	1,8	2,30	50K	CRUISE	YST	AUTO	MAX	AUTO	AUTO	
67	7,8B	2,10	45K	CRUISE	0	AUTO	MAX	MINRD	MINRD	
68	7	2,10	45K	LIMIT	0	AUTO	MAX	MINRD	MINRD	
69	8B	2,10	45K	CRUISE	YST	AUTO	MAX	AUTO	AUTO	
70	5	1,90	45K	CRUISE	0	AUTO	MAX	MINRD	MINRD	
71	9	1,90	45K	CRUISE	0	AUTO	IDLE	MINRD	MINRD	
72	5	1,90	45K	LIMIT	0	AUTO	MAX	MINRD	MINRD	
73	9	1,90	45K	LIMIT	0	AUTO	IDLE	MINRD	MINRD	
74	5	1,90	45K	CRUISE	YST	AUTO	MAX	AUTO	AUTO	
75	2,8	1,60	45K	CRUISE	0	AUTO	MAX	MINRD	MINRD	
76	9	1,60	45K	CRUISE	0	AUTO	IDLE	MINRD	MINRD	
77	8B	1,60	45K	LIMIT	0	AUTO	MAX	MINRD	MINRD	
78	9	1,60	45K	LIMIT	0	AUTO	IDLE	MINRD	MINRD	
79	8	1,60	45K	CRUISE	YST	AUTO	MAX	AUTO	AUTO	
80	3,4	1,40	41K	CRUISE	0	AUTO	MAX	MINRD	MINRD	
81	3,6A,7	1,40	41K	CRUISE	0	AUTO	PTPWR	MINRD	MINRD	
82	*	1,40	41K	CRUISE	0	AUTO	IDLE	MINRD	MINRD	
83	6A	1,40	41K	LIMIT	0	AUTO	MAX	MINRD	MINRD	
84	7	1,40	41K	LIMIT	0	AUTO	PTPWR	MINRD	MINRD	
85	*	1,40	41K	LIMIT	0	AUTO	IDLE	MINRD	MINRD	
86	3,4	1,40	41K	CRUISE	YST	AUTO	MAX	AUTO	AUTO	
87	3,6A	.90	45K	CRUISE	YST	AUTO	MAX	AUTO	AUTO	
88	1,2,3	.54	10K	CRUISE	0	AUTO	APR 1,8	AFT	MANUAL	

MUTLIM — WIND UP TO ALPHA LIMIT
YST — YAW TILL ENGINE STALL
PTPWR — PART POWER NAR11000,RPM
MINRD — FIND MINIMUM RD FACTOR
MAX — THROTTLE SETTINGS MAY BE ADJUSTED BETWEEN MIL AND MAX PRIOR TO EVENT TO HOLD MACH CONDITIONS
* — EVENT DELETED

MIMAIDMI — MIL-MAX-IDLE-MIL Transient

Table 5.2-2 HIGH RESPONSE DISTORTION DATA FROM IPCS BLFT

HIGH RESPONSE DISTORTION DATA FROM IPCS BLFT

FLT	TIME	Mn∞	PLA	ALT	EVENT
3	14:07:03:825	.5	Mil	10K	Stall
3	14:44:57:200	.9	Mil	45K	Cruise
3	14:45:07:100	.9	Max	45K	Cruise
3	14:45:14:400	.9	Idle	45K	Cruise
3	14:46:07:300	.9	Mil	45K	15° AOA
3	14:46:24:100	.9	Idle	45K	13° AOA
4	09:20:07:000	0	Mil	0	S.L. Static
4	09:20:30:000	0	Idle	0	S.L. Static
4	09:48:35:000	1.6	Idle	45K	Cruise
4	09:48:48:000	1.6	Mil	45K	Cruise
4	09:51:24:200	1.6	Max	45K	Manual Cone,$+\theta_2$
4	09:51:45:200	1.6	Max	45K	Manual Cone,$-\theta_2$
4	09:52:07:000	1.6	Max	45K	Manual spike,+X/R
4	09:52:24:000	1.6	Max	45K	Manual spike,-X/R
4	09:53:23:000	1.6	Max	45K	+2° Sideslip
4	09:54:11:000	1.6	Max	45K	9° AOA
4	09:54:21:000	1.6	Max	45K	15° AOA
4	10:02:39:000	1.4	Max	41K	Cruise
4	10:02:49:000	1.4	Idle	41K	Cruise
4	10:04:32:500	1.4	Max	41K	Manual Cone,$+\theta_2$
4	10:04:49:400	1.4	Max	41K	Manual Cone,$-\theta_2$
4	10:05:50:300	1.4	Max	41K	Manual Spike,-X/R
4	10:06:45:500	1.4	Max	41K	+2° Sideslip
5	09:45:58:600	1.9	88°	45K	Manual Cone,$-\theta_2$
5	09:46:34:800	1.9	88°	45K	Manual Spike,-X/R
5	09:46:57 800	1.9	88°	45K	Manual Cone,$+\theta_2$
5	09:46:57:700	1.9	88°	45K	Manual Cone,$+\theta_2$
5	09:46:58:300	1.9	88°	45K	Manual Cone,$+\theta_2$
5	09:46:58:750	1.9	88°	45K	Stall
5	09:46:58:950	1.9	88°	45K	Stall Recovery
5	09:47:02:400	1.9	88°	45K	Stall Recovery
5	09:48:41:600	1.9	95°	45K	+2.4° Sideslip
5	09:49:09:300	1.9	Max	45K	Cruise
5	09:19:14:000	1.9	Idle	45K	Cruise
5	09:55:43:600	1.9	Max	45K	13.5° AOA
5	09:55:48:700	1.9	Idle	45K	13.5° AOA
5	09:59:00:000	1.9	105°	45K	Min KD,+X/R,+θ2
5	09:59:08:000	1.9	105°	45K	Min KD, increasing
5	09:59:16:000	1.9	105°	45K	" " " "
5	09:59:27:200	1.9	105°	45K	Stall
5	09:59:27:400	1.9	105°	45K	Stall Recovery
5	09:59:27:600	1.9	105°	45K	Stall Recovery
5	09:59:31:100	1.9	105°	45K	Stall Recovery
6A	09:25:36:000	.5	Max	10K	Cruise
6A	09:25:46:400	.5	Idle	10K	Cruise
6A	09:29:14:600	.7	Max	10K	Cruise
6A	09:29:24:000	.7	Idle	10K	Cruise
6A	09:55:56:400	1.4	54°	41K	Manual Cone,$-\theta_2$
6A	09:56:05:300	1.4	54°	41K	Manual Cone,$+\theta_2$
6A	09:56:21:200	1.4	54°	41K	Manual Spike+X/R
6A	09:56:33:000	1.4	54°	41K	Manual Spike,-X/R
6A	09:58:23:100	1.4	82°	41K	-X/R,$-\theta_2$,16° AOA
6A	10:01:02:200	1.4	82°	41K	+X/R,$+\theta_2$,16° AOA
6A	10:09:25:800	1.4	Max	41K	16° AOA
6A	10:09:36:300	1.4	74°	41K	Inlet Turbulence
6A	10:12:53:700	1.4	55°	41K	17° AOA
6A	10:18:05:900	.9	Max	45K	Cruise
6A	10:18:13:800	.9	Idle	45K	Cruise
6A	10:20:09:300	.9	Max	45K	-3° Sideslip
6A	10:20:29:000	.9	Max	45K	+3° Sideslip
6B	10:58:16:000	.9	Max	10K	Cruise
6B	10:58::29:000	.9	Idle	10K	Cruise
6B	11:25:05:600	1.6	97°	45K	$-\theta_2$,-X/R 16° AOA

Table 5.2-2 HIGH RESPONSE DISTORTION DATA FROM IPCS BLFT (Cont'd)

FLT	TIME	Mn	PLA	ALT	EVENT
6B	11:26:23:000	1.6	97°	45K	$+\theta_2$,+X/R 16 AOA
6B	11:30:48:200	1.6	48°	45K	16° AOA
6B	11:34:01:000	2.1	Max	45K	Cruise
6B	11:34:11:400	2.1	Idle	45K	Cruise
6B	11:37:30:200	2.1	Max	45K	Cruise, Turbulence
6B	11:37:43:400	2.1	Max	45K	Inlet Buss
6B	11:37:43:600	2.1	Max	45K	Inlet Buss
6B	11:37:43:800	2.1	Max	45K	Inlet Buss
6B	11.37.44.300	2.1	Max	45K	Inlet Buss
6B	11:37:44:500	2.1	Max	45K	Stall
7	10:01:19:000	1.4	58°	41K	$+\theta_2$,+X/R
7	10:07:23:200	1.4	46°	41K	Stall
7	10:09:22:500	1.4	55°	41K	$+\theta_2$,+X/R 16° AOA
7	10:09:25:500	1.4	89°	41K	High K_D
7	10:12:54:000	1.6	Idle	45K	Cruise
7	10:13:00:100	1.6	Idle	45K	9° AOA
7	10:15:43:000	2.1	Max	45K	15° AOA
7	10:18:31:650	2.1	99°	45K	Inlet Buss
7	10:18:31:850	2.1	99°	45K	Stall
7	10:20:05:000	2.1	90°	45K	Cruise
7	10:21:36:000	2.1	30°	45K	13° AOA
7	10:25:13:400	.9	92°	45K	16° AOA
7	10:25:17:400	.9	92°	45K	Cruise
7	10:25:49:00	.9	92°	45K	Cruise
8	09:37:46:400	2.3	Max	50K	Cruise
8	09:37:50:000	2.3	Max	50K	High K_D
8	09:38:17:900	2.3	Max	50K	Cruise
8	09:38:48:600	2.3	104°	50K	Stall
8	09:39:40:100	2.3	94°	50K	Cruise
8	09:39:46:400	2.3	99°	50K	16° AOA
8	09:41:12:900	2.3	Max	50K	Stall
8	09:41:42:000	2.3	Max	50K	Manual Cone,-θ_2
8	09:41:50:500	2.3	Max	50K	Inlet Buss
8	09:41:50:700	2.3	Max	50K	Stall
8	09:44:24:200	1.0	105°	45K	Stall
8	09:49:17:400	.9	77°	45K	16° AOA
8	09:51:18:000	.9	Idle	45K	16° AOA
9	14:09:23:000	2.3	Max	45K	Inlet Turbulence
9	14:12:44:000	2.4	110°	52K	Inlet Turbulence
9	14:13:32:600	2.44	110°	52K	Cruise
9	14:14:32:800	2.4	Max	52K	Inlet Buss
9	14:14:33:900	2.44	Max	52K	16.5° AOA
9	14:14:34:100	2.44	Max	52K	Stall
9	14:16:26:100	1.9	47°	45K	Inlet Buss
9	14:16:26:300	1.9	47°	45K	Stall
9	14:18:55:000	1.9	52°	45K	Cruise
9	14:23:39:100	1.6	53°	45K	Stall
9	14:25:01:000	1.6	53°	45K	Stall Recovery
9	14:32:48:100	.7	84°	19K	Stall Recovery
9	14:33:57:700	.5	80°	18K	Stall Recovery
9	14:34:52:000	.7	80°	18K	Stall Recovery
9	14:34:58:400	.7	80°	18K	High K_D
9	14:37:21:200	.6	Idle	12K	Stall

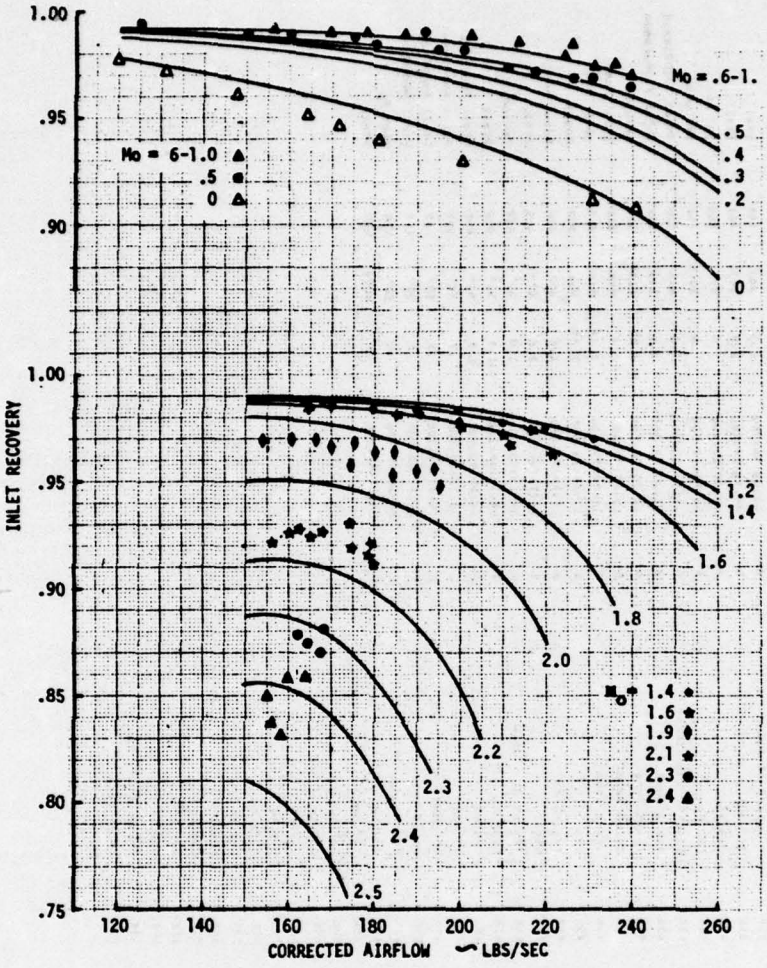

Figure 5.2-5 Mass Flow Effects on Inlet Recovery

5.2.3.1 Recovery and Distortion (Continued)

inlet pressure recovery as a function of corrected airflow for Mach numbers 0 to 2.5. The recovery curves shown were obtained from F-111 and FB-111A flight tests conducted by General Dynamics, while the data points were obtained from the baseline flight test. Good agreement is shown. Figure 5.2-6 presents the correlation of steady state inlet distortion with corrected airflow for Mach numbers 0 to 2.4 obtained from the BLFT.

Test events defined as WUTLIM (wind up turn to alpha limit) were used to evaluate the effects of angle of attack changes on recovery and distortion. Figure 5.2-7 shows the effect of angle of attack on recovery from the BLFT. Supersonically, increasing angle of attack increased recovery due to the lower Mach number produced by the wing glove compression. Effect of angle of attack subsonically is unclear due to lack of data but it appears that increasing angle of attack reduced recovery. No consistent effect of angle of attack on distortion was found. Engine surges which occurred during high supersonic wind up turns were likely caused by a sudden random boundary layer separation and not by angle of attack effects on distortion per se. Analysis of both steady-state and instantaneous distortion have not shown significant changes prior to surge during these events.

5.2.3.2 Manual Inlet Control Testing

Several of the test events flown during the IPCS baseline flight testing were conducted with the inlet geometry under manual control. Using cockpit mounted controls, the spike and cone position were varied while the aircraft was under cruise and high angle of attack conditions. The major objective of the testing was to generate high distortion levels to define the distortion probe location. Data defining the optimum inlet geometry settings for distortion and inlet recovery were also desired.

Figures 5.2-8 and 5.2-9 show the effects at cruise of off-design geometry settings on distortion and recovery for Mach numbers 1.4 and 1.6, respectively. The bill-of-materials design points for spike and cone position are identified on the figures.

5.2.3.3 On-Line Distortion Sensing

The scheme for on-line instantaneous distortion sensing was evaluated and location for the probes selected from data from the BLFT. Conceptually, this distortion sensing scheme treats instantaneous distortion as the composite of a steady-state component superimposed with a turbulent component. To this end, the distortion sensor would be composed of five pressure probes located at the compressor face. Four of the probes estimate the steady-state component while the fifth measures a turbulent component.

The locations selected for the four steady state probes was made on the basis of a computer analysis of 110 data samples taken at various flight configurations over the entire F-111 flight envelope tested during the BLFT. The probe configuration selected, shown in Figure 5.2-10, is comprised of widely separated probes which accommodate the rotation of the pressure pattern for high speed conditions. Figure 5.2-11 shows four compressor face plots for flight Mach numbers .9 and 2.3. Note that the four probe locations were selected to sample the high and low pressure areas within the inlet and that their spacing accommodates the rotation of the pressure pattern that occurs at high speeds.

The distortion signal, $\frac{P_{MAX} - P_{MIN}}{P_{MIN}}$, computed from the four probes, was used to estimate the actual steady-state distortion factor, KD, computed from the full 40-probe rake readings.

The fifth pressure probe in the distortion sensor was used to measure the turbulence intensity of the inlet airflow. The probe was a high frequency response Kulite whose output was processed to provide a filtered signal proportional to the rms of the pressure fluctuations.

The final correlation with actual instantaneous distortion was made using data from the 110 IPCS baseline flight tests data samples. A relationship of the form:

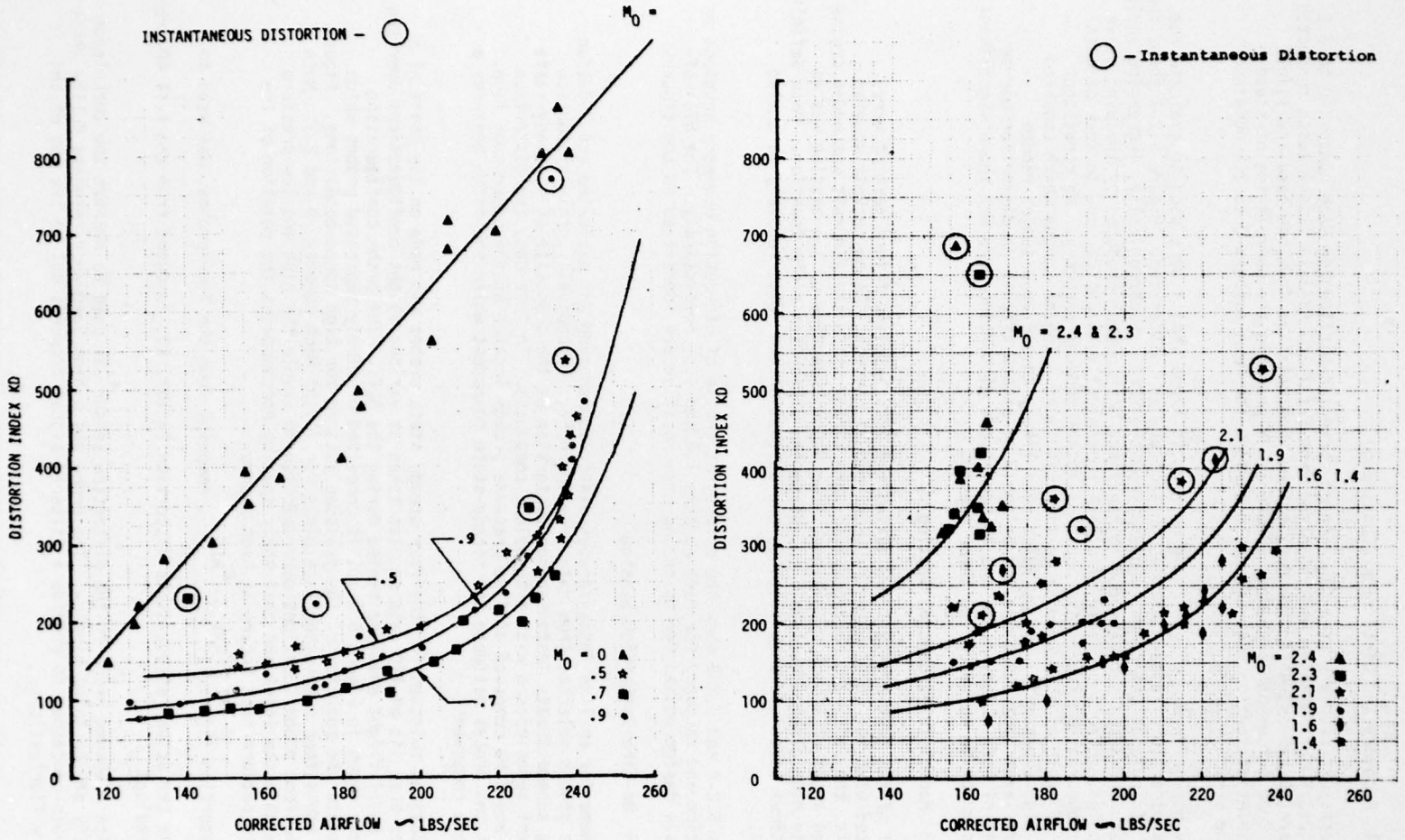

Figure 5.2-6 Mass Flow Effects on Inlet Distortion

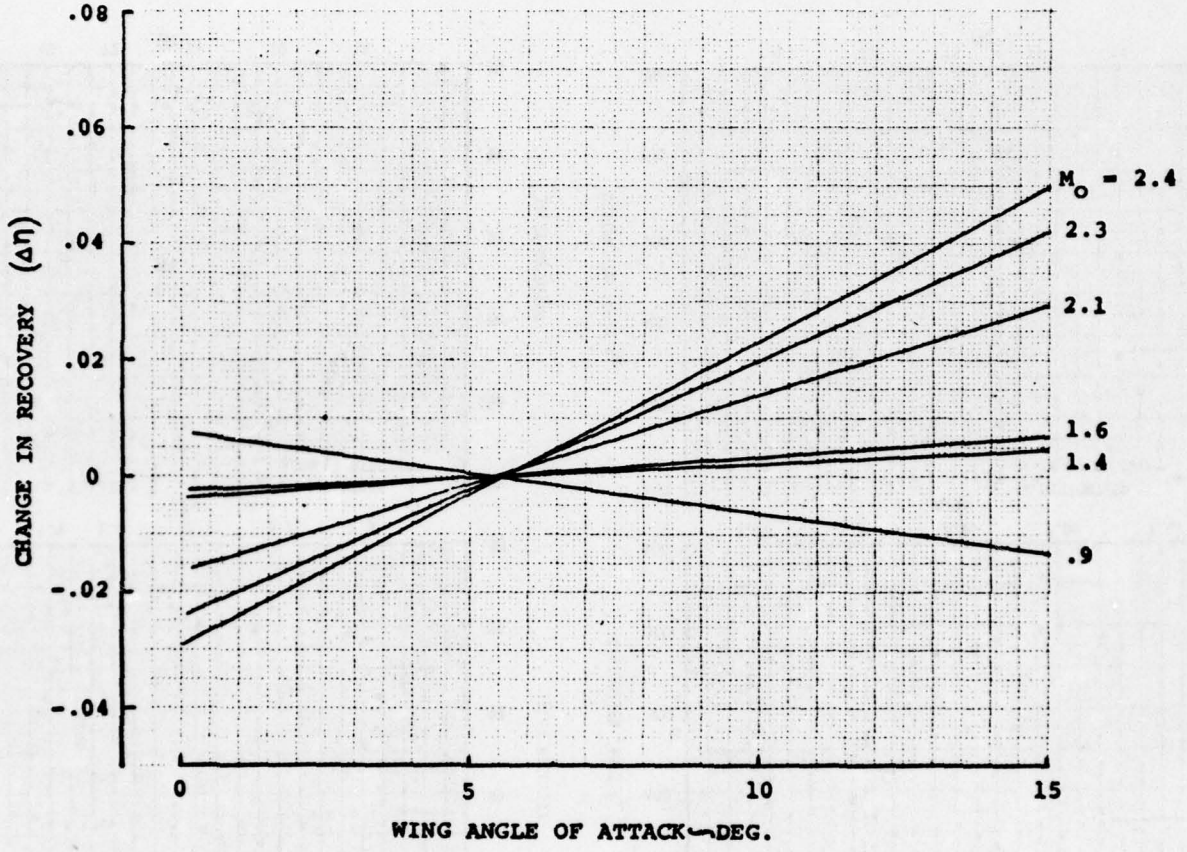

Figure 5.2-7 Angle of Attack Effects on Inlet Recovery

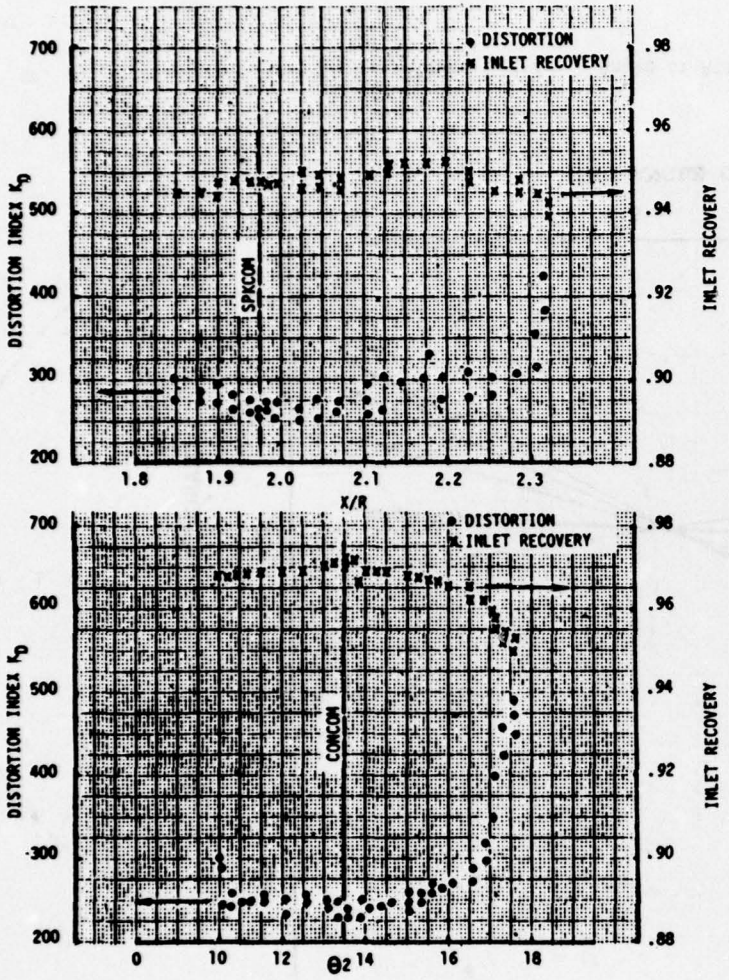

Figure 5.2-8 Effect of Off-Design Inlet Geometry at Mach 1.4

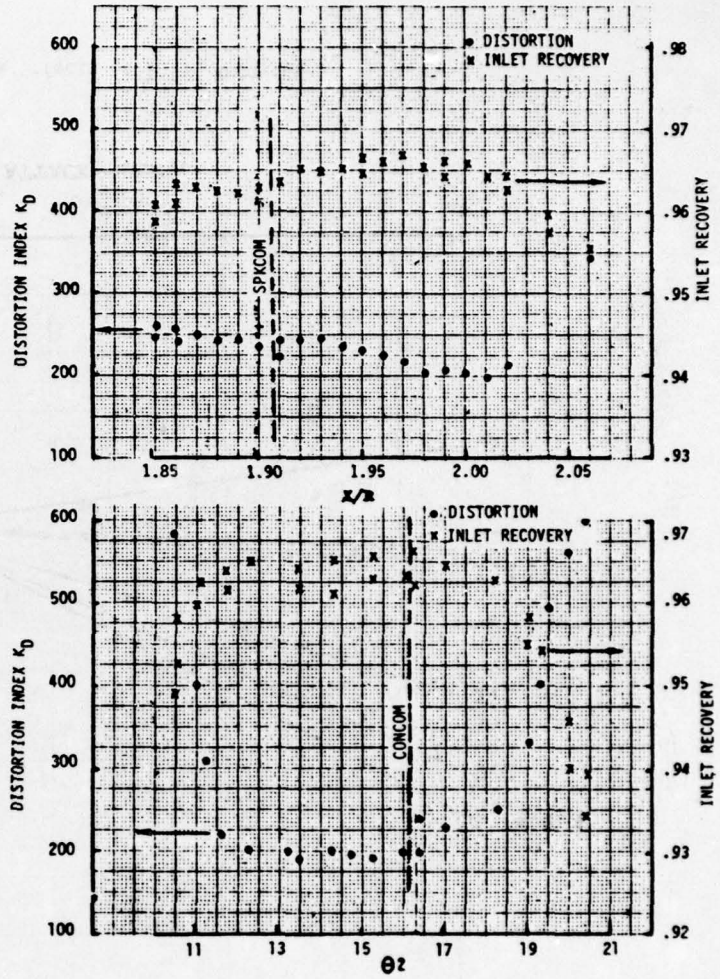

Figure 5.2-9 Effect of Off-Design Inlet Geometry at Mach 1.6

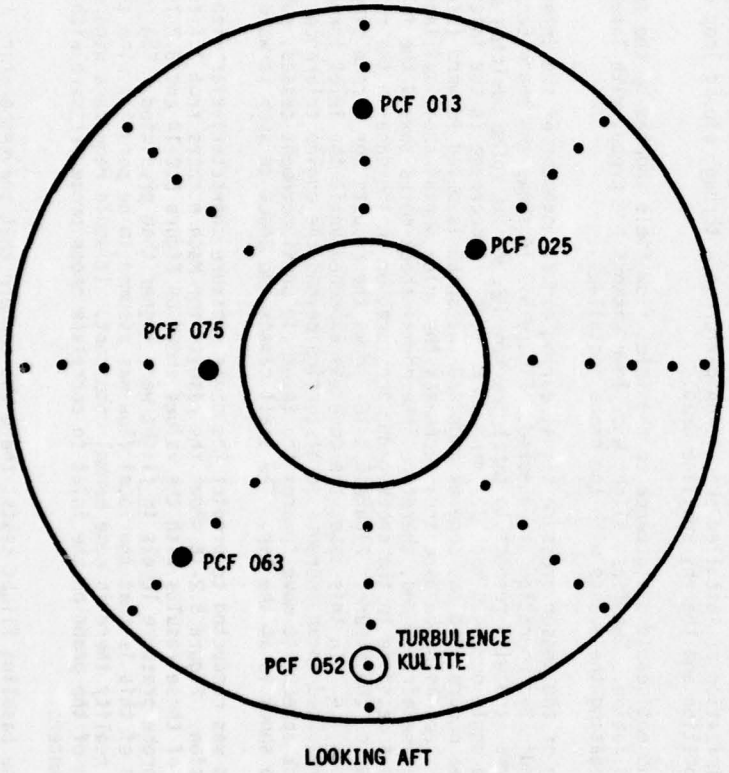

Figure 5.2-10 Distortion Sensor Probe Locations Selected

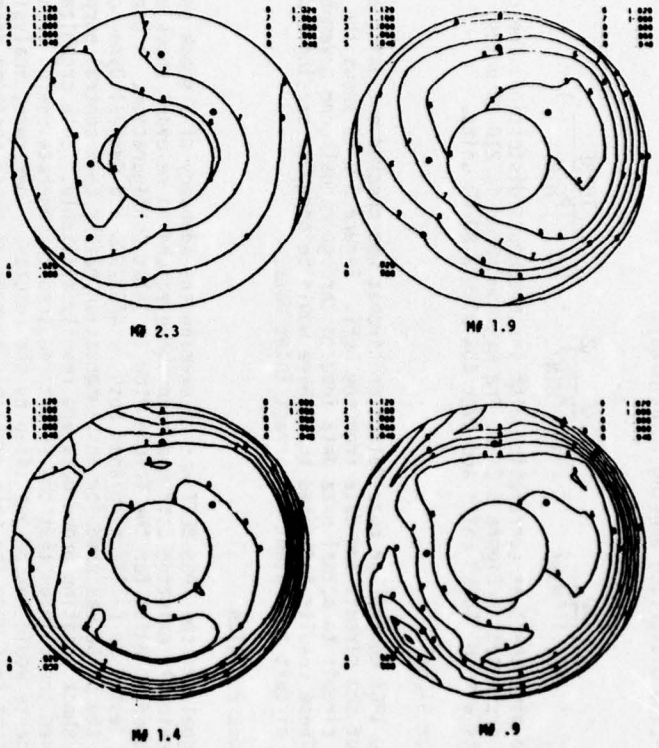

Figure 5.2-11 Typical Compressor Face Pressure Plots

5.2.3.3 On-Line Distortion Sensing (Continued)

$$C_1 + C_2 \left(\frac{\Delta P}{P_{MIN}}\right) + C_3 \left(\frac{\Delta P}{P_{MIN}}\right)^2 + C_4 \left(\frac{TURBF}{P_{MIN}}\right)$$

was found to give the best correlation with instantaneous distortion. The correlation obtained is presented in Figure 5.2-12. The maximum error is 210 KD units, with 85% of the points within 150 KD units and over 50% within 80 KD units.

5.2.3.4 Buzz Signal

The proposed IPCS controller buzz detection circuit was checked out using a computer simulation of the circuit and data from the BLFT. Figure 5.2-13 shows the response of the buzz circuit to actual buzz data induced through manual cone movement during the BLFT. These results indicated that there would be adequate sensing and response by the buzz circuit to prevent or correct inlet buzz.

5.2.3.5 Shock Position

One of the goals of the IPCS BLFT was to examine the adequacy of a shock position sensor. Previously existing data had been surveyed and no relevant shock position data were found to exist for the Triple Plow II inlet configuration. A probe had been flight tested on F-111A airplanes both by NASA/FRC and General Dynamics. In these tests the probe was used for instrumentation rather than control purposes. None of the shock position probe data are readily available. Both organizations have expressed the opinion that the effort required to generate useful data from these past tests would not be justified by the results. Therefore, analysis and the baseline flight test were the only available sources of shock position data.

Although a shock position signal is not being applied as an IPCS control loop, a Boeing built shock position sensor was installed and flown on the F-111E aircraft during the baseline flight test. The goal was to evaluate use of a single transducer to obtain an indication of shock position and its possible future application to in-flight optimization of installed propulsion performance through closed loop control on shock location and thereby spillage drag.

There was no noticeable disturbance to the inlet flow field induced by the shock probe installation. The first flight was flown without the probe, with later flights repeating the events with the probe installed.

Examination of the sensor pressure signal during manual movement of the inlet spike and cone indicated operation as expected. Figure 5.2-14 shows the shock sensor signal, normalized with respect to total pressure P2, versus spike position and second cone angle during a Mach 2.1 minimum KD test. A decrease in the inlet capture area occurs when the cone expands and the spike is moved forward (X/R increase). Decreasing capture area decreases the inlet normal shock spillage for constant engine airflow and, therefore, the normal shock moves toward the inlet lip. This causes a decrease in the shock probe pressure, or an increase in the ratio PT/PS, as shown on the figure. Figure 5.2-15 shows the results for a cone expansion and stall at Mach 1.4. In this case, the cone was expanded until the inlet throat area reduction resulted in an increase in distortion beyond the engine tolerance. The normal shock appears to move towards the inlet lip until movement ceases, possibly because the shock is at the lip. The stall causes the shock to jump forward.

An analysis was conducted to predict the probe pressure characteristics with normal shock location. Figure 5.2-16 shows the results for Mach numbers from 1.4 to 2.5. Comparison of these results with the values shows on Figure 5.2-14 and 5.2-15 indicates probe pressure levels in flight were higher than predicted. The probable explanation of this is that the local flow was assumed to be parallel with the probe, whereas in reality there is some normal component. It would require a wind tunnel calibration of the probe on the inlet to correlate shock probe pressure with other inlet parameters.

Prior to the baseline flight tests, there was concern that the temperature limit of the shock sensor pressure transducer (+275°F) might be exceeded at the high Mach numbers, which would necessitate removal of the transducer to preserve its integrity. An

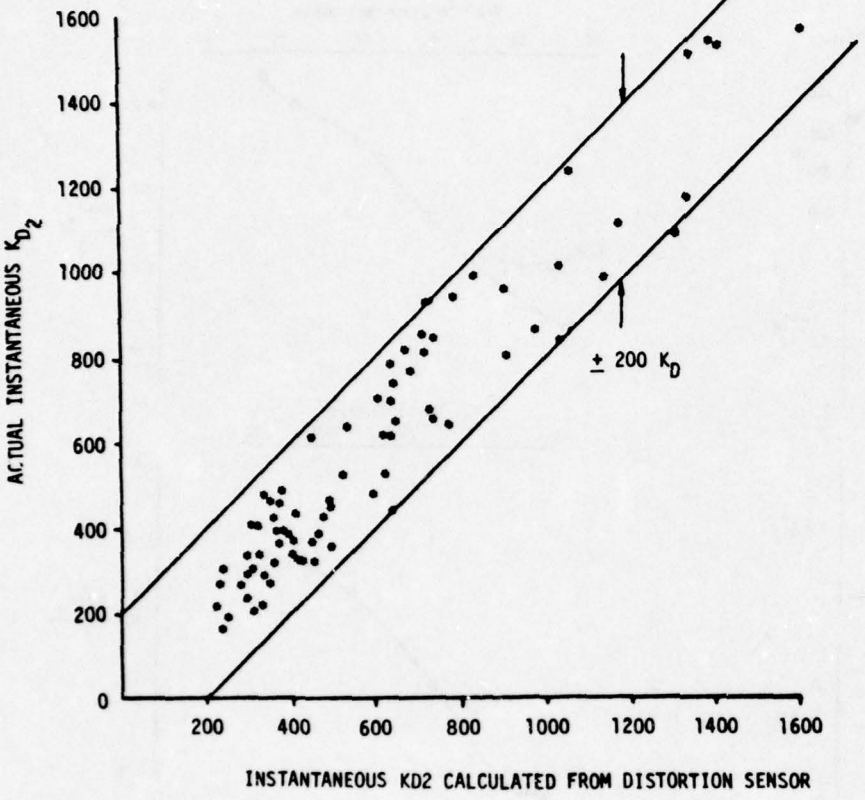

Figure 5.2-12 Correlation of Distortion Sensor Output with Instantaneous Distortion

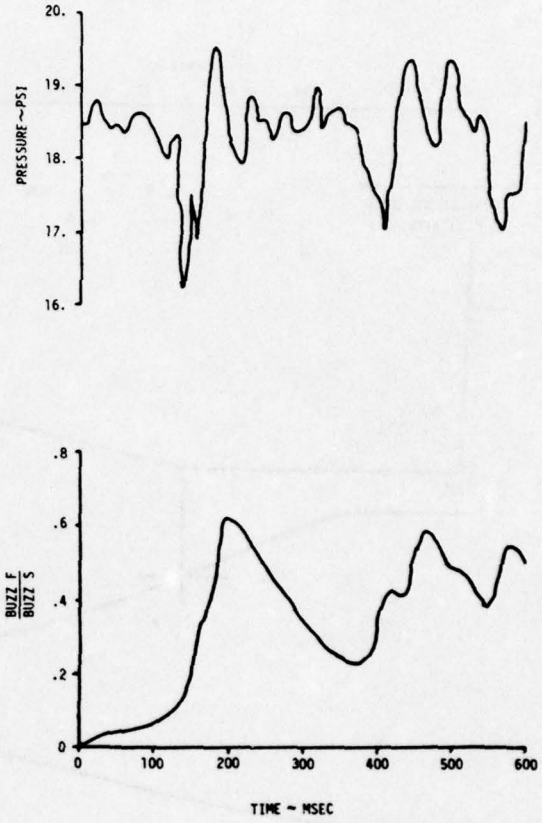

Figure 5.2-13 Buzz Circuit Response to Flight Data

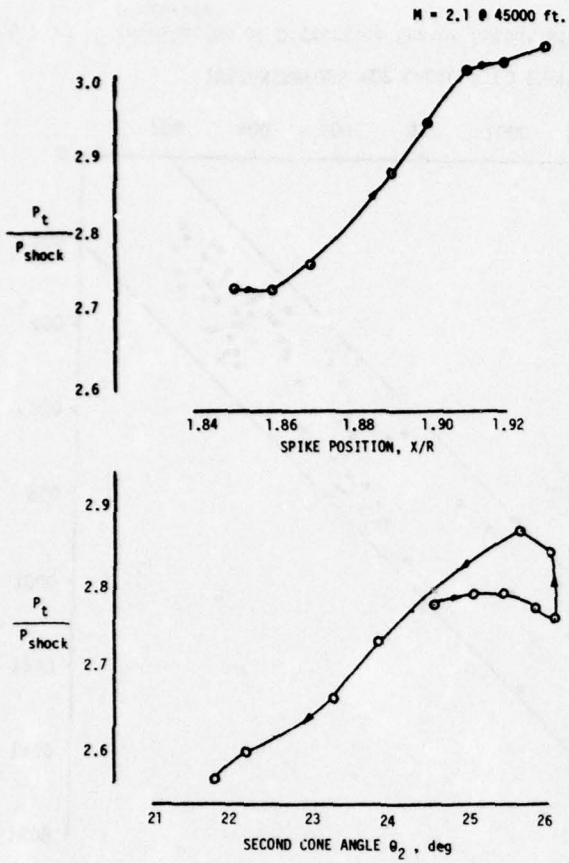

Figure 5.2-14 Effect of Spike and Cone Position on Shock Probe Signal

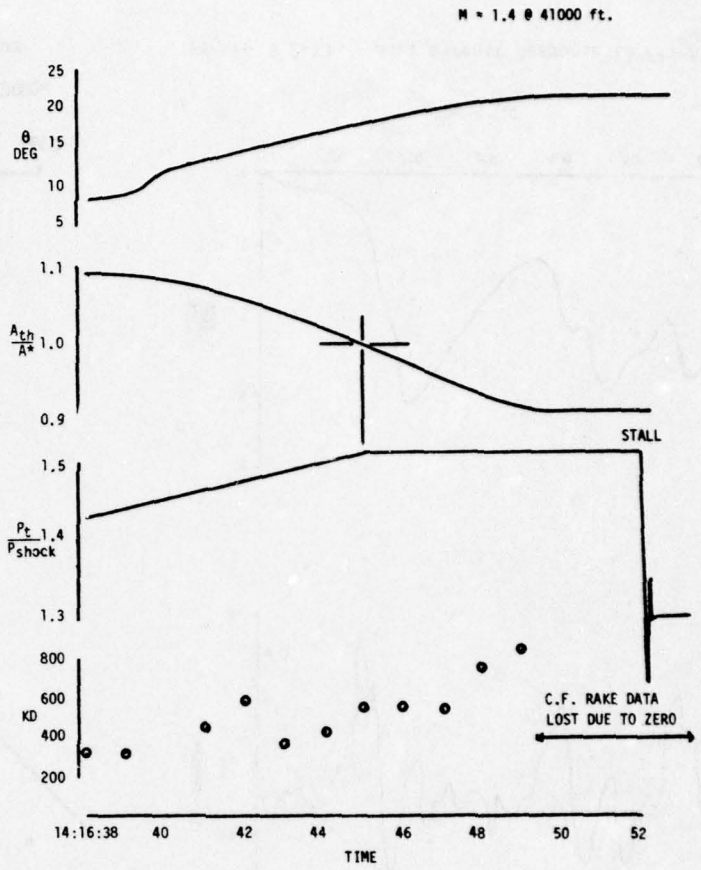

Figure 5.2-15 Effect of Cone Expansion on Shock Probe Signal and Distortion

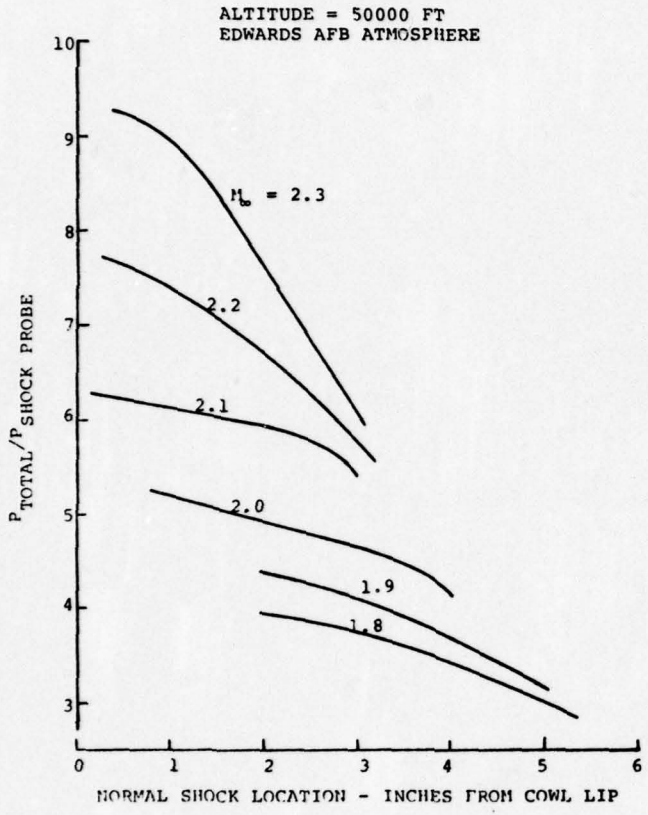

Figure 5.2-16 Shock Probe Theoretical Calibration Curve

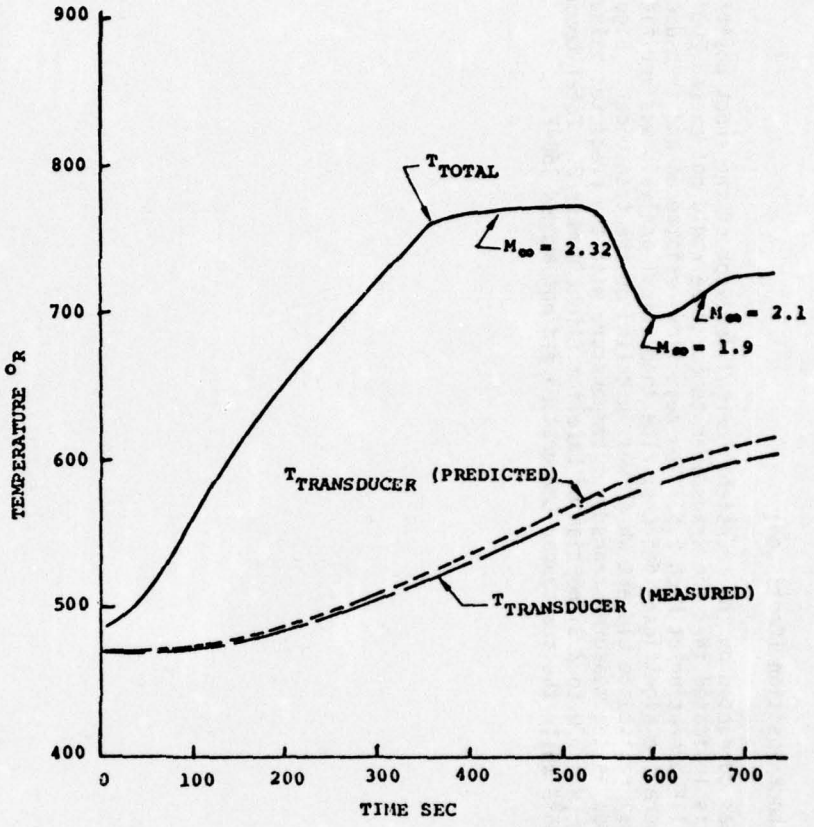

Figure 5.2-17 Shock Probe Transducer Temperature

5.2.3.5 Shock Position (Continued)

analysis was conducted on the transient thermal behavior of the shock position sensor. The analysis indicated that the transducer temperature would not exceed 200°F for normal F-111E operation at Mach 2.5. The heat flow resistances and transducer heat capacity were the significant factors. The theoretical analysis was verified by a thermal resistance element which was installed on the transducer. Figure 5.2-17 compares the measured transducer temperature with the predicted value for the supersonic (M = 1.0 to 2.3) portion of baseline flight number 2. Total temperature reached 335°F while the transducer temperature did not exceed 160°F.

6.0 BENCH TEST

A closed loop bench test (CLBT) for evaluation of the IPCS components, was conducted per reference 2, during the period 15 October 1974 to 18 December 1974.

6.1 BENCH TEST OBJECTIVES

The objectives of the bench test program were as follows:

1. Verify the performance of the control components when operated as a complete system.
2. Verify the performance of the control software when operated in conjunction with the system hardware and a real time dynamic simulation of the propulsion system.
3. Verify the suitability of the complete control system for sea level engine testing.

6.2 BENCH TEST CONFIGURATION

The configuration for the bench test included the IPCS modified fuel controls, engine nozzle actuators, engine sensors (actual and simulated) inlet actuators, the DPCU with its test set, and analog simulations of the engine, inlet and afterburner.

Figure 6.2-1 illustrates the test configuration for the components tested, and Figure 6.2-2 defines the signal paths for the bench test setup.

6.2.1 Test Facility

6.2.1.1 Closed Loop Test Bench Description

The closed loop test bench facility (X-262) consisted of an analog computer, discussed in Section 6.2.1.2, interface hardware that provided a real time engine (RTE) simulation, and a fuel flow bench incorporating two variable speed drive systems.

Figure 6.2-3 is a photograph showing the real time engine simulator portion of the closed loop facility (analog computer is on the left). The operator's control panel can be seen at the center. Figure 6.2-4 is a photograph showing the test bench portion of the closed loop facility. The two 400 horsepower drive system output pads can be seen on the left and the 7.5 horsepower output pad is in the center of the photograph.

6.2.1.2 Real Time Engine Sumulation

The Real Time Engine (RTE) simulation used for the IPCS Closed Loop Bench Test was developed from SOAPP digital simulation data which agree well with TF30-P-9 test data. The RTE simulation was a more simplified model than the digital simulation due to the limited amount of nonlinear function generating capability of the Beckman EASE analog computer. This limitation confined RTE simulation operation to sea level static, standard day conditions with all compressor bleeds closed.

The initial RTE simulation used the Beckman EASE analog computer for all calculations except for static pressure and afterburner calculations which were performed by an AD-32 analog computer. This configuration required the use of all available multipliers and amplifiers of the Beckman, which called for peak power supply output. The maximum power supply loading caused excessive down time for service requirements. Since this created a situation leading to probable program delays, a PDP-11/40 digital computer was used to perform the rotor speed calculations in a hybrid configuration.

This eliminated 6 amplifers and 4 multipliers in the EASE analog simulation thereby alleviating the power requirements. Ultimately, this configuration, shown in Figure 6.2-5 provided excellent support to the Closed Loop Bench Test.

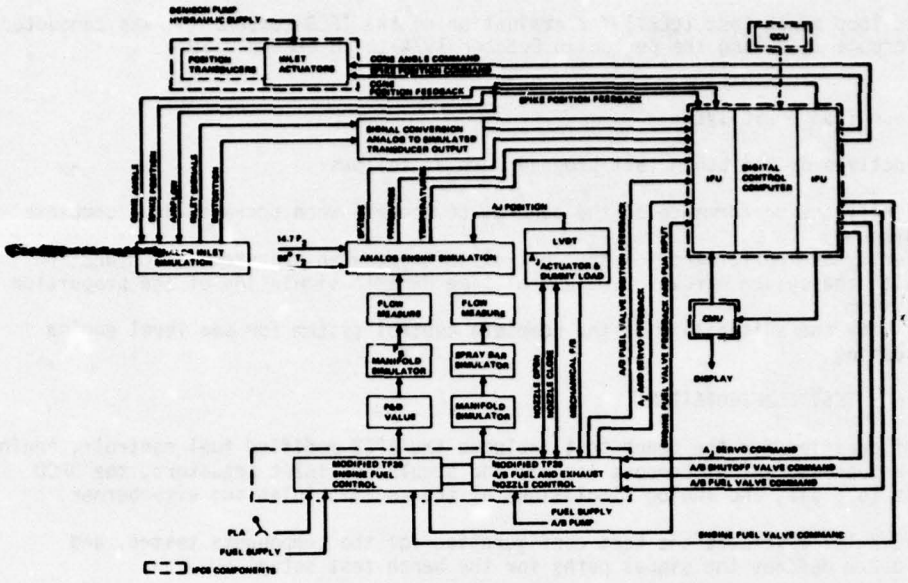

Figure 6.2-1 IPCS Closed Loop Bench Test Schematic

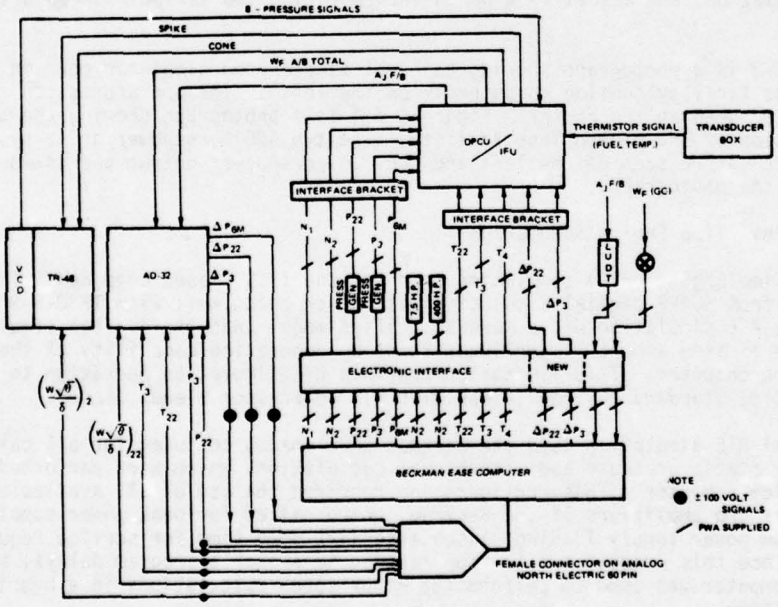

Figure 6.2-2 CLB Interface Signal Paths

Figure 6.2-3 CLB Control Room

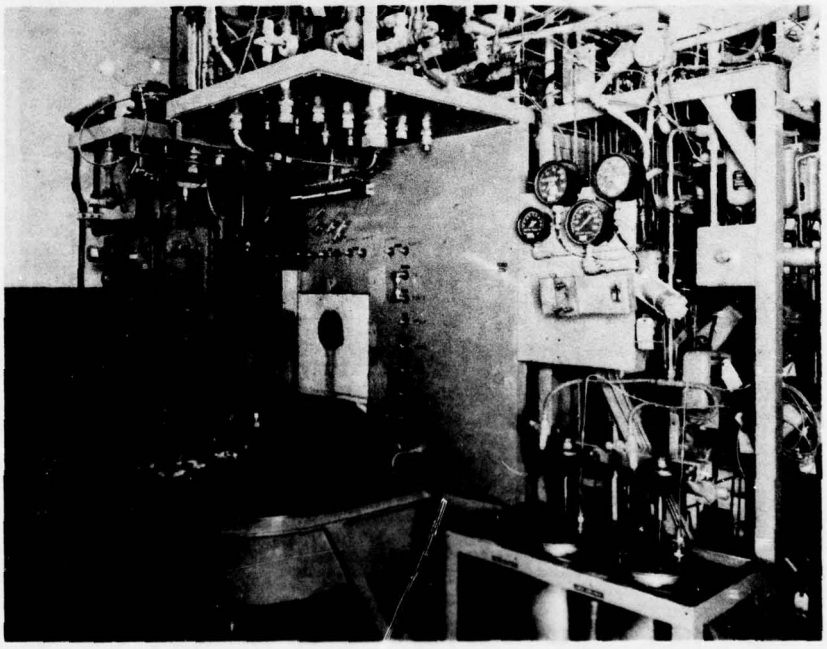

Figure 6.2-4 Closed-Loop Test Bench

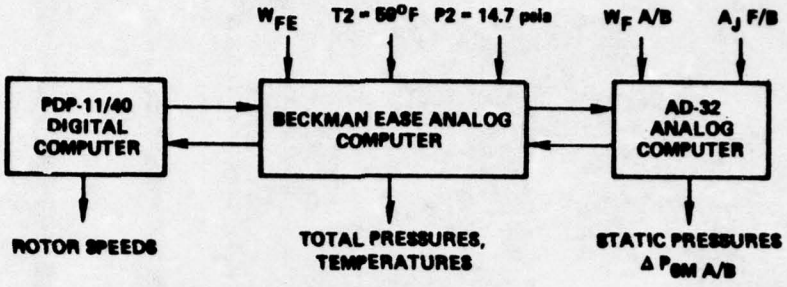

Figure 6.2-5 Real Time Engine Simulation Diagram

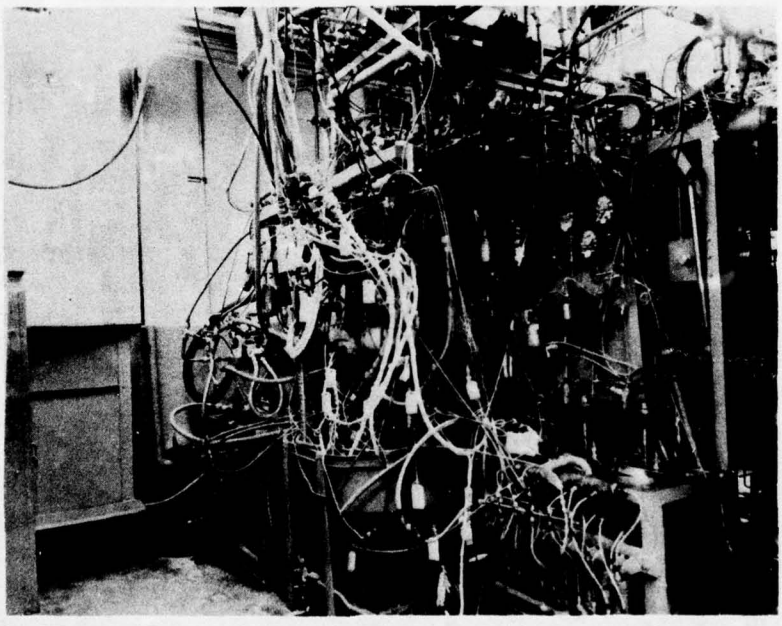

Figure 6.2-6 IPCS Closed Loop Bench Test Showing Engine Mounted Components on Test Bench

6.2.2 Test Hardware

6.2.2.1 Engine-Related Hardware

The following IPCS components were evaluated as a system to assess the IPCS system compatibilities:

Component	Part Number
CJ-U1 Main Fuel Control	749008
AA-R1 A/B and Exhaust Nozzle Control	749009
TF30-P-9 B/M Exit Nozzle Actuators	575073
P_{22} M/B Alinco Transducer	750361
P_3 M/B Alinco Transducer	750363
Thermistor	750364
Engine Harness	724792
Engine Harness	751168
Engine Harness	751169
Engine Harness	751302

Other characteristics of the fuel system (manifold volumes, fuel nozzle pressure drop, P&D valve, etc.), were simulated by auxiliary bench test equipment.

Figure 6.2-6 shows the modified IPCS controls and the TF30 nozzle actuators mounted on the flow bench.

6.2.2.2 DPCU

The DPCU-related components which were tested included the power supply unit, digital computer unit, interface unit, computer monitor unit and the test set unit.

These components are shown schematically in Figure 6.2-1 and in photograph Figure 6.2-7.

6.2.2.3 Inlet Hardware

A Boeing hydraulic test fixture (HTF) was used for inlet evaluation. The HTF contained F-111 cone and spike actuators with proper movement and inertial loads, LVDTs for position feedback, IPCS servo controller and F-111 hydraulic hoses. During the running of the CLB, MIL-H-5606 hydraulic fluid was used when testing the HTF. The HTF with cone and spike actuators is shown in Figure 6.2-8.

Figure 6.2-1 and photograph Figure 6.2-9 show four other items of test-related equipment used for test. These are: A TR48 analog computer for programming the inlet simulation, eight voltage-controlled oscillators and associated gear (patch panel, amplifiers), and the ASR-35 teletype used to communicate with DPCU.

6.2.2.4 Connector and Cable Interfacing

The IPCS designed connectors and cables required for interfacing the engine related, DPCU related, and inlet related components were used as allowed by the bench test configuration. Experimental connectors and cables were used where necessary because of the use of simulated signals instead of real hardware.

6.2.3 Instrumentation

Several sources of instrumentation were used during the bench test: direct outputs from the analog simulators, readout from the transducers, and data from the DPCU. The instrumentation diagram, Figure 6.2-10, shows the recorder interfaces. The data from the DPCU were obtained from 11 selectable digital to analog (D-A) channels for transient recordings, and octal display on the TSU for steady state data and the pulse code modulated (PCM) data signals for post-test analysis and reporting. The PCM data were tape recorded during the bench test and then sent to USAF/FDL for processing.

Figure 6.2-7 IPCS CLB Test Showing Electronic Test Equipment

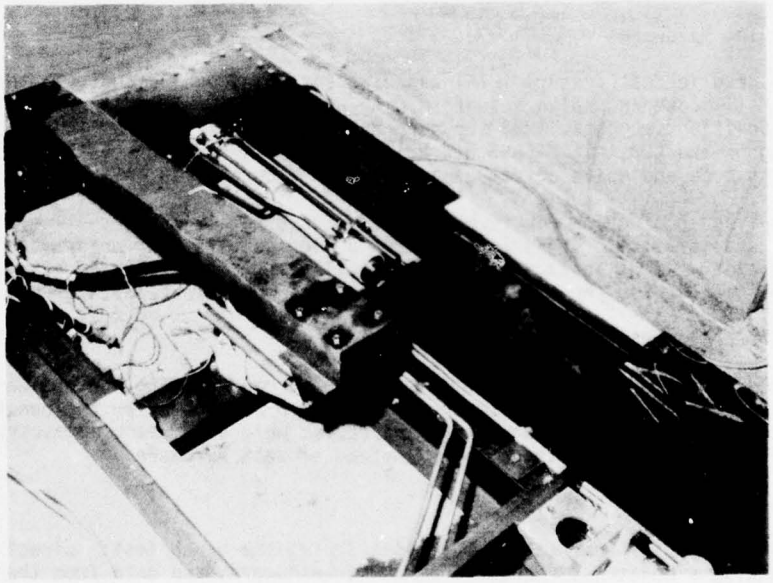

Figure 6.2-8 Inlet Hydraulic Test Fixture

Figure 6.2-9 IPCS CLB Test Showing Teletype, AD32 and TR48

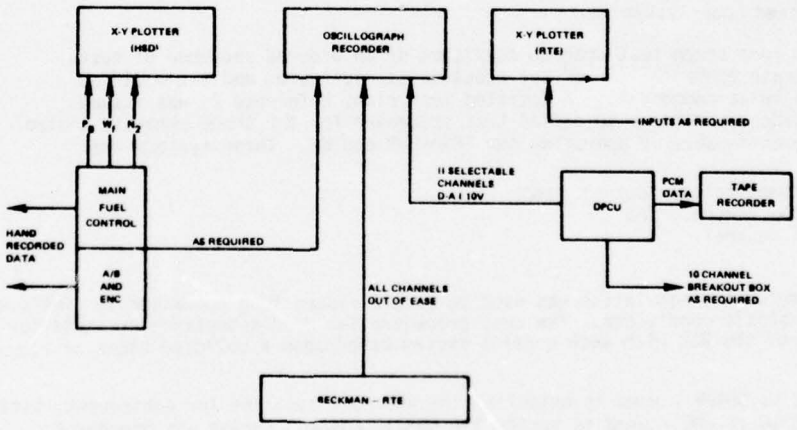

Figure 6.2-10 CLB Instrumentation Diagram

6.2.4 Inlet Simulation

Simulation of the F-111E inlet during the closed loop bench test was achieved using an analog TR48 computer and a hydraulic test fixture. The aerodynamics of the inlet were represented by an analog simulation programmed on the TR48. while the hydraulic test fixture simulated the inlet mechanical properties. A block diagram of the inlet simulation is given in Figure 6.2-11.

The inlet simulation implemented on the TR48 used engine airflow and inlet geometry signals received from the real time engine simulation and the DPCU to compute eight inlet pressures. Total pressure, airplane Mach number, and angle of attack were input using potentiometers. The eight inlet pressures were then converted to frequency modulated signals by VCO's and input to the IFU. The VCO's were used to simulate the Paroscientific transducers that were used in the flight test.

The Boeing built hydraulic test fixture was used in evaluating the interface between the DPCU and the inlet hardware. The fixture contained flight qualified hardware including F-111 cone and spike actuators with proper movement and inertial loads, an IPCS servo controller, LVDTs for position feedback, and F-111 hydraulic hoses. Aerodynamic loads were not simulated.

6.3 TEST PROCEDURE

6.3.1 Open Loop Acceptance Test

A separate set of tests was conducted on each of the modified main fuel controls and afterburner and exhaust nozzle controls as part of the PWA Flight Assurance Test (FAT) Plan. These tests on MFC S/N 200838 and S/N 200874 and A/B-ENC S/N 1974 and S/N 1860 consisted of a component calibration schedule test as defined in the PWA FAT plan. The tests were conducted on an open loop test bench in conjunction with the Bendix test set unit which was used for setting the required conditions.

6.3.2 Comparison of Real Time Engine (RTE) Simulation with Digital Simulation

Comparisons of the RTE simulation with the digital SOAPP simulation and available OCALC overhaul test data were made for steady state operation in order to assess the differences between actual and simulated engine operation. In addition a comparison of the RTE and SOAPP simulation engine parameter response to ramp and step fuel flow inputs was performed. These tests were done prior to closed loop testing. Refer to Section 6.4.3.1.

6.3.3 Closed Loop System Test

The closed loop bench test program consisted of an ordered sequence of tests to demonstrate compatibility of the electronics, software, and the modified engine and inlet components. A detailed test plan, Reference 2, was issued prior to bench operations to define test procedure for the three separate control systems, each capable of operating the TF30-P-9 engine. These systems are:

1. Hydromechanical Control (HMC)
2. BOMDIG Control, and
3. IPCS control.

A real-time engine simulation was used to permit closed loop operation at simulated sea level static conditions. The test procedure included acceptance criteria for operation of the RTE with each control system based upon a building block of comparison data:

1. HMC vs SOAPP - used to establish the HMC as a baseline for subsequent testing.
2. BOMDIG vs HMC - used to verify the BOMDIG control during gas generator operation.
3. BOMDIG vs SOAPP - used to verify the BOMDIG control during afterburner operation.
4. IPCS vs BOMDIG - used to verify the IPCS control and identify operational differences.

In each case the RTE model was the same to provide consistent data.

An open loop schedule definition was run in addition to the closed loop testing to evaluate the schedules in the DPCU at conditions other than standard day. This test was run because the simplified RTE model limited the closed loop system evaluation to a sea level static, standard day condition.

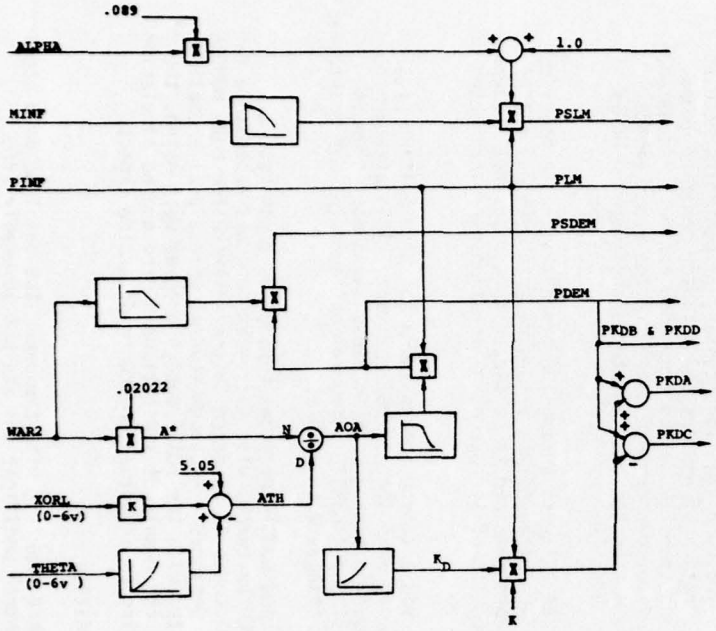

Figure 6.2-11 Inlet Simulation Block Diagram

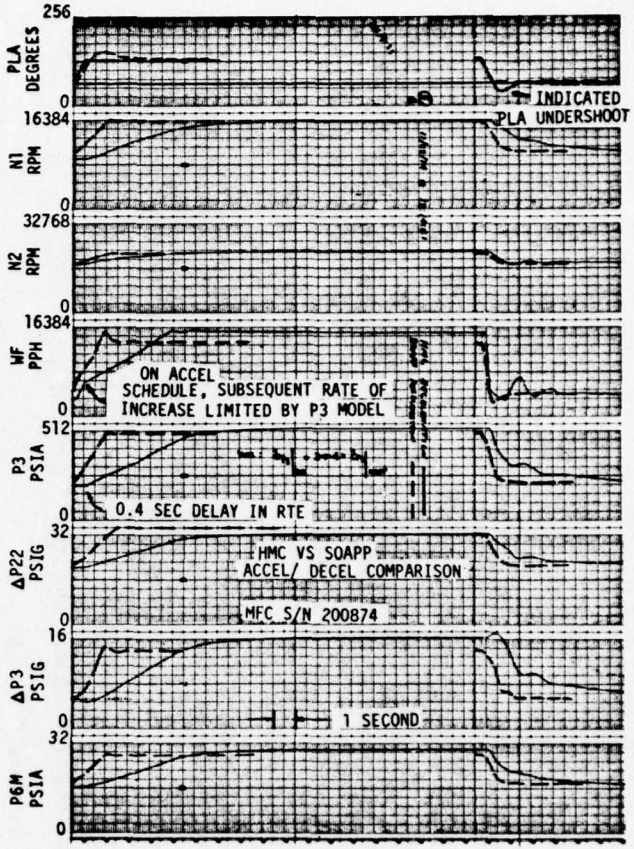

Figure 6.4-1 HMC vs SOAPP - Accel/Decel Comparison

6.4 BENCH TEST RESULTS

6.4.1 Hardware Compatibility

The closed loop bench test permitted system evaluation of the hardware and software for the IPCS program in a configuration similar to that expected on the engine.

The influence of the modified IPCS control hardware characteristics on system performance was determined to be consistent with design criteria. The functional check of the modified hydromechanical control components operating within the complete system demonstrated overall hardware compatibility with the DPCU with one exception. An incorrect sign in software, on the command signal to the Aj stepper motor, resulted in the Aj stepper motor being driven against the closed mechanical stop in the control when a request for open nozzle area was made. As a result of this the stepper motor gear head failed.

An analysis of the failed parts indicated that the failures were due to overstressing the gear train when the stepper motor ran into its end-of-travel mechanical stops. Additional failures were prevented by a combination of software and hardware changes. The software was changed to eliminate the conditions that caused the stepper motor to run into the stops. The stop configuration was modified to increase the distance between the mechanical stops from ± 8 1/2 degrees travel to +22 degrees travel and build in more spring in the stops to reduce dynamic loads. The DPCU hardware operated throughout the test without significant problems.

6.4.2 Bench Test Software Checkout

Continuation of software checkout at the system level was a major bench test goal. The extremely tight schedule (five months from final design review to software delivery) and the limitations of hybrid simulation facility used for closed-loop testing at Honeywell meant that the software development cycle extended well into the program test phase. Bench test procedures included open loop testing of control schedules and trim ranges, steady-state calibration of sensors and actuator position loops, closed-loop transient operation, and transfer to and from DPCU control. Acceptance criteria were based upon comparisons of performance data with the requirements document and with results obtained during the baseline tests and from the SOAPP simulation.

A number of changes were made to the software during the bench test. The majority of these resulted from updating of requirements or errors made in previous definition of requirements. A few coding errors remained to be picked up and several hardware compatibility problems (e.g., direction of stepper motor rotation) were corrected by software changes.

Changes to the software were made via teletype hookup and a software editing program (MEDIC) that was coresident in memory with the control software. This arrangement provided great flexibility and speed in making modifications, with most changes requiring only minutes to make. IPCS and BOMDIG software configuration was maintained and controlled by documenting all changes with SFCO's.

The software checkout of the IPCS and BOMDIG programs during the bench test was successful in proving that the DPCU software, with modifications, was acceptable for engine testing. The basic control modes implemented in the software for both BOMDIG and IPCS were found to operate as designed. Although several operational anomalies relative to performance demonstrated with the SOAPP design program were noted, the differences were determined to be the result of limitations of the engine simulation or design problems requiring testing on an actual engine to determine impact.

6.4.3 Control Mode Test and Validation

The test was performed in a sequence starting with the HMC. The baseline data acquired with the HMC verified that the control modifications did not adversely effect operation of the hydromechanical control. Subsequent testing with the Honeywell DPCU in the BOMDIG mode demonstrated operation similar to the HMC. The afterburner and exhaust nozzle control operation was compared to SOAPP simulation results. Similar operation was demonstrated. The last test sequence involved operating the Honeywell DPCU in the IPCS mode, which demonstrated operation similar to BOMDIG. This was done after control gains were adjusted to provide stable operation of the RTE.

6.4.3.1 HMC Closed Loop Testing

The objective of this test was to obtain transient data from the analog RTE model to document baseline gas generator operation using the HMC control. A comparison was made with SOAPP model operation to identify differences to be expected during SLS engine test. A series of transients was performed with each control. Figure 6.4-1 shows an acceleration followed by a deceleration. Differences were noted when compared with the SOAPP engine model operations. The acceleration shown on the figure indicates that the RTE accelerated slower than the SOAPP model. This was not anticipated for the engine test as the ratio unit plot shown on Figure 6.4-2 indicated close correlation. The slow acceleration was attributed to the RTE burner pressure pneumatic generator, which was observed to be slower than the SOAPP model. Since the HMC acceleration acted as a baseline for subsequent BOMDIG testing, these differences were accepted. The decelerations shown on Figure 6.4-1 and 6.4-2 compare favorably with the exception of a deceleration hook ringing that was observed on the fuel versus time and ratio unit plot. This ringing was observed only with HMC decelerations. Subsequent BOMDIG and IPCS decelerations did not exhibit this characteristic. The recorded data indicate that the HMC throttle undershot during a deceleration. This undershoot was attributed to the air in the hydraulic lines used to actuate the throttle linkage on the control. In addition, the N2 drive for the HMC was determined to be sluggish. Both BOMDIG and IPCS were driven off a different PLA system and had a different N2 signal, thus supporting the conclusion.

The resultant excursions during accelerations and decelerations for each control were within the limits bounded by the limiting schedules formed on the ratio unit plot, Figure 6.4-2. The controls were accepted for subsequent SLS engine testing.

6.4.3.2 BOMDIG Closed Loop Testing - Gas Generator

The objective of this test was to operate the RTE using the BOMDIG DPCU obtaining transient data for comparison with HMC operation. Figures 6.4-3 and 6.4-4 show the transient data comparisons. The BOMDIG deceleration did not ring as was the case with the HMC. The PLA for BOMDIG did not undershoot, and N2 came from RTE, not HMC, motor drive. The BOMDIG acceleration compares almost point on point with the HMC acceleration. The acceleration and deceleration transient envelopes shown on the ratio units versus rotor speed plot, Figure 6.4-4, are similar with the exception of the idle hook ringing and the BOMDIG deceleration proceeding to a lower PLA. The data indicate the BOMDIG and HMC operation were similar, with engine transient protection provided, thereby, validating the software.

6.4.3.3 BOMDIG Closed Loop Testing - Afterburner Control

A thorough investigation of the Aj servo-actuator loop was performed to select the various loop gains. The gain settings were identified at Honeywell as critical to ENC stability. A simple sketch of the Aj control loop is shown on Figure 6.4-5. The inner loop was investigated first and resulted in uncovering the incorrect sign of the stepper command signal. Closure of the outer loop to permit control of the Aj actuator uncovered a software problem. The pilot valve position command signal was compared with the LVDT feedback to generate the stepper command. The software used to generate the stepper command caused all increase signals to start with two steps. The software was corrected to permit a single step. Subsequent testing of the inner and outer loops operating together indicated a problem that was diagnosed as "actuator drift". Figure 6.4-6 illustrates the problem as it existed in steady state with the "TRIM LOOP" locked. The data indicated that a single step travel of the pilot valve was either too large to achieve a steady point, or the actuator was too responsive to the pilot valve travel. It should be noted that the test apparatus had six "Bill-of-Material" actuators. However, only one actuator had its position fed back to the control. In steady state the other five actuators would saturate. This resulted in all the pilot valve flow being ported to a single actuator for steady operation. The results were repeated with the saturated actuators removed from the system. Thus, the cause of the instability was attributed to the actuators being too responsive to a single step. The test was repeated toward the end of the test program when the test apparatus was reworked to tie six actuators together and feed back their common position. This resulted in all six actuators being governed in steady state and greatly improved the servo actuator drift problem as noted on Figure 6.4-7.

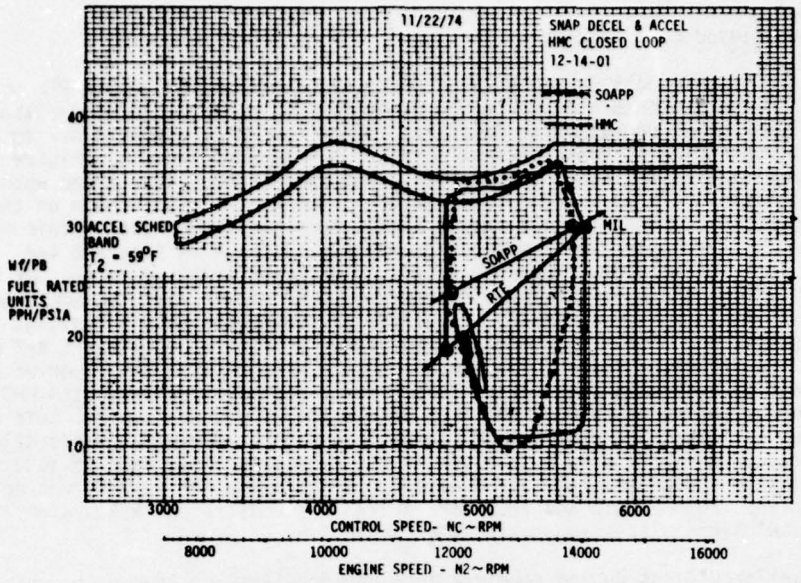

Figure 6.4-2 HMC Closed Loop - Snap Accel and Decel

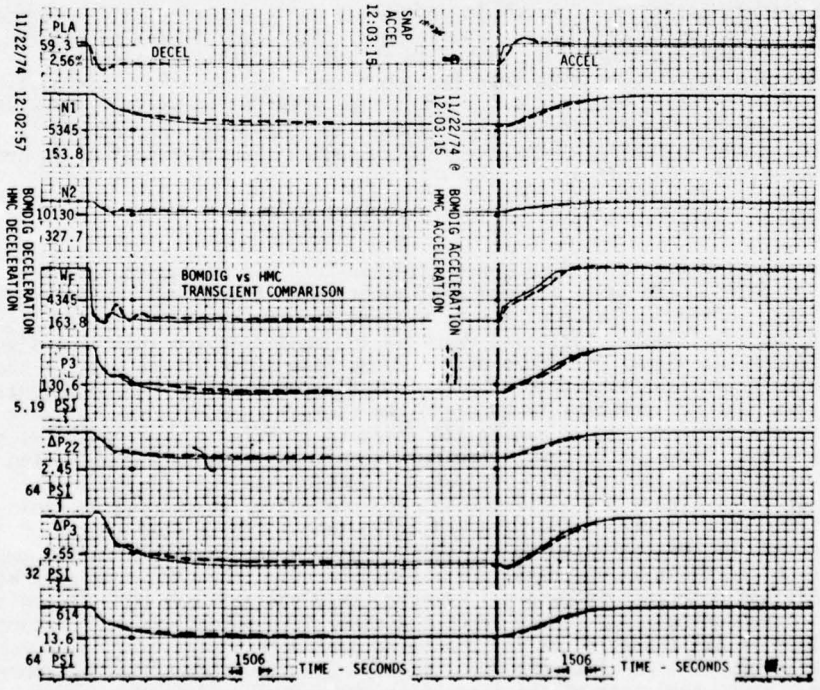

Figure 6.4-3 BOMDIG vs HMC - Transient Comparison

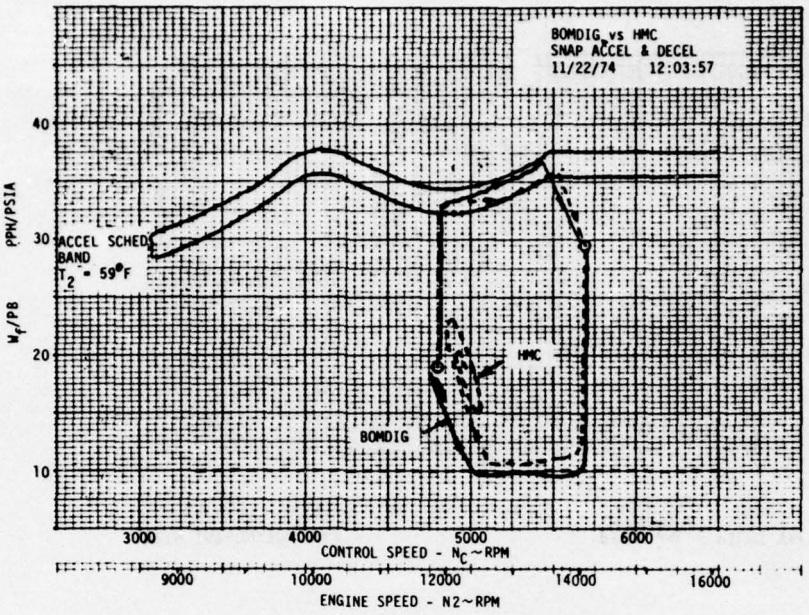

Figure 6.4-4 BOMDIG vs HMC - Snap Accel and Decel

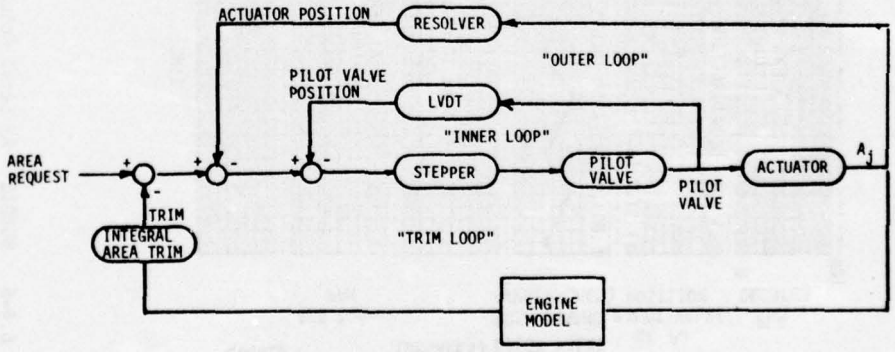

Figure 6.4-5 Definition of Aj Servo Actuator Loops

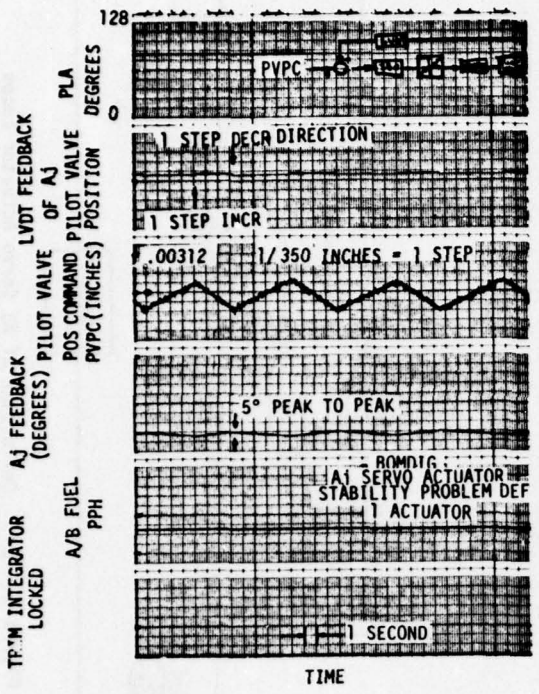

Figure 6.4-6 BOMDIG - Aj Servo Actuator Stability

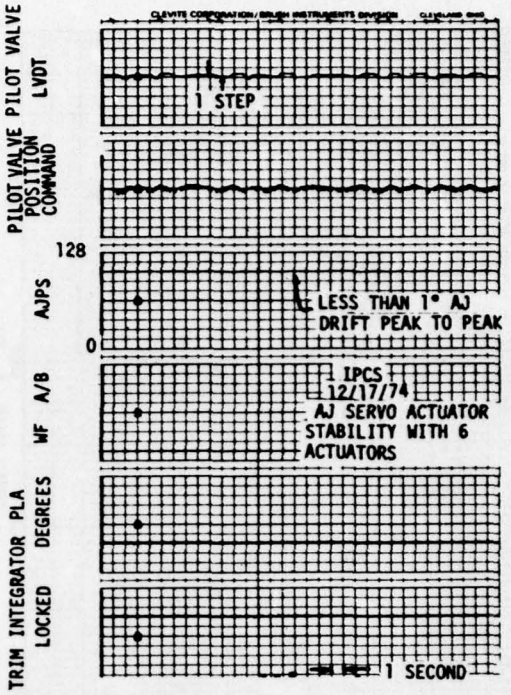

Figure 6.4-7 IPCS Aj Servo Actuator Stability

6.4.3.3 BOMDIG Closed Loop Testing - Afterburner Control (Continued)

The servo actuator testing highlighted the need for providing a control adjustment that would reduce the impact of a single step on the travel of the pilot valve. This adjustment is being made with the existing hardware by incorporating a gain reduction cam on the output of the stepper. The hardware presently has a unity gain cam at this location. A cam design was generated to reduce the gain by a factor of eight in the steady state null region. The trade-off involved slowing down the time to achieve maximum Aj slew by 0.04 seconds (the added time for the stepper to travel to achieve max. slew pilot valve position) which was considered acceptable. Figure 6.4-8 shows the unity cam presently in the control and the new design cam. The new design cam was fabricated and held in reserve in the event that subsequent engine test results indicated the need for its incorporation. Subsequent engine testing indicated that this cam was not required.

The transient afterburner (A/B) and exhaust nozzle control (ENC) operation assured logic validity and demonstrated interface operations. The data were also used as a baseline for comparisons with IPCS. The data were acquired in two sequences. The first sequence was obtained during the preliminary testing phase with a single Aj actuator system. The second sequence was obtained during the final testing phase with a six-actuator system.

The first set of data was compared with the SOAPP program to identify differences that might exist. Figure 6.4-9 shows a Mil to Max. A/B transient followed by a Max. to Mil deceleration transient. These data were acquired with known system anomalies that were duplicated on the SOAPP deck. The suppression parameter used P22/P6M instead of the conventional TF30-P-9 parameter PS22/P6M, and the trim integrator null logic had a gain that was too high, resulting in the trim integrator not going as close to null as it should during not-lit operation. The data comparison shown on Figure 6.4-9 shows a close correlation between the two operations indicating that the software and hardware were performing according to design.

The second set of data acquired for BOMDIG afterburner transient operation shows the Mil to Max and Max to Mil performance with six actuators as shown on Figure 6.4-10. At Max. PLA, the A/B model operated unsuppressed with maximum fuel and downtrimmed area operating in an attempt to satisfy suppression requirements. The Max. to Mil deceleration transient shows Aj closing faster than fuel was turned off as requested by the suppression trim loop. When Aj achieved the appropriate position, afterburner cutoff was sequenced to achieve the transition to MIL power.

A combined gas generator and afterburner accel/decel was performed by snapping the throttle from below Mil up to Max and returning to the RTE idle setting as shown on Figure 6.4-11. The A/B initiation delay may be observed to occur at the start of the transient. Subsequent zone sequencing followed with the Max. power point attained, at which time the throttle was chopped to idle. Simultaneously the gas generator and afterburner decelerated as expected. However, A/B RTE model created a blow-out signal. This resulted in the normal shutdown sequencing being overridden, as expected, wtih the attendant maximum slew closure of Aj and the immediate shut off of the zone fuel valves. The gas generator deceleration masked the blowout derichment action of the main burner fuel.

6.4.3.4 IPCS Closed Loop Testing - Gas Generator

The objective of the transient calibration testing was to operate the RTE using the IPCS DPCU, obtaining data for comparison with BOMDIG operation.

The accel/decel comparison is shown in Figure 6.4-12 which shows IPCS parameters, on Figure 6.4-13 which shows the comparison data with BOMDIG, and on Figure 6.4-14 which shows the Wf/Pb versus N2 excursion comparison. These data illustrate that IPCS and BOMDIG compared favorably, with differences primarily due to the ΔP/P schedule impact. The Wf/Pb excursion envelope tells the story about the differences. As shown on Figure 6.4-14 both controls set similar idle points. However, the acceleration with the IPCS control did not fall within the Wf/Pb maximum allowed band. The high compressor discharge Mach schedule that controlled the IPCS acceleration acted to slow down the acceleration. This was primarily due to the difference bewteen the RTE and the SOAPP engine. The deceleration transient comparison shows the IPCS control undershooting the BOMDIG minimum Wf/Pb ratio by at least 1-1/2

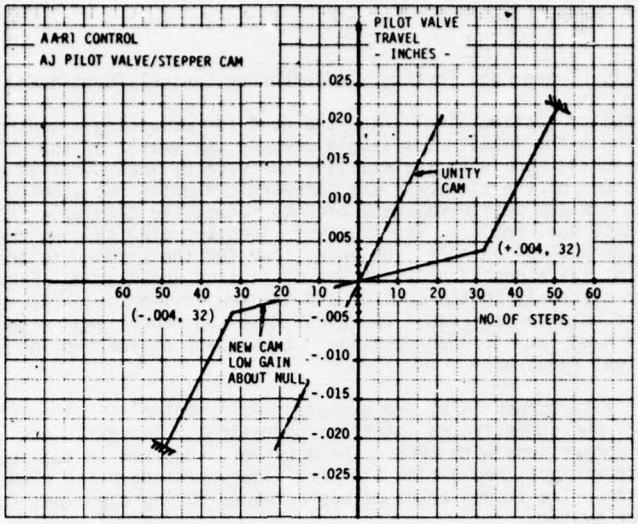

Figure 6.4-8 AA-RI Control Aj Pilot Valve/Stepper Cam

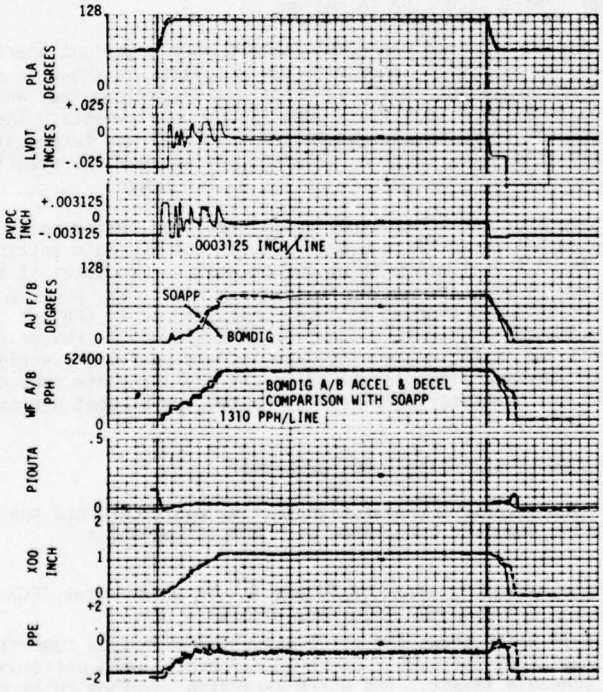

Figure 6.4-9 BOMDIG vs SOAPP - A/B Accel and Decel

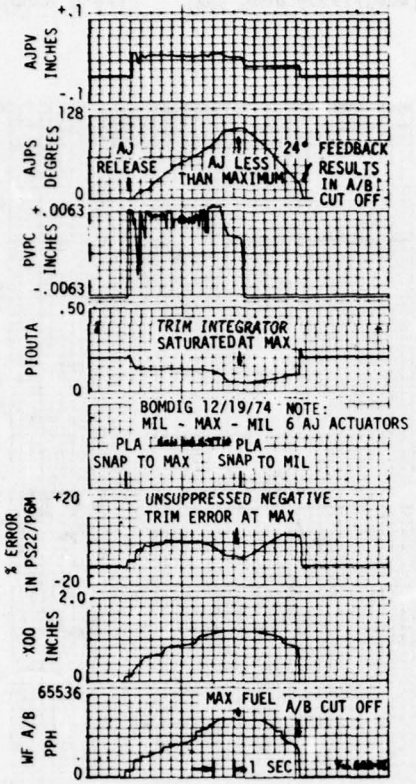

Figure 6.4-10 BOMDIG - MIL to MAX to MIL

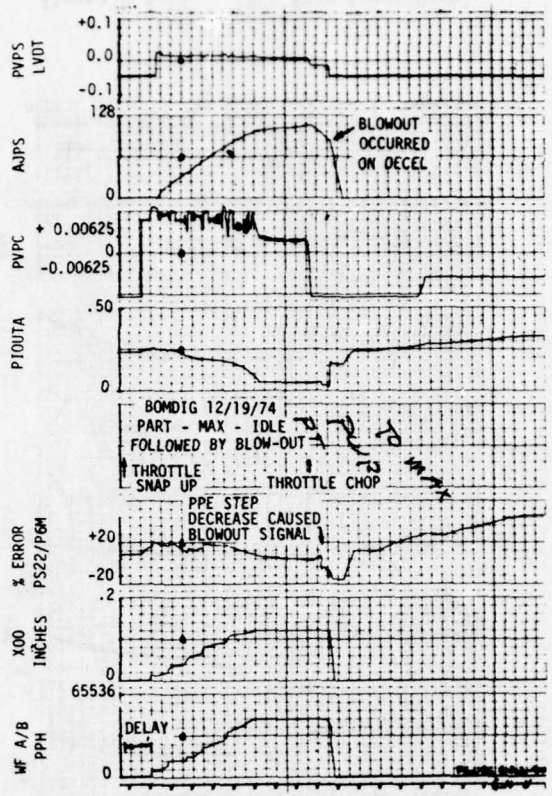

Figure 6.4-11 BOMDIG - Part to Max. to Idle

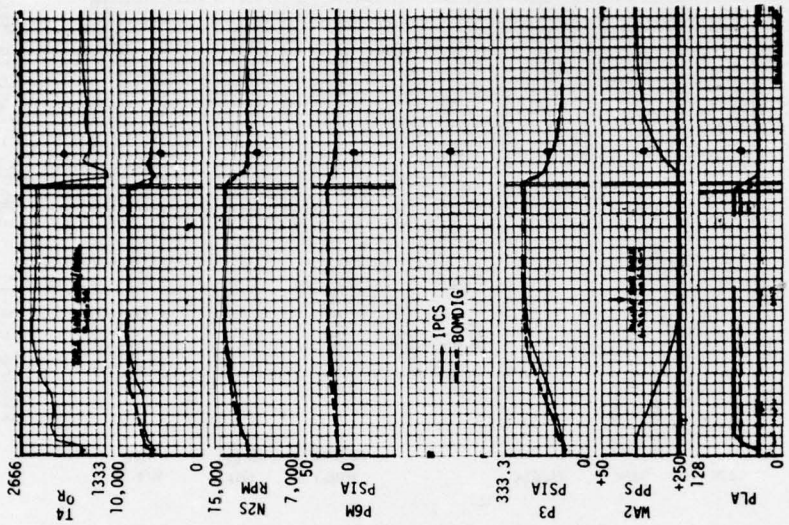

Figure 6.4-13 IPCS Snap Accel/Decel

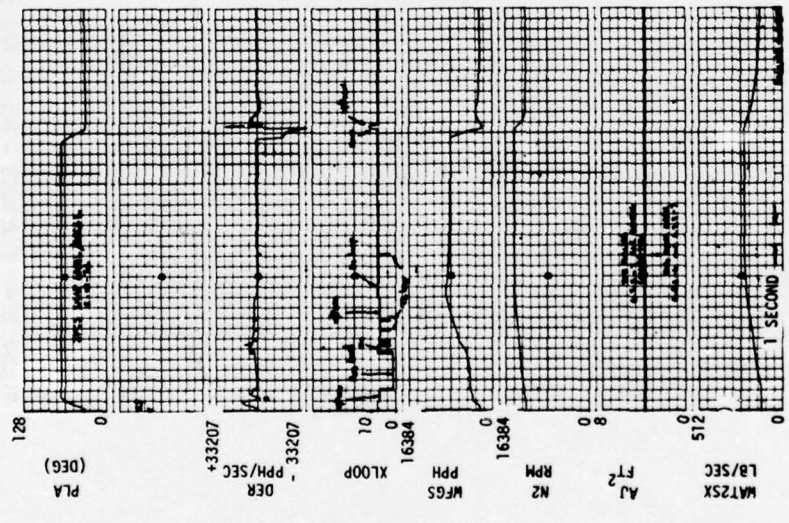

Figure 6.4-12 IPCS Snap Accel/Decel

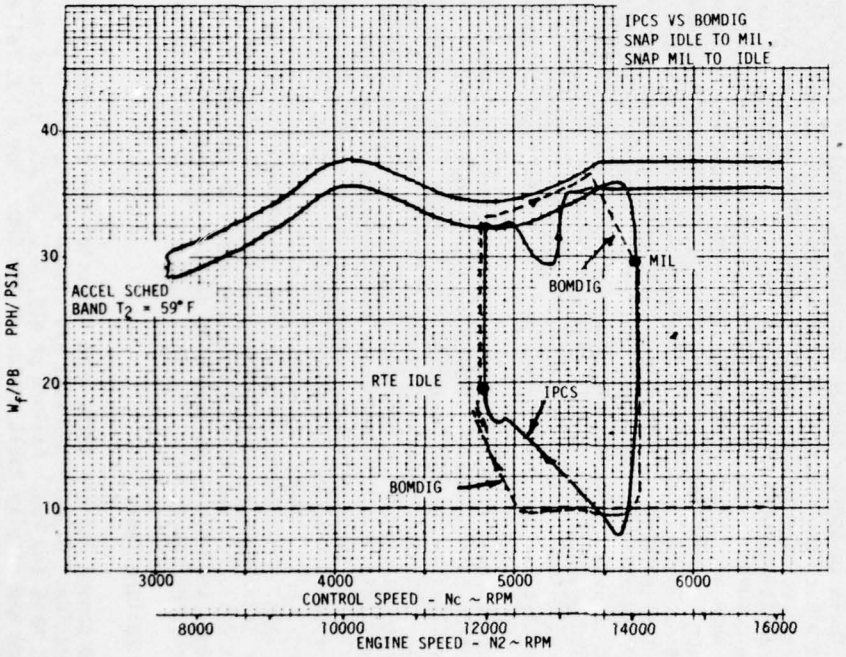

Figure 6.4-14 IPCS vs BOMDIG - Snap Idle to MIL, Snap MIL to idle

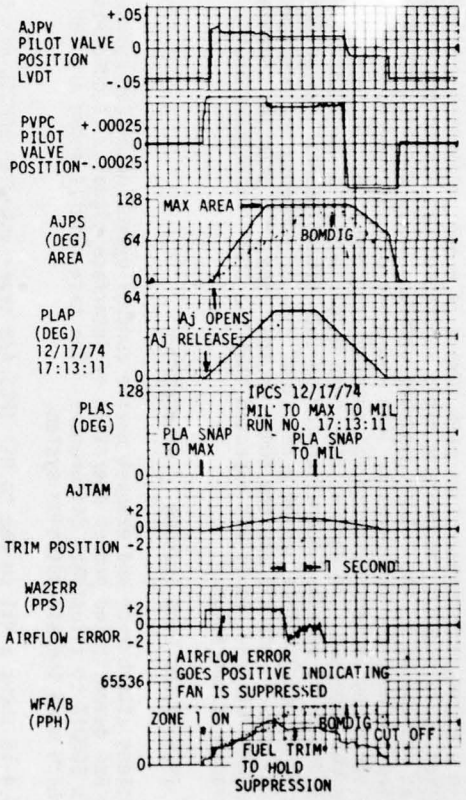

Figure 6.4-15 IPCS MIL to Max. to MIL

6.4.3.4 IPCS Closed Loop Testing - Gas Generator (Continued)

units with a subsequent deceleration path toward Idle that indicates a slower deceleration would occur. The minimum ratio undershoot was due to the tracking error that was caused by the actual hardware metering valve position in the control and implied the need for deceleration loop compensation. Such a change, however, was not made since engine test data did not substantiate the need. Instead, the Wf/Pb loop gain was reduced. The deceleration path which indicates the IPCS will decelerate slower is due to N2 governor operation coming into effect sooner than anticipated with the SOAPP model. This may be a result of gain or compensation requirement differences between the RTE and the SOAPP engine. The IPCS gain and compensation schedules were retained, as it was expected that the SOAPP model more nearly duplicated actual transient operation.

6.4.3.5 IPCS Closed Loop Testing - Afterburner

The transient afterburner and exhaust nozzle control operational test assured logic validity and demonstrated proper operation of interface signals. A comparison was made with BOMDIG to illustrate differences. The test results shown are for the system which used the six-actuator system.

Figure 6.4-15 shows a Mil to Max to Mil IPCS A/B transient with BOMDIG A/B fuel and area superimposed for comparison. When the IPCS Zone 1 turned on, the trim integrator reacted to increase area faster than the PLAP (the rate limited control power lever signal) signal commands. This effect, coupled with the prefill logic, that sequenced the zone fuels to operate sooner than BOMDIG, resulted in a transient that took less time to achieve Max. power. The area transition was smooth, although delayed by the pilot valve response to the command signal. (This delay was also observed on the BOMDIG transition shown on Figure 6.4-10.) The transition to steady Max. power operation occurred with the transfer of suppression control from area to fuel. This occurred when area hit the maximum stop. The result was to downtrim fuel to hold suppression. A momentary overshoot of about one second occurred. The deceleration transient shows fuel reduction following PLAP while Aj was held at its maximum value until Aj trim reduced to close area. This resulted in an unsuppression with fuel cut-off occurring while area was still half open. Cutoff tripped the Aj locking solenoid which closed area at its maximum slew rate. The amount of oversuppression and under-suppression demonstrated by this test was masked by the airflow error term being amplitude limited. Suppression mismatch was also observed during later SLS testing, and corrective measures were identified and implemented to minimize it.

A combined gas generator and afterburner accel/decel was performed by snapping the throttle from Idle to Max., followed by a snap back to Idle. The data shown on Figure 6.4-16 show the A/B parameters, and Figure 6.4-17 shows the gas generator parameters. The "fig sync mark" on each figure identifies a common point in time. The gas generator acceleration occurred first with A/B permission being achieved when speed was within 5% of the reference and the controlling loop was not on a transient limiting loop. Subsequent zone sequencing followed with Max. power achieved, at which time suppression trim was transferred to fuel downtrim. These data were acquired prior to solving a trim integrator release logic problem, with the result that trim action occurred late. This anomaly did not impair the mode verification testing of gas generator interlocks on Idle to Max transients. The deceleration portion of the transient was different than BOMDIG, wherein both the A/B and gas generator decelerated simultaneously. The IPCS mode delayed the gas generator deceleration until the afterburner turned off. The test data verified the logic to do this.

6.4.3.6 Failure Tests

Simulated sensor failure tests were conducted per the bench test plan for BOMDIG and IPCS operation. Primary emphasis was placed on the safety of flight parameters, N1S, N2S, WFGS and P3S. Failure of N1S, N2S, or WFGS should cause reversion to the track mode and display fault status on the CMU. For a P3S failed the system should compute P3S = PS3S + PDP3S and display the backup light on the CMU.

Simulated failure of N1S, N2S, and WFGS caused immediate reversion to the HMC mode with fault status indicated on the CMU. Refer to Figures 6.4-18, and 6.4-19 for examples of transfer to the HMC mode upon sensor failure.

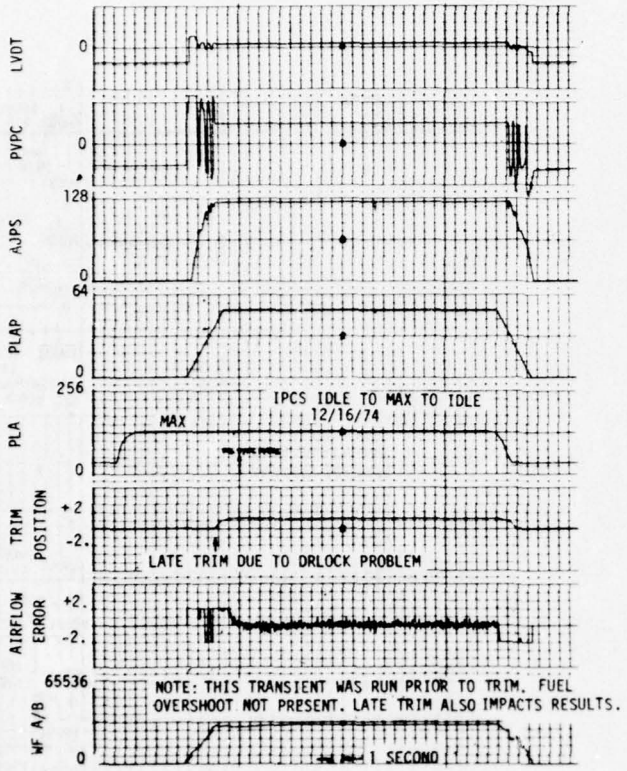

Figure 6.4-16 IPCS Idle to Max.to Idle

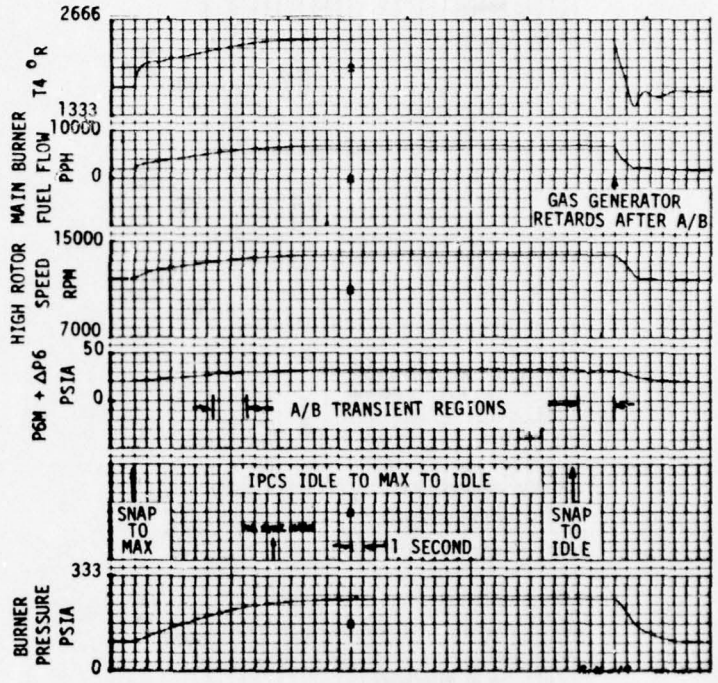

Figure 6.4-17 IPCS Idle to Max. to Idle

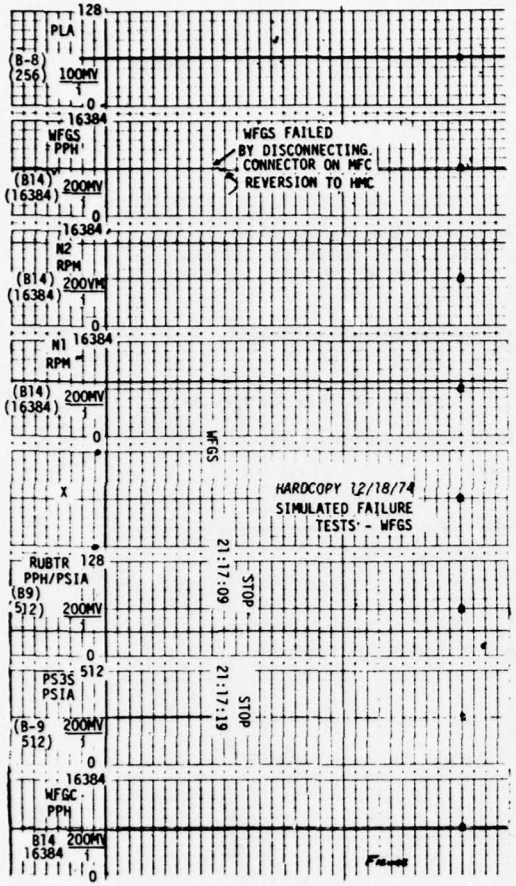

Figure 6.4-18 IPCS Simulated Failure Tests - N1

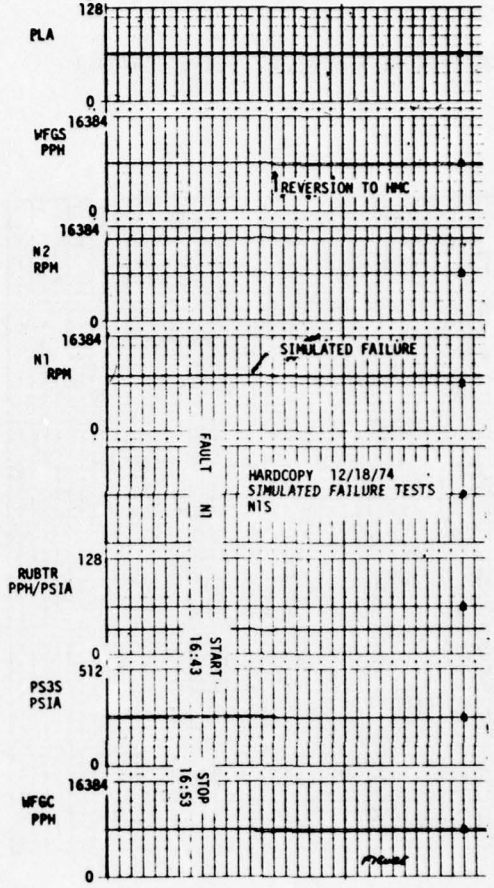

Figure 6.4-19 IPCS Simulated Failure Tests - Wf

6.4.3.6 Failure Tests (Continued

In addition to the parameters listed in the CLB test plan requiring a simulated failure test, T4S was also monitored during IPCS testing to determine if reversion to T4 synthesis occurred when the T4S signal was out of range. This reversion did occur with the backup light being displayed on the CMU.

6.4.4 Bench Test Conclusions and Recommendations

The closed loop bench test permitted evaluation of the hardware and software for the IPCS program in a system configuration similar to that expected on the engine. After the appropriate adjustments and modifications were made, the system was accepted and was recommended for further testing on the engine.

The functional check of the modified hydromechanical control components verified their performance when operated as a complete system. The influence of hydromechanical hardware characteristics on system performance was determined to be consistent with design assumptions and was accepted for engine test.

The DPCU software was found to have some compatibility problems with the system hardware and the dynamic, real time simulation of the propulsion system, but after modifications were made, subsequent testing proved the software acceptable for engine test. The DPCU hardware operated throughout the test without problems and was determined to be acceptable for engine testing.

The control modes implemented in the software for both BOMDIG and IPCS exhibited several operational anomalies relative to performance demonstrated with the SOAPP design program. The differences were determined to be caused by the limitations of the engine model used in the bench test, or by design problems requiring further investigation and testing on the actual engine to determine impact. In either case the control modes were accepted for further testing on the engine.

7.0 SEA LEVEL STATIC ENGINE TEST

Sea level static engine tests were conducted for evaluation of the two IPCS engines and components per reference 4.

The calendar time for testing engine P-676629 was 21 January 1975 through 12 February 1975 with a total engine time of 69 hours and 35 minutes. The calendar time for testing engine P-676627 was 20 March 1975 through 27 March 1975 with a total engine time of 28 hours and 22 minutes.

7.1 SEA LEVEL TEST OBJECTIVES

The objectives of the sea level static engine tests were as follows:

1. Obtain engine calibration and baseline data to determine the effects of IPCS modifications on engine performance.
2. Document engine acceptance after rebuilding.
3. Conduct a preliminary evaluation of the IPCS control system hardware components in the sea level engine environment.
4. Verify IPCS control modes and software with actual engine hardware.
5. Obtain baseline IPCS performance data for the altitude engine test at NASA/LeRC and the ground test at NASA/FRC.
6. Substantiate the structural integrity of the engine modifications.

7.2 ENGINE TEST CONFIGURATION

The test configuration consisted of the modified IPCS TF30-P-9 engines P-676629 and P-676627 installed in the X-16 sea level static test stand at P&WA, the DPCU monitored with the test set, and a limited inlet simulation consistent with the fixed geometry operation of the inlet under SLS conditions. Figure 7.2-1 illustrates the signal paths for the test setup. The test configuration was the same for both engine tests.

All of the engine sensors were installed for the SLS test. The transducer box and harness were the flight hardware. Cables between the engine interface and the IFU duplicated the flight cables both in length and construction. Table 7.2-1 lists the engine sensors and command inputs. The photographs, Figures 7.2-2, 7.2-3 and 7.2-4 show the modified engine mounted in X-16 stand and the DPCU electronic test equipment mounted in the Control Room.

Because of the fixed geometry operation of the inlet at low speeds, only a limited simulation was required for this test. Table 7.2-2 presents the normal signal and command flow between the DPCU and the inlet/airplane combination. Table 7.2-2 lists the sources of these signals during the SLS test. Because the geometry remains fixed in the takeoff configuration, neither the position feedback signals nor the pressure ratios which position the geometry (local Mach and duct exit Mach) were required. Since no actuators were used, the position commands were not required either. The four Paroscientific pressure transducers at the compressor face which are used for the distortion and average P2 signals were simulated. A single transducer was connected to a compressor face total pressure probe. The output of the transducer was paralleled to the four IFU input channels. This produced the correct P2 and zero distortion signal which is representative of operation with a bellmouth inlet. Because the distortion signal is zero, a separate signal source was required to checkout the distortion control features. A pot on the TSU was used to supply a KD signal to the DPCU through one of the spare A/D channels. A software change was made which bypassed the normal KD calculation and substituted the input value. The airplane angle of attack and Mach number signals were set to zero through a minor change to the software. A Kulite transducer was installed, vented to ambient pressure, to present the IFU with the proper impedance characteristics for the buzz and turbulence detectors.

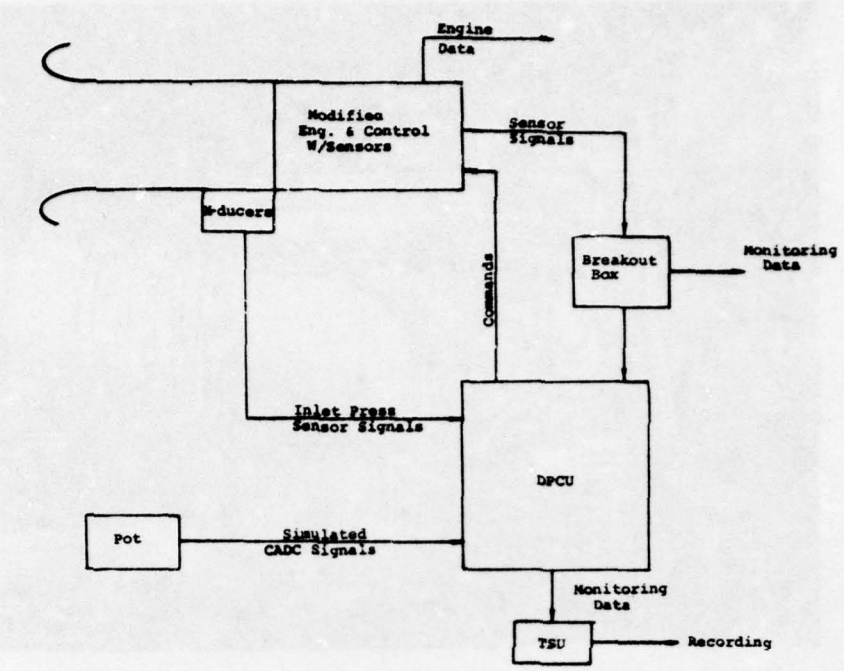

Figure 7.2-1 Signal Paths - SLS Test

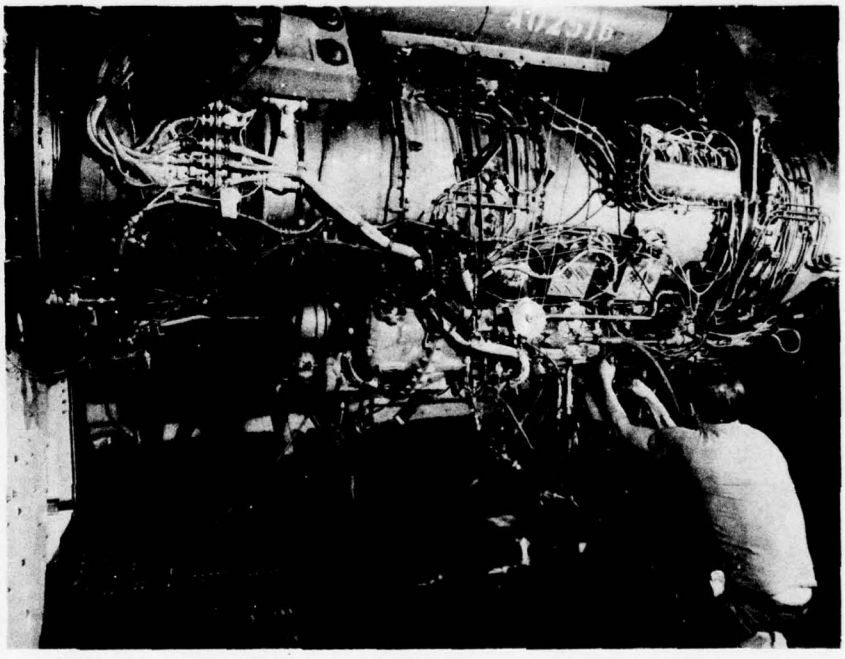

Figure 7.2-2 IPCS Engine P-676629 Mounted In X-16 Stand Left Side View

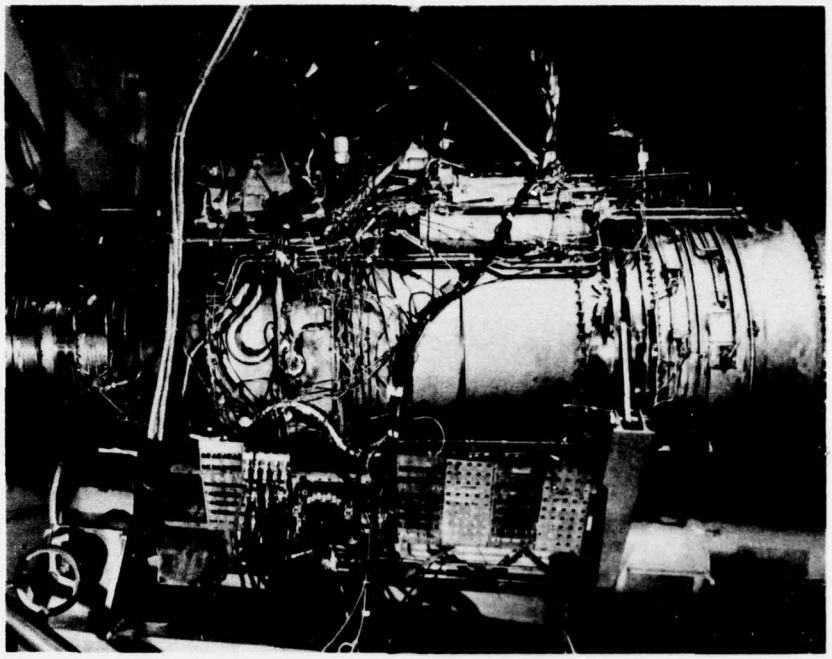

Figure 7.2-3 IPCS Engine P-676629 Mounted in X-16 Stand - Right Side View

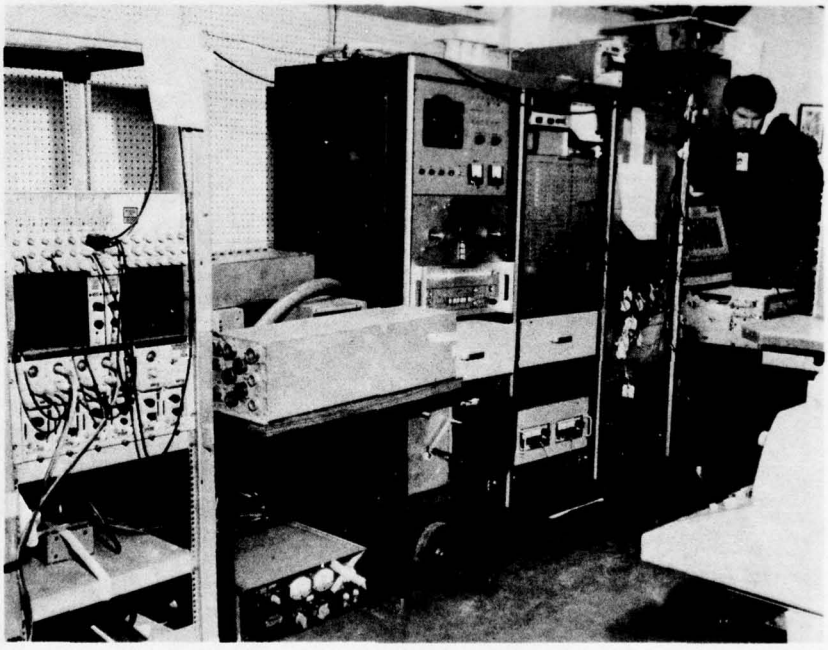

Figure 7.2-4 IPCS SLS Engine Test Showing Electronic Test Equipment

Table 7.2-1

Engine Control Signals

Sensed Parameters

Low Rotor Speed, N1
High Rotor Speed, N2
LPC Exit Total Pressure, P22
LPC Exit Static Pressure, PS22
LPC Exit Differential Pressure, (P-PS) 22
HPC Exit Total Pressure, P3
HPC Exit Static Pressure, PS3
HPC Exit Differential Pressure, (P-PS) 3
LP Turbine Exit Total Pressure, P5
Compressor Face Total Temperature, T2
LPC Exit Total Temperature, T22
HPC Exit Total Temperature, T3
Turbine Inlet Gas Temperature, T4
Fuel Inlet Temperatures
Nozzle Area
Fuel Valve Position - Main & 5 A/B Zones
Power Lever Angle
Bleed Positions

Commands

Main Fuel Flow
A/ B Zone Fuel Flow - 5 Zones
Nozzle Area
Bleed Positions

Table 7.2-2

Inlet/Airplane Interface Signal Sources for the SLS Test

Signal	Source
Local Mach and Duct Exit Mach Pressures	Not Sensed
4-Probe Distortion Pressures	Paroscientific transducer installed on total pressure - paralleled into the 4 distortion pressure input channels. Pot input of KD through A/D channel to checkout distortion control.
Turbulence/Buzz Sensor	Kulite Installed - vented to ambient pressure
Spike/Cone Feedback LVDTs	Not Input
Spike/Cone Position Command	Not Needed
CADC Angle of Attack and Mach Number Signal	Not Input - set to zero in the software
Airplane Squat Switch	Simulated with a voltage source and input to the DPCU through the normal input channel.

7.2.1 Engine Test Facility

The X-16 is a gas turbine engine test facility designed to develop both afterburning and non-afterburning turbojet and turbofan engines. Total airflow in the stand is limited by the inlet sound treatment to 1800 lb/sec. Engine testing can be conducted only at ambient temperatures and pressures.

The controls and instrumentation necessary to operate the engine and monitor its performance are located in the test stand control room. This room is located at an intermediate elevation between this stand and X-15 stand. An observation window is provided in the Control Room for visual inspection of the test cell interior during engine operation. Test stand support equipment and services are located beneath the Control Room.

7.2.2 Test Hardware

7.2.2.1 Engine Related Hardware

The major IPCS components which were tested on both engines are shown in Table 7.2-3.

Table 7.2-3

Major Engine IPCS Components

IPCS Component	P-676629	P-676627
CJ-U1 Main Fuel Control	P/N 749008 S/N 200838	P/N 749008 S/N 200874
AA-R1 Afterburner and Exhaust Nozzle Control	P/N 749009 S/N 1860	P/N 749009 S/N 1974
Transducer Box Assembly	P/N 724790	P/N 724790
P3 Pressure Probes	P/N 724786-300	P/N 724786-300
N1 Tachometer	P/N 751103	P/N 751103
N2 Tachometer	P/N 751103	P/N 751103
T4 Fluidic Probe	P/N 24788	Not Installed
P22-T22 Combination Probe	P/N 686202 (Experimental)	P/N 724784-300
Electrical Harnesses		
Main Fuel Control	P/N 724792	P/N 724792
Transducer Box	P/N 751168	P/N 751168
Afterburner Control	P/N 751169	P/N 751169
Thermocouple	P/N 751170	P/N 751170
N1 Tachometer	Experimental	P/N 751240
Afterburner Control	P/N 751302	P/N 751302

7.2.2.2 DPCU Related Test Hardware

The DPCU related components which were tested included the power supply unit (PSU), digital computer unit (DCU), interface unit (IFU), computer monitor unit (CMU) and the test unit (TSU), as shown on Table 7.2-4. A configuration change was made to the CMU during testing of P-676627 engine to allow the 7th stage bleeds to be opened upon a disengagement from DPCU control to Hydromechanical Control (HMC) and thus prevent N1 overspeed. This was done by installing a relay, supplied with 28 VDC. A disengage signal from the CMU opened the relay and allowed the 28 VDC power supply to be directed to the manual override of the 7th bleeds.

Table 7.2-4

IPCS "DPCU Related" Part Numbers

DPCU Component	P-676629	P-676627
Power Supply Unit (PSU)	P/N BG 1097AA01 S/N V1	P/N BG 1097AA01 S/N V1 and V2
Digital Control Unit (DCU)	P/N DBG 8239B1 S/N V1	P/N DBG 8239B1 S/N V1 and V2
Interface Unit (IFU)	P/N HG 1026AA01 S/N V1	P/N HG 1026AA01 S/N V1 and V2
Test Set Unit (TSU)	P/N UG 2568AA01	P/N UG 2568AA01
Computer Monitor Unit (CMU)	P/N CG 1064AA01	P/N CG 1064AA01

7.2.3 Instrumentation

The test instrumentation included the normal test cell sensors used during TF30 testing. The data were recorded on a number of data systems. A steady state automatic recording system was used to record performance data, and normal test gages were used to monitor the steady state engine operation. An oscillograph and an X-Y plotter were used to record transient performance, and a continuous tape system was used to record critical parameters for analysis in the event of an engine failure.

The data from the DPCU were obtained from 11 selectable digital-to-analog (D-A) channels for transient recordings, an octal display on the TSU for steady state data, and the pulse code modulated (PCM) data signals for post-test analysis and reporting. The PCM data were tape recorded during the engine test and then sent to USAF/FDL for processing.

7.3 TEST PROCEDURES

7.3.1 Engine P-676629

IPCS Sea Level Static Engine Test Plan, reference 3 which was issued and approved prior to the testing, outlined the procedures required to accomplish the test objectives in an orderly progression. The procedure was divided into two categories, Verification Tests and Documentation Tests. Testing of engine P-676629 followed this plan without significant deviation.

The Verification Tests allowed for engineering evaluation of the system while operating in the HMC mode, the BOMDIG mode, and the IPCS mode. The Documentation Test, which was to include a cyclic endurance test and the official engine acceptance test, was modified to include only the acceptance test. Sufficient time and operational cycles were accumulated on the engines during the Verification Tests to preclude further cyclic endurance testing.

7.3.2 Engine P-676627 Test Procedure

The procedure for testing P-676627 was revised to place primary emphasis on the operational problems which were not resolved during P-676629 engine testing, and at the same time, to evaluate the overall system on this engine per the IPCS Sea Level Static Engine Test Plan.

The problems identified and not resolved during the P-676629 engine testing were as follows:

1. T2 offset of approximately 10°F between the engine harness readings and the DPCU reading (BOMDIG and IPCS modes).

7.3.2 Engine P-676627 Test Procedure (Continued)

An open loop test (engine off) was run to establish that the millivolt output of the cold reference junction probe and the resistance of the thermistor, when measured at the engine harness, were the same level (after conversion to temperature through appropriate conversion tables) as the T2 measured by the engine harness system and the experimental thermocouple installed in the transducer box.

The follow-on step was to monitor the DPCU T2 and thermistor reading during the engine test and compare to the T2 engine harness reading and the experimental thermocouple in the transducer box.

2. Low Wf/Pb level during the engine transients Idle to Military (BOMDIG and IPCS modes).

Special instrumentation was installed to determine, during engine steady state operation and transients, the differences in burner pressure (PS3) between what the main fuel control sensed and what the DPCU sensed. A fuel flow calibration was also run to determine the difference between the measured Wf out of the main fuel control and the Wf measured by the DPCU.

3. Incorrect 12th bleed opening and closing point (BOMDIG and IPCS modes).

Special instrumentation was installed to determine the steady state dynamic differences in the PS22 level sensed by the Pressure Ratio Bleed Control (PRBC) and the DPCU. Instrumentation was also installed in the override signal line from the Main Fuel Control (MFC) to the PRBC to determine if the hydromechanical system was overriding the DPCU command when operating in either the BOMDIG or IPCS modes.

4. N_1 overspeed during transfer from DPCU to HMC at Max. A/B.

The configuration of the CMU (refer to paragraph 7.2.2.2 of this report) was modified to cause the 7th stage bleeds to pop open upon DPCU disengagement. Disengagement tests from DPCU to HMC control were run from Zone 1 to Max. A/B to determine the amount of N_1 overspeed when the 7th stage bleeds were opened at point of disengagement.

The following problems were tested during the Verification Test portion of the test plan with the software logic correction being incorporated prior to the tests.

1. Zone 2 Wf cycling on/off during slow transients through Zone 2 turn-on region (BOMDIG mode).
2. Inconsistent Wf/Pb tracking caused by noise on the DER signal (IPCS mode). See paragraph 6.5.1.1.
3. Engine remaining at Max. A/B following a snap power lever movement from Max. A/B to Idle (IPCS mode).
4. Engine stall during bodie transient, Max. A/B to Military to Max. A/B (IPCS mode).
5. Delay in Aj and A/B Wf during a snap transient, Military to Max. A/B (IPCS mode).

7.4 SEA LEVEL ENGINE TEST RESULTS

7.4.1 Hardware Validation

The sea level static engine tests conducted on both engines P-676629 and P-676627 served a two-fold purpose, acting in one case as a means to evaluate and verify control and engine modifications, and in another case to document engine acceptance.

The engines were tested with the hydromechanical control, and evaluation showed that the modifications to the fuel control did not impair operation of the engine between idle and military rated power.

The engine testing done with the DPCU in either the BOMDIG mode or IPCS mode verified the various control loops and transducers while operating in the engine environment between idle and maximum rated power.

Satisfactory completion of a total of 98 hours of steady state and transient testing, and satisfactory periodic inspection of engine hardware and IPCS probes provided assurance of the structural integrity of the engine modifications.

7.4.1.1 Sea Level Engine Acceptance Tests

Engine P-676629

The steady state calibration of P-676629 after the sea level static test indicated engine performance and low and high compressor operating lines were within the acceptable maintenance bands and below upper limits (Figures 7.4-1 through 7.4-4.) Final acceptance data taken on 12 February 1975 showed slight decreases in corrected high rotor speed, XNHR2 and overall compression ratio, PS3Q2 from original calibration levels (0.4 and 0.5 percent respectively) and this could indicate a slight increase in first turbine nozzle area or a slight loss in high turbine efficiency during the 69 hour 35 minute duration of the sea level static test. The Wf/Pb ratio unit comparison in Figure 7.4-4 shows the post-test P-676629 data shifted approximately 0.5 ratio unit up from the pre-test level. This may have also been caused by a slight increase in high turbine area or a slight drop in high turbine efficiency. A post-acceptance test borescope inspection did not reveal bowed or warped first turbine vanes. Engine trim was within the acceptable maintenance bands, and acceleration time was within limits.

Engine P-676627

The steady state calibration of P-676627 after the sea level test indicated engine performance and low and high compressor operating lines were within the acceptable maintenance bands and below upper limits (Figures 7.4-5 through 7.4-8). Final acceptance data taken on 27 March 1975 showed no change in engine performance from the original calibration conducted on 19 March 1975. An apparent improvement in fuel consumption can be noted on Figure 7.4-8 but the differences are within normal data scatter.

Engine trim was within the acceptable maintenance bands and acceleration time was within limits.

Comparing the acceptance test data of the two engines, P-676627 performance was better than P-676629 demonstrating a 0.5 - 1% lower LPC operating line, and at constant EPR, 20° - 30°F lower turbine inlet temperature and 1.5% lower fuel consumption.

7.4.2 Control Mode Development

The engine test program was conducted to perform a control mode evaluation in the actual engine environment. The test was conducted to conform to the test plan requirements where practical. The engine test with the hydromechanical control established base line gas generator steady state and transient performance. The IPCS probe data were reviewed, and correction factors were included in the control.

BOMDIG

The BOMDIG gas generator testing was conducted to parallel the testing performed with the hydromechanical control and resulted in program changes to account for the following problems:

1. Operation of the engine in the prestart and start region resulted in modifications to sensor validity checks.
2. Operation during steady state indicated the N_2 tachometer to be noisy. The N_2 signal was filtered.

The resultant engine operation was acceptable.

The BOMDIG afterburner testing was conducted to evaluate the software and to establish a baseline for the IPCS mode. The control program was changed during the test to account for the following problems.

1. Steady state A/B fuel flow oscillations were occurring at a 10 Hz frequency. A correction to the integration routine for the power piston eliminated the problem.

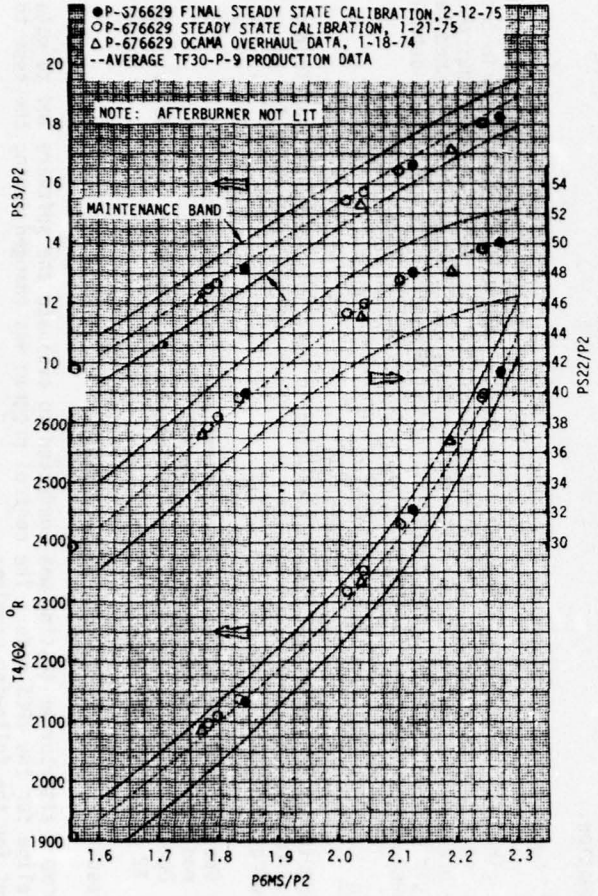

Figure 7.4-1 IPCS - P-676629 SLS Test - Steady State Calibration

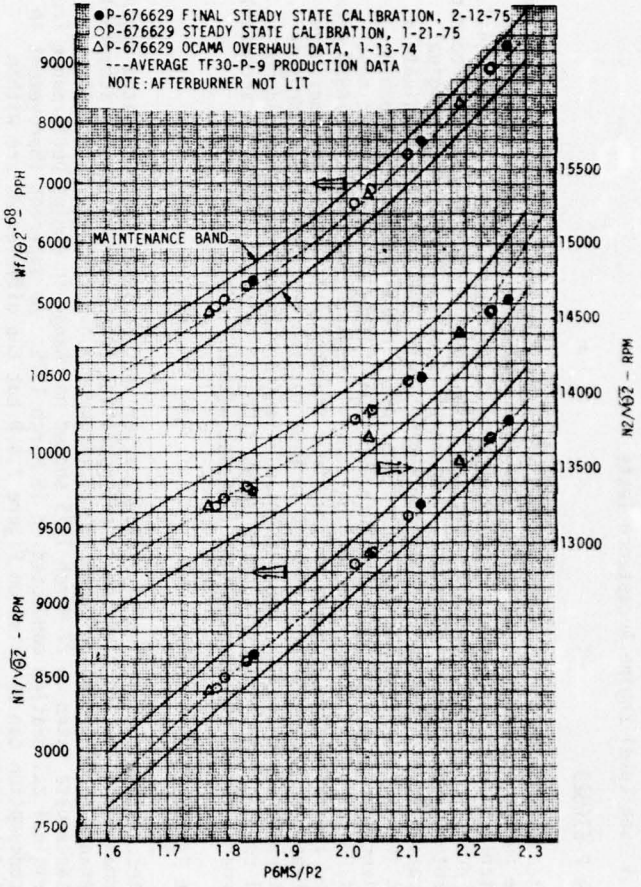

Figure 7.4-2 IPCS P-676629 SLS Test - Steady State Calibration

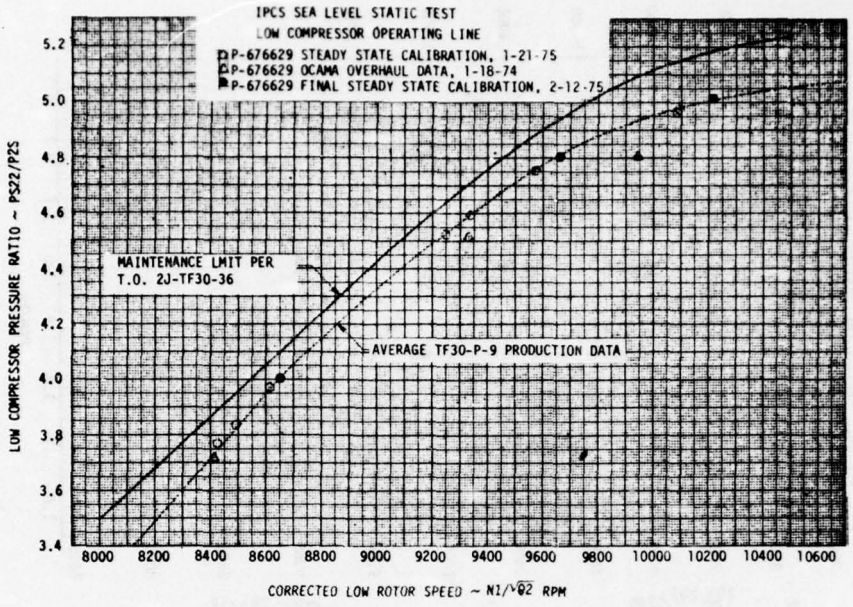

Figure 7.4-3 IPCS P-676629 SLS Test - Low Compressor Operating Line

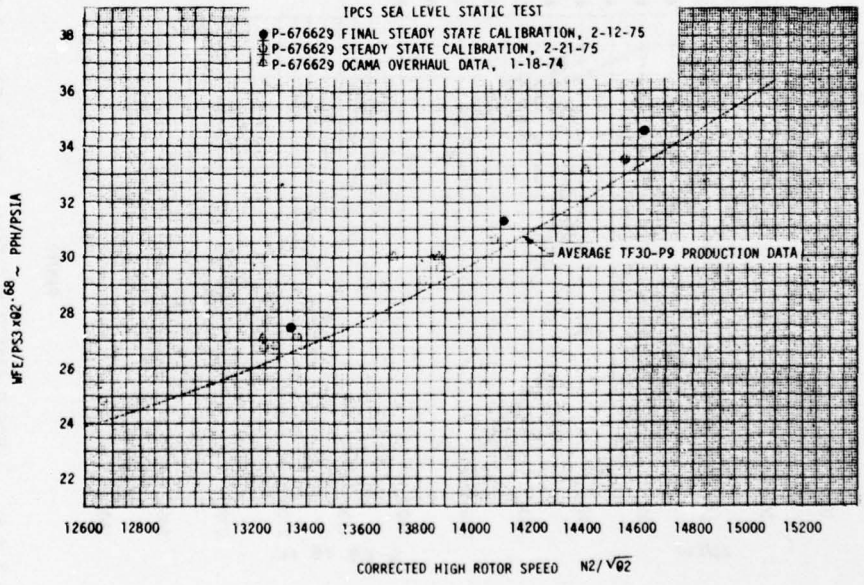

Figure 7.4-4 IPCS P-676629 SLS Test - WFE/PS3 vs CORRECTED N2

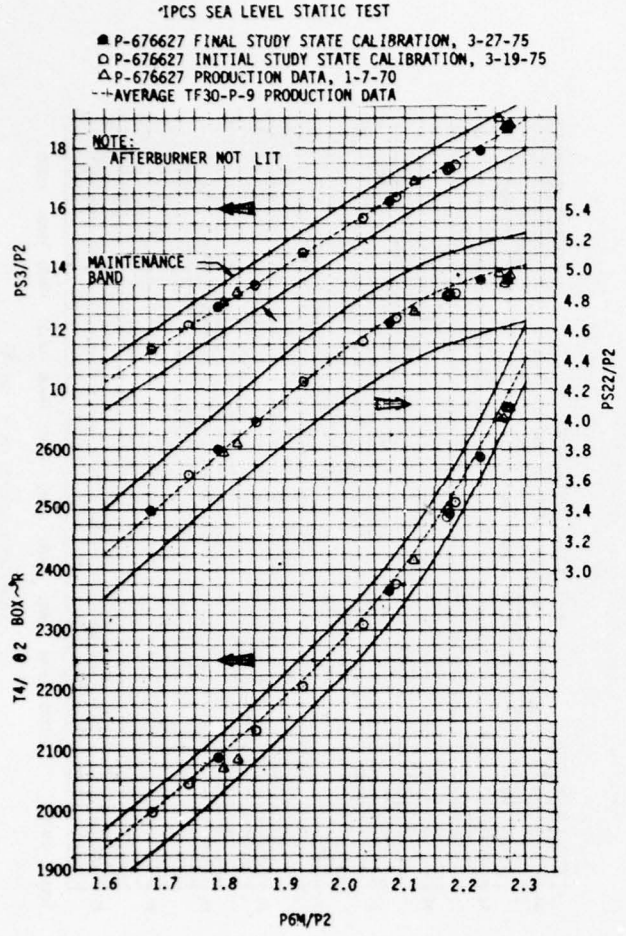

Figure 7.4-5 IPCS P-676627 SLS Test - Steady State Calibration

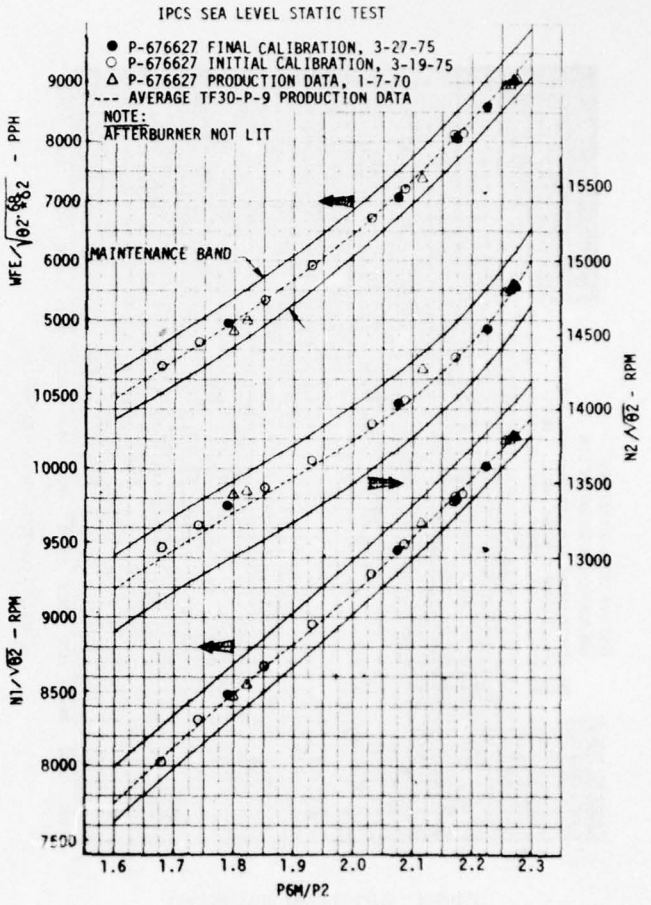

Figure 7.4-6 IPCS P-676627 SLS Test- Steady State Calibration

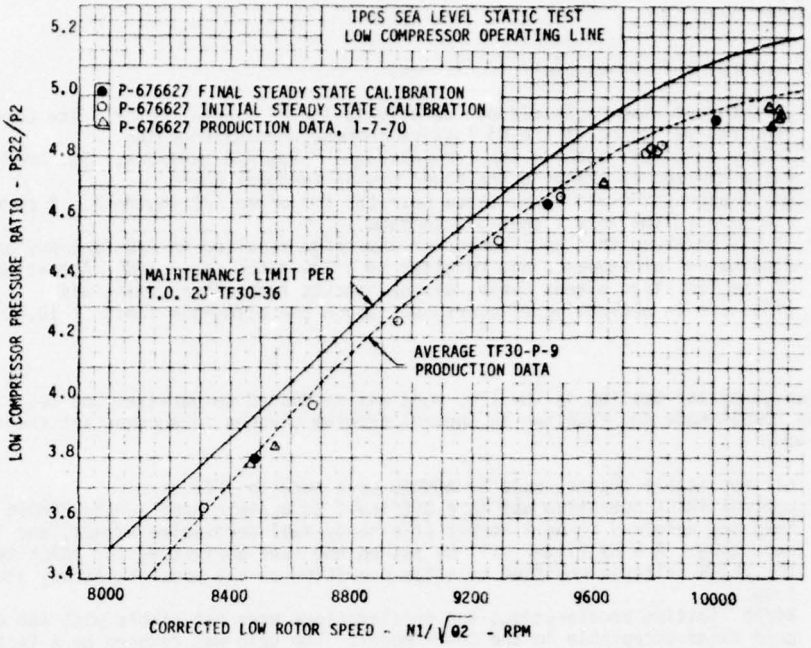

Figure 7.4-7 IPCS P-676627 SLS Test - Low Compressor Operating Line

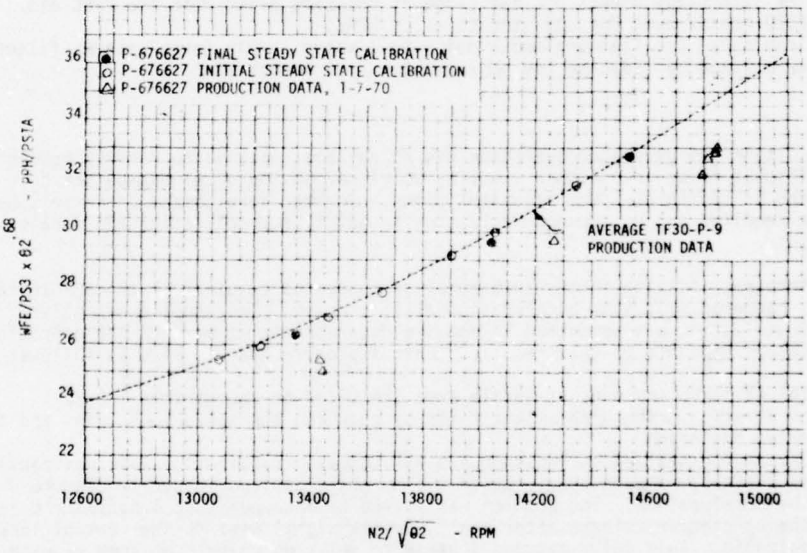

Figure 7.4-8 IPCS P-676627 SLS Test - WFE vs XNH

7.4.2 Control Mode Development (Continued)

2. Afterburner disengages did not deactivate the Aj stepper motor. The correction required was to reset the Aj locking command when disengaging.
3. A Zone 2 "on-off bobble" was encountered on slow A/B advances. The problem was minimized by changing the power piston feedback curve.
4. An unsuppression was encountered near the end of an A/B shutdown. A correction was made to the Zone 1 shut-off command.
5. It was observed that an afterburner disengage resulted in A/B fuel and area closing out of sequence and resulted in a low rotor overspeed. Actuation of the 7th stage bleeds during disengagements from afterburning was effective in preventing N1 overspeeds above the allowable limit of 10,500 rpm.

IPCS

The gas generator testing in the IPCS mode was conducted to parallel the tests made in the BOMDIG mode and resulted in control program changes to account for the following problems:

1. All applicable changes made to BOMDIG were made to IPCS.
2. Control TRACK operation was more difficult to achieve than in the BOMDIG mode. This was resolved to be a result of a noisy fuel derivative signal, and loop switching. A 5 Hz filter will be put on the fuel derivative for TRACK test and the TRACK criteria modified to allow operation on all possible steady state loops.
3. Wf/Pb limiting accelerations and decelerations were not stable with the control gain found acceptable in the SOAPP model. The gain was reduced by a factor of 2.
4. The acceleration Mach limiting schedule was found to be sensitive to small adjustments, whereas the deceleration Mach limiting schedule was insensitive. Schedules were designed that permitted partial operation on these loops.
5. The 12th stage bleeds were cycling in steady state due to a noisy fuel derivative signal. Filtering solved the problem.
6. The 12th stage bleeds did not close at the same point that the PRBC did. The PS22 measurement was adjusted to match PRBC.
7. Idle speed oscillations and a noisy fuel valve at Mil (even with N2 filtered) were fixed by reducing the N2 loop gain by a factor of 2.

The resultant gas generator operation was acceptable relative to BOMDIG; however, it was difficult to achieve a Mach limiting acceleration and deceleration schedule that permitted achieving the same transient times. Further development of these schedules will be required during subsequent testing to optimize acceleration and deceleration transients.

The afterburner testing in the IPCS mode was conducted to parallel the BOMDIG testing and was hampered by a snap acceleration stall problem. The problem was solved, and subsequent testing was conducted to acquire data demonstrating IPCS A/B operations. The problems encountered that required control program changes were as follows:

1. The Aj servo and exhaust nozzle area exhibited an undesirable 1/2 Hz oscillation. The problem was fixed by changing the servo loop gains and the trim loop gains.
2. The engine stalled during snap A/B Mil to Max. transients. This was caused by an unstable exhaust nozzle servo system that resulted in nozzle closure during the acceleration. The problem was solved by incorporating a software delay on the Aj stepper release after the Aj unlock signal went to the control locking solenoid. This delay matched a hardware delay which held up area release. Without the software delay, the stepper would "wind up" upon the initial release signal trying to open area which was not free to respond. This caused a situation where the pilot valve was spring loaded against the null-flapper, and, without any stepper feedback, the pilot valve system was free to react in response to external disturbances (such as hydraulic pressure fluctations).
3. A Max. -Mil-Max, A/B bodie stall problem was attributed to the Zone 1 enrichment coupled with the manifold prefill. A control modification which delays prefill when area is opening fast eliminated the bodie stall problem.
4. A slow area closure problem during a Max. to Mil snap was caused by a slow trim reset. The problem was corrected by including an airflow error term to unlatch area.

7.4.2 Control Mode Development (Continued)

5. A noisy airflow measurement signal (intermittent one pass error) caused an early Aj release and created an erratic stepper command. A 5 Hz filter was added to the airflow measurement.
6. A Max. to Idle deceleration with pop-open area at Idle throttle position resulted in a limited Nl overspeed since the gas generator deceleration was delayed until the A/B transient was completed. Simultaneous deceleration of the gas generator and afterburner eliminated the possibility of Nl overspeed.
7. A snap acceleration from Mil to Max. operated smoothly with the exception of an intermittent hold that occurred at the top of Zone 3. A/B gain changes minimized the intermittent hold.

The resultant A/B transients demonstrated that prefill does work to result in a fast smooth transient.

7.4.3 Engine Response Comparison

The mode evaluation and verification testing program required engineering evaluation of system operation during the test to formulate an acceptance. Basically, this was done by a series of comparisons with experience and the SOAPP design deck used for a baseline. The operation of BOMDIG was compared against the HMC for gas generator operation, and against SOAPP for afterburner operation. The operation of IPCS was compared against BOMDIG, keeping in consideration the demonstration of the basic operational requirements described at the program design reviews. In all cases, the engine T.O. 2J-TF30-36 was referenced to define steady state and transient engine operating limits.

7.4.3.1 BOMDIG Mode

Gas Generator Transients

The test on engine P-676629 was conducted with the 7th stage bleeds closed and with the pop-open nozzle feature at idle. Figure 7.4-9 shows the Wf/Pb vs N2 path for the selected throttle snaps. Superimposed is the HMC accel-decel envelope obtained during the same test conditions. The BOMDIG control resulted in lower ratio units during the accel and decel. Figure 7.4-10 is the time transient comparison for the idle to mil snap, which shows the engine accelerating slightly faster with the HMC control. A review of the steady state probe calibration data after this test was run showed the DPCU burner pressure measurement PS3S reading about 2 psi lower than the HMC burner pressure. A post-test SOAPP simulation with this -2 psi offset in burner pressure measurement indicated a slower accel with the Wf/Pb path being about 1 1/2 ratio units lower.

Subsequent testing on engine P-676627 was conducted to verify the PS3S probe calibration effects. However, an across-the-board +2 psi shift was not attempted due to concern about this shift during high altitude operation, where the shift would have a large impact during low pressure conditions. Instead, a temporary slope adjustment of +2 psi at mil pressure level with no change at idle was implemented. As shown on Figure 7.4-18 BOMDIG was still slower than HMC because of lower ratio units during the snap accel (Figure 7.4-17.)

Afterburner Transients

Figure 7.4-11 shows a mil to max accel, followed by a max to mil to max bodie, and engine in a max to mil snap decel. Figure 7.4-12 shows a mil to max to mil bodie transient. These data were obtained to verify the operation of the engine with the BOMDIG control. A comparison was made with the SOAPP simulation to illustrate the degree of BOMDIG compliance with requirements. This is shown on Figure 7.4-13. The key to the zone sequencing is the relationship between the zone turn-on points, the hold time, and the zone enrichment on a mil to max transient. The data show the zones turned on at the correct point during the mil to max transient, and the suppression levels were consistent. The max to mil transient comparison indicates a premature Zone 1 shutoff occurred during the test, resulting in an undersuppression near the end of the transient. Post-test analysis revealed an improper Zone 1 shutoff command caused the early shutoff. The correction was implemented and tested during the altitude test.

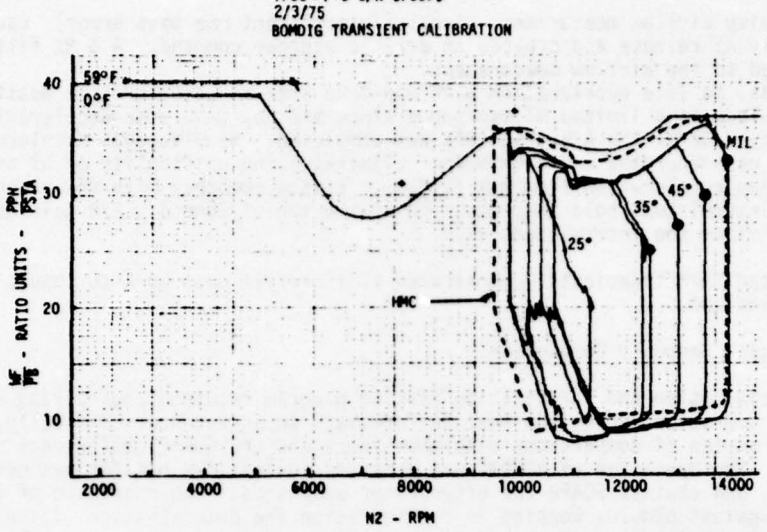

Figure 7.4-9 P-676629 BOMDIG Transient Calibration

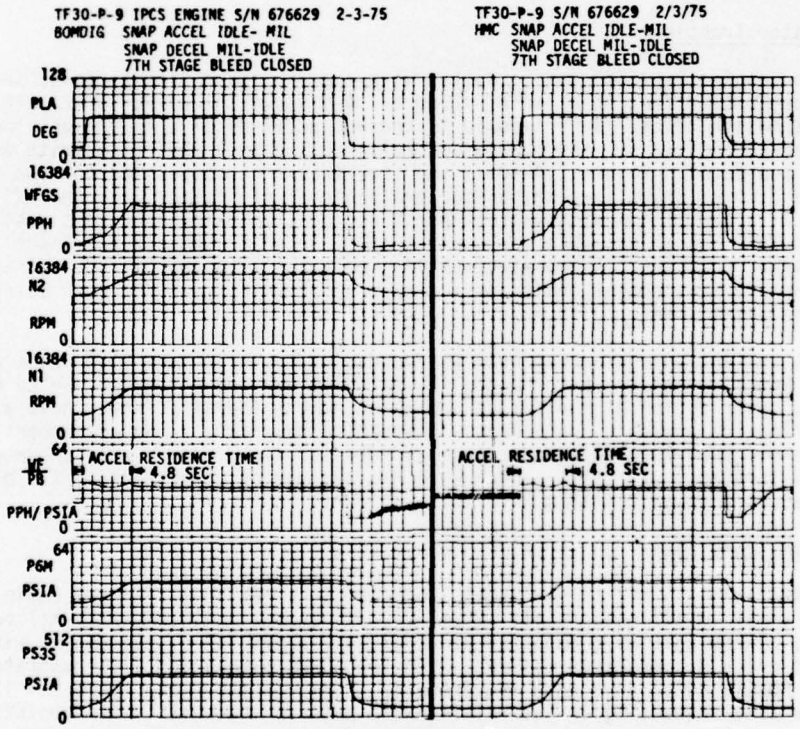

Figure 7.4-10 P-676629 Snap Accel - Idle to MIL, and Snap Decel - MIL to Idle BOMDIG vs HMC

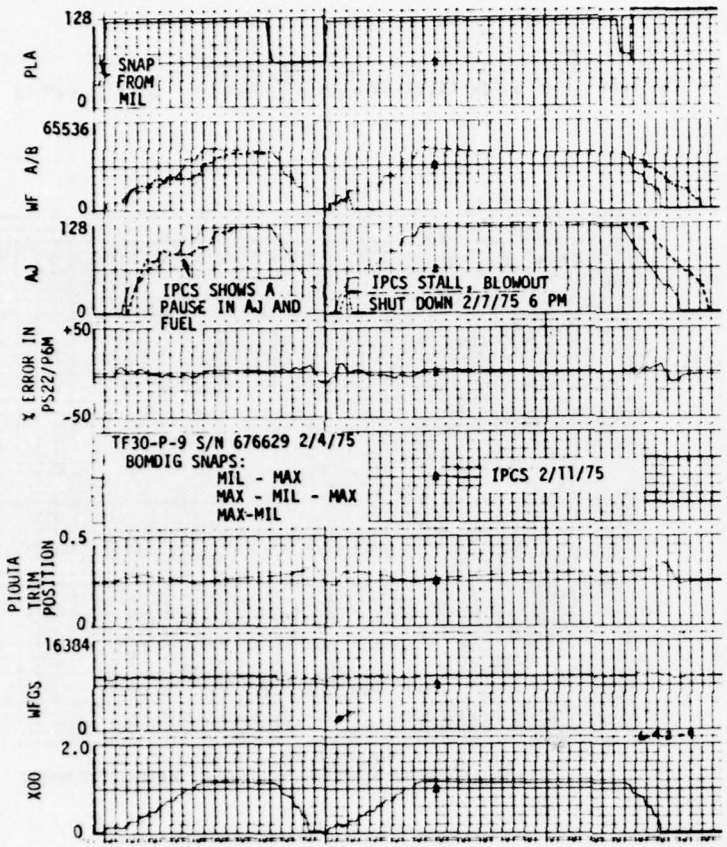

Figure 7.4 -11 P-676629 BOMDIG Snaps, MIL to Max, Max to MIL to Max, and Max. to MIL

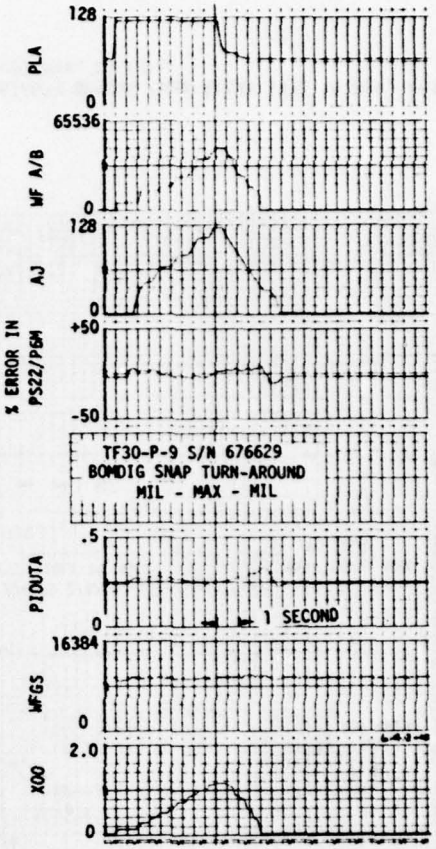

Figure 7.4-12 P- 676629 BOMDIG Snap Turnaround MIL to Max to MIL

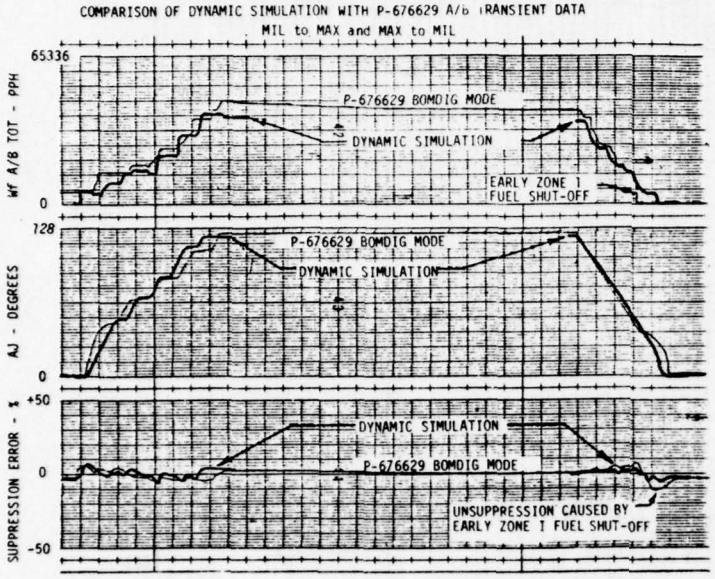

Figure 7.4-13 P-676629 A/B Transients, MIL to Max, and Max to MIL

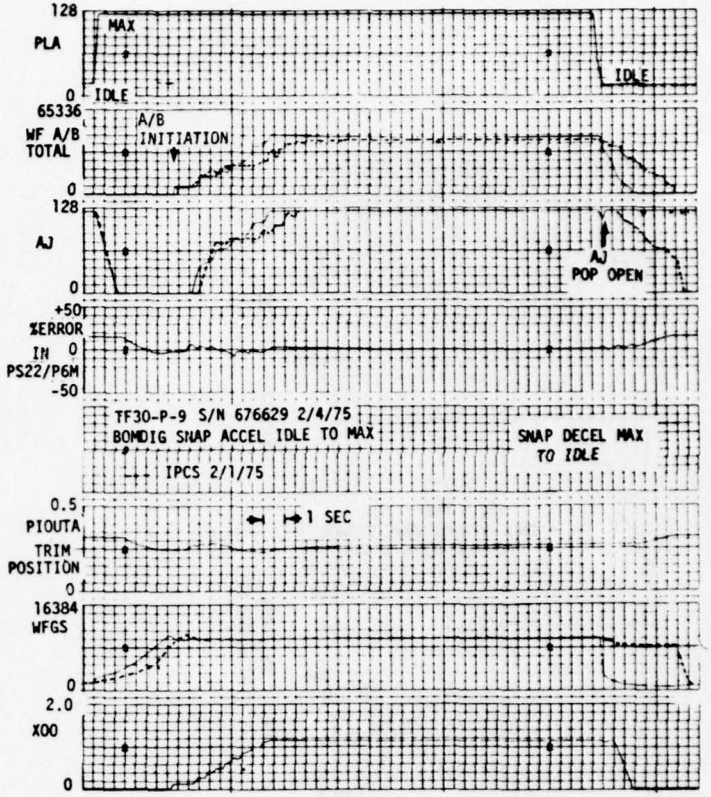

Figure 7.4-14 P-676629 BOMDIG Snap Accel Idle to Max. and Snap Decel Max. to Idle

7.4.3.1 BOMDIG Mode (Continued)

Gas Generator/Afterburner Transient

Figure 7.4-14 shows the idle to max and max to idle transient data for engine P-676629. The BOMDIG data are presented with a continuous line. The figure shows the A/B initiation occurring after the gas generator fuel increased to the vicinity of mil.

The actual control check performed to permit A/B ensures that throttle is in the A/B region, and the gas generator is on the mil governor. The nozzle was open at idle (on the ground), and closed during the gas generator accel with eventual reopening to max to maintain fan suppression. The max to idle transient shows the nozzle starting to close for the A/B decel, and turnaround to full pop-open, as required by the idle throttle setting. A/B fuel turned off and the gas generator snapped to idle at the same time.

7.4.3.2 IPCS Mode

Gas Generator Transient

The transient calibration for P-676629 with the IPCS control mode is summarized on Figure 7.4-15 and 7.4-16 which is a comparison with HMC and BOMDIG. As shown by these data, the IPCS control mode resulted in an accel that was slower than with the BOMDIG mode. The P-676629 IPCS accel was slower by two seconds as seen on Figure 7.4-16. A post-test review using the SOAPP dynamic simulation indicates the cause being the error that existed with an integrator. A dynamic error was required to drive the integrator to increase fuel. This dynamic error was on the order of one to two ratio units.

The subsequent test with P-676627 engine was run with changes determined from the above analysis. The data are shown on Figures 7.4-17 and 7.4-18. These data were obtained for BOMDIG and IPCS control mode operating the engine and are compared with the HMC. The DPCU control included an adjustment to the burner pressure calibration curve which increased measured PS3S by 2 psi at mil and was reduced to no change at idle. In addition, the IPCS data were obtained with the Wf/Pb accel schedule increased by two ratio units to account for the dynamic lag. The result was to improve the accelerations such that the IPCS accels to mil within 1/2 sec. of the time the HMC takes.

Another factor contributing to the slightly slower BOMDIG and IPCS accelerations was the longer time required to close the 12th stage bleeds after initiation of the acceleration. Figure 7.4-17 indicates the 12th stage bleed closed at a lower N2 speed for the HMC control than for either the BOMDIG or IPCS controls. The 12th bleeds were closed in the HMC mode by the pressure ratio bleed control (PRBC) once a low compressor discharge static pressure (PS22) threshold was exceeded. The PRBC function was duplicated in the DPCU logic. The DPCU could override the PRBC to open the 12th stage bleed. Although the 12th stage bleed operation was checked for all three control modes and found acceptable during the prescribed slow transients, the dynamic characteristics of the PS22 sensed by the PRBC and the DPCU were different for snap transients. This was measured by connecting these two signals to a ΔP transducer for the P-676627 testing.

Afterburner Transients

P-676627 engine test time parameters for the mil to max transient in IPCS mode are shown on Figure 7.4-19 as compared with BOMDIG.

The IPCS accel occurred 1.2 seconds faster than BOMDIG, as measured by time to achieve max Aj.

The max to mil decel was demonstrated during P-676629 test, as shown on Figure 7.4-11 for time parameters, and on Figure 7.4-20 for fan suppression. The fan suppression excursion for IPCS was less than BOMDIG. Both excursions were acceptable from a fan stability viewpoint; however, the impact of the excursion at altitude required assessment. Figure 7.4-21 shows the max to mil time parameters for engine P-676627.

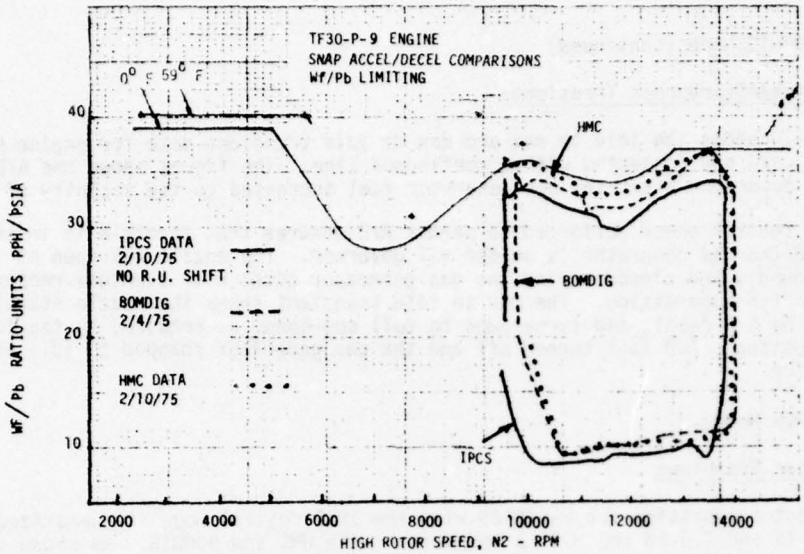

Figure 7.4-15 TF30-P-9 IPCS Snap Accel and Decel, HMC, BOMDIG and IPCS

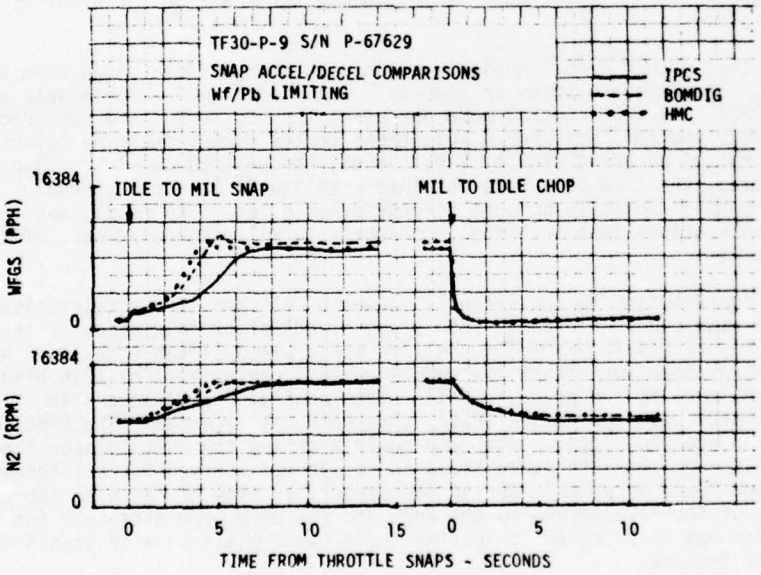

Figure 7.4-16 P-676629 Snap Accel and Decel, Wf/Pb Limiting - IPCS, BOMDIG and HMC

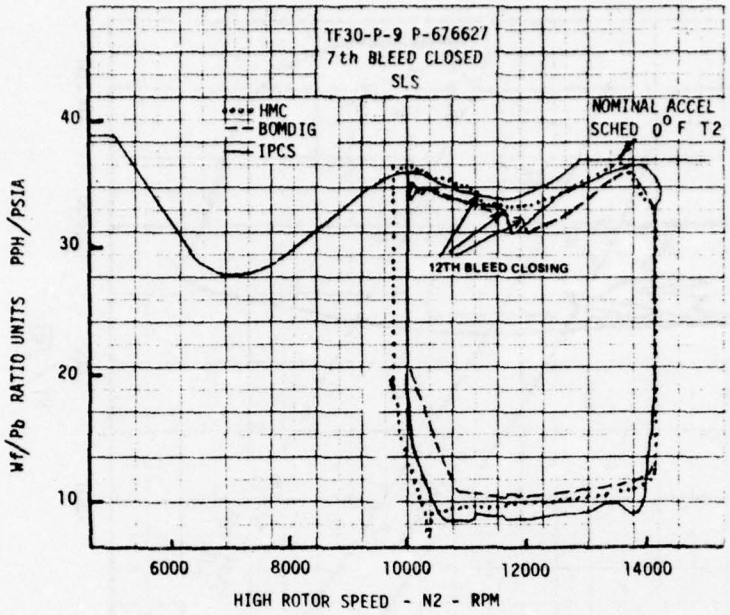

Figure 7.4-17 P-676627 Snap Accel and Decel IPCS, BOMIDG and HMC

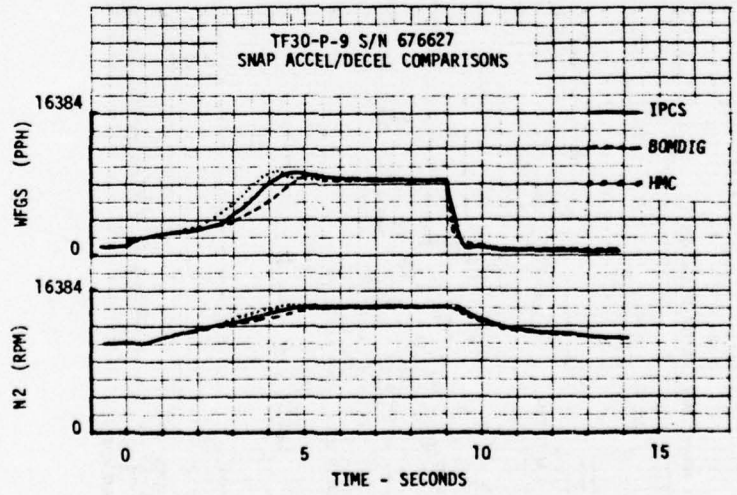

Figure 7.4-18 P-676627 Snap Accel and Decel IPCS, BOMDIG and HMC

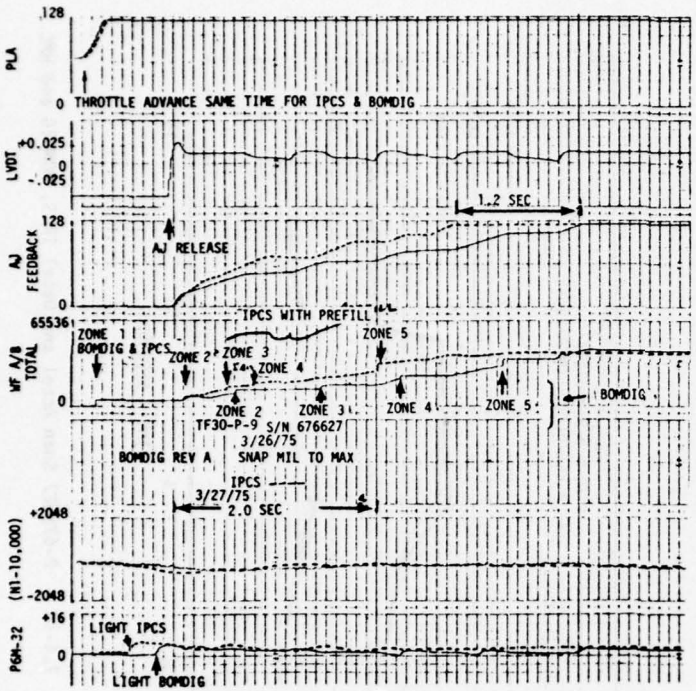

Figure 7.4-19 P-676627 Snap MIL to Max., BOMDIG vs IPCS

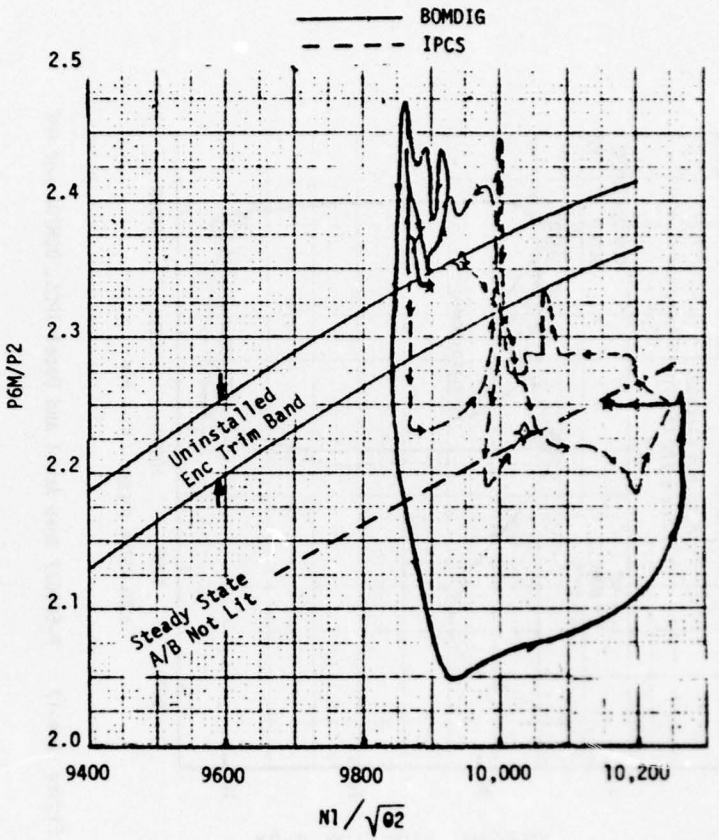

Figure 7.4-20 P-676629 Snap MIL to Max., BOMDIG vs IPCS

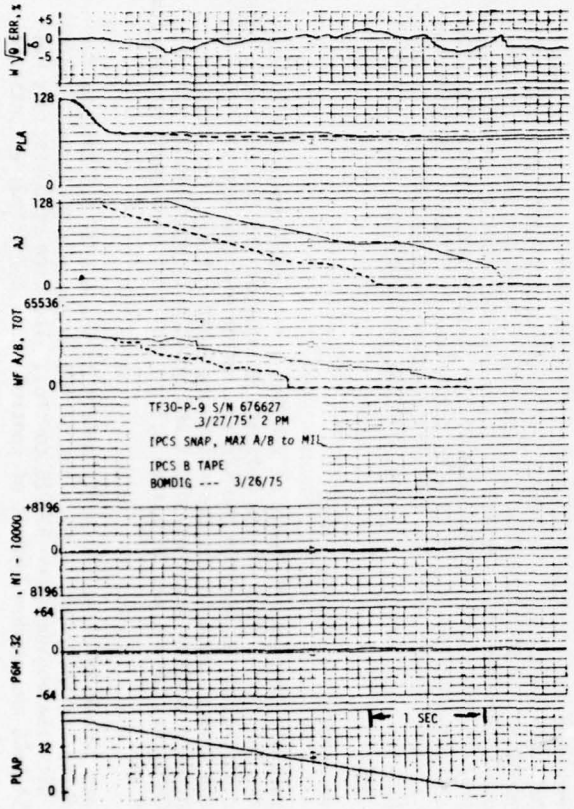

Figure 7.4-21 P-676627 Snap Max. to MIL, BOMDIG vs IPCS

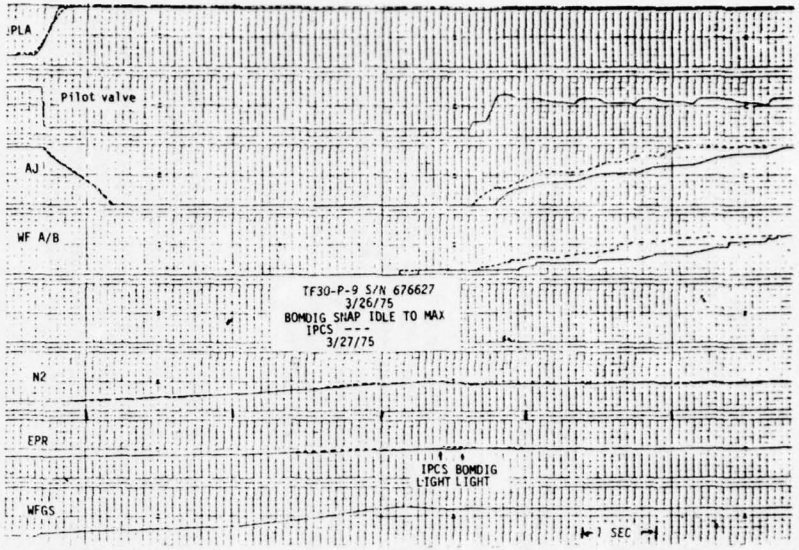

Figure 7.4-22 P-676627 Snap Idle to Max., BOMDIG vs IPCS

7.4.3.2 IPCS Mode (Continued)

The IPCS A/B control mode featured a new prefill concept for eliminating the need for manifold filling delay times during snap accels, thus improving accel times. This was accomplished with the control computer precalculating the time it takes to fill a zone manifold. Prefill was then accomplished by opening the zone shutoff valve early by an amount equal to fill time. The result was a faster acceleration transient which was nearly uniform throughout the flight envelope.

The SLS engine test verified the prefill concept. Figure 7.4-19 shows the throttle snap from mil to max for IPCS as compared with BOMDIG. The prefill logic reduced the time from light-off detection to max A/B from 4.2 seconds to 3.2 seconds.

Gas Generator and Afterburner Transient

The objective of this test was to verify A/B interlock logic during accel and to evaluate the IPCS mode concept during decels. The IPCS and BOMDIG accels had the same design criteria and restraints, thus the transients should have been similar. However, the IPCS mode design criteria during decels was different than BOMDIG. During a max to idle decel, BOMDIG decelerated the A/B and gas generator at the same time, whereas the IPCS decelled them sequentially, turning off the afterburner prior to decelerating the gas generator. This change was made to minimize the potential for high mach decel stalls, when the engine is decelerating and mismatched due to A/B shutoff.

The idle to max transient was run during both engine tests. The data shown on Figure 7.4-14 were obtained during P-676629 engine test and are compared with BOMDIG. IPCS was slower for two reasons. The gas generator accel was slower, and the Zone 4 Wf had an unnecessary pause. The data shown on Figure 7.4-22 were obtained during P-676627 engine test and show operation with these problems corrected by the IPCS Revision B tape. The IPCS-controlled engine took 8.7 seconds, whereas the BOMDIG took 10.2 seconds, to get from idle to max A/B (measured from throttle snap to max Aj).

The max to idle transient with the pop-open nozzle feature was not performed during P-676629 engine test because of a potential N1 overspeed problem. The IPCS control was designed to turn off the afterburner before decelerating the gas generator. The problem occurred when the throttle was snapped from max to idle (with the squat switch on), and the nozzle remained open while afterburner fuel shut off. Without the gas generator decelerating, the low rotor would overspeed (similar to a blowout). The IPCS software was revised prior to P-676627 test to permit simultaneous A/B and gas generator decel if the pop-open nozzle feature were armed. This was demonstrated, as shown on Figure 7.4-23 with comparison to BOMDIG. The test was repeated with a throttle excursion to a position above pop-open arming. In this case, the figure shows the nozzle closing, and the gas generator decelerating, after the A/B turned off.

7.4.4 Software Checkout at the SLS test

System level software development begun at the bench test (paragraph 6.4.2) was continued at the SLS test. Most of the software changes at the SLS test were made to correct for discrepancies between the RTE simulation and the actual TF30-P-9 and to implement changes made to the control modes (para 7.4.2). Revision B of the IPCS software program was checked out and brought to operational status. Checkout of BOMDIG Revision B was initiated but was not completed until the Altitude Test was under way.

The software was judged to be sufficiently mature by the end of SLS testing for formal delivery to the government. Portions of the acceptance tests on 27 March 1975 were run with the engine under BOMDIG control. The site of operations was shifted to NASA LeRC and co-development of control modes and software continued there.

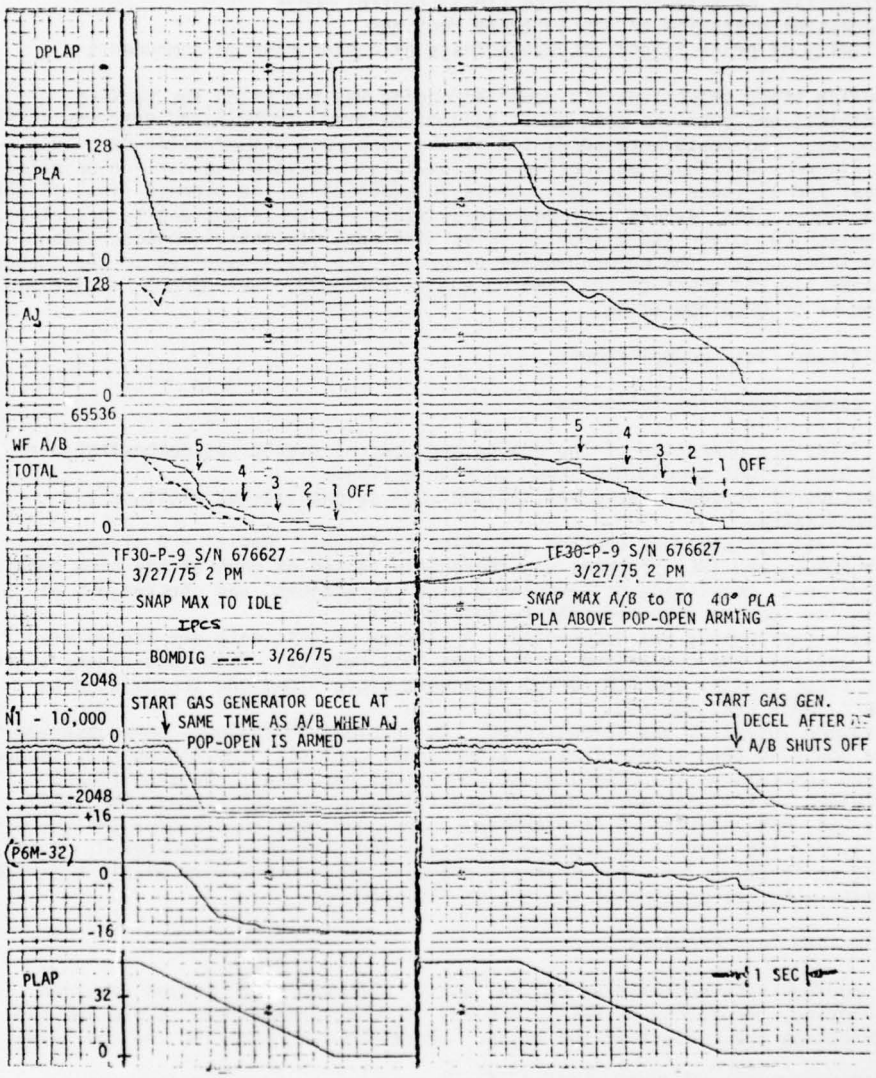

Figure 7.4-23 P-676627 Snaps Max. to Idle, BOMDIG vs. IPCS

8.0 ALTITUDE TEST PROGRAM

8.1 ALTITUDE TEST OVERVIEW

Approximately 14 weeks of altitude tests of the IPCS hardware and software were conducted at the NASA LeRC PSL facility to complete the system flight worthiness demonstrations prior to proceeding to the final flight evaluation test program. The objectives of the altitude tests were to demonstrate the following:

1. operational compatibility of mechanical and electronic components
2. suitability of selected advanced (IPCS) control modes
3. successful operation of the software routines
4. validity of prior flight assurance tests of engine mounted components

To accomplish these objectives the modified engine was run using the back-up hydromechanical and both the programmed bill-of-material (BOMDIG)and advanced (IPCS) control modes. The tests were conducted at the nine Mach number/altitude points shown on Figure 1.3-2 thus duplicating as closely as possible the earlier baseline flight test and altitude engine test points in addition to the planned final flight test conditions. Test events included steady state and transient engine operation, control switching, clean and distorted inlet airflows, distortion induced engine stall and inlet buzz. The comprehensive nature of the tests resulted in the accumulation of approximately 243 hours of run time on engine P-676629, including 70 engine stalls, and 655 hours of DPCU operation.

8.1.1 Altitude Test Accomplishments

The test accomplished the following:

1. Satisfactory operation of the engine and control system was demonstrated at the nine flight conditions shown on Figure 1.3-2.
2. The control schedules were refined and mode suitability at altitude was demonstrated.
3. The final software was checked out prior to flight. Revision B of each of the BOMDIG and IPCS programs was thoroughly tested at each of the nine conditions. Revision C, consisting of Revision B plus corrections, was checked out at selected low and high temperature test points.
4. Engine performance was documented. A library of test data was accumulated for analysis and comparison with flight test results. Processed steady state, transient digital and PCM (DPCU) data were microfilmed and transmitted to AFAPL, NASA LeRC and FRC.
5. Hardware integrity was demonstrated. No problems or failures were observed in the modified Bendix main fuel or afterburner controls, the 7th and 12th stage bleed controls or the plumbing and electrical harnesses. No significant problems or failures were found in the following special probes; P22, PS22, P3, PS3, P6M and T22. A T4 probe and redesigned heat shield operated successfully for 146 hours. No speed measurement problems were encountered. A post-test calibration indicated that all pressure transducers were within acceptable limits. No malfunction of the IFU or PSU occurred.

8.1.2 Altitude Test Problems

Various problems were encountered in the tests. Although each problem required troubleshooting, the method or resolution was in most cases rather simple and had little impact on the conduct of the tests. These problems included the following:

1. A P3 pressure transducer shifted slope requiring replacement by a spare.
2. A T3 cold reference junction probe failed requiring replacement by a spare.
3. The transducer box insulation blanket eyelets sustained damage requiring greater caution during installation.
4. It was found to be necessary to grease the P3 probe sealing gaskets to prevent them from falling into the fan duct during probe removal for inspection.
5. An oil leak around the gear box filter cover required repair.
6. Excessive power lever linkage play was resolved by replacing the worn parts with spare linkage.
7. All six standard TF30 T5 probes shorted requiring replacement.

8.1.2 Altitude Test Problems (Continued)

8. A crack in one of the inlet guide vanes required stop drilling per the TF30 overhaul manual.
9. Shipment damage to the TSU required component replacement and on-site functional repair. Refurbishment of the unit was postponed until after the test.

Four problems of greater significance occurred. Two resulted in redesign and two required post test equipment repair.

1. Errors of up to 25°F in the DPCU measurement of T2 resulted in changes to the transducer box insulation and in a revision in the location of one of the transducer box thermistors and the T3 cold reference junction probe. The probe relocations required an engine electrical harness modification.
2. Mechanical problems associated with the installation and removal for inspection of the T4 fluidic probe resulted in a design change to the probe heat shield to reduce the possibility of chipping the protective silicide coating and exposing the base material to erosion.
3. The DCU intermittently malfunctioned near the end of the test program with the result that the 12th bit of random core locations was not reset after interrogation. The system reacted correctly to this failure and was always fail-safe; i.e., disengage, power down and refuse to accelerate.

4. At the end of the program the engine (P/N 676629) performance displayed a marked deterioration accompanied by an increased occurrance of stalls during slow decelerations. A post test examination of the engine resulted in a major overhaul by the OCALC.

Refinement of the two software control programs for altitude operation required considerable effort and resulted in numerous changes which were implemented by means of patch tapes. Configuration control of the software was maintained through the use of software field change orders (SFCO) since modifications to the basic programs was not permitted in the field. Procedures and responsibilities of the contractor and NASA personnel were established in advance for maintaining accountability and control of the IPCS hardware and software configurations.

8.1.3 Altitude Test Conclusions

The following conclusions were drawn from the altitude test:

1. The IPCS hardware and software were demonstrated to be ready to proceed to the flight test phase.
2. Testing in the altitude facility was a cost effective way to subject the engine controls to operating conditions that simulate most of the flight envelope. This significantly reduced the cost, calendar time and risk in subsequent flight testing.
3. The software configuration control procedure developed for the IPCS program provided the flexibility required for on-site software development without sacrificing the rigor required for satisfactory software management.

Review of the test results indicated that various hardware and software changes should be incorporated prior to flight testing to provide the best possible operation. The recommended changes were:

1. BOMDIG gas generator accel time was slower than HMC at high altitude and low Mach number. The PRBC schedule should be revised to permit DPCU bleed operation at a point similar to the HMC.
2. The IPCS gas generator accel should show an improvement relative to the BOMDIG mode. The recommendation was to raise the Wf/Pb backup protection schedule and use the compressor discharge Mach number limiting loop more often.
3. The IPCS gas generator decel was slower than BOMDIG. A change in the minimum airflow loop compensation would permit faster decels. At the high supersonic flight conditions the buzz protection feature should be removed to provide basis for faster decels, except when activated by sense switch position.

8.1.3 Altitude Test Conclusions (Continued)

4. The IPCS afterburner decels were slower than BOMDIG. The rate of afterburner shut down should be increased to improve the decel time.
5. The IPCS combined gas generator and afterburner decel times were slower than BOMDIG. The sequential decel feature should be removed.
6. The hardware modifications devised to improve the DPCU T2 measurement should be incorporated in the flight test engine.

8.2 TEST CONFIGURATION

As noted in Section 7.0, the engine and DPCU hardware used in the altitude tests had previously been subjected to sea level static tests and were formally accepted by the Government. The following describes the altitude test configuration.

8.2.1 Test Facility

The NASA LeRC PSL cell 2 was used for the tests. To keep the length of the electrical cabling between the engine and the DPCU consistent with the F-111 installation, it was necessary to locate the DPCU and related equipment adjacent to the test tank in a temporary "contractors' room". Control of test configurations, engine operation and data recording periods was managed from the cell 2 control room by the LeRC test director who maintained voice communication with the remote data recording locations and the contractor room. Test support was provided by contractor personnel who operated the contractor room equipment. This equipment consisted of the test set unit, teletype, brush recorder, X-Y plotter, line printer, PCM data recorder, A TR-48 analog computer and voltage controlled oscillators. Communication with the control room was provided by a voice link, PDP-11 data display and time and status lights. Since the DPCU was controlled from the contractor room, the computer monitor unit status was also displayed in the control room.

The installation in the test tank primarily consisted of the modified IPCS engine, the LeRC furnished bellmouth inlet, airflow distortion generator and water cooled 40 probe compressor face rake; the normal complement of engine and facility instrumentation and duplicates of the flight type electrical cables between the engine and DPCU.

Two TR-48 analog computers were used. The one in the contractors' room closed the loop for the F-111 inlet and airplane parameters unavailable in the test configuration. The second, operated by the LeRC personnel, was used to drive the airflow distortion generator during the stall and buzz tests. Inlet controlled distortion was provided by using the inlet simulation to drive the distortion generator. Compressor face total pressure distortion was computed on-line by an analog computer developed for this purpose and previously flown during the IPCS baseline test flights, Section 5.2. Figure 8.2-1 is a schematic of the various signal paths involved in the DPCU control of the engine.

8.2.2 Test Articles

TF30-P-9 engine S/N 676629 was selected for the altitude tests. The installation in the cell is shown in Figure 8.2-2. Since being used for the baseline engine tests described in Section 5.1 it had been modified to the IPCS configuration as described in Section 3.1. During the test a change was made to the transducer box assembly to improve the DPCU T2 measurement (the T2 problem and its resolution are discussed in detail in Section 7.3.1 of the Reference 3, Altitude Test Report). The change consisted of insulating the rear mount flange of the box from the engine fan case to reduce an observed thermal gradient across the box and the relocation of a thermistor so that it was adjacent to the T2 cold reference junction probe, thus minimizing the impact of any remaining thermal gradient.

Remote control and position indication were provided in the control room for the 7th and 12th stage bleeds to permit setting of unscheduled conditions. A modification of the 7th stage bleed actuation was incorporated to open the bleed whenever control was transferred from the DPCU to the hydromechanical controller. This change resulted from the sea level static test observation of an N1 speed increase following control reversion at high afterburning power settings. Flight type relays were provided by the NASA LeRC in order to bring the test system as close as possible to the flight configuration.

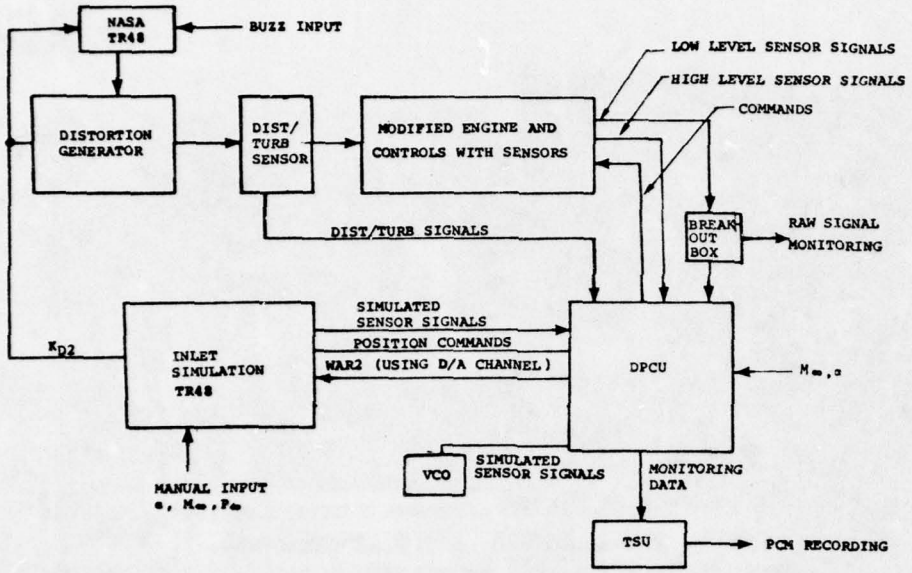

Figure 8.2-1 Signal Paths

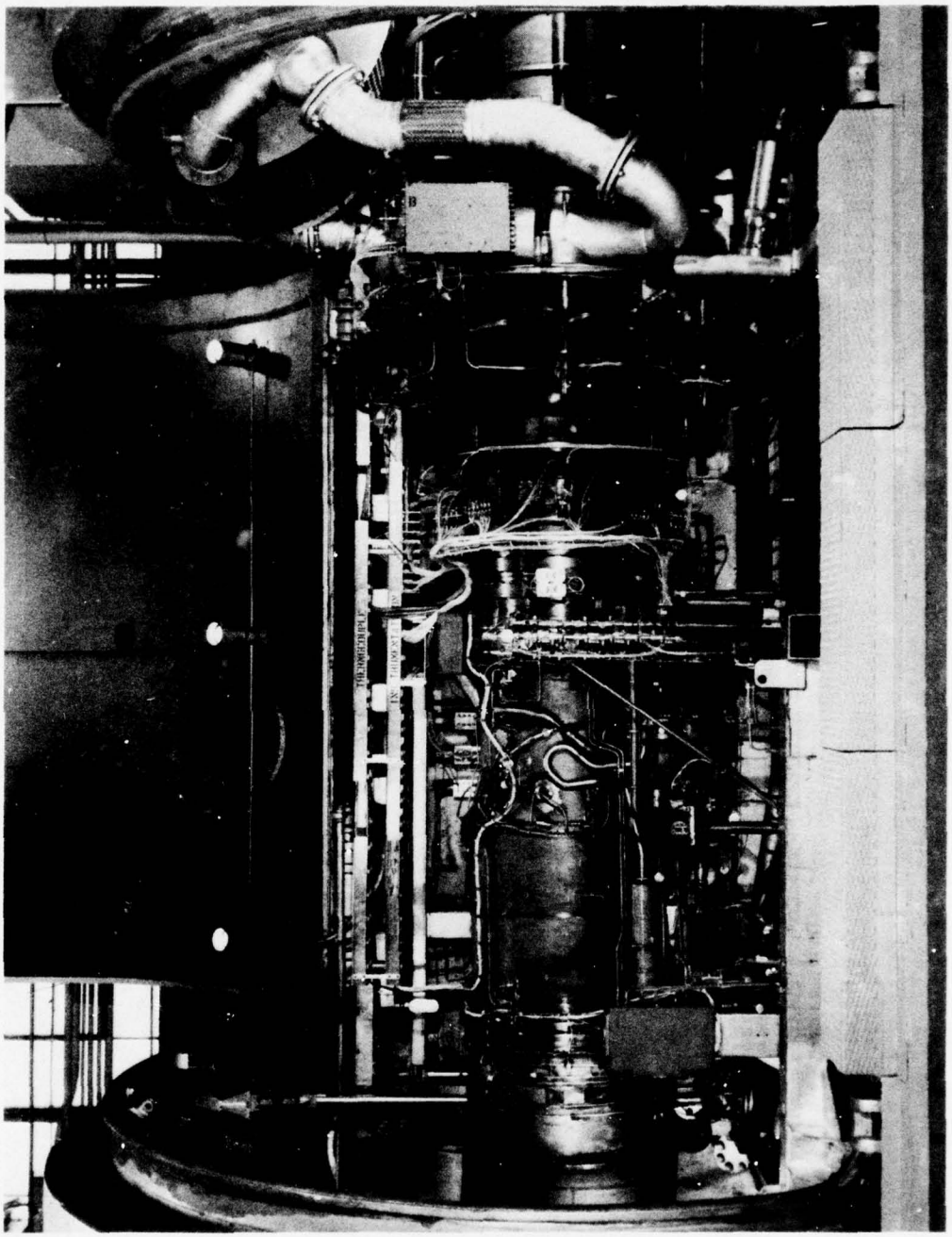

Figure 8.2-2 Test Engine in Altitude Cell

8.2.2 Test Articles (Continued)

The DPCU components used in the altitude tests were the following: CMU (S/N 2), PSU (S/N 1), DCU (S/N 5) and IFU (S/N 1)*. Considerable vibration was evidently experienced in transit by the TSU (S/N 2) resulting in damage to various components. Inspection revealed structural failure or electrical malfunction in the following: tape reader, CCU, DVM, power supply meters, engine/inlet simulation panel and middle storage drawer. Functional repairs were made on-site and included replacement of the defective CCU with the unit from TSU (S/N 1). (At the conclusion of the altitude test the TSU was returned to Honeywell, Inc. for refurbishment and repair). The TTY was not damaged in shipment and operated satisfactorily during the tests. The Tally high speed paper tape punch, a TSU component, was undergoing overhaul by the vendor at the start of the tests and was not available until the second month of the test period. This had no impact on the testing. The long form ATP was conducted on the DPCU to verify the functional readiness of the components prior to conduct of the altitude tests.

The software configurations in use at the conclusion of the second sea level static tests, Section 7.0, were used to start the altitude tests and additional program changes were made as the test progressed. These Revision B programs and the accumulated SFCOs were reviewed by Honeywell and new BOMDIG and IPCS configurations, identified as revision C of each program, were checked out in the concluding week of the test. Patch tapes were generated as needed for the revision C software, primarily to correct coding errors.

With the exception of a DCU failure near the end of the test program, the DPCU hardware and software operated satisfactorily throughout the test. The failure, which was ultimately traced to a bit-12 inhibit driver resulted in unpredictable program execution and occasionally prohibited loading of the software. Quite by accident, the failure provided a practical demonstration of a system fail-safe design feature; when the malfunction would intermittently occur, the system would disengage, power down and refuse to accelerate. Electronic Memories, the vendor of the SEMS-9 memory module, considered the failure to be an isolated case from the failure trend point of view and should not affect the second IPCS HDC 601 computer, S/N 06.

8.2.3 Instrumentation

Test data were acquired from two separate sources of instrumentation. In all, about 400 channels were used to obtain the desired engine and facility performance data for the steady state, transient digital and analog recording systems. Nearly one-third of the total was required for facility measurements (airflow, reference pressure, etc.) and roughly one half of the remaining channels were data common to all three recording systems.

The second source of data was the instrumentation unique to the operation of the digital control system. These parameters included sensed variables, position feedback signals and computer commands used to evaluate and monitor control performance. The data were transmitted from the DPCU as 59 variables at a 20 samples per second per variable rate in the form of a multiplexed digital signal and were recorded on one track of an analog tape recorder in the contractor room. On-line monitoring of the control system parameters were provided by selectable sets of 11 channels of analog data and high level signals hard wired to TSU jacks for display on Brush or oscillograph recorders.

Compressor face total pressure was sensed by Kulite transducers in the 40-probe water cooled rake. Distortion pressure levels were input to the DPCU for the advanced control mode tests from Paroscientific transducers which were substituted for four of the Kulites. One of the remaining Kulites provided the turbulence and buzz signal to the DPCU. Locations of the transducers are shown on Figure 8.2-3. The distribution of the Paros sensors provided two dynamic measurements in each of the high and low pressure regions. The distortion pattern created by the distortion generator represented that observed in the F-111 inlet during the baseline flight tests, Section 5.2; i.e., circumferential with a single low pressure area. The location of the turbulence/buzz sensor was rather immaterial since the turbulence and shear flow were not simulated. Buzz testing, for example, provided a uniform, but cyclic, pressure oscillation that could be detected at any pickup location.

*This set of components was designated DPCU V-2.

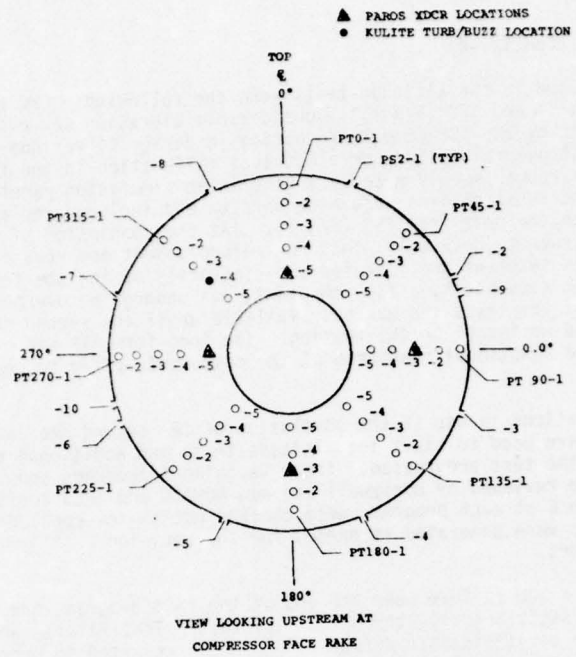

Figure 8.2-3 Distortion and Buzz Transducer Locations

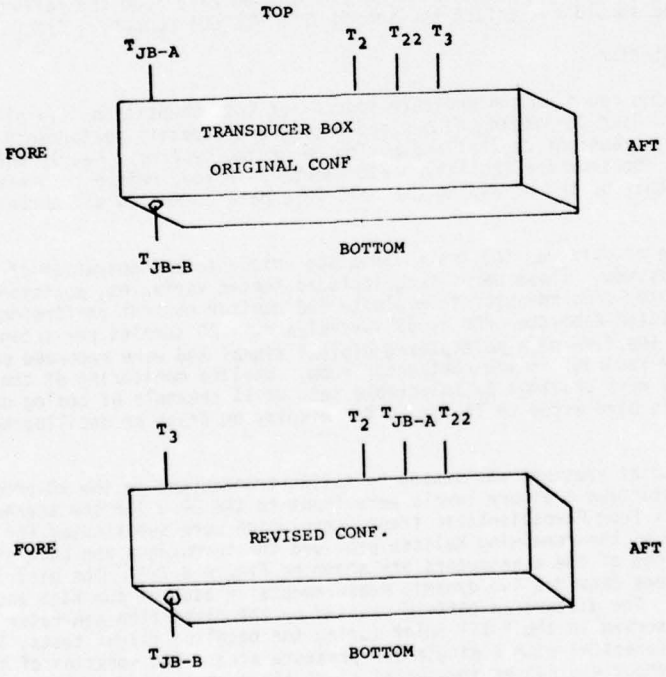

Figure 8.2-4 Transducer Box Configuration

8.2.3 Instrumentation (Continued)

The inlet temperature measurement problem referred to in Section 8.2.2 resulted in the addition of thermocouples on the outside of and adjacent to the transducer box to assist in the study of the differential heating of the box. Further study involved a special test in which the T2 cold junction probe and reference thermistor were by-passed by using a LeRC 150°F reference junction oven for reference. One of the results of the investigations was a recommendation to relocate the TJB-A thermistor and T3 and T22 cold reference junctions as shown in Figure 8.2-4.

8.3 TEST OPERATIONS

8.3.1 Test Procedures

The tests were conducted at the nine Mach number and altitude conditions shown in Figure 1.3-2. The type of test events varied as a function of the flight condition being simulated. Distortion and buzz tests, for example, were limited to 80°F inlet temperatures by the distortion generator. Table 8.3-1 summarizes the tests noting which events were conducted with each control mode. Briefly, the events were as follows:

Switching - transfers from BOMDIG or IPCS control to HMC and back at 25°, 40° and 55° PLA where not restricted by flight idle.
Steady state GG - up to 5 power line performance points
Steady state A/B - performance at mid zones 1, 2, 3, 4, 5 and max A/B
Snap Transients - a single direction throttle movement between two PLA values at a rate corresponding to less than one second from ground idle to MIL
Bodie - Snap decel between two PLA positions followed by snap accel at the time the N2 speed reaches the designated value (or nozzle change is complete).
Random - rapid selection of increasing and decreasing PLA between 18° and 69° at the snap rate in a random manner beginning at 50° PLA.
Airflow trim - a check on the IPCS mode airflow bias logic which is designed to match the inlet operating point and engine demand by varying inlet geometry and/or engine speed.
Rumble - a check on the IPCS mode rumble logic to observe if duct stream fuel flow changed in response to an A/B rumble condition induced by reducing primary stream fuel flow to off-design levels
Distortion tolerance - engine distortion tolerance determined for various manual and automatic bleed position combinations by increasing distortion level until engine stalled. In the IPCS mode the bleeds were positioned in response to a direct distortion measurement to provide stall protection.
Inlet controlled distortion - throttle transients with variable distortion levels controlled by the inlet simulation as a function of airflow.
Buzz - inlet pressure fluctuations at 10 Hz (with and without superimposed distortion) were detected and IPCS buzz loop responsed by increasing airflow demand

Simulated failures of the sensors critical to flight safety and other sensor validity test limit checks were conducted during the Bench Tests, Section 6.0. One of the four critical sensors, P3S, could not be tested due to test electronics and was deferred to the altitude program where the failure test was successfully conducted. Validity limit checks of inlet parameters were again performed as was the T4 upper validity limit check. It was agreed in the Interim Altitude Test Review that tests performed up to that time had satisfactorily demonstrated the system response to out-of-valid ranges and additional tests at other Mach/altitude conditions could be omitted.

Priorities were assigned to the various test events since not all of the data were deemed necessary to demonstrate the flight-worthiness of the system. In general, the requirement was to successfully complete the following events with additional comparative data being provided by the remaining tests.

No distortion

HMC: gas generator powerline and selected transients at M 1.4/41000 ft and M 0.8/30000 ft
BOMDIG and IPCS: switching, gas generator and A/B powerlines, selected transients and failure simulations at M 1.4/41000 ft, M 0.8/30000 ft and M 2.1/45000 ft.

8.3.1 Test Procedures (Continued)

Distortion

HMC: ramp distortion to stall with bleed variations at M 1.4/41000 ft.
IPCS: ramp distortion to stall with auto bleeds at M 1.4/41000 ft.

TABLE 8.3-1 ALTITUDE TEST EVENTS

Condition			CLEAN INLET FLOW								DISTORTED FLOW			
			Steady State		Transients									
Mo	Alt	Switching	GG	A/B	GG	A/B	Bodie	Random	Air flow trim	Rumble	Dist. Tol. Bleeds Man.	Dist. Tol. Bleeds Auto	Dist Inlet Cont.	Buzz
1.4	41K		H*		H		H				H			
		B	B*	B	B	B	B	B					B	
		I	I*	I	I	I	I	I	I		I	I	I	I
0.8	30		H		H									
		B	B	B	B	B	B	B						
		I	I	I	I	I	I	I						
2.1	45													
		B	B	B		B	B							
		I	I	I		I	I							
0.9	45													
		B			B	B	B							
		I			I	I	I			I				
1.4	52													
		B			B	B	B							
		I			I	I	I						I	
1.06	22													
		B			B	B	B							
		I			I	I	I							
0.9	10													
		B			B	B	B							
		I			I	I	I							
1.6	45													
		B			B	B	B							
		I			I	I	I							
2.25	48.5													
		B				B	B							
		I				I	I							

*H=HMC; B=BOMDIG; I=IPCS

8.3.2 Data Recording and Processing

The LeRC CADDE, SEL and FM analog systems were used to record the steady state, transient and the high response compressor face measurements. DPCU control data were recorded separately on analog tape. On-site processing by the LeRC provided Boeing with CADDE and SEL data tapes in engineering units and scaled decimal output for the PCM data. Processing of the high frequency FM analog data and final data reduction were performed by Boeing.

Most of the high frequency data consisted of signals from the compressor face rake to be used to compute instantaneous total pressure distortion during periods of high distortion or engine stall. The raw data were edited to select 200 millisecond intervals of interest, demultiplexed and digitized at 1000 samples per second. PCM data from the DPCU required editing to retain only the significant portions and labeling of the data output. Final processing on a CDC6600 computer produced plot tapes and data printouts which were permanently recorded on 16 and 35 mm microfilm. Copies of the CADDE, SEL and PCM microfilm were distributed to the AFAPL, NASA LeRC and NASA FRC and were accompanied by copies of the test logs.

8.4 TEST RESULTS

The altitude tests were conducted with both clean and distorted inlet airflows. Clean inlet testing refers to tests with the distortion generator removed or not flowing. The distortion generator was limited to operation at 80°F inlet total temperature and was removed for the simulated high Mach number conditions.

8.4.1 Clean-Inlet Tests

Clean-inlet tests were performed using each control mode with the HMC data serving as a comparative baseline for the BOMDIG and IPCS results. Since A/B operation was only possible with the BOMDIG and IPCS modes, comparative HMC A/B data were taken from the S/N 676629 baseline tests, Section 5.0.

8.4.1.1 Gas Generator Steady State

Engine trimming was initially performed with the distortion generator installed (not flowing) at the M 1.06/22000 ft. condition by adjusting the sea level static military trim band for altitude and Mach number effects. A performance comparison with the distortion generator removed indicated that a final downtrim, applicable to all three control modes, had accounted for generator blockage and engine deterioration effects, thus providing turbine inlet temperatures consistent with the baseline test data. The DPCU and HMC idle trim settings established in the sea level tests remained unchanged; however, the omission of a fuel flow calibration curve had the effect of reducing the normal BOMDIG idle setting. The BOMDIG Wf/Pb control is open loop and thus sensitive to errors in commanded fuel flow. The IPCS Wf/Pb limiting loop closes on Wf/Pb in the software, thus was not affected by the error.

High compressor discharge static pressure, PS3, sensed by the DPCU, was calibrated to the main fuel control burner pressure, PB. Good agreement was obtained by incorporating slope and offset conditions to the PS3 pressure transducer characteristics.

The DPCU determines total engine inlet airflow from a corrected low-rotor speed, engine pressure ratio correlation. A correction to the Reynolds number bias resulted in close agreement between computed airflow and the CADDE airflow measurement.

Repeatable inlet temperature measurement by the DPCU was difficult to achieve. This was briefly discussed in Sections 8.2.2 and 8.2.3. Most of the altitude testing was conducted with a fixed DPCU T2 input for each condition.

The steady state tests permitted checking the BOMDIG mode schedule biases and the high rotor speed schedules, airflow limits and turbine inlet temperature limit for the IPCS mode. A comparison of HMC, BOMDIG and IPCS military power settings is presented in Figure 8.4-1 and the associated turbine inlet temperatures in Figure 8.4-2. The BOMDIG agrees within 1.3 percent of the HMC EPR for all test conditions. Schedule adjustments were made to the IPCS inlet pressure bias to provide better agreement at M 1.4/52000 ft and M 1.6/45000 ft. A comparison of throttle sensitivities indicated that all three control modes had the same EPR lapse rates.

Operation of the engine with the Honeywell TIGT fluidic sensor was not completely successful. The TIGT measurement is used as a redline topper in the IPCS mode. A backup signal synthesized from high compressor discharge temperature, T3, and main burner fuel-air ratio exhibited more stable and repeatable measurement and was used for most of the testing, compare Figures 8.4-3 and 8.4-4. The backup correlated reasonably well with the harness T4E providing much quieter operation; however, the fluidic probe signal wandered at a relatively low frequency and high amplitude. The cause of the wander has not been identified, but the observed signal may be characteristic of a single sample taken in the gas stream at the selected location.

Transfers to and from BOMDIG/HMC and IPCS/HMC were demonstrated at all test conditions. No adverse effects were observed.

8.4.1.2 Gas Generator Transients

A comparison of idle to mil snap accel times (initiation of PLA movement to achievement of 95 percent of change in high rotor speed) is presented in Figure 8.4-5. BOMDIG times were comparable to HMC except at high altitude and low Mach number where the time was increased by a combination of the fuel calibration error and the 12th bleed closure which occurred at a higher power setting than for HMC. The effect of the fuel error was most significant at the lowest fuel flow conditions where the percentage error was the greatest. A software change was recommended to eliminate the error before flight testing. Since the DPCU overrides the HMC PRBC to open the 12th stage bleeds, consideration was also given to incorporating the low limit of the PRBC schedule in the DPCU to provide 12th bleed actuation consistent with the HMC during flight testing.

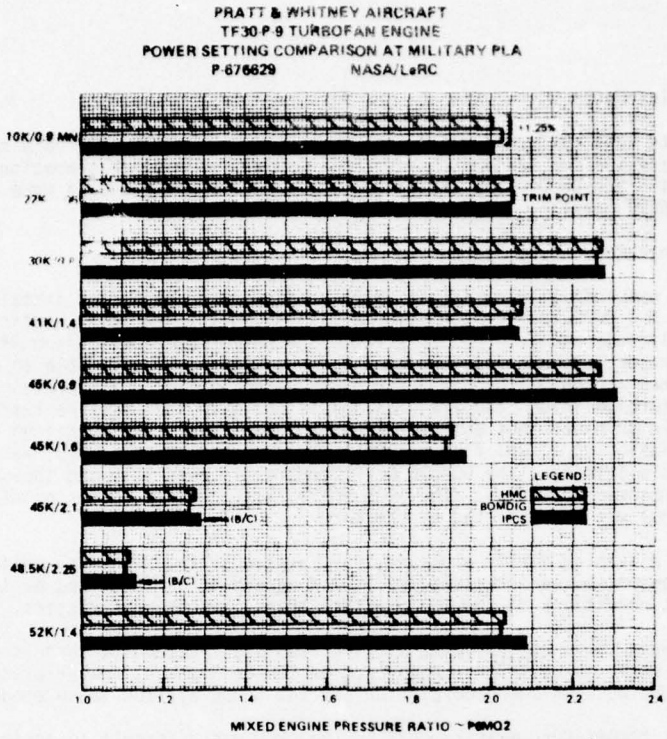

Figure 8.4-1 MIL Power Setting Comparison

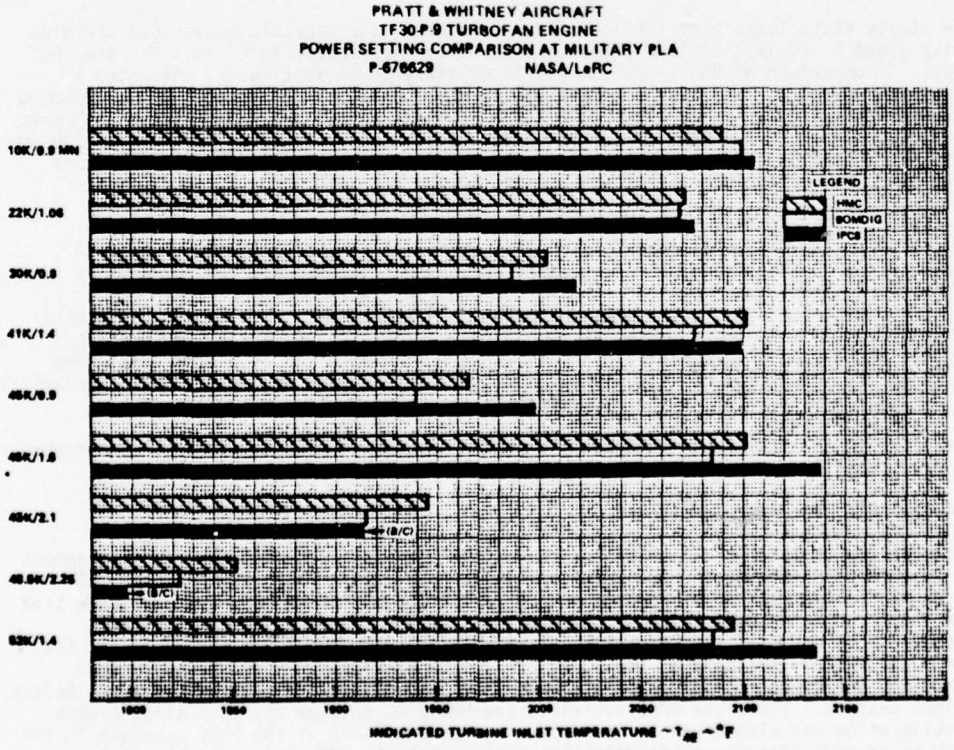

Figure 8.4-2 MIL T4E Comparison

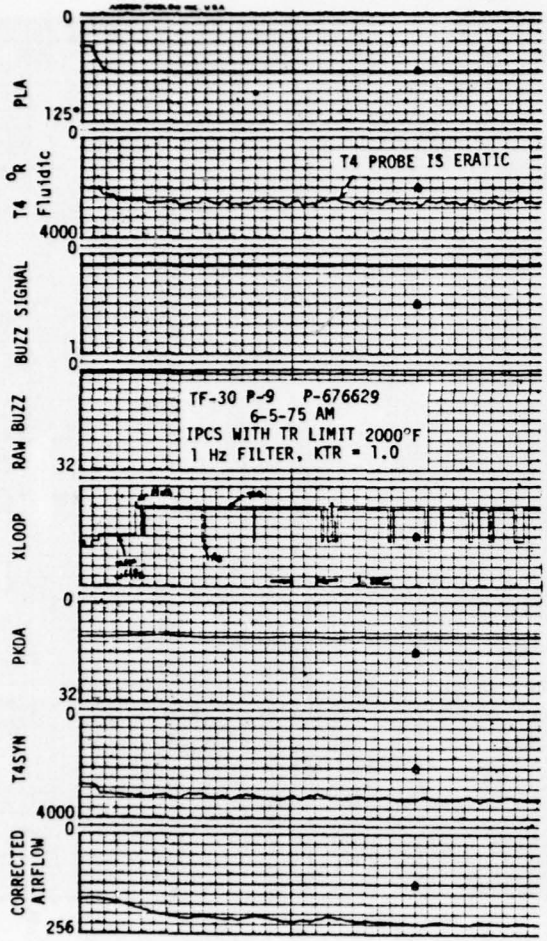

Figure 8.4-3 Fluidic Probe T4 Limiting, M1.4/41000

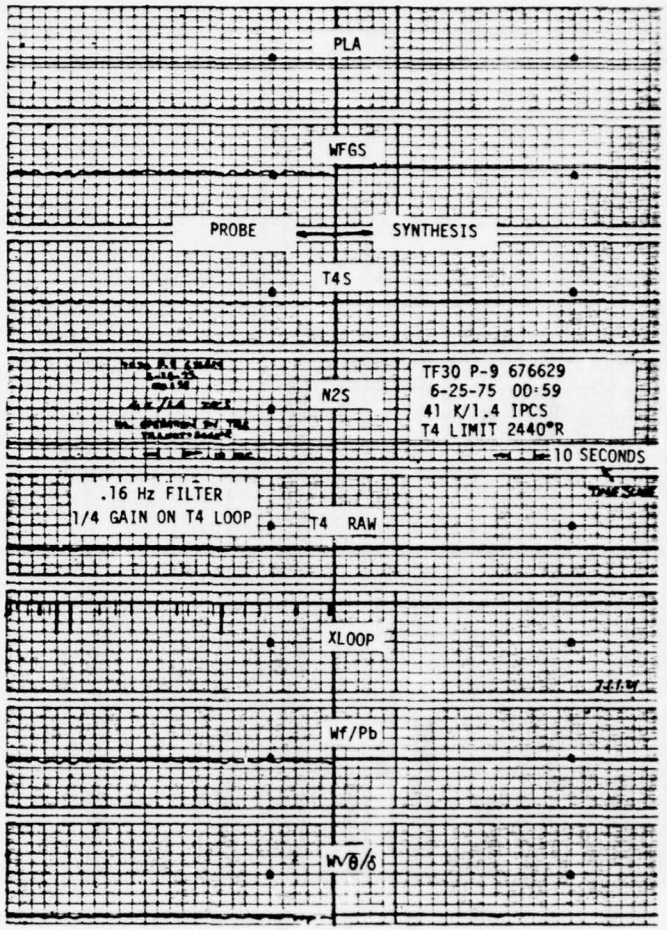

Figure 8.4-4 IPCS T4 and T4SYN Limiting

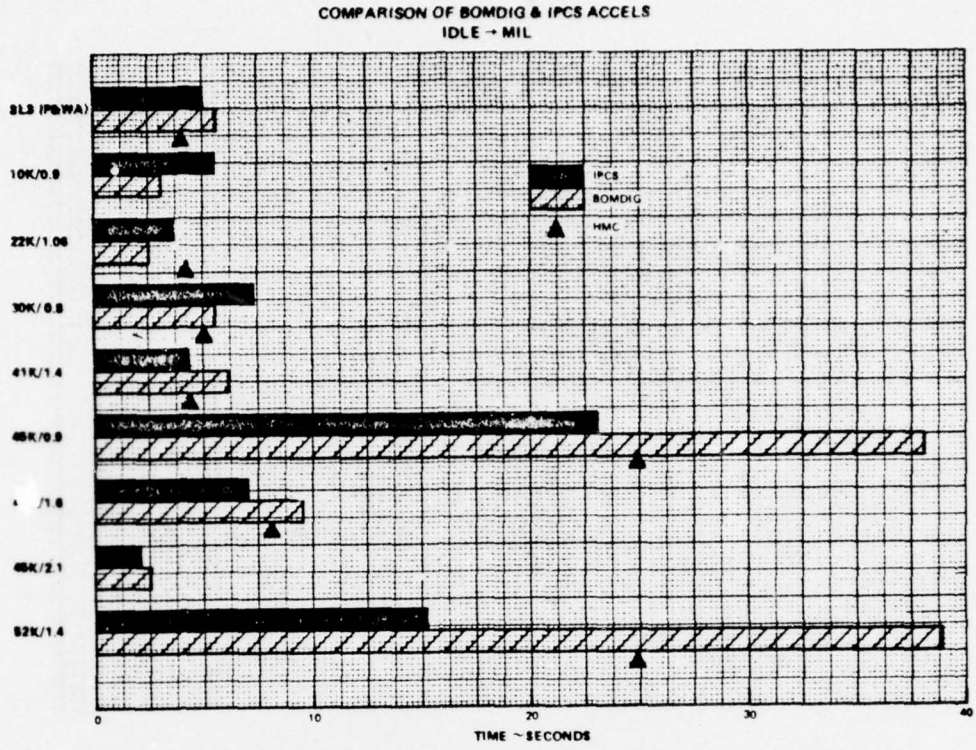

Figure 8.4-5 Accel Time Comparison, Idle to Mil

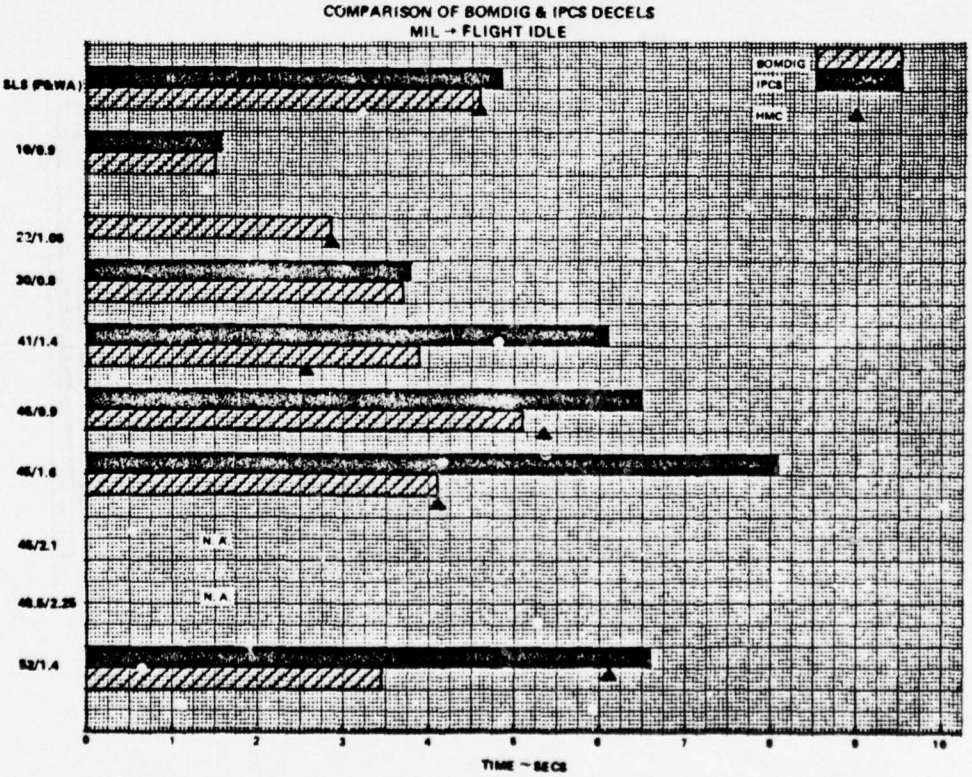

Figure 8.4-6 Decel Time Comparison, MIL to Idle

8.4.1.2 Gas Generator Transients (Continued)

IPCS accels were slower than BOMDIG at three conditions. At M 0.8/30000 ft this was attributed to the accel starting from a 12th bleed open idle, while the HMC and BOMDIG accels started from slightly higher power settings where the bleeds were closed. At M 0.9/10000 ft and M 1.06/22000 ft. the increased times were caused by operation on the high compressor discharge Mach number loop (to avoid off-idle high compressor stall by scheduling a high compressor transient path limit). Following the altitude test, the MN3 schedule was adjusted to prevent slow accels at low altitudes and high Mach numbers during flight testing.

Decels were timed in the same manner as accels. A comparison for the three modes, Figure 8.4-6, generally showed good agreement between BOMDIG and HMC; however, the IPCS control was consistently slower. The longer BOMDIG decel time at M 1.4/41000 ft and shorter times at M 1.4/52000 ft were attributed to differences in the manually controlled HMC idle and the DPCU controlled setting. In the IPCS cases the M22 limiting, minimum airflow limiting and fuel flow rate limiting control loops, which are intended to improve propulsion system stability, produced slower decelerations. Schedule refinements were developed to improve deceleration times during the flight tests without adversely affecting engine stability.

Gas generator bodies (mil-part power-mil) were successfully demonstrated in all but the very high Mach number conditions where the idle-to-mil power range was very small. Bodie transients were of interest because they result in higher compressor excursions than occur during cold (idle-mil) transients due to more heat energy being available to the gas path from the hot metal parts during the power lever turnaround. A BOMDIG bodie at M 0.9/10000 ft. resulted in a one percent larger high compressor excursion than occurred with the cold idle-mil snap accel. As a comparison, an IPCS bodie at the same condition did not exceed the cold accel excursion since the IPCS control features a high compressor excursion M3 limiting loop. No bodie stalls were encountered on HMC or DPCU control.

Random throttle transients were demonstrated in the IPCS mode at M 1.4/41000 ft. The sequence was; 50° PLA to mil (snap accel) to flight idle to Mil (Bodie) to flight idle (hot decel). Controlling schedules were; snap accel governed by the max Wf/Pb accel schedule, bodie governed by the M3 accel schedule because of the larger high compressor excursion associated with the bodie turnaround, and decel governed by the minimum airflow loop.

8.4.1.3 Afterburning Steady State

Afterburner lighting was not a problem in the BOMDIG mode except for a zone 2 blowout at M 0.9/45000 ft. during an idle to max accel which was consistent with normal TF30 operational experience. The IPCS mode, using a new concept for light-off detection that basically measures the rate of change of the fan operating point, also worked well at all test conditions. An IPCS software A/B release logic change was needed, however, for flight Mach numbers greater than 2.0.

Mid zone 3 trimming was performed in both control modes at M 1.06/22000 ft. and checked at other altitude conditions to verify fan operating line control. Figure 8.4-7 shows the desired fan operating line and trim check data. The IPCS data falls right on the fan operating line since the target schedule is used as a reference for the control integrator. The BOMDIG point did not fall on-line for all conditions due to the mode of the control which indirectly sets fan match using PS22/P6M as a function of corrected high rotor speed. Thrust checks were made with both control modes. Max A/B EPR comparisons were performed at all conditions, figure 8.4-8. A change to the IPCS speed set schedules reduced the difference between IPCS and BOMDIG at M 1.4/52000 ft.

8.4.1.4 Afterburning Transients

Transient afterburning tests were conducted with BOMDIG and IPCS controls at each altitude test condition. Accel time (start of throttle snap to the point where the exhaust nozzle area reached its max A/B position) comparisons for mil-max snap accels are shown in Figure 8.4-9. IPCS was always faster, primarily due to the manifold prefill logic, whereas the accel was interrupted to permit the manifolds to fill in BOMDIG. Filling duration was proportional to PS3, so longer times were experienced at low pressure conditions. The change in EPR was not adversely affected by prefill.

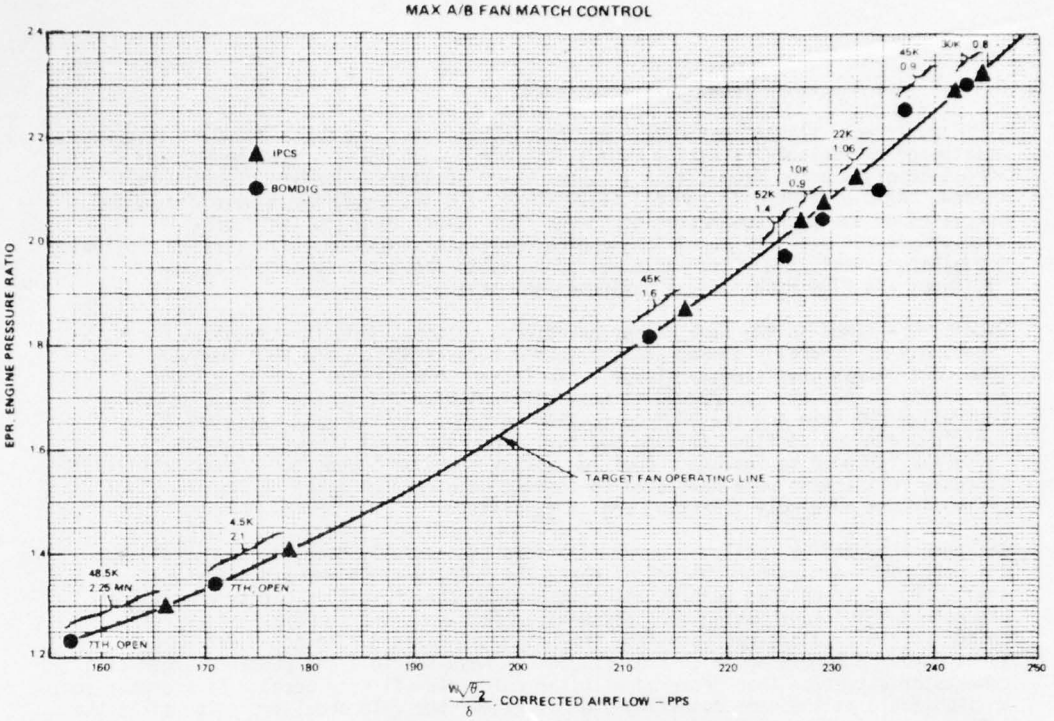

Figure 8.4-7 BOMDIG, IPCS Max A/B Fan Match Control

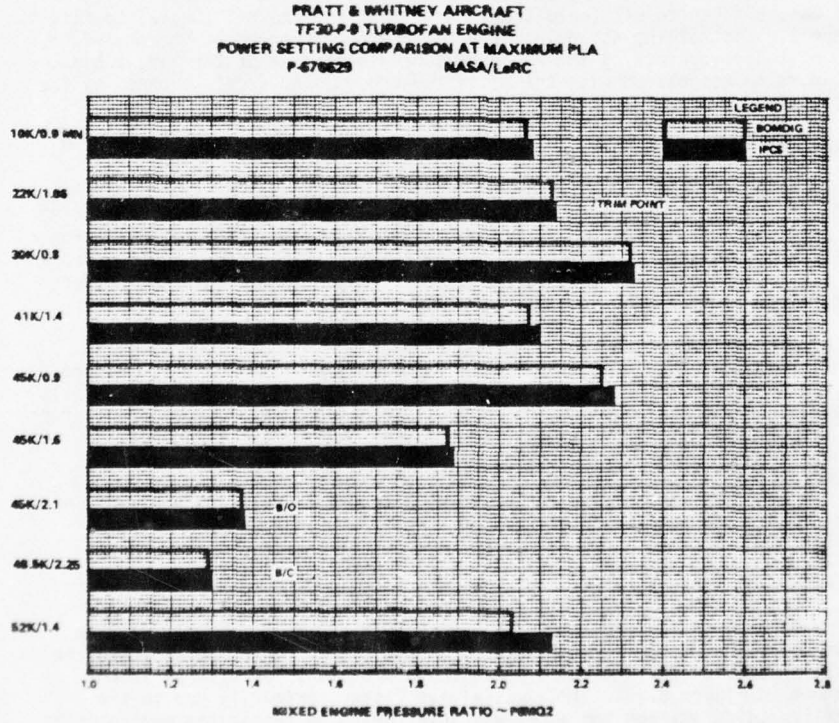

Figure 8.4-8 BOMDIG, IPCS Max Power Comparison

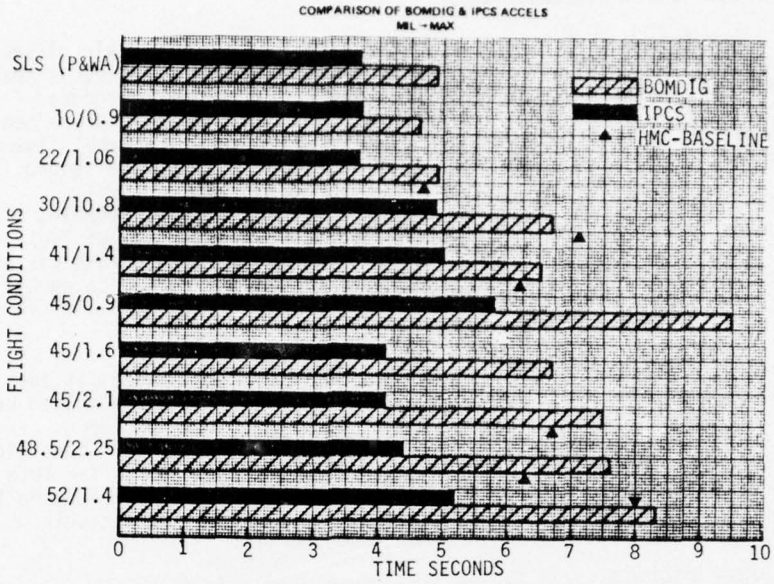

Figure 8.4-9 Mil-Max Accel Time Comparison

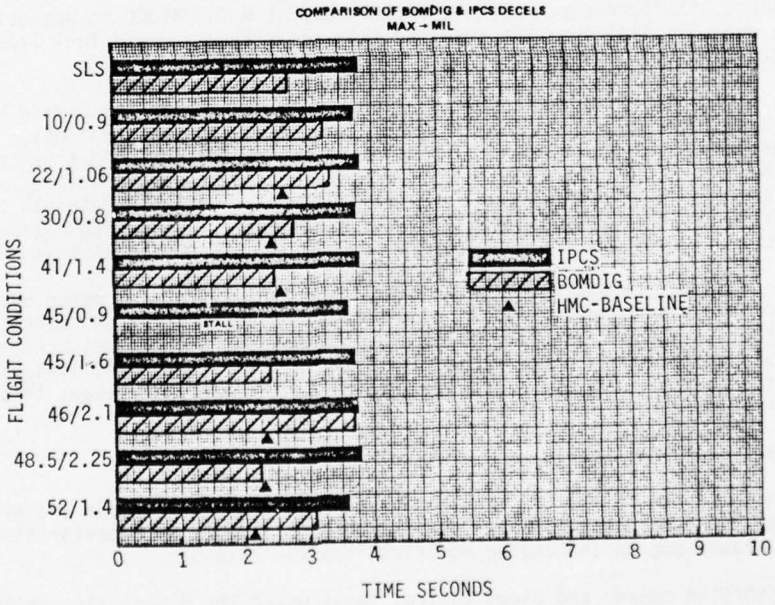

Figure 8.4-10 Max-Mil Decel Time Comparison

8.4.1.4 Afterburning Transients (Continued)

Max to mil decel times (start of PLA snap to point where the exhaust nozzle closed) are shown in Figure 8.4-10. Both control modes produced more consistent decel than accel times. BOMDIG basically followed the area closure rate and IPCS produced unsuppressed decels by following a rate limited PLA (PLAP) rate of -15 degrees/sec. At the conclusion of the altitude tests it was decided to improve IPCS decel time by increasing PLAP to -21 degrees/sec, improving the decel time by about one second.

The IPCS mode delayed area closure resulting in less over-suppression. BOMDIG, however, produced a suppression stall at M 0.9/45000 ft due to insufficient fuel modulation above the minimum fuel stop and the fact that nozzle closure rate was not varied with fan suppression. Figure 8.4-11 shows that compressor exit Mach number (MN22 and MN3) did not vary significantly during the stall and is not suitable as an incipient stall indicator during A/B operation.

Max-mil-max A/B bodies were successfully conducted with both control modes at each test condition and demonstrated that prefill would not stall the IPCS controlled engine.

Idle to max snap accels were also successful except at the M 0.9/45000 ft condition where blowout occurred in the BOMDIG mode and on two of three attempts in the IPCS mode. It was concluded that the blowouts were caused by the pressure level being too low for A/B lightoff. Figure 8.4-12 compares accel times. IPCS is faster than BOMDIG due to earlier lightoff permission and manifold prefill.

The IPCS mode provided more fan stall margin than the BOMDIG mode during max to idle decels at the expense of decel time, Figure 8.4-13. At the conclusion of the tests it was decided to improve the IPCS decel times by replacing the sequential feature, where the A/B decel is completed prior to the gas generator decel, with simultaneous deceleration, as in BOMDIG.

8.4.1.5 Miscellaneous Tests

An attempt to induce afterburner rumble in the IPCS mode at M 0.9/45000 ft was not successful. The duct oscillations that resulted from the off-design A/B fuel flow were not characteristic of rumble.

The IPCS mode airflow bias logic matches inlet operating point and engine demand by varying inlet geometry and/or engine speed. Without an inlet, the checkout was limited to the engine speed variation. The tests were successful during gas generator operation when the bias signal resulted in engine acceleration or deceleration, as required, to obtain the inlet/engine match. Removal of the bias signal returned the engine to its initial state. Operation in A/B was unsatisfactory producing nozzle oscillations. Further investigation was deferred to the ground and flight tests.

Test data acquired during the sea level tests showed a potential for low rotor overspeed when the DPCU was disengaged during A/B operation. A control fix was made to add a relay to open the 7th stage bleeds for three seconds when the DPCU was disengaged or powered down. This feature was tested at sea level and all altitude conditions with the result that the peak N1, following disengagement from max A/B, was always less than the 10,500 rpm limit.

8.4.2 Tests with Distortion Generator

Engine distortion tolerance in the HMC mode was measured for several speeds and all bleed combinations for comparison with the baseline engine tests. No deterioration in distortion tolerance due to the engine modifications was observed.

The IPCS mode distortion sensor and bleed control logic using the direct distortion measurement pressure transducers described in Section 8.2.3 operated as desired. The 7th and 12th bleeds were opened in response to an increase in measured distortion levels and, when distortion was increased to stall, the control sensed the stall and resulted in a deceleration to idle for a period of two seconds, as programmed. An example of the IPCS stall reaction at M 1.4/41000 ft is shown in Figure 8.4-14.

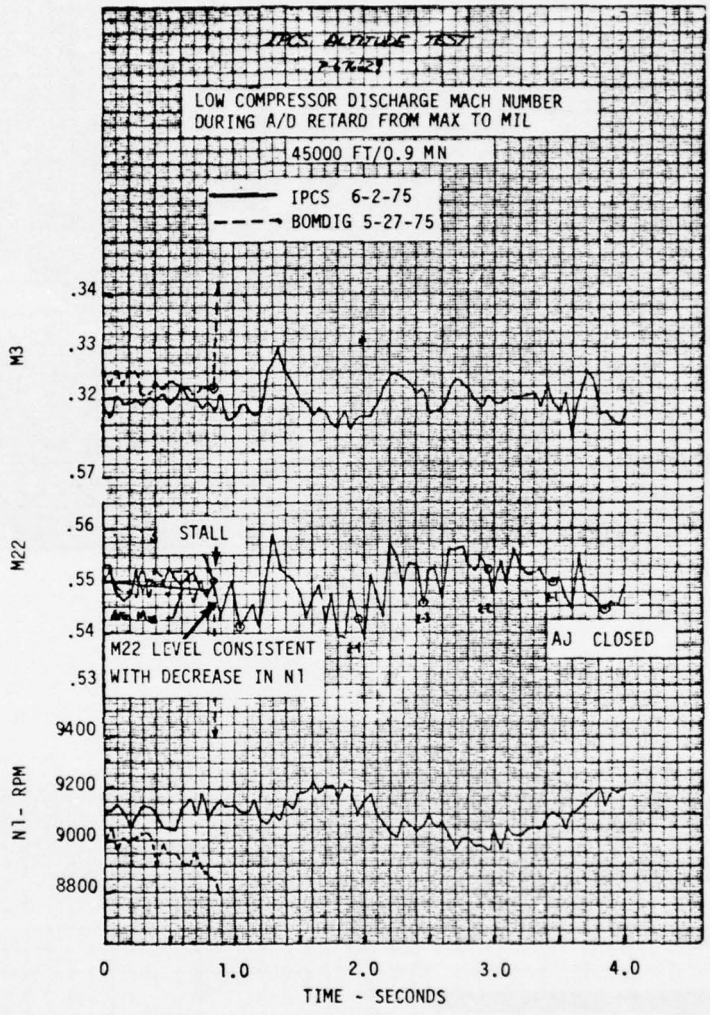

Figure 8.4-11 M22, M3 BOMDIG Max-Mil Stall

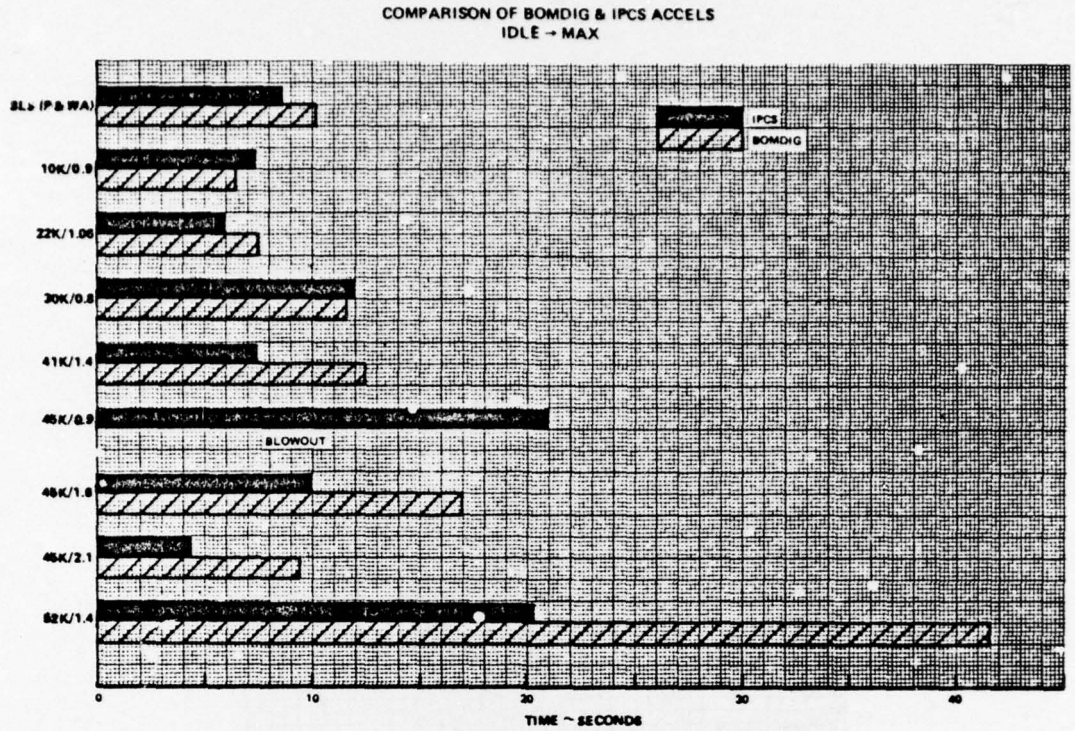

Figure 8.4-12 BOMDIG, IPCS Idle-Max Time Comparison

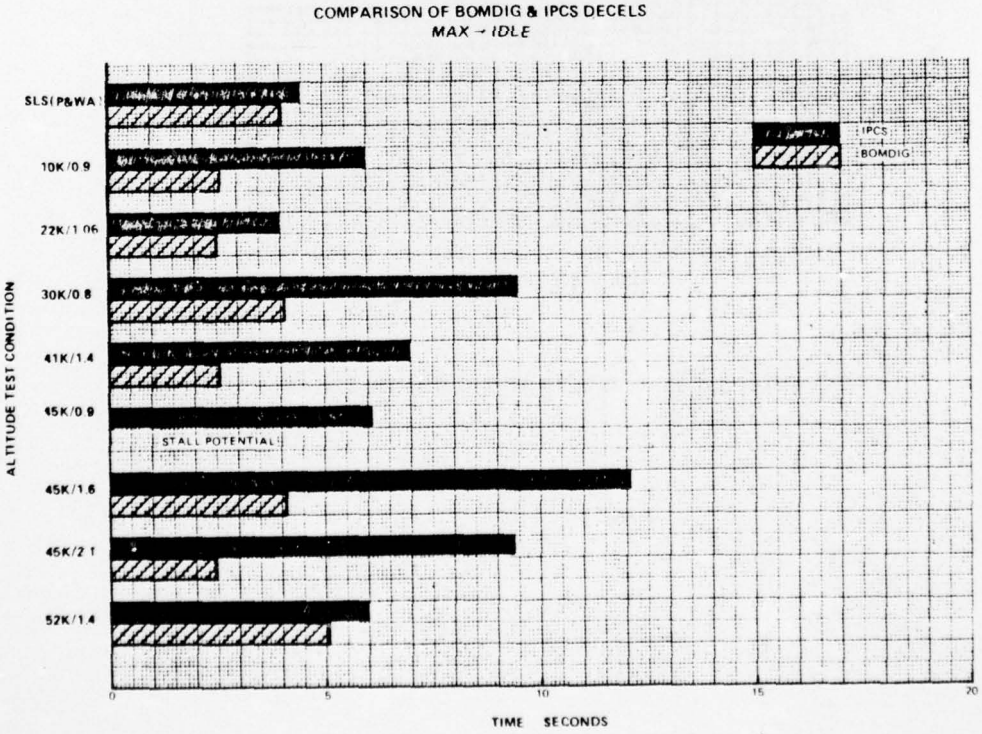

Figure 8.4-13 Max-Idle Decel Time Comparison

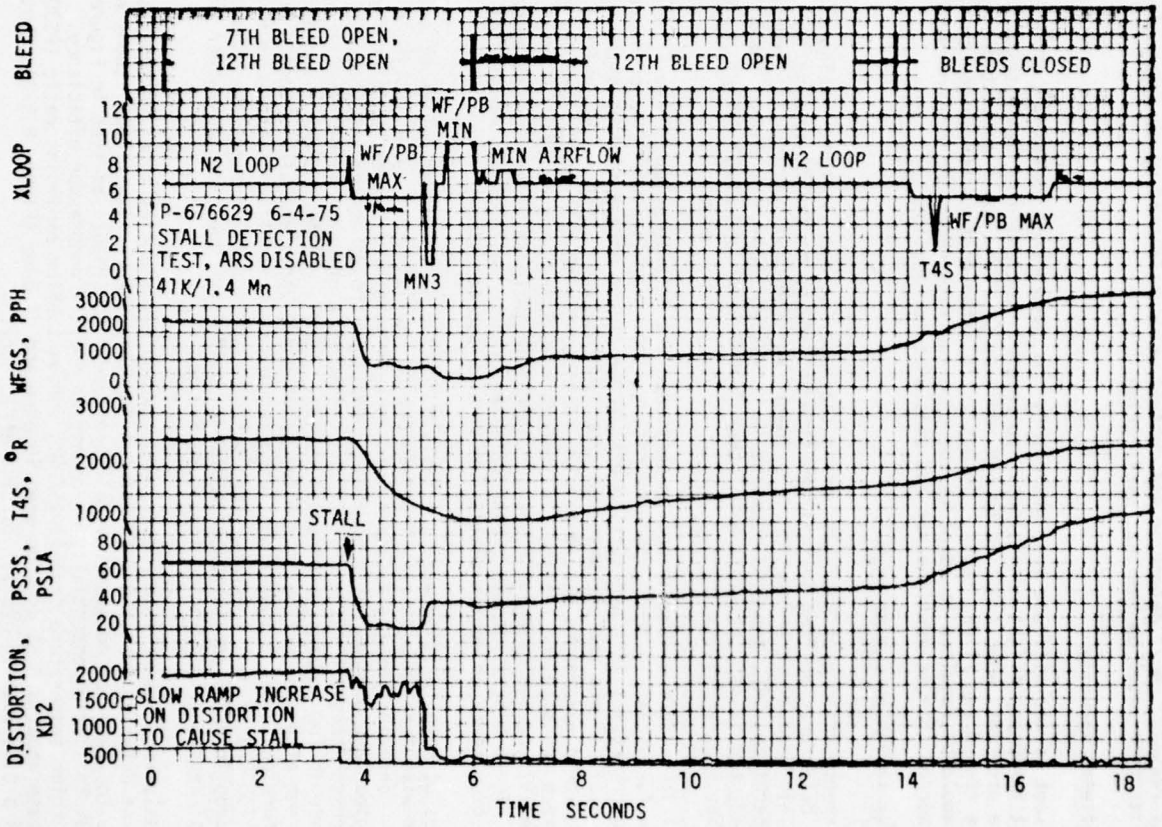

Figure 8.4-14 IPCS Stall Reaction

8.4.2 Tests with Distortion Generator (Continued)

Operation of the IPCS buzz detector and loop was demonstrated by pulsing all six control valves of the distortion generator at a typical F-111E buzz frequency of 10 Hz. Figure 8.4-15 shows that the engine accelerated to move the inlet out of buzz as the pressure fluctuations increased and returned to its initial state when the buzz signal was reduced. Buzz detection and control were unaffected by superimposing a 500 Kd distortion level on the buzz oscillation.

8.4.3 Software Maturity

The last week of the altitude test was devoted to checkout of BOMDIG and IPCS revision C tapes at three key flight conditions. Successful conclusion of these tests assured that these programs, when modified by the revision C SFCOs, would be suitable for use during the ground and flight tests. It was anticipated that modifications to these programs would be required to adapt to the airplane interfaces and to incorporate the recommended changes mentioned at the conclusion of Section 8.1.

8.5 ENGINE STATUS AT END OF TEST

The performance history of P-676629 during the baseline and altitude testing showed a gradual deterioration from initial baseline testing up to the 24-30 June 1975 period. This gradual deterioration is evident from the 0.5% increase in turbine inlet temperature, T4E, and 0.6% decrease in corrected high-rotor speed, XNHR2, over this period, and it is consistent with other TF30-P-9 T4H and XNHC2 deterioration rates. (See Figure 8.5-1).

Additional indicators of engine health confirmed the deterioration of P-676629. Changes in fuel flow, low-compressor operating line, overall compressor pressure ratio, and compressor exit and turbine exit temperatures were estimated with influence coefficients and the observed drop in high-rotor speed. The observed changes in these parameters were generally consistent with the estimated deterioration rates between the baseline testing, 26 September 1973 and 24 June 1975. During the 24-30 June 1975 period (350-365 hours) a noticeable increase in deterioration was observed (Figure 8.5-1), and this change in performance was also accompanied by an increased occurrence of engine stalls during slow decelerations.

Two sources of deterioration were initially suspected: (1) contamination of the high compressor with foreign particles ingested during facility shaking at the M .9/ 10000 ft condition, or (2) a sudden loss in high turbine efficiency and/or first-stage turbine vane bowing. Both of these conditions could have caused the drop in high-compressor pressure ratio (PS3Q2) and corrected high-rotor speed (XNHC2) and the increase in low-compressor pressure ratio (PS22Q2). High-compressor contamination was ruled out after inspection of the fan inlet guide vanes and blades showed no signs of foreign particle ingestion. High-turbine deterioration is the most likely deterioration source, but a marked drop in high rotor corrected speed in conjunction with the drop in PS3Q2 and increase in PS22Q2 would have been expected rather than the gradual decrease in N2 noted in Figure 8.5-1.

Further analysis of overall compressor and turbine efficiencies tends to support high-turbine deterioration. Overall compressor temperature rise (T3PC2) shows no noticeable increase for constant overall pressure rise (PS3Q2) as seen in Figure 8.5-2, thus indicating essentially no change in overall compressor efficiency. Overall turbine temperature drop (1-T5/T4H) versus turbine expansion ratio (PS3Q6M) does indicate about a 0.5% drop between 10 June and 24 June (Figure 8.5-3), thus indicating a 0.5% loss in overall turbine efficiency.

In view of the performance changes observed for P-676629 together with the increased incidence of compressor stalls during decelerations, a thorough examination of the high pressure turbine was recommended during the post-test engine teardown and inspection. Specific recommendations were as follows:

1. Examine the high turbine seals for excessive wear. P-676629 does not have the extended first vane platform (T.O. 2J-TF30-678), so the first outer air seal should be closely inspected for wear.
2. Examine the first turbine vanes for bowing or burned areas.
3. Check the burner and transition duct for signs of distress.

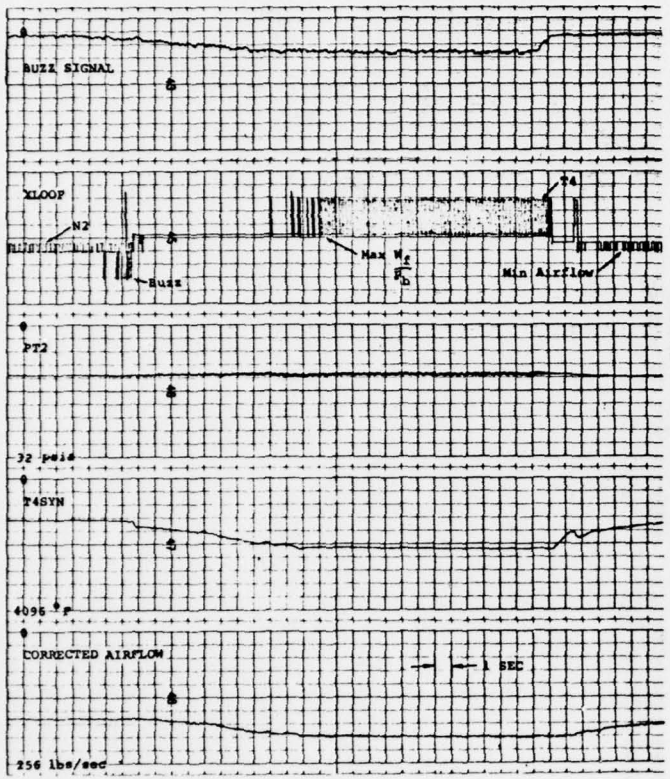

Figure 8.4-15 IPCS Buzz Loop Operation

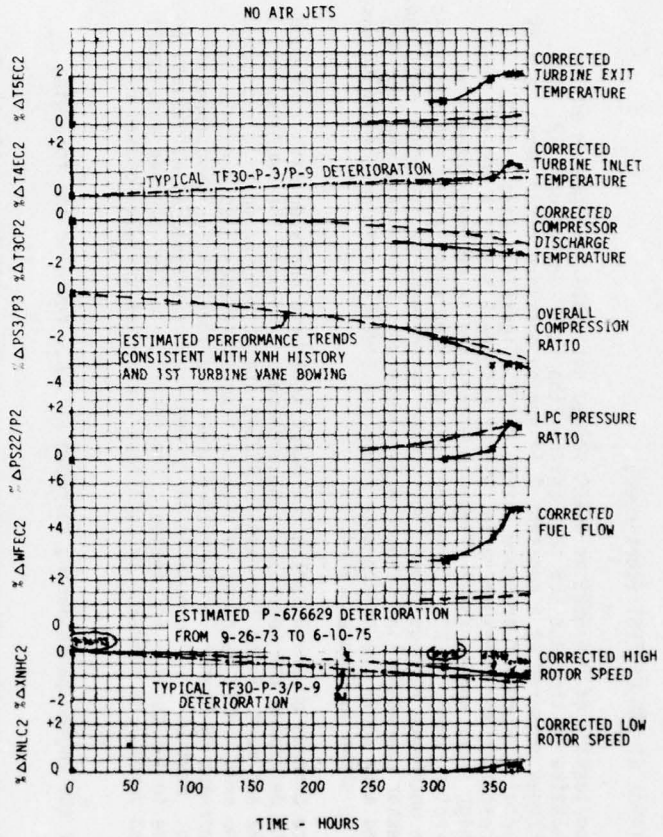

Figure 8.5-1 TF30-P-9, P-676629, Performance History, NASA LeRC 41K/14 Mn

8.5 ENGINE STATUS AT END OF TEST (Continued)

The as-received testing of P-676629 at OCALC showed noticeable changes in engine performance relative to the last SLS test calibration taken on February 12, 1975. The largest changes measured at a constant 2.14 engine pressure ratio were: a 3.2% decrease in overall compressor pressure ratio, PS3Q2 (Figure 8.5-4a); a 2.7% increase in low-compressor pressure ratio, PS22Q2 (Figure 8.5-4a); a 200 rpm drop in corrected high rotor speed, XNHR2 (Figure 8.5-4b); and an 80 rpm decrease in corrected low-rotor speed, XNLR2. Corrected turbine inlet temperature and corrected fuel flow were unchanged at high power, but showed an increase at low power settings. The low-compressor operating line (Figure 8.5-4c) was 3.5% higher than the last SLS calibration and also above the maintenance limit. A 3 Wf/Pb ratio unit increase was also observed as shown in Figure 8.5-4d.

The performance changes observed during the OCALC test were analyzed with influence coefficients to determine the sources of these changes. Most of the decrease in PS3Q2 and XNHR2 and most of the increase in PS22Q2 are attributed to a 3% increase in high turbine area. A 1% decrease in high turbine efficiency also accounts for some of the decrease in high-rotor corrected speed and increase in low-compressor pressure ratio. Most of the decrease in corrected low-rotor speed is attributed to a 1.5% decrease in low turbine efficiency. The increase in high-turbine area could be due to bowed vanes, and decrease in turbine efficiencies could be caused by seal wear.

Examination of the engine parts during teardown at OCALC revealed the following discrepancies:

All the first stage turbine stator vanes were bowed from .010 in. - .040 in. (increase in high turbine area).
The first turbine outer air seal was burned and cracked in a number of places
The transition duct was burned and warped in some spots.
Burner cans showed some slight evidence of burning and warping, but were considered normal for an overhaul engine.

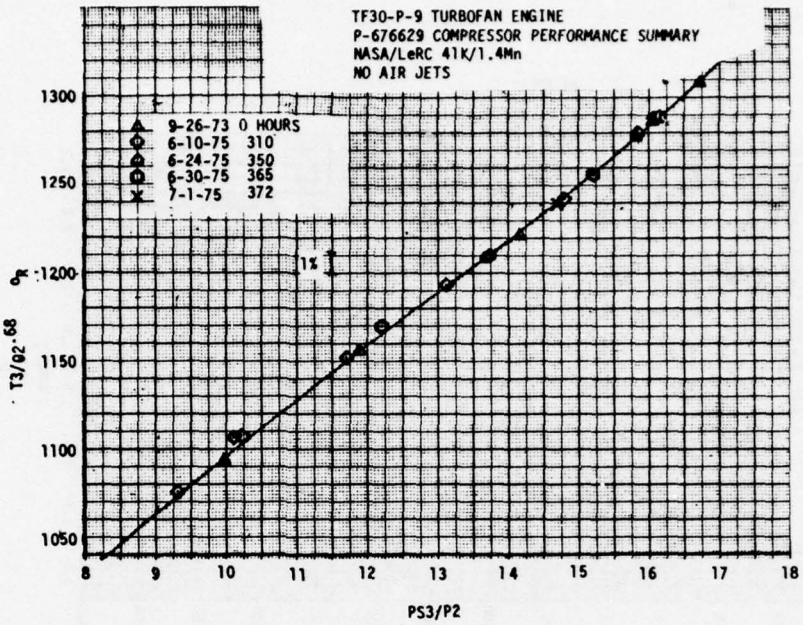

Figure 8.5-2 TF30-P-9, P-676629, Compressor Performance Summary, NASA LeRC 41K/1.4 Mn

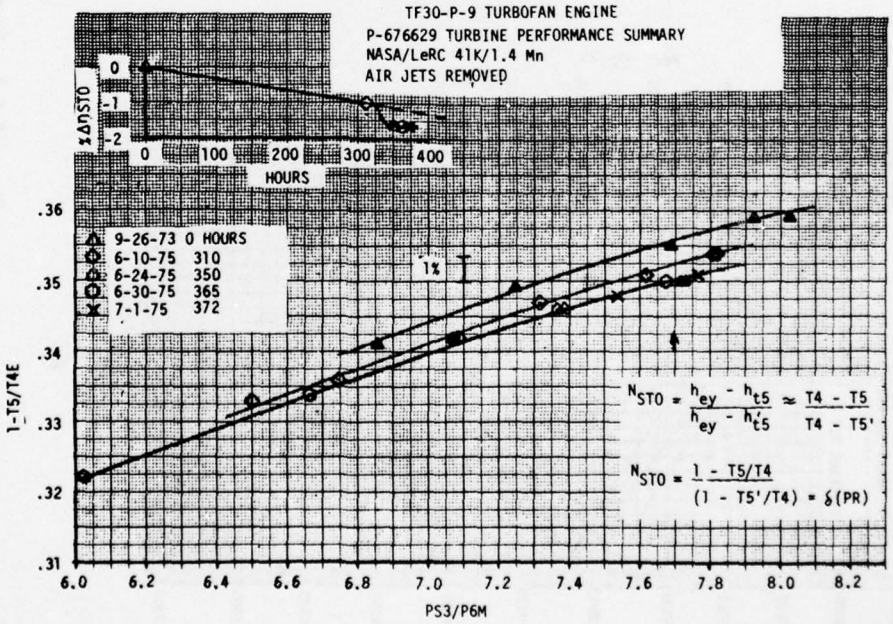

Figure 8.5-3 TF30-P-9, P-676629, Turbine Performance Summary, NASA LeRC 41K/1.4 Mn

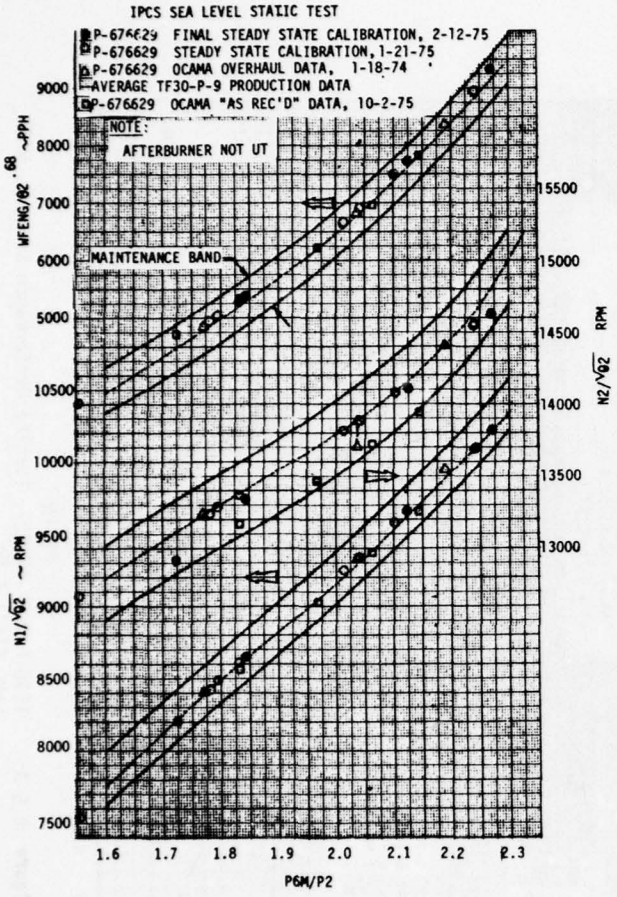

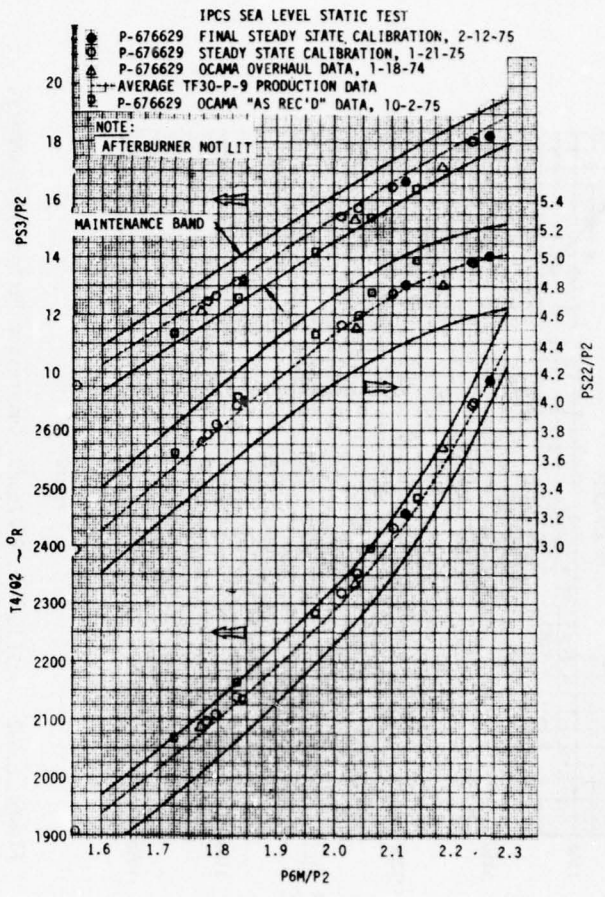

Figure 8.5-4 Performance Summary Curve

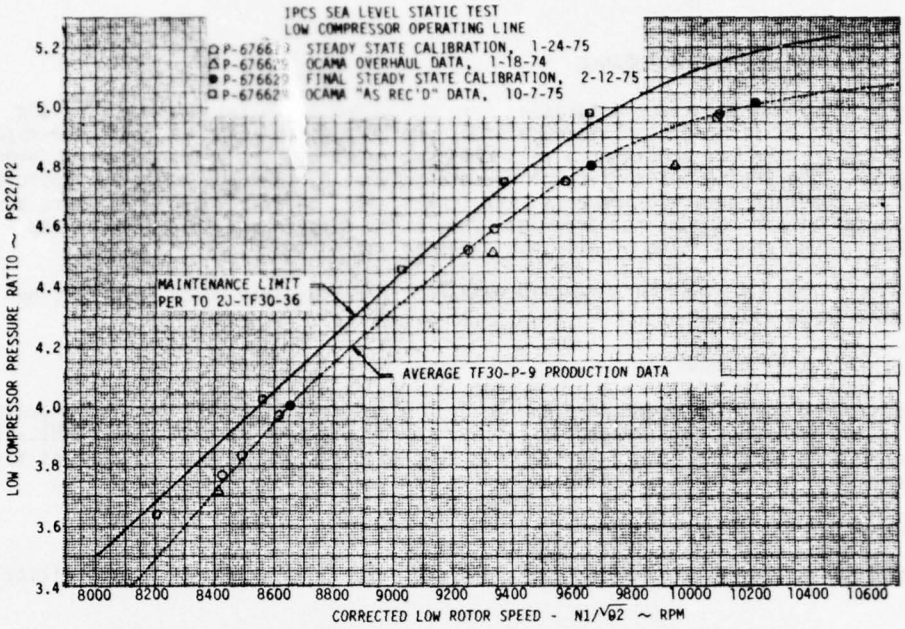

C

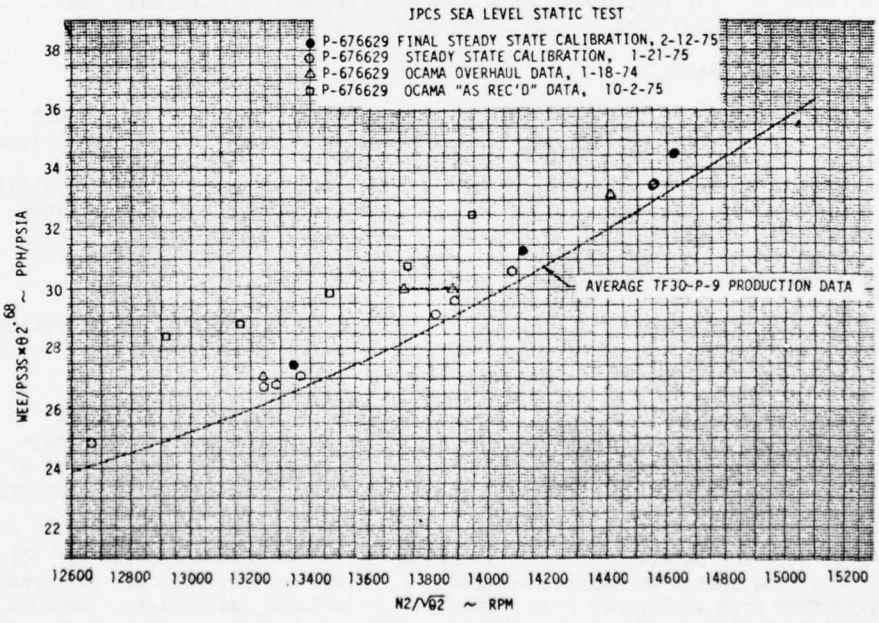

D

Figure 8.5-4 Performance Summary Curve

9.0 RELIABILITY AND QUALITY ASSURANCE

Reliability and quality assurance activities were conducted as an integral part of the IPCS program. Formal program plans in each area were prepared by each of the three major contractors and checked for consistency with contract requirements, government standards, and each other. The Boeing reliability plan was submitted to the government for approval as part of the Contract Data Requirements List (CDRL), item A-00B. These plans were updated as appropriate throughout the program. They had a significant influence on the design, fabrication, and testing of all IPCS hardware and software.

The paragraphs below describe the composite reliability and quality program pursued by the three major IPCS contractors.

9.1 IPCS RELIABILITY PROGRAM

The Reliability Program Plan identified and described the controls, methods, and organizational responsibilities that were implemented to satisfy the appropriate requirements of MIL-STD-785A, as amended by Contract F33615-73-C-2035. This plan was the governing document for the performance of all reliability disciplines associated with the contract.

9.1.1 Application of Military Standards

The documents listed below provide the basis and the authority for the IPCS reliability program.

MIL-Q-9858	Quality Program Requirements as interpreted by the Boeing IPCS Reliability Program Plan
MIL-STD-785A	Reliability Program Requirements as interpreted by the Boeing IPCS Reliability Program Plan
MIL-HDBK-217A	Reliability Stress and Failure Rate Data for Electronic Equipment
MIL-STD-721B	Definitions of Effectiveness Terms for Reliability, Maintainability, Human Factors, and Safety

A task list was drawn up that referenced these documents and Boeing procedures that were responsive to their requirements. This task list is given in Table 9.1-1.

9.1.2 Reliability Requirements

The IPCS reliability engineer was responsible for implementation and direction of all reliability tasks. He reported directly to the IPCS program manager. Directives originated by the reliability engineer to promulgate reliability policies and procedures were signed by the program manager to assure compliance by affected personnel. All reliability management and engineering tasks were listed on Task Sheets (Table 9.1-1) that defined each task, showed prime responsibility, supporting organizations, completion criteria, disposition, schedule/phasing task number referenced to MIL-STD-785A paragraph number and company policies, and procedures and controls.

Specifications for subcontractors and suppliers of equipment were prepared as appropriate. Reliability requirements for each procurement activity were allocated proportional to the relative complexity and criticality of the item being procured.

The Boeing reliability engineer coordinated directly with the reliability engineers assigned to the IPCS program by Honeywell and P&WA. These engineers worked with their respective designers by providing specialized guidance, parts approvals, and support of reviews. This close working relationship assured an integrated interdisciplinary assurance effort without duplication.

A Preferred Parts List was established to serve as the basis for part selection for all new design and modified design hardware. Selection of parts for this list was performed by design engineering with assistance from component applications specialists. Because of their specialized training, their data sources, and their experience, these engineers were equipped to recommend part selections after detailed design requirements has been established by the designer.

Table 9.1-1 Reliability Program Task List

MIL-STD-785 REF & Task No.	Task Description	Applicable Procedure	Responsible Organization	TASK OUTPUT Description	CDRL Item
4.0	Reliability Planning				
4.4	Prepare and document a Reliability Program Plan	MIL-STD-785A	Reliability Engineer	Reliability Program Plan Document	Yes
5.1	Reliability Management				
5.1.1	Prepare or revise Engineering Directives, procedures and instructions for implementing specific reliability functions	Not applicable	Reliability Engineer	Boeing Aerospace Co. directives, procedures, instructions and revisions thereof	No
5.1.2.1	List all Reliability Program Task in accordance with DI-R-3533/R-101-2	Not applicable	Reliability Engineer	Reliability Program Task Lists	Yes
5.1.3	Prepare reliability requirements for inclusion in specifications for subcontractors and vendors as appropriate	Not applicable	Reliability Engineer	Memos to Materiel	No
5.1.4	Prepare reliability program status data for monthly reviews and PDR, FDR, and CDR	Not applicable	Reliability Engineer	Design review presentation data	No
5.2	Reliability Design and Evaluation				
5.2.1	Support design in selection and derating of parts consistent with reliability requirements	MIL-HDBK-217A, BAC, MH and PWA data	Reliability Engineer	Memos, lists and/or discussion	No
5.2.2	Conduct and document reliability prediction analysis	MIL-STD-785A	Reliability Engineer	Reliability Analysis	Yes
*(5.1.4.2)	Accomplish Failure Mode Analysis	R&D Plan	Design	FMA	No
5.2.3	Use preferred parts listed in para 5.4, Task IV-A of Contract F33615-73-C-2035 with exceptions as noted in this plan	Program Direction	Design	Drawings	No
5.2.3	Prepare non-standard parts list	As stated in this plan	Design	Lists	No
5.2.3	Review and approve parts usage	Program Direction	Reliability Engineer	Signature on drwg's and/or memo to Material for subcontractors	No

AD-A033 774 BOEING AEROSPACE CO SEATTLE WASH F/G 21/5
INTEGRATED PROPULSION CONTROL SYSTEM (IPCS). VOLUME II. TECHNIC--ETC(U)
AUG 76 L O BILLIG F33615-73-C-2035
UNCLASSIFIED AFAPL-TR-76-61-VOL-2 NL

3 OF 3
AD
A033 774

END
DATE
FILMED
2-77

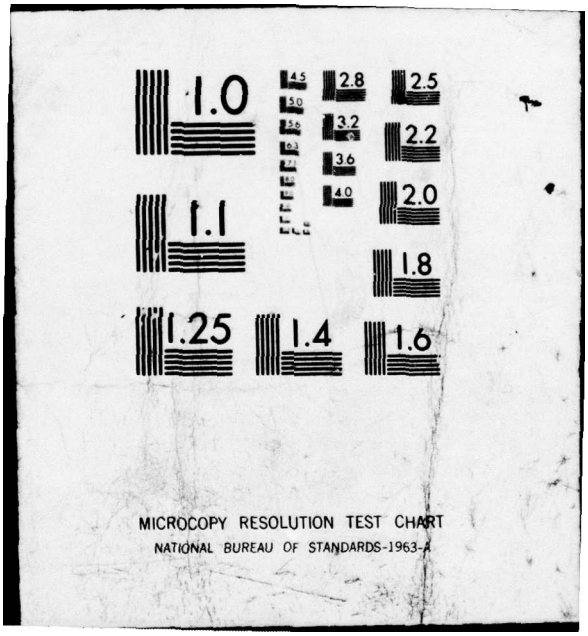
1.0
1.1
1.25
1.4
1.6
1.8
2.0
2.2
2.5
2.8
3.2
3.6
4.0
4.5
5.0
MICROCOPY RESOLUTION TEST CHART
NATIONAL BUREAU OF STANDARDS-1963-A

Table 9.1-1 Reliability Program Task List (Continued)

MIL-STD-785 REF & Task No.	Task Description	Applicable Procedure	Responsible Organization	TASK OUTPUT Description	CDRL Item
5.2.4	Accomplish failure mode effect and criticality analysis	D2-24144-1	Design	FMECA	No
5.2.5	Identify critical items, controls, and/or special handling	Program	Design	Memos	No
5.2.6	Identify effects of storage, shelf-life, packaging, transportation, handling and maintenance	Program Direction	Design	Memos	No
5.2.7	Prepare reliability analysis data and participate in design reviews	D2-24144-1	Reliability Engineer	Design review presentation data	No
5.4	Failure Data				
5.4.1	Provide for reliability data collection as a part of the IR's (UERs) including subcontractor data	D2-4800	Quality Control	UERs and subcontractors reports	No
5.4.1	Analyze failure data, recommend corrective action and inform management. Correct problems	As required	Reliability Engineer Design	TFARs	No
5.4.2	Prepare failure summaries	Not applicable	Reliability Engineer	Reports	Yes
5.6	Prepare reliability inputs to monthly status reports	CDPL/ D1-A-3002/A-113-1	Reliability Engineer	Reliability status report	Yes

9.1.2 Reliability Requirements (Continued)

All parts used in airborne components of new design were selected on the basis of at least one of the following criteria:

Material, parts, and processes that have been used in prevous applications and are in accordance with Government specifications and standards.

Suitable, reliable parts that have been procurred to industrial specifications and appear on the preferred parts list of similar programs.

Materials, parts and processes that have been determined necessary to meet systems requirements and have adequately documented reliability characteristics warranting their use.

The order of precedence followed for DPCU part selection for new design is given below.

9.1.2 Reliability Requirements (Continued)

1. Established reliability (ER) and screened parts as defined below:

Part Type	Military Spec
Resistors, capacitors, and relays	MIL-R-55182, and MIL-R-39000 Series, level M or better
Transistors and diodes	MIL-S-19500, JAN or JANTX
Microcircuit	MIL-M-38510 Class B or vendor's high reliability program per MIL-STD-883, Class B

2. Other MIL-STD parts

Parts that were not included in any of the above categories were considered nonstandard. The Honeywell G&AP Divisional Preferred Parts List (DPPL) was used as a guide for initial selection of nonstandard parts. A nonstandard electrical parts list was prepared and submitted to Boeing for review. This list included the following for each part:

Part identification and description
Reason for selection

Parts used in DPCU airborne components of new design were derated in accordance with the Honeywell standard Design Margin Criteria with approval from Boeing.

9.1.3 Reliability Analysis

A reliability analysis of the IPCS was performed concurrently with the design process. This analysis consisted of a detailed reliability block (functional) model and a set of equations relating equipment reliability (to the piece part level) to the reliability of the basic system functions. The exponential mathematical model, $R(t) = \lambda\exp(-\lambda t)$, $t \geq 0$, was selected since all three contractors had historical data on their electronic and mechanical hardware that indicated a constant failure rate process.

Inputs to the reliability model consisted of identification of the required functions and critical time periods for each function (assumed to be two hours per flight).

The results of the analysis were presented at the Final Design Review, held May 29, 30, and 31, 1974. The analysis, summarized in Figure 9.1-1, indicated a 98% probability of successful operation of the IPCS hardware for a given two-hour flight.

9.1.4 Failure Mode, Effects and Criticality Analysis

Failure mode, effects, and criticality analysis (FMECA) were conducted to identify all potentially catastrophic and critical failure modes that may occur during a two-hour test flight. Failures were divided into four categories as listed in Table 9.1-2.

Table 9.1-2 Failure Mode Classification

I	Loss of Aircraft
II	Engine Shutdown
III	DPCU Shutdown
IV	Nuisance

The data used to conduct the analysis included the following:

A. System performance specification
B. IPCS Block Diagram
C. IPCS Inlet Functional Schematic
D. IPCS DPCU Functional Schematic
E. IPCS Transducer Package Schematic
F. IPCS Engine/Afterburner/Nozzle Functional Schematic
G. Assembly/Part Performance Specifications
H. Boeing, Honeywell, Pratt & Whitney ICD's.

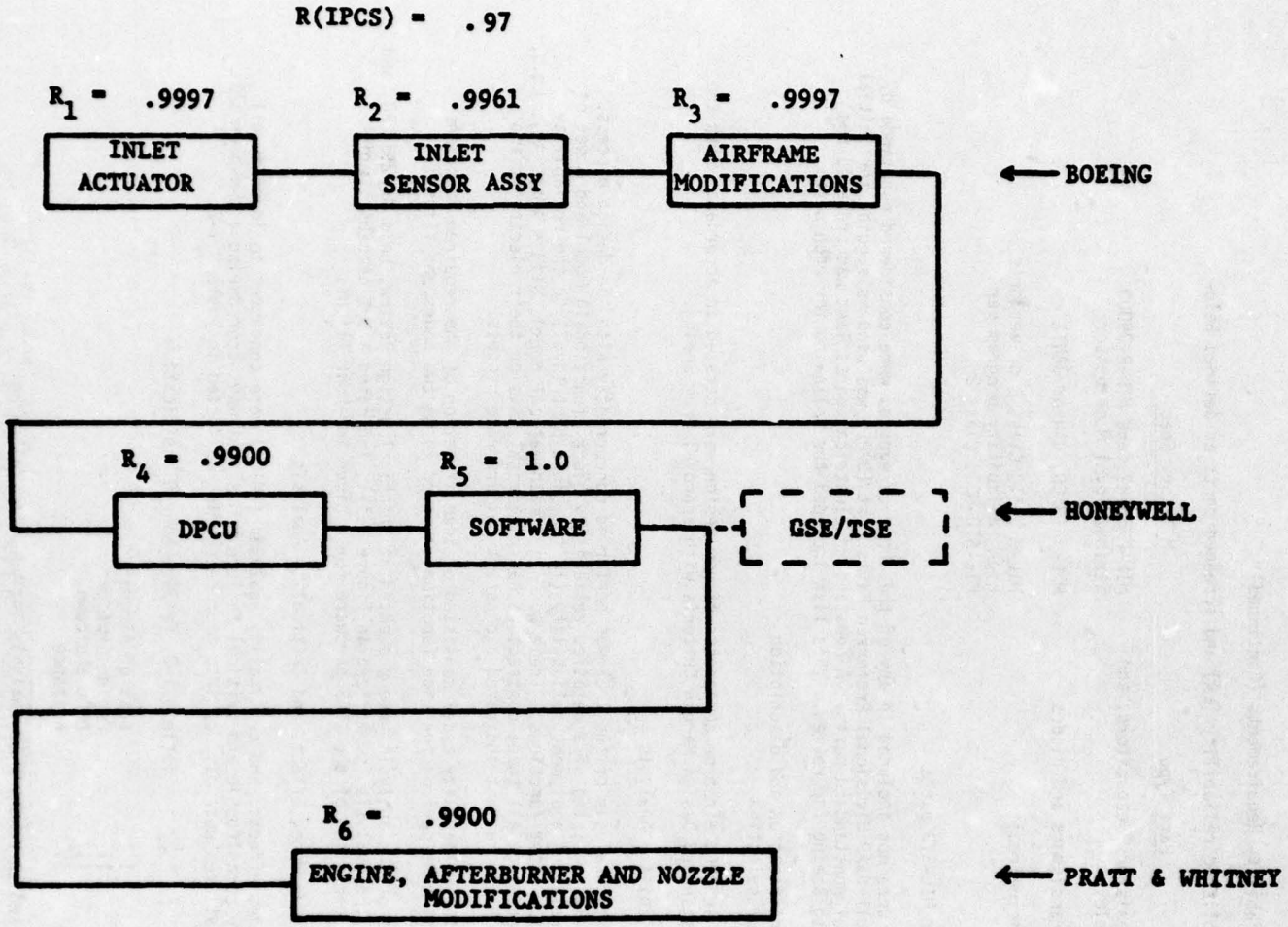

Figure 9.1-1 IPCS Reliability Prediction

9.1.4 Failure Mode, Effects and Criticality Analysis (Continued)

The initial analysis was primarily concerned with those failure modes that would cause engine operating limits to be exceeded or would prevent switch-over to hydromechanical control. To provide for flight safety, the system was designed to monitor critical propulsion parameters and to disengage the DPCU (revert to hydromechanical control) if a potential hazard was detected or if the integrity of the IPCS was in doubt. (See para 2.3.3).

The final FMECA summary is given in Table 9.1-3

Table 9.1-3 FMECA Summary

	I	II	III	IV
Boeing	0	4	1	60 21*
Honeywell	0	0	237	61 45*
P&WA	0	5	105	145
Bendix	0	0	84	5
Total	0	9	426	333

*Classification is IV if Mach ≤ 1.0; otherwise it is III

The predicted failure rate was calculated for class II failures. This probability is 0.00003 for a two-hour flight. This probability is based on the total failure rates of all the components involved.

9.1.5 Failure Reporting, Analysis and Corrective Action

A formal failure reporting, analysis and corrective action program was established for IPCS. This program was tailored to accommodate the existing failure reporting systems within Boeing, Honeywell and Pratt and Whitney. Failure reports were prepared on all failures, describing the history of the failed item, the test conditions at the time of failure, the results of the failure investigation (including tear-down analyses) and the recommended corrective action. These reports were approved by Boeing and submitted to the Government under CDRL A00A.

9.2 QUALITY ASSURANCE

IPCS Program quality assurance requirements specified in the contract statement of work required that the IPCS Quality Program conform with the requirements of MIL-Q-9858A, "Quality Program Requirements"; MIL-C-45662, "Calibration System Requirements", and USAF Specification Bulletin NR 515 "Control of Nonconforming Supplies". The basic quality assurance disciplines used during the development procurement, fabrication, assembly, and test of the IPCS are set forth in Aerospace Group Quality Control Manual D2-4800 Directives.

The IPCS Program Quality Control Manager reported to and was accountable to the Boeing Aerospace Company Director of Quality Control, who has delegated responsibility and commensurate authority for directing all IPCS quality assurance functions to the IPCS Quality Control Manager. The IPCS Quality Control Manager was responsible for IPCS product quality and for providing functional quality assurance direction to all organizations that supported the IPCS program. He received program direction from the IPCS program manager.

9.2.1 Procurement Control

Procurement quality control covered the selection, approval, and surveillance of suppliers furnishing materials, parts, and components for incorporation into IPCS. The nature and extent of controls depended on the type of procurement, the suppliers demonstrated performance capabilities on similar articles, and the suppliers' system for control of quality. Disciplines were imposed as follows:

9.2.1 Procurement Control (Continued)

1. The major subcontractors, Pratt & Whitney and Honeywell, were required to comply with MIL-Q-9858A, MIL-C-45662, and NR 515.

2. Suppliers of off-the-shelf parts and components were required to be an approved Boeing source and meet the applicable purchase order requirements.

Design requirements were reviewed by Quality Control engineers to ensure that adequate provisions were included for determining and controlling the quality of procured hardware and services. All purchase orders were reviewed and approved by Quality Control prior to release to ensure the inclusion of technical and quality requirements and configuration and inspection system provisions.

The Quality Control personnel monitored the major subcontractors' quality control activities as necessary to confirm that they comply with requirements levied upon them by purchase orders and subcontract. They participated in functional and detailed design reviews, process specifications compliance reviews, and hardware inspections. All testing classified by engineering as critical to quality assurance was witnessed and certified by Quality Control personnel. Assistance was provided to all IPCS suppliers in interpreting purchase orders, configuration management requirements, and technical requirements affecting quality.

9.2.2 Material Control

All purchased material and parts were checked for conformance to purchase orders and material specifications. The inspections and tests were planned in advance with special emphasis applied to the location of tests and criticality of the item.

As supplier-furnished material arrived in the receiving inspection area, a data package was reviewed for evidence of supplier's inspection and source control requirements. The material was then subjected to a visual, dimensional laboratory, and functional tests as required. All functional test data were provided to the Reliability organization for inclusion in the equipment log.

9.2.3 Inspection and Test System

Records of inspection and test performed throughout the fabrication, test, and acceptance process were maintained by Quality Control in accordance with the requirements of Quality Control Manuals as applicable.

The quality planning function ensured that manufacturing work orders were developed that defined sequential operations compliant with contract requirements during fabrication, processing, and assembly of deliverable hardware and that provided for the recording of configuration, accountability, acceptance, malfunctions, reliability data, and nonrecurrent action.

Quality Control personnel monitored fabrication operations and inspected all completed items. Additionally, Quality Control personnel witnessed in process and end item acceptance testing. The results of these inspections and tests was documented and the parts identified as having been accepted.

9.2.4 Nonconforming Material

Quality Control identified and segregated all nonconforming material as it was detected. A rejection form was initiated on each nonconformance and became part of the historical record. The disposition of non-confirming material was controlled by Material Review Boards.

10.0 REFERENCES

1. "Automatic Detection and Suppression Of Inlet Buzz", by L. O. Billig, Instrumentation for Airbreathing Propulsion, Progress in Astronautics and Aeronautics, Vol. 34, The MIT Press, 1973.

2. "IPCS Closed Loop Bench Test Plan", P&WA Report No. 5110, 25 September 1974.

3. "Integrated Propulsion Control System Control Component Flight Assurance Testing Closed Loop Bench Test", P&WA Report No. 5247, 12 March 1975.

4. "IPCS Sea Level Static Engine Test Plan", P&WA Report No. 5166, 26 November 1974.

5. "IPCS Sea Level Static Engine Test Report", P&WA Report No. 5268, 4 June 1975.

6. "IPCS Altitude Test Plan", Boeing Aerospace Company Document No. D251-10029, 7 March 1975.

7. "IPCS Altitude Test Report" Boeing Aerospace Company Document No. D251-10037, 16 November 1975.

8. NASA Flight Research Center Process Specification No. 21-2, Flight Assurance Testing (Environmental) Electronic and Electromechanical Equipment, 24 July 1972.

9. "Pratt & Whitney Aircraft Design Data Summary, PWA Hardware", Integrated Propulsion Control System Components, Revised 15 March 1974.

10. "Baseline Engine Test Plan, Integrated Propulsion Control System", Boeing Aerospace Company Document No. D251-10003, 4 June 1973.

11. "Data Reduction Requirements, Integrated Propulsion Control System Program", Boeing Aerospace Company Document No. D251-10005, 15 May 1973.

APPENDIX: LINEAR MODELING TECHNIQUE

The method used to extract linear state models of the F-111/TF30-P-9 propulsion system from a digital dynamic simulation is described below. The linear state models were subsequently used to generate transfer functions for stability analyses and as bases for the hybrid simulation as described in Section 2.0 of this document.

Consider a state model of the form

$$\dot{X} = AX + BU, \; Y = CX \tag{1}$$

where X is the state vector, Y is the vector of signals available to control the plant, U is the control vector, and A, B, and C are matrices. A model of the form of (1) will in general have only a limited useful domain when applied to a non-linear plant. Hence we must specify points X_o, U_o for which we must determine the corresponding matrices A. B. and C.

Equation (1) may be expanded to the form

$$\begin{aligned}
\dot{x}_1 &= a_{11} x_1 + \ldots + a_{1n} x_n + b_{11} u_1 + \ldots + b_{1m} u_m \\
&\vdots \\
\dot{x}_n &= a_{n1} x_1 + \ldots + a_{nn} x_n + b_{n1} u_1 + \ldots b_{nm} u_m
\end{aligned} \tag{2}$$

with a similar expression for Y. The X and U vectors in (2) define the points X_o and U_o. It is conventional, but by no means necessary to choose X_o and U_o such that $\dot{x} = 0$. The choice of points depends entirely upon the application for which the model is employed.

We begin by perturbing x_1 *by a "small" increment* Δx_1 *and substitute into* (2) to obtain the following expression:

$$\begin{aligned}
\dot{x}_1 + \Delta\dot{x}_1 &= a_{11}(x_1 + \Delta x_1) + \ldots + a_{1n} x_n + b_{11} u_1 + \ldots + b_{1m} u_m \\
&\vdots \\
\dot{x}_n + \Delta\dot{x}_n &= a_{n1}(x_1 + \Delta x_1) + \ldots + a_{nn} x_n + b_{n1} u_1 + \ldots + b_{nm} u_m \\
y_1 + \Delta y_1 &= c_{11}(x_1 + \Delta x_1) + \ldots
\end{aligned} \tag{3}$$

Subtracting (2) from (3) we obtain

$$\begin{aligned}
a_{11} &= \frac{\Delta \dot{x}_1}{\Delta x_1} & c_{11} &= \frac{\Delta y_1}{\Delta x_1} \\
a_{21} &= \frac{\Delta \dot{x}_2}{\Delta x_1} & c_{21} &= \frac{\Delta y_2}{\Delta x_1} \\
&\vdots & &\vdots
\end{aligned} \tag{4}$$

Repeating this operation $x_2 \ldots x_n$ and $u_1 \ldots u_m$ will give the entire A, B, and C matrices.

The density of points X_0, U_0 around which to linearize depends upon the accuracy required and the degree of non-linearity of the function. A total of 38 linear models were generated during the IPCS program as discussed in section 2.3.2. This number may have been larger than necessary; due to the exploratory nature of the IPCS program, a very dense set was chosen to increase confidence in the results.

☆ U. S. GOVERNMENT PRINTING OFFICE: 1976 — 757-001/49